Heterogeneity and Impaired IGF1R Signalling in Aged B cell Development

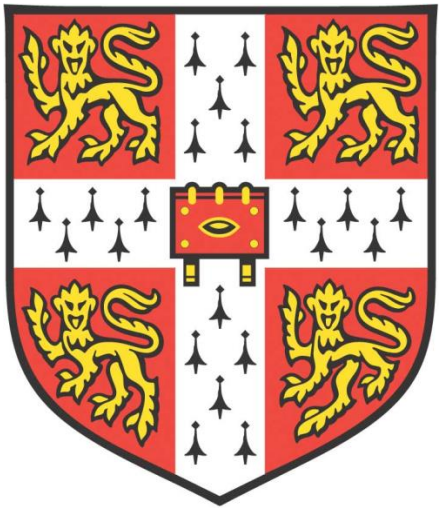

Sam Rees

Christ's College

The Babraham Institute

Department of Lymphocyte Signalling and Development

University of Cambridge

This dissertation is submitted for the degree of Doctor of Philosophy

July 2020

In dedication to Godfrey Bannister

DECLARATION

This thesis is the result of my own work and includes nothing which is the outcome of work done in collaboration except as declared in the Preface and specified in the text. It is not substantially the same as any that I have submitted, or, is being concurrently submitted for a degree or diploma or other qualification at the University of Cambridge or any other University or similar institution except as declared in the Preface and specified in the text. I further state that no substantial part of my thesis has already been submitted, or, is being concurrently submitted for any such degree, diploma or other qualification at the University of Cambridge or any other University or similar institution except as declared in the Preface and specified in the text.

In accordance with the School of Biology guidelines, this thesis is does not exceed 60,000 words, and it contains less than 150 figures.

Date: 31/07/2020

Sam Rees

Cambridge

ABSTRACT

B cells are a vital component of humoral immunity. Upon activation, their immunoglobulin B cell receptor (BCR) is secreted as antibody to neutralise pathogens or mediate the immune response. A diverse repertoire of immunoglobulin molecules is therefore essential for immune surveillance. As we age however, antibody diversity declines, as does our ability to mount a sufficient humoral immune response to vaccines and infections.

The process of generating the BCR, and its diversity therein, begins in the bone marrow. B cell progenitors undergo tightly-regulated recombination of different V_H, D_H, and J_H gene segments of the immunoglobulin heavy chain (Ig_H) gene loci, followed by recombination of the Ig light chain loci, to produce the heavy (μ/Mu) and light (κ/λ) chain proteins that make up an immunoglobulin BCR (IgM). Signalling via the interleukin-7 receptor (IL7R) and the preBCR are required for successful progenitor B cell development in mice. There has also been mounting evidence implicating insulin-like growth factor 1 receptor (IGF1R) signalling to progenitor B cell development at the Pro-B and Pre-B cell stages.

Aged progenitor B cells exhibit reduced output, both in terms of cell number and immunoglobulin repertoire diversity. These defects are suggestive of disrupted differentiation, and correlate with downregulation of several IGF1R signalling components, which may also be regulated at multiple levels. However, given the inherent heterogeneity of the ageing process, it has not yet been fully elucidated that disruption of the IGF1R signalling pathway is a hallmark of ageing progenitor B cells.

I therefore hypothesise that, despite their heterogeneity, progenitor B cells from all aged individuals have impaired IGF1R signalling, and that this suppressed response to IGF1 contributes to their reduced biological output.

In this thesis, I aim to characterise the intrinsic defects of aged progenitor B cells through transcriptomic, V-DJ_H repertoire, and cell cycle analyses. To achieve this, I developed an innovative analytical approach for grouping individual aged mice based on the transcriptomic variability of their Pre-B cell populations, and demonstrate how this reflects the severity of their aged phenotype. To explore the role of IGF1 – the cognate ligand of IGF1R – in early B cell development, I developed a novel in-vitro system for differentiating bone marrow haematopoietic progenitors into B cells that preferentially undergo V(D)J recombination to express IgM in response to IGF1. With this system, it has been possible to demonstrate aged B cell developmental defects in response to IGF1, and highlight the B cell intrinsic nature of these aged defects through mixed chimeric cultures of young and aged cells. Utilisation through this in-vitro system of small molecule inhibitors to the histone H3K27 demethylase JMJD3, and the methyltransferase Ezh2, has also provided evidence to support a hypothesis of polycomb-mediated IGF1R signalling suppression in ageing B cell progenitors. Finally, I provide scope for clinical translation from these aged murine findings by demonstrating similar aged defects, including downregulation of IGF1R transcripts, in older human bone marrow-derived B cells.

ACKNOWLEDGEMENTS

I'd like to acknowledge my colleagues at the Babraham Institute, with special mention to those in the Nuclear Dynamics and Lymphocyte Signalling departments, and my PhD companion Elena Stoyanova.

I would also like to thank my supervisor Anne Corcoran and members of the Corcoran lab – Ola, Peter, Caz, Louise, Luba, Dan, and Elise – for your scientific support throughout the years.

Further thanks goes to my collaborators at GSK, with particular acknowledgements for Clare Thomas and David Tough, who were immensely supportive. I had a wonderful time when I came to work in your labs, and for that I also give thanks.

Extended thanks go to my family for their continued dysfunctionality. I'm incredibly proud of them all, and hope I have done them proud with this work.

I reserve most of my gratitude for my amazing partner Meg, who has shared in the highs and endured the lows. Your strength and stability are qualities I have always admired, and in you I am eternally grateful. Onto the "next chapter"!

TABLE OF ACKNOWLEDGMENT OF ASSISTANCE

Initial training in techniques and laboratory practice and subsequent mentoring:

Dr Anne Corcoran (supervisor, Babraham Institute)

Dr Michelle Linterman (assessor, Babraham Institute)

Dr Clare Thomas (supervisor, GSK)

Dr David Tough (supervisor, GSK)

Dr Peter Chovanec (Babraham Institute)

Dr Olga Mielczarek (Babraham Institute)

Dr Vicki Moignard (GSK)

Dr Wendi Bacon (single-cell RNAseq analysis course, Welcome Sanger Institute)

Data obtained from technical service provider:

Flow Cytometry Dept, Babraham Institute – FACS sorts and training

GSK (Dr Clare Thomas) – FACS sorts

Bioinformatics Dept, Babraham Institute – Training and support

Sequencing Dept, Babraham Institute – Illumina sequencing

Biological Services, Babraham Institute – Animal maintenance and in-vivo studies

Data produced jointly:

Bone marrow extractions:

Dr Daniel Bolland

Dr Peter Chovanec

Miss Carolyn Rogers

Murine culture set-ups:

Miss Irina Ferapontova

Data/materials provided by someone else:

Dr Daniel Bolland – Nuclear RNAseq data

Dr Felix Krueger – Quality trimming and fastq reads

Dr Peter Chovanec – sciRNAseq primers

GSK – Human CD34+ BM cell samples; LC-MS/MS of culture supernatants

Dr Elisa Monzon-Casanova – BrdU flow cytometry protocol

Kayla Friedman and Malcolm Morgan – Microsoft Word thesis template

CONTENTS

List of Tables

List of Figures

List of Abbreviations

Abbreviation	Description
#	Number
3'RR	3' regulatory region
7AAD	7-Aminoactinomycin D
ABCs	Age-associated B cell
AID	Activation-induced cytidine deaminase
ANOVA	Analysis of variance statistical test
ATM	Ataxia telangiectasia mutated
BAD	BCL2 Associated Agonist Of Cell Death
BAFF	B cell activating factor
BCL2	B-cell lymphoma 2
BCR	B cell receptor
BIM	Bcl-2 Interacting Mediator Of Cell Death
BLNK	B Cell Linker
BM	Bone marrow
bp	Base pair
BrdU	Bromodeoxyuridine
BRWD1	Bromodomain and WD repeat-containing protein 1
CAR	CXCL12-abundant reticular
CB	Cord blood
CBE	CTCF binding elements
cDNA	complementary DNA
CDR	Complementarity-determining region
C_H	Constant region
ChIP-qPCR	Chromatin immunoprecipitation paired with quantitative PCR
ChIPseq	Chromatin immunoprecipitation sequencing
CJ	Coding joint
CLP	Common lymphoid progenitor
COVID-19	Coronavirus disease 2019
CSR	Class switch recombination
CTCF	CCCTC-binding factor
CXCL12	C-X-C motif chemokine 12

CXCR4	C-X-C chemokine receptor type 4
CytoMu	Cytoplasmic Mu protein expression
DAMP	Danger associated molecular pattern
DE	Differentially expressed
DepC	Diethyl Pyrocarbonate
DICER	Double-Stranded RNA-Specific Endoribonuclease
DMSO	Dimethyl sulfoxide
DNA	Deoxyribonucleic acid
DNMT	DNA methyltransferase
dNTP	Deoxynucleoside triphosphates
(D)PBS	(Dulbecco's) phosphate buffered saline
dsDNA	Double-stranded DNA
DTT	Dithiothreitol
EB	Elution buffer
EBF	Early B cell factor
EDTA	Ethylenediaminetetraacetic acid
ERK	Extracellular regulated kinases
Eμ	Igh intronic enhancer Mu
Ezh2	Enhancer of zeste homolog 2
Ezh2i	Ezh2 small molecule inhibitor
FACS	Fluorescence-activated cell sorting
Fc	Fragment crystallisable region (constant region of Ig molecule)
FCS	Foetal calf serum
FDR	False discovery rate
FFS/SSC	Forward/Side scatter
FLT3L	Fms Related Receptor Tyrosine Kinase 3 Ligand
FO	Follicular B cells
FOXO	Forkhead box O
FR	Framework region
FrA/FrBC/FrC'/FrD/FrE/FrF	Hardy fractions
FVD	Fixable viability dye
G0-phase	Growth zero phase
G1-phase	Growth phase 1
G2M-phase	Growth phase 2/ mitotic phase

GH	Growth hormone
GO	Gene ontology
Grb2	Growth Factor Receptor Bound Protein 2
GSEA	Gene set enrichement analysis
GSK3	Glycogen synthase kinase-3
GVHD	Graft versus host disease
H3K27me3	Histone 3 lysine 27 trimethylation
HDAC	Histone deacetylase
HEPES	4-(2-hydroxyethyl)-1-piperazineethanesulfonic acid
HS1-4/HS5-8	Dnase hypersensistive sites 1-4 and 5-8
HSC	Haematopoietic stem cell
ID3	DNA-binding protein inhibitor
Ig/IgM/IgG/IgA/IgE/IgD	Immunoglobulins and their isoforms
Igα/Igβ	Immunoglobulin subunits alpha and beta
IGCR1	Intergenic control region 1
IGF1	Insulin-like growth factor
IGF1R	Insulin-like growth factor receptor
IGFBP	Insulin-like growth factor binding protein
IgJ	Immunoglobulin J polypeptide
IL2Rα/CD25	Interleukin 2 receptor subunit alpha
IL7	Interleukin 7
IL7Ra	Interleukin 7 receptor subunit alpha
IMDM	Iscove's Modified Dulbecco's Medium
ImmGen	Immunological Genome Project
IR	Insulin receptor
IRF4/IRF8	Interferon regulatory factors 4 and 8
Irs1/2	Insulin receptor substrates 1 and 2
JAK	Janus kinase
JMJD3/KDM6B	Jumonji Domain Containing 3, Histone Lysine Demethylase
JMJD3i	JMJD3 small molecule inhibitor
KEGG	Kyoto Encyclopedia of Genes and Genomes
LepR	Leptin receptor
LFC	Log fold change
LNA	Locked nucleic acids

MHC	Major histocompatability complex
miRNA	Micro-RNA
mRNA	Messenger RNA
mt-DNA	Mitochondrial DNA
mTOR/mTORC1/mTORC2	Mammalian target of rapamycin complexes 1 and 2
MZ	Marginal zone B cells
ncRNA	noncoding RNA
NES	Normalised enrichment score
NGS	Next generation sequencing
NHEJ	Non-homologous end joining
NOM p-val	Nominal p-value
oligo-dT	Primer with an oligomer of T nucleotides
OPN	Osteopontin
ORF	Open reading frame
osx	Osterix
p38	P38 mitogen-activated protein kinases
PAIR	Pax5-Activated Intergenic Repeats
PCR	Polymerase chain reaction
PI3K	Phosphoinositide 3-kinase
pIC50	Negative log of the half maximal inhibitory concentration
PKB/AKT	Protein kinase B
PRC1/2	Polycomb repressive complexes 1 and 2
preBCR	Pre-B cell receptor
PTEN	Phosphatase and tensin homolog
RAG1/2	Recombination-activating gene
RISC	RNA-induced silencing complex
RNA	Ribonucleic acid
RNAseq	RNA sequencing
ROS	Reactive oxygen species
RPM	Reads per million reads
RSS	Recombination signal sequences
RT	Reverse transcription
RTK	Receptor tyrosine kinase
SASP	Senescence-associated secretory phenotype

SCF	Stem cell factor
sciRNAseq	Single-cell combinatorial-indexing RNA-sequencing
siRNA	Small interfering RNA
SJ	Signal joint
SLC	Surrogate light chain
Socs2	Suppressor of cytokine signaling 2
S-phase	Synthesis phase
SSC	Saline Sodium Citrate buffer
STAT	Signal transducer and activator of transcription
SYK	Spleen Associated Tyrosine Kinase
T1/T2/T3	Transitional 1-3 B cells
TCR	T cell receptor
TdT	Terminal deoxynucleotidyl transferase
TET	Ten-eleven translocation methylcytosine dioxygenases
TNFα	Tumor necrosis factor alpha
TSLP	Thymic stromal lymphopoietin
TSS	Transcription start site
μ/Mu	heavy chain Mu
UMAP	Uniform Manifold Approximation and Projection
UMI	Unique molecular identifier
UTR	Untranslated region
UTX/UTY	Ubiquitously transcribed tetratricopeptide repeat, X/Y chromosome
V-DJh	V-to-DJ recombination of the heavy chain loci
VDJseq	VDJ sequencing
$V_H/D_H/J_H$	V, D, and J gene segments of the heavy chain loci
Vkl/Jkl	V and J gene sements of the light chain loci (l and k)
WT	Wildtype
YY1	Yin And Yang 1

List of Appendices

1 INTRODUCTION

1.1 Adaptive immunity

Haematopoietic stem cells (HSC) have the potential to differentiate into a wide spectrum of functionally distinct immune cell lineages. These self-renewing cells asymmetrically divide and commit to either erythroid, myeloid or lymphoid progenitor cells, which themselves branch off to produce all the blood cells of the body. Immune cells in particular originate from the myeloid and lymphoid progenitors and predominantly form the innate and adaptive immune system respectively (Figure 1-1). The innate immune system acts as a non-specific first line of defence against pathogens and foreign particles, and consists of specialised phagocytic cells such as macrophages and dendritic cells (DC), granulocytes such as neutrophils, eosinophils and basophils, and T cell-like innate lymphoid cells (ILC) and natural killer cells (NK).

The adaptive immune system provides a more specialised, antigen-specific long-term immunity to a pathogen. The predominant lymphoid cells are B cells and T cells, whose antigen-specific immunoglobulin B cell receptor (BCR) and T cell receptor (TCR) are generated and fine-tuned throughout development, and govern the humoral response.

T cell development begins in the bone marrow, but generation of TCR via V(D)J recombination of the α and β chain loci (or the less common γ and δ chain loci), and

expression of the mutually exclusive CD4 or CD8 co-receptors, occurs in the thymus. T cells will bind via the TCR to processed antigen epitopes that are associated with major histocompatibility complexes (MHC) on the surface of antigen-presenting cells (such as dendritic cells or macrophages) for either a cytotoxic (CD8) or helper (CD4) T cellular response[1]. $CD4^+$ cells are themselves made up of functionally distinct groups of helper T cells. For example, $CD4^+$ Th1 cells can activate antigen-presenting macrophages upon secretion of IFNγ to facilitate their phagocytic and inflammatory immune functions[2]. In germinal centres, $CD4^+$ T follicular helper cells (Tfh) can activate B cells that have internalised a pathogen via a complementary BCR and expressed an epitope via MHC class II on its surface. Co-stimulation of these B cells with CD40L from Tfh cells induces clonal expansion and antibody class switching in secondary lymphoid organs[3]. Regulatory T cells (Tregs) are another subpopulation of $CD4^+$ T cells, classified also by their expression of the transcription factor FOXP3 (forkhead box P3), and are involved in immune modulation through, for example, the production of immunosuppressive cytokines IL10, IL35 and TGFβ[4]. $CD8^+$ T cells on the other hand are cytotoxic, and via MHC class I will function to kill cells that have been virally infected or present with abnormalities (such as cancer)[5,6].

Unlike T cells, most of B cell development occurs in the bone marrow. Immature B cells, with functioning BCR on their surface, migrate to secondary lymphoid tissues, such as the spleen or lymph nodes, to develop further into transitional, then mature naïve B cells[7,8,9]. Activation of B cells also occurs in secondary lymphoid organs such as lymph nodes upon antigen engagement, and can be T cell dependent (as described[10]) or independent[11]. Through clonal expansion, affinity maturation of BCR by somatic hypermutation, and antibody class switching, activated B cells differentiate into plasma

cells, secreting splice variants of their BCR into circulation as antibody[12]. While T cells are only able to respond to antigen via its TCR through epitopes on antigen presenting cells, antibodies are able to bind directly to its antigen and so work to neutralise or direct non-specific immunoinflammatory responses[3].

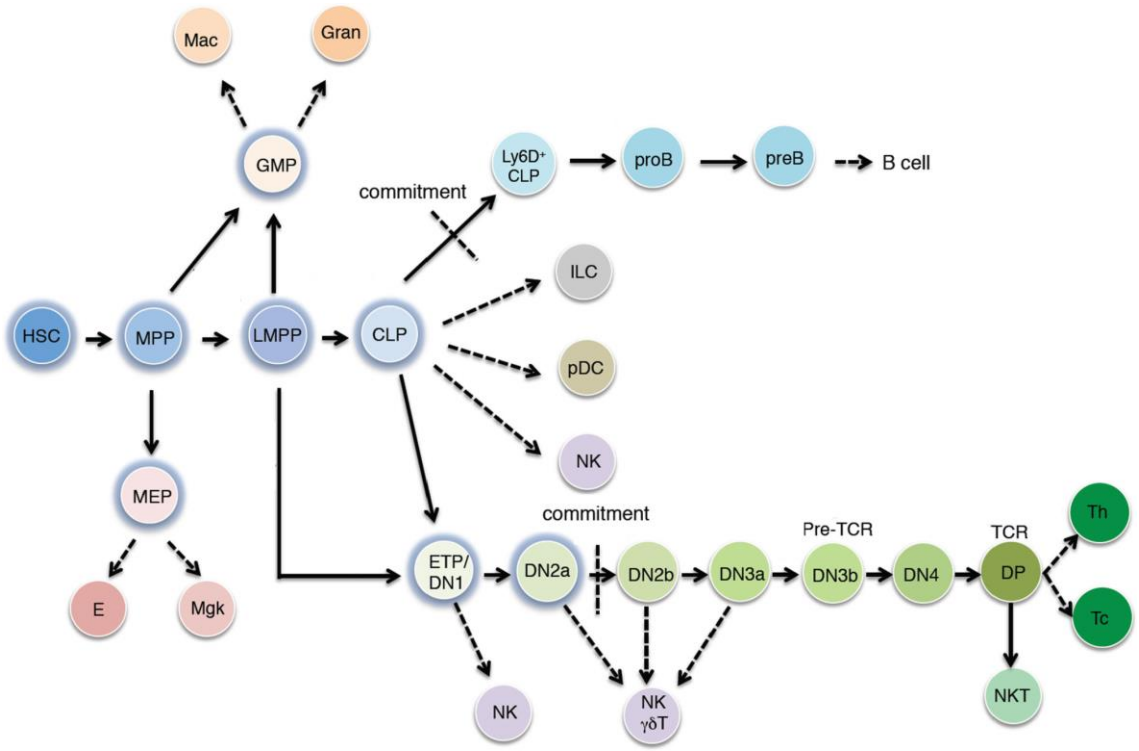

Figure 1-1: Generation of B cells by haematopoiesis. Haematopoietic stem cells (HSC) reside in the bone marrow and differentiate into all blood cells. Multipotent progenitor cells (MPP) can differentiate into either megakaryocyte-erythrocyte progenitors (MEP; erythrocytes E, megakaryocytes Mgk), granulocyte-macrophage progenitors (GMP; granulocytes Gran, macrophage Mac), or can be primed down the lymphoid lineage as lymphoid-primed multipotent progenitors (LMPP). Common lymphoid progenitors (CLP) can differentiate into natural killer cells (NK), dendritic cells (DC) and innate lymphoid cells (ILC) of the innate immune system, or T cells and B cells of the adaptive immune system. Early thymocyte progenitors (ETP) start out double-negative (DN) for CD4 and CD8 expression, but as they undertake thymocyte development, will undergo V(D)J recombination to produce their TCR, becoming double-positive (DP) for both CD4 and CD8, before committing to a single-positive $CD4^+$ T-helper (Th) or $CD8^+$ cytotoxic T cell (Tc). Conversely, B cell development occurs in the bone marrow, also undergoing V(D)J recombination to produce their immunoglobulin BCR. (Adapted from Miyazaki et al[13]).

1.2 The structure and isoforms of immunoglobulin

Immunoglobulins (antibodies) are members of the immunoglobulin superfamily that includes the TCR. They are heterodimeric proteins made up of two identical heavy chains and two identical light chains (Figure 1-2). Each chain has a unique variable region, which bind antigens for recognition, and a constant region, which can bind to Fc receptors or activate the complement cascade for a targeted immune response[14]. The constant region of immunoglobulin is C-terminal and determines the isotype, of which there are five: IgM, IgG, IgA, IgD and IgE. Each isotype has its own set of constant genes that can be expressed with variable regions to form an antibody of differing structures and functions[15]. The variable region is N-terminal and composed of moderately constant framework regions (FR) and hypervariable complementarity determining regions (CDR) that make the fragment antigen binding (FAB) site of the antibody. The 4 β sheets of heavy and light chain polypeptide are held together by disulphide bonds to form the classic Y-shaped immunoglobulin molecule[16,17].

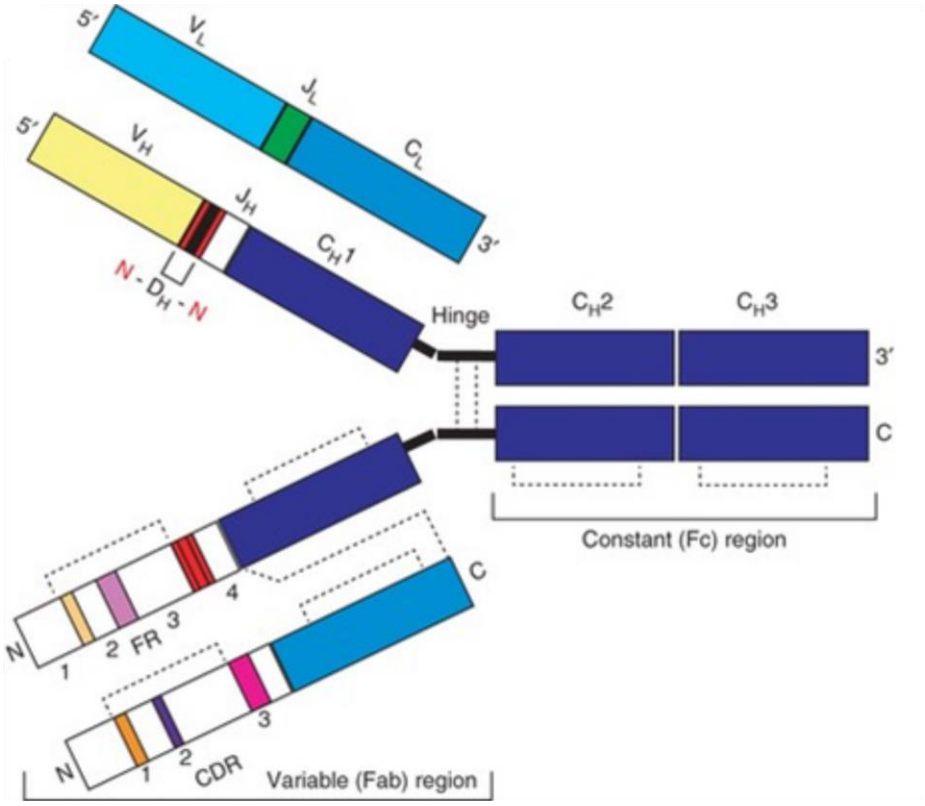

Figure 1-2: The structure of a typical immunoglobulin molecule (IgG). Immunoglobulin is composed of a heavy and light chain protein as the result of V(D)J recombination to produce the variable fragment antigen binding (Fab) and constant (Fc) portions, held together by disulphide binds. The Fab portion contains moderately constant regions (FR) and hypervariable regions (CDR). The Fc portion determines the immunoglobulin isotype, and can be IgM (default), IgG, IgA, IgD or IgE. (Schematic adapted from Schroeder and Cavacini[17]).

The genetic components of the heavy and light chains are located at the Ig_H and Ig_κ or Ig_λ loci respectively. The heavy chain variable region is composed of variable (V_H), diversity (D_H) and joining (J_H) gene segments, whilst the light chain is variable (V) and joining (J) only. During development, differentiating B cells will undergo V(D)J recombination of their germline Ig_H, then $Ig_{\kappa/\lambda}$ loci, in an attempt to productively align one V, (D), J and C gene segment and express a functioning BCR/immunoglobulin. The process of V(D)J recombination requires, among other enzymes in the recombination reaction, the Recombination-activating gene 1 and 2 (RAG1/2) recombinases for double-strand DNA (dsDNA) breakage, and the terminal deoxynucleotidyl transferase (TdT)

polymerase to add nucleotides at the break sites, thus directing non-homologous end joining (NHEJ) for the alignment of VDJ_H and $VJ_{\kappa/\lambda}$ genes. Splicing of VDJ_H-recombined primary mRNA transcripts in mature naïve B cells leads to their expression predominantly with constant region Mu for an IgM isotype immunoglobulin BCR. It is believed that alternative splicing events of this primary mRNA transcript also leads to the co-expression of IgD isotype BCRs with IgM found on naïve B cells prior to class switch recombination to any of the other immunoglobulin isotypes (IgG, IgA, IgE), which occurs in secondary lymphoid organs during T cell-dependent activation[18,19].

1.3 Early B cell development

Commitment of HSCs to the B cell lineage occurs in the bone marrow. The ultimate goal for B cells during these early stages of development is to successfully V(D)J recombine their Ig_H and Ig_κ/Ig_λ loci in an attempt to produce a functioning, non-autoreactive BCR. To achieve this, B cells pass through many stages, expressing a variety of unique surface and cytoplasmic markers, including RAG1/2, and must pass through several developmental checkpoints of positive or negative selection.

1.3.1 Bone marrow B cell subsets

Early progenitor B cell development can be broken down into distinct subpopulations based on their V(D)J recombination status and expression of different biomarkers. In mice, bone marrow B cells have been characterised by *Hardy et al* and *Rolink and Melchers*[8,20,21] as the Prepro-B (FrA), Pro-B (FrBC), Early/Large Pre-B (FrC'), Late/Small

Pre-B (FrD), Immature B (FrE), and Mature (recirculating) B (FrF) cell fractions (Figure 1-3). The pan-B cell marker B220 (CD45R) – an isoform of the pan-leukocyte marker CD45 – defines all B cells in the bone marrow, but it is co-expression of the cell adhesion molecule AA4.1 (CD93) that delineates the progenitor B cell niche.

Prepro-B cells (FrA) represent the earliest B lineage stage of development and can be characterised as $B220^{+}CD19^{-}CD43^{+}$. Their Ig_H and $Ig_{\kappa/\lambda}$ loci are still in the germline configuration, but are in the process of D-J_H recombination as they express RAG1/2.

Pro-B cells (FrB/C) develop from Prepro-B cells to express CD19, which is retained on all subsequent B cell subsets. Pro-B cells can be defined as $B220^{+}CD19^{+}CD43^{+}HSA^{low}$ (FrB being $BP1^{-}$ and FrC $BP1^{+}$). All Pro-B cells have DJ_H recombined both Ig_H alleles, and are in the process of V-DJ_H recombination through continued expression of RAG1/2.

Early Pre-B cells (FrC') can be defined as $B220^{+}CD19^{+}CD43^{low}HSA^{hi}$ and differ from FrC as they have completed V-DJ_H recombination and thus, if productive, will express heavy chain (μ/Mu) in the cytoplasm. Their $Ig_{\kappa/\lambda}$ loci are still in the germline configuration, so Mu protein will complex instead with a surrogate light chain protein (SLC) – comprised to two polypeptides λ5 and VpreB – to form the preBCR on their cell surface. Signalling via the preBCR induces a proliferative burst, which represses RAG1/2 expression and gives Early Pre-B cells their "large" cellular morphology.

Late Pre-B cells (FrD) have a characteristic "small" morphology due to their quiescent state, brought about by the progressive loss of SLC expression resulting in loss of preBCR signal. Exit from the cell cycle allows Late Pre-B cells to re-express RAG1/2 and engage the $Ig_{\kappa/\lambda}$ loci for V-$J_{\kappa/\lambda}$ recombination. Within the progenitor B cell niche, Late Pre-B cells are unique in their expression of the IL2Rα chain protein CD25, and so can be defined as $B220^{+}CD19^{+}CD25^{+}IgM^{-}$.

Immature B cells (FrE) represent the last progenitor B cell subset. Upon successful V-$J_{\kappa/\lambda}$ recombination, the light chain protein (κ or λ) product will complex with cytoplasmic heavy chain Mu and present on the surface of the progenitor B cell as BCR in the form of IgM. Immature B cells can be defined as $B220^{+}CD19^{+}CD25^{-}IgM^{+}$. Provided the BCR produced is not autoreactive, Immature B cells will then leave the bone marrow and migrate to secondary lymphoid organs – such as the spleen and lymph nodes – where they differentiate into mature naïve B cells, encounter antigen, and undergo isotype switching and somatic hypermutation[7,8,9].

Mature B cells (FrF) are also found in the bone marrow. These cells have recirculated back into the bone marrow from the periphery for storage. Mature B cells co-express IgM and IgD isoforms of their BCR and are not part of the progenitor B cell niche. As a result, Mature B cells in the bone marrow can be defined as $B220^{+}CD19^{+}AA4.1^{-}IgM^{+}IgD^{+}$.

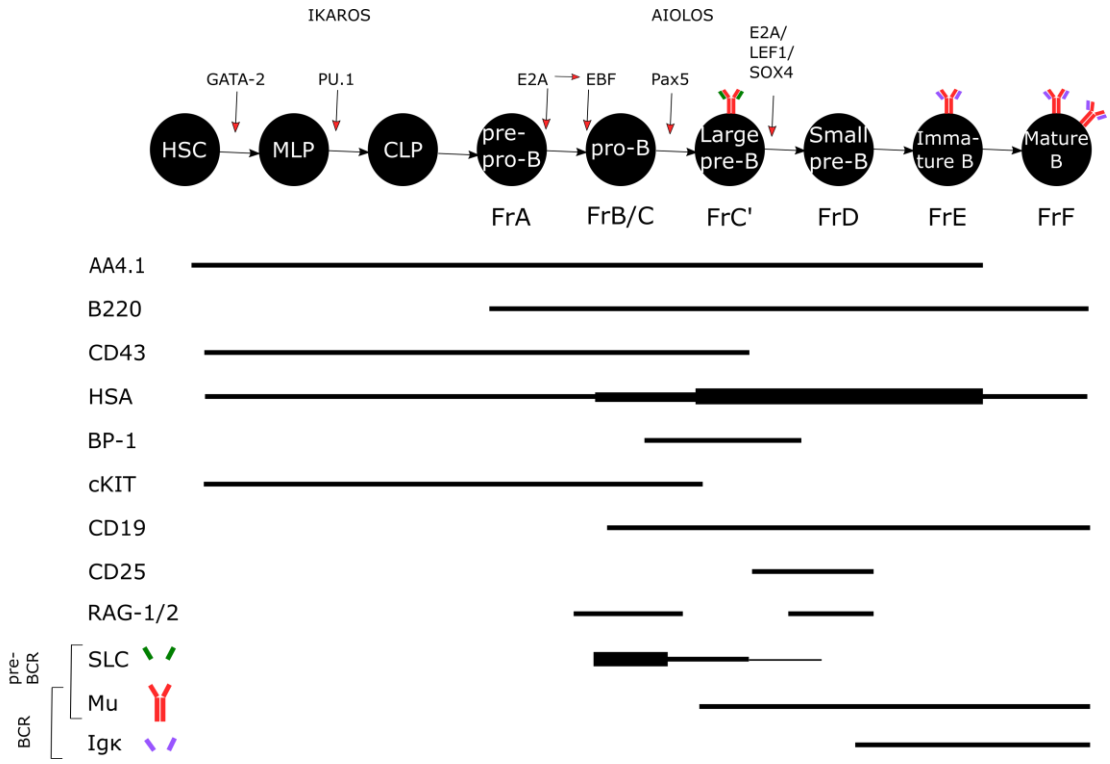

Figure 1-3: Early B cell development in the bone marrow. HSCs differentiate into multipotent multi lymphoid and common lymphoid progenitors (MLP and CLP) before committing down the B-lineage. B cells

in the bone marrow have been characterised in mice as "Hardy Fractions" (FrA-F), which correspond to their classical nomenclature of Prepro-B, Pre-B, Large/Early Pre-B, Small/Late Pre-B, Immature B, and Mature B cells. Expression of surface and cytoplasmic markers throughout development define each B cell subpopulation. Different transcription factors are expressed at each stage to direct the B cell intrinsic network towards a mature naïve B cell. (Schematic adapted from Hardy et al[22]).

1.3.2 Peripheral B cell subsets

Once immature B cells have developed in the bone marrow, they are trafficked to the spleen, during which they go through transitional stages (T1/T2/3) as a selection checkpoint for autoreactive BCR until they become mature naïve B cells[23,24]. In secondary lymphoid organs such as lymph nodes, naïve B cells are classified into follicular (FO) or marginal zone (MZ) B cells based on their position inside the tissue, fulfilling different immune functions. For example, FO B cells eventually become plasma cells that contribute high affinity antibodies or give rise to long-lived memory B cells[22,25], whereas MZ B cells have a more limited BCR repertoire that contributes to the clearance of blood-borne bacterial pathogens and cell debris[26].

The aforementioned B cell subsets constitute the classical B-2 B cell lineage, but there is also a rare B cell lineage known as B-1 (broken down into $CD5^+$ B-1a and $CD5^-$ B-1b cells) that is derived from foetal liver and form their own pool of self-renewing cells in the spleen and peritoneal cavity of adults[27,28]. They possess more autoreactive BCRs that are released as "natural antibody" and can be found in Peyer's Patches as they aid in mucosal homeostasis[28].

1.3.3 V(D)J recombination

The Ig_H locus in mice is ~3Mb in size and is located on chromosome 12, consisting of 195 V_H, 13 D_H, 4 J_H, and 8 C_H gene segments (Figure 1-4)[29]. Of the 195 V_H genes, 85 are pseudogenes with either non-functional Recombination Signal Sequences (RSS), no start codon, or an intergenic stop codon located in the open reading frame (ORF)[30]. V_H genes span 2.5Mb and are characterised into 16 evolutionarily conserved families based on sequence homology[30-31], which are geographically grouped into 3' proximal (e.g. V_H7183 and Q52), middle (e.g. V_HS107), and 5' distal (V_HJ558 and V_H3609) V_H genes.

There are 2 light chain loci: Igκ and Igλ – although the ratio of representation in mature murine B cells is 90-95% and 5-10% respectively[32]. Igκ is ~3.2Mb in size and located on chromosome 6, consisting of 140 $V_κ$, 5 $J_κ$, and 1 $C_κ$ gene segment(s). $Ig_λ$ on the other hand is only 250kb and on chromosome 16, with only 3 $V_λ$, 4 $J_λ$ and 4 $C_λ$ gene segments[33].

As a vital part of early B cell development, V(D)J recombination of these gene segments is achieved through non-homologous end joining (NHEJ), with the Ig_H locus recombining first in a sequential D-J_H, followed by V-DJ_H fashion[34]. Unique to lymphocytes and V(D)J recombination are RAG1/2 recombinase and TdT polymerase, which are key enzymes in this reaction. RAG1/2 are responsible for dsDNA breaks at recombination signal sequence (RSS) sites – DNA sequences consisting of conserved heptamer and nonamer sequences separated by either a 12bp or 23bp non-conserved spacer sequence – flanking each gene segment of the Ig loci. V_H and J_H genes are flanked by 23-RSS, and D_H genes are flanked by 12-RSS[35]. The significance of this being that RAG1/2 have an intrinsic preference to recombine 23-RSS flanked genes with 12-RSS flanked genes (known as the 12/23 rule). Therefore V_H and J_H genes cannot directly join, but rather join

through D_H genes, which can join both – thus achieving sequential VDJ_H recombination. Similarly, Vκ genes have 12-RSSs and Jκ genes have 23-RSSs to allow $VJ_κ$ recombination.

Cleavage of V, D, and J gene segments at their RSSs results in the formation of hairpin loops, which are opened for repair by the endonuclease Artemis (part of the DNA-dependent protein kinase complex). Depending on where the hairpin Is excised, Artemis will leave a palindromic "P" nucleotide overhang at the exposed 3' ends of the DNA, then the TdT polymerase adds more random "N" nucleotides. These 3' overhangs at the dsDNA strand ends subsequently anneal and ligate the ends together to leave repaired genomic DNA, with aligned gene segments and their newly-formed coding joint (CJ) sequence, along with either an inverted or excised sequence containing the signal joint (SJ) sequence. The repair process therefore results in additional junctional diversity to the diversity obtained from recombining different combinations of V, D, and J gene segments together. Consequently, the process of V(D)J recombination contributes to the estimated 10^{12} different possible immunoglobulin BCR variants that can be made per human B cell[36].

Recombination of the C_H gene segments does not take place at the same time as VDJ_H recombination, but instead later in development during isotype switching in secondary lymphoid organs upon antigen engagement. Therefore, Immature B cells express BCR in the form of IgM by default[37].

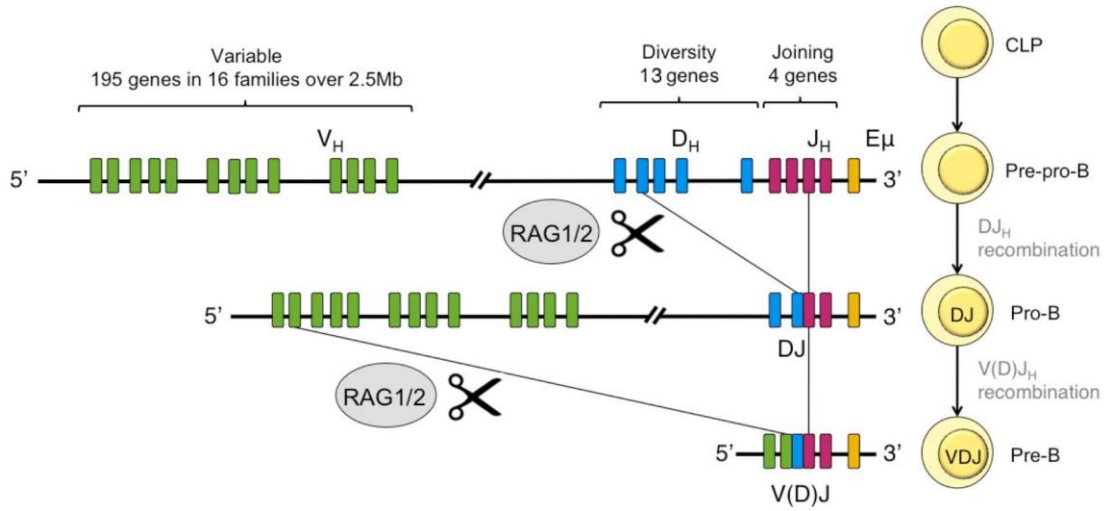

Figure 1-4: VDJ recombination of the Ig_H locus. During early B cell development, the Ig_H loci recombines sequentially, with D-J_H during Prepro-B to Pro-B followed by V-DJ_H during Pro-B to Pre-B cell stages. In mice, there are 195 V-genes, 13 D-genes, and 4 J-genes spread over the 3Mb locus. Recombination of these gene segments is achieved through NHEJ, whereby RAG1/2 induce dsDNA breaks at RSSs flanking V, D, and J gene segments. These gene segments are then joined together to form a productive VDJ_H gene that is expressed as heavy chain protein Mu. Antibody repertoire diversity is in large part down to the different VDJ_H gene segment combinations, as well as the junctional diversity acquired through the process of DNA repair by NHEJ.

1.3.4 Transcription factors

In response to external signals from the microenvironment, intrinsic signals are initiated within developing progenitor B cells by transcription factors. Transcription factors regulate the transcription of genes by binding to promoter or enhancer regions of DNA to influence transcription of associated genes. Key transcription factors therefore direct the tightly regulated stage-specific V(D)J recombination, the transcription programme of individual stages of B cell development, and ultimately production of immature B cells. B cells have several key transcription factors, the most important are shown in Figure 1-3, and described below.

IKAROS and AIOLOS

IKAROS is a zinc finger protein that is important from the HSC stage onwards, with pleiotropic effects throughout early B cell development, such as modulating chromatin accessibility over B-lineage genes by recruiting chromatin-remodelling factors such as histone deacetylases (HDAC)[38]. IKAROS has been shown to play an important role in the commitment of many stages of early B cell development. In Prepro-B cells, IKAROS upregulates the expression of Flt-3 and c-Kit – receptors required for B cell survival through interaction with nearby mesenchymal cells[39]. In Pro-B cells, expression of RAG1/2, TdT and the surrogate light chain (SLC) genes λ5 and VpreB are activated by IKAROS[40]. IKAROS also facilitates V-DJ_H recombination in Pro-B cells by compacting the Ig_H locus, bringing the gene segments spatially closer together for recombination[41]. When VDJ_H recombination has occurred, IKAROS can also recruit the unrecombined or non-functionally-recombined Ig_H loci to pericentromeric heterochromatin as part of allelic exclusion[42]. At later stages of B cell development, when heavy chain protein Mu has successfully complexed with SLC to form the pre-BCR on its surface, an alternate IKAROS family member, named AIOLOS, downregulates λ5 expression to progressively terminate the pre-BCR signal initiated by IKAROS[43].

PU.1

Like IKAROS, the transcription factor PU.1 regulates early stages of lymphocyte development. Levels of PU.1 determine the myeloid versus lymphoid lineage commitment: High levels of PU.1 direct HSC to differentiate into common myeloid progenitors (CMP) whereas low levels of PU.1 promote commitment to common lymphoid progenitors (CLP)[44]. During B lineage differentiation, PU.1 upregulates other transcription factors involved at later stages of development – namely EBF1 and Pax5 –

along with the IL7Rα gene[45,46]. PU.1 has also been shown to bind regulatory enhancer regions on the light chain loci to influence Ig_{κ} recombination[47,48].

E2A

Encoding 2 proteins, E12 and E47, the E2A transcription factor is involved in early Prepro-B cell development through targeted chromatin accessibility[49]. It has an implicit role in initiation of D-J_H recombination, as E2A knockout mice lack any recombination, whilst inducing expression of E2A with RAG1/2 in non-lymphoid cells can induce such rearrangements. E2A is also able to upregulate expression of early B lineage specification factor 1 (EBF1), and the 2 transcription factors then act together to regulate further stages of B cell development[50]. The functions of E2A act as an ultimate B lineage-committing stage, as loss of EBF1 and exposure to Notch1 signalling has been shown to divert lineage commitment away from B cells towards T cell development[51,52].

EBF1

Activation of EBF1 through the chromatin remodelling actions of E2A and the histone deubiquitinase MYSM1[53] also marks an important stage of B lineage commitment. As such, there are multiple positive feedback mechanisms involving EBF1. Firstly, EBF1 expression is governed by two promotors: one is activated by E2A, IL7R signalling and EBF1 itself; the other promotor is activated by PU.1 and Pax5[54]. Subsequent expression of EBF1 via E2A/PU.1 activation results in further activation of its own promotor both directly and indirectly. Indirect positive feedback is achieved through the activation of the two transcription factors FOXO1, which upregulates IL7Rα and Pax5 expression. Pax5 and EBF1 then regulate many of the same target genes to drive and maintain B cell differentiation. Knockout deficiencies in either Pax5 or EBF1 leads to B cells being unable to differentiate beyond the Prepro-B and Pro-B cell stages[55,56], whilst knockdown in B

lineage-committed B cells results in divergence down another haematopoietic lineage[57,58]. Therefore, EBF1 is important in B cell commitment, specification, and V(D)J recombination.

Pax5

Pax5 regulates nearly a third of all gene expression during differentiation from Common Lymphoid Progenitors (CLP) to Pro-B cells. It acts by both activating B lineage-specific genes, such as CD19, BLNK and FOXO1, whilst also inhibiting alternative lineage genes[59,60]. During V-DJ_H recombination, Pax5 binds to Pax5-activated intergenic repeat (PAIR) elements – found interspersed amongst the V_H gene segments – to facilitate V-DJ_H recombination[61].

LEF-1 and SOX-4

Lymphoid enhancer binding factor (LEF-1) and SRY-related HMG box 4 (SOX-4) are involved in B cell-proliferation and survival at the Pro-B and Pre-B cell stage of development. Inhibition studies show that these factors are not essential for B cell development, but loss of LEF-1 or SOX-4 results in reduced Pro-B and Pre-B cell numbers[62,63]. LEF-1 is known to contribute to the regulation of Wnt/β-catenin transcription, and it is this signalling pathway that increases proliferation and decreases apoptosis of early B-lineage cells[63].

1.3.5 Bone marrow niche

As murine HSCs develop into B cells in the bone marrow, they migrate from the endosteum (inner surface of a bone cavity) of the metaphysis (near the heads of long

bones) to sinusoid vessels in the diaphysis (shaft of long bones), encountering many microenvironment niches along the way that facilitate their differentiation[64,65]. The mesenchymal progenitors that make up these different supportive stromal cell niches are found in specific locations in the bone marrow. For example, multipotent $Sca1^{+}$ mesenchymal cells tend to associate with blood vessels in the diaphysis, whereas osteogenic $Sca1^{-}$ mesenchymal cells tend to associate with blood vessels in the metaphysis[66].

In their quiescent state, HSCs remain in tight association with the endosteum through signals such as osteopontin (OPN) from osteocytes and adrenergic signals from neurones. Endosteum-proximal peri-arteriolar $Sca1^{+}NG2^{+}Nestin^{+}$ mesenchymal cells provide long-term maintenance of these quiescent HSCs in this niche[67,68]. Haematopoietic progenitor cell commitment and progression down the B cell lineage has been shown to be dependent on factors such as interleukin-7 (IL7), C-X-C motif chemokine 12 (CXCL12), FMS-like tyrosine kinase 3 ligand (FLT3L), stem cell factor (SCF/c-kit), Receptor activator of nuclear factor kappa-B ligand (RANKL), and insulin-like growth factor-1 (IGF1)[69,70,71,72,73,74]. Exposure to these factors in different combinations at different developmental stages drives successful differentiation. FLT3L for example is required for Prepro-B cell development, and combined with IL7 drives greater commitment of the multipotent progenitors down the B cell lineage[72]. Dependency on IL7 and SCF is seen at the Pro-B cell stage[70,75], whilst RANKL and IGF1 are known to be important in Pre-B and Immature B cell development[73,74], although in the case of RANKL these effects may be indirect[76]. The chemokine CXCL12 provides a chemoattractant signal throughout development that can direct progenitor B cells to their different bone

marrow niches, such as CLPs towards IL7-producing stromal cells, or Pre-B cells away from IL7-producing stromal cells (Figure 1-5)[69,77,78].

There are many mesenchymal lineage cells that are known to produce these different factors to support B cell development. The most abundant morphology of these stromal cells in the bone marrow is that of a fibroblast reticular cell. In-vivo studies have shown that a subset of these reticular cells are abundant in CXCL12, and are therefore referred to as CXCL12-abundant reticular (CAR) cells[79]. Interestingly, IL7-producing stromal cells – such as $Lepr^{+}$ (Leptin receptor) reticular cells – tend to be positioned away from CXCL12-producing cells in the bone marrow and so generally represent a distinct stromal niche to CAR cells[79]. However recent studies would suggest that this distinction is somewhat overlapping, and that stromal niches constitute cells expressing both CXCL12 and IL7 at different intensities[80,81].

Although these CXCL12/IL7-producing stromal cell niches are themselves heterogeneous, one of the more defined mesenchymal lineage cells known to play a role in progenitor B cell development are osteoblasts. In-vivo and in-vitro studies have demonstrated the supportive role that osteoblasts play on B cell development, due in part to their expression of CXCL12, IGF1, and RANKL[67,73,82]. In particular, expression of IGF1 by osx^{+} osteoprogenitor cells, expressing the osterix transcription factor, is known to stimulate autocrine osteoblast formation and survival[83], whilst also promoting B cell development in-vitro by stimulating cytoplasmic μ expression[84]. Loss of osx^{+} cells or osx-specific deletion of IGF1 production in-vivo also results in impaired Pre-B cell development that can be restored with IGF1 injection[67]. It is therefore considered that dysregulation of osteogenesis has a direct impact on B cell development.

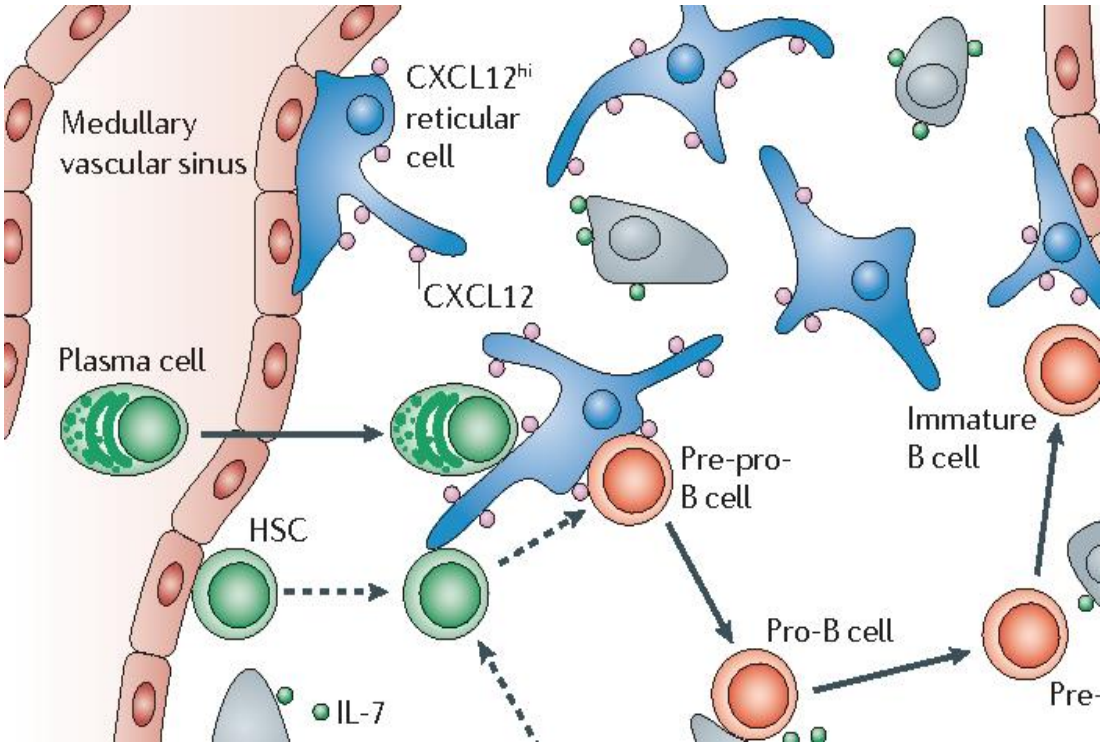

Figure 1-5: Bone marrow niche(s) facilitating B lymphopoiesis. HSCs reside in tight association with the endosteum in a quiescent state. As they differentiate into CLPs, they are attracted to CXCL12-expressing CAR cells and commit down the B-lineage to Prepro-B and Pro-B cells in the presence of IL7. As they differentiate into Pre-B cells, are drawn away from IL7 by means of CXCL12 homing to allow differentiation to immature B cells, which then leave the bone marrow and enter circulation destined for the spleen. (A simplified schematic, taken from Takashi Nagasawa et al[85]).

1.3.6 Selection checkpoints

In order for progenitor B cells to progress in these niches, they must pass through their own intrinsic selection checkpoints. During Prepro-B and Pro-B cell stages of development, both Ig_H alleles undergo D-J_H recombination. However in order for B cells to express just one heavy chain, V-DJ_H recombination occurs on one allele first, with recombination on the other allele only occurring if the VDJ_H product of the first allele is non-productive or unable to form a preBCR with SLC. Allelic exclusion of the unwanted allele is achieved through recruitment of ataxiatelangiectasia mutated (ATM) – a

serine/threonine protein kinase that is recruited to the RAG-induced dsDNA breakage to initiate a signalling cascade which relocates the second allele to pericentromeric heterochromatin region[86]. Additionally, the repressed Ig_H allele has been shown to decontract, which prevents recombination by keeping the V gene segments spatially apart from the DJ_H gene segment on the locus[87]. Allelic exclusion is pre-determined by the asynchronous replication of each allele, with the allele replicating first being the allele that recombines first[88].

When V-DJ_H recombination at the Pro-B cell stage has been achieved on this first Ig_H allele, the pro-B cell must produce a productive heavy chain that can complex with SLC. However, it has been modelled that only one in three recombination events are productive[89]. The remaining unsuccessful events will have recombined with a pseudo-V_H gene, or the process of recombination has introduced sequence or frame shift mutations, resulting in premature stop codons or a shift in the ORF that ultimately produces a non-productive VDJ_H gene. In this scenario, the Pro-B cell has another opportunity to V-DJ_H recombine the second Ig_H allele. To progress through this selection checkpoint, the Pro-B cell must be able to express preBCR on its surface and initiate its Pre-B cell-associated downstream signals. Therefore, productive VDJ_H Pro-B cells are positively selected, whereas non-productive VDJ_H cells are negatively selected[90,91].

Affinity for SLC to complex with heavy chain varies depending the V_H gene used. For example, the 3' D-proximal V_H gene 81X is preferentially recombined in Pro-B cells, however due to its weaker affinity for SLC this V_H gene loses its representation in the overall VDJ_H repertoire by the Pre-B cell stage. Thus, the repertoire diversifies through negative selection of certain V_H genes used, such as 81X[92].

Light chain recombination must also be productive in order to complex with cytoplasmic Mu. Therefore, successive non-productive Ig_{κ}/Ig_{λ} recombination events will lead to negative selection of Pre-B cells at this stage, whereas BCR production positively selects for immature B cells. Immature B cells with autoreactive BCR products also undergo further receptor editing during their transitional (T1/T2) stages towards a mature B cell, but only 10% of Immature B cells survive this selection process[93,94,95].

1.4 Key signalling pathways

It is evident that successful differentiation of progenitor B cells in their bone marrow niche(s) is reliant on a combination of extrinsic signals that induce a cell intrinsic network of transcription factors and specialised enzymes (such as RAG1/2) which drive V(D)J recombination and subsequent production of the BCR, in addition to signals for survival and proliferation. For coordinated progression, progenitor B cells depend on temporal signalling from a combination of surface receptors with overlapping downstream pathway activation.

1.4.1 Interleukin 7 receptor signalling

IL7 Receptor (IL7R) signalling in mice is an essential pathway for B cell development and is considered a master regulator of Pro-B cell proliferation and differentiation in mice. The IL7 receptor is a heterodimer of an IL7-binding IL7Rα chain and the common-γ chain (shared with other receptor complexes, such as IL2R)[96,97]. Upon binding of IL7, intracellular domains of both IL7Rα and cγ engage several downstream signalling

cascades – most notably in B cells the Janus kinase/signal transducers and activators of transcription (JAK/STAT)[98,99], phosphoinositide 3 kinase (PI3K)/AKT[99,100], and phospholipase-Cγ/Diacylglycerol (PLCγ/DAG)[99,101] pathways (Figure 1-6). Together, these signalling pathways drive progenitor B cell development by supporting proliferation, survival, differentiation, and Ig_H recombination. This is made evident from knockout studies of the IL7Rα chain leading to a near complete block in B cell development at the CLP stage, with the small number of cells that do progress to the Pro B cell stage displaying severely limited D-J_H and V-DJ_H gene usage and repertoire diversity[102,102,103] (*Baizan-Edge et al*, submitted work from the Corocoran lab). In support of this, STAT5a and STAT5b deficient mice have a developmental block at the Prepro-B cell stage[104,105], and deletion of the p110α and p110δ catalytic subunits of PI3K leads to a block at the Pro-B cell stage[106].

B cell differentiation by IL7R signalling is sustained through STAT5-mediated upregulation of B-lineage transcription factors (such as EBF and Pax5) [102,106]. Regulation of progenitor B cell proliferation by IL7R is shared between PI3K and STAT5 signalling, via upregulation of cell cycle proteins such as Cyclin D3[99,107]. PI3K and STAT5 also share in the survival role for progenitor B cells through IL7R signalling, with PI3K suppressing pro-apoptotic factors (such as BAD and BIM)[108] and STAT5 activating anti-apoptotic factors (such as BCL2 and MCL1)[109,110]. IL7R signalling has also been shown to support cell metabolism pathways through mTOR/mTORC1 signalling, and this is thought to occur through the shared signalling of PI3K/AKT and PLCγ/DAG[111,112].

While on the one hand supporting Ig_H recombination, IL7R signalling is also known to actively suppress premature $Ig_κ$ recombination. This is achieved both through the act of proliferation, but also through STAT5/Polycomb-mediated H3K27me3 histone

suppression of the Ig_{κ} locus during Pro-B cell development[113]. Therefore, in order for progenitor B cells to undergo $Ig_{\kappa/\lambda}$ recombination, they must escape IL7R signalling.

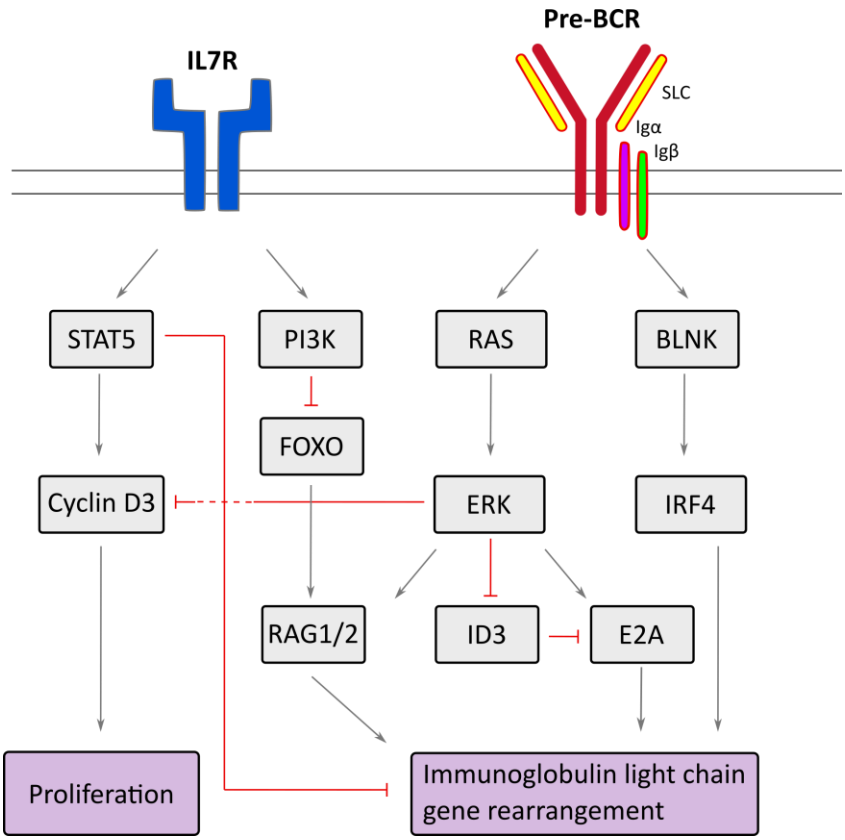

Figure 1-6: IL7R/preBCR signalling and interplay in early B cell development. IL7R signalling is important in driving commitment of CLPs down the B-lineage. Downstream signalling pathways – in particular JAK/STAT5, PI3K/AKT (and PLCγ/DAG) – facilitate cell proliferation and Ig_H recombination, whilst suppressing Ig_{κ} recombination. preBCR signalling replaces IL7R signalling to allow Ig_{κ} recombination (see Figure 1-7 for more detail). (Adapted from Clark et al[114]).

1.4.2 Pre-B cell receptor signalling

Successful VDJ_H recombination and complexing of heavy chain protein Mu with SLC (composed of VpreB and λ5 subunits) on the cell surface of a Pre-B cell leads to preBCR formation (Figure 1-6 and Figure 1-7)[115]. Combined with the Igα/β heterodimer subunit, preBCR signalling is initiated. Progenitor B cells must be able to express the preBCR in

order to progress, as knockout of Igα and Igβ block cells at the Pro-B cell stage[116]. Similarly, knockout of RAG1/2 – and thus inability to recombine the Ig_H locus – also blocks cells at the Pro-B cell stage[117], but transgenic BCR expression in RAG1/2-deficient B cells can bypass this inefficiency[118,119]. As well as acting as a checkpoint for successful Ig_H recombination, so too does preBCR signalling select for self-tolerant BCRs, since knockout of the SLC leads to an increase in autoreactive BCR progression[120,121].

preBCR signalling coordinates temporally first with IL7R via PI3K/AKT to induce a proliferative burst at the Early "large" Pre-B cell stage[122,123]. However once preBCR signalling via the Spleen Tyrosine Kinase (SYK) and B Cell Linker (BLNK, also known as SLP-65) adaptor proteins is established, this IL7R/preBCR driven PI3K/AKT pathway is suppressed[123,124]. In doing so, B-lineage transcription factors such as FOXO1, Pax5, IKAROS and AIOLOS can be re-expressed, acting to both feed-forward the expression of SYK/BLNK and interferon-regulatory factors 4 and 8 (IRF4/IRF8), as well as re-express RAG1/2 for $Ig_{\kappa/\lambda}$ recombination[123,125]. IKAROS and AIOLOS enable further cell cycle repression by suppressing PI3K/AKT-induced MYC and Cyclin D3 (via p27 expression)[126]. Meanwhile, IRF4 and IRF8 signalling facilitate Ig_κ recombination through downregulation of the SLC to progressively dampen the preBCR signal[125,127]. Further signals enabling Igκ recombination are provided by the preBCR through RAS/ERK (extracellular signal-regulated kinases) signalling, via the Growth-factor-receptor-bound protein-2 (Grb2) adaptor, which works to reactivate the transcription factor E2A, whilst at the same time supressing its inhibitor ID3[124]. Both E2A and IRF4/IRF8 are able to bind to Ig_κ enhancers, thus facilitating Ig_κ recombination directly[124,128].

It is therefore the role of the preBCR to first synergise with IL7R via PI3K/AKT to drive the Early Pre-B cell proliferative burst, but then also through SYK/BLNK signalling to both

suppress PI3K/AKT and activate Ig_{κ} recombination (with the help of RAS/ERK). In support of this, deficiencies in SYK or BLNK result in a block in early B cell development[129,130].

1.4.3 C-X-C chemokine receptor type 4 signalling

As the IL7R is considered a master regulator for Pro-B cell proliferation and differentiation, so C-X-C chemokine Receptor Type 4 (CXCR4) is considered a master regulator for the retention of progenitor B cells in the bone marrow, and for their trafficking between different stromal niches. Deficiencies in CXCR4 lead to reductions in Pro-B and Pre-B cells in the bone marrow, and subsequent increased numbers in blood circulation[131].

CXCR4 has seven transmembrane regions that bind the chemokine CXCL12 (Figure 1-7). Compartmentalisation of bone marrow stromal niches into high IL7-expressing and high CXCL12-expressing stromal cells allows preBCR-expressing Pre-B cells to migrate away from high IL7 concentrations to facilitate the temporal transition in receptor signalling dependencies[79,80,81]. Given that IL7R signals can override preBCR signals[77,78,113] , and that preBCR-mediated IRF4 activation leads to increased CXCR4 expression[77], suggests that Pre-B cells signal via CXCR4 as they progress through this stage of development, perhaps as a means of migration away from IL7 concentrations. Moreover, a recent study has implicated CXCR4 signalling not only in progenitor B cell homing, but also in a more direct role in Pre-B cell differentiation and Ig_{κ} recombination, by synergising with the preBCR signal. It has been suggested that signalling by CXCR4 acts as a feed-forward activator of IRF4 along with the preBCR, as well as activating NFκB to facilitate $Ig_{\kappa/\lambda}$ recombination[77]. Another feed-forward mechanism for CXCR4 can be found in its

induced expression of the Bromodomain and WD Repeat Domain Containing 1 (BRWD1), which mediates chromatin accessibility at the Ig_{κ} locus[132]. Loss therefore of the IL7R-induced suppression of the Ig_{κ} locus through H3K27me3 – a suppressive histone mark that prevents BRWD1 binding – leads to greater Ig_{κ} accessibility for RAG1/2[113]. Indeed, CXCR4 deficient Late Pre-B cells had reduced Ig_{κ} recombination and a skew in V_{κ} gene usage in-vivo[77].

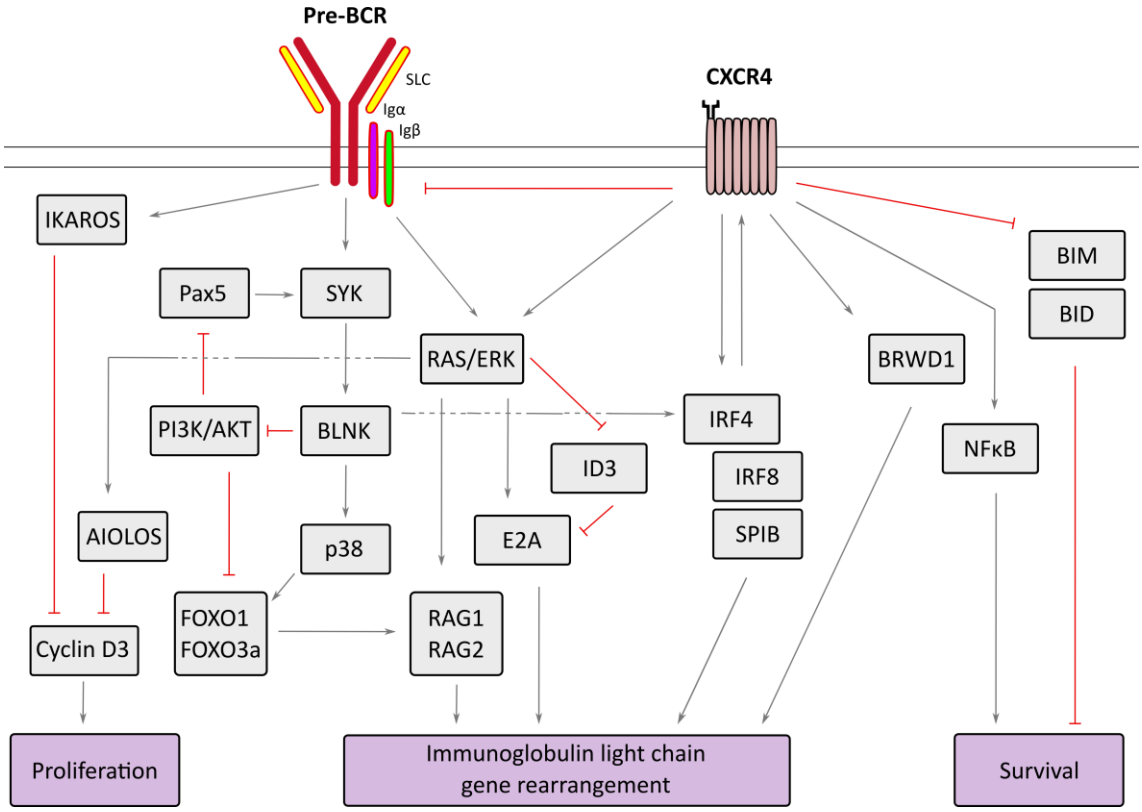

Figure 1-7: preBCR/CXCR4 signalling and interplay in early B cell development. preBCR signalling initially coordinates with IL7R via PI3K/AKT to induce a Pre-B cell proliferative burst. Establishment of SYK/BLNK and RAS/ERK arms of preBCR signalling suppress PI3K and cell proliferation, allowing B-lineage transcription factors such as PAX5, IKAROS, AIOLOS, E2A, and RAG1/2 to be (re)expressed and Ig_{κ} recombination to occur. CXCR4 signalling acts not only as a chemokine for cell homing, but also as a feed-forward mechanism to facilitate preBCR signalling via IRF4, RAS/ERK, and NFκB for B cell survival and Ig_{κ} recombination. (Adapted from Mandal et al[77]).

1.4.4 Insulin-like growth factor receptor signalling

In collaboration with IL7R, preBCR, and CXCR4, there is growing evidence to suggest that signalling via Insulin-like Growth Factor 1 Receptor (IGF1R) also has an influential role in progenitor B cell development. In mice, this role seems to be at the Pro-B and Pre-B cell stages. Early studies demonstrated that IGF1 has a synergistic effect on proliferation of in-vitro derived progenitor B cells in response to IL7[133,134], and promotes ex-vivo derived Pro-B cells to express cytoplasmic Mu when cultured on the IGF1-producing S17 stromal cell line[84]. In-vivo studies have shown that ablation of osx^+ osteoblasts, or targeted ablation of IGF1 expression from osx^+ osteoblasts, leads to a block at the Pro-B cell stage, that strikingly can be rescued upon IGF1 injection into these osteoblast-depleted mice[67].

The IGF1R is a receptor tyrosine kinase (RTK) protein composed of two extracellular α-subunits and two transmembrane β-subunits with intracellular domains, which complex together to form a tetrameric IGF1R[135]. Together with the Insulin Receptor (IR), the IGF1R has been extensively studied due to its central role in cell growth and metabolism (Figure 1-8). These two RTKs work in an endocrine paradigm with one another that is evolutionarily conserved, using the same downstream signalling components to transduce their complementary signals. In fact, their relationship is so intimate that IR and IGF1R subunits can heterodimersise to form a functioning hybrid receptor, and that at much lower affinities IGF1/Insulin can bind to and activate IR/IGF1R respectively (approximately 100X lower)[135,136]. In mammals, Insulin signalling via IR regulates cellular glucose homeostasis by initiating glucose uptake[137,138], whilst IGF1 signalling via IGF1R drives cell growth in the presence of sufficient glucose uptake[139]. Both receptors have downstream effects on metabolic pathways[140,141,142]. Most of the circulating IGF1 is produced by hepatocytes in response to Growth Hormone (GH)[143,144], but tissues

including the bone marrow are known to produce it locally[145,146,147]. In these extracellular environments, IGF1 is rarely found in a free form, but rather is in complex with one of six known IGF Binding Proteins (IGFBP1-6) that extend half-life or alter its binding to IGF1R[148]. For example, in the context of B cell development, through binding IGF1, IGFBP3 has been found to inhibit human Pro-B cell development in-vitro, whilst IGFBP6 is in fact required for Pro-B cell development[149].

Upon binding of IGF1 to IGF1R, key adaptor proteins Insulin Receptor Substrate 1/2 (Irs1/2) and Grb2 are activated to predominantly drive PI3K/AKT and RAS/ERK signalling respectively[140,150,151]. IGF1 is able to drive cell proliferation through both of these pathways, but it is through AKT/mTOR signalling that cell growth, protein synthesis, and an increase in glucose metabolism is predominantly instigated[152]. IGF1R knock-out in mice leads to premature neonatal death[153,154] and conditional knockout studies of IGF1R in the B-lineage have yet to be explored. A study with the approach of reconstituting sub-lethally irradiated $RAG2^{-/-}$ mice with $IGF1R^{-/-}$ foetal liver cells reported no defects in B cell development in the bone marrow of these mice[155]. However, as already mentioned, B-lineage deletion of the p110α and p110δ catalytic subunits of PI3K downstream of IGF1R (though, not the only receptor to utilise this pathway) results in a block in development at the Pro-B cell stage. More specifically to mTOR signalling, targeted disruption of the mTORC1 complex in the B-lineage also results in a comparable block at the Pro-B cell stage[156], thus demonstrating the precise role of PI3K/AKT/mTOR signalling in early B cell development. In addition to this, equivalent disruption of the mTORC1 complex in osx^{+} osteoblasts results in a similar deficiency in Pro-B and Pre-B cells, further emphasising the intimate relationship these two cell lineages share[157].

Although not fully understood, it is postulated that IGF1R signalling contributes to normal progenitor B cell development. Given that there is considerable overlap in downstream pathway utilisation with IL7R, preBCR, and CXCR4, one could speculate that an ever-present IGF1R signal throughout development could provide a sustained metabolic and biosynthetic signal that is required for these high-energy processes – such as proliferation, Ig recombination, and production of subsequent heavy and light chain protein. Shared regulatory mechanisms – such as Phosphatase and tensin homolog (PTEN) to suppress PI3K, and Suppressor of cytokine signalling 2 (SOCS2) for STAT5 and IGF1R inhibition – also point to a shared functional purpose of these different receptors in early B cells[158,159].

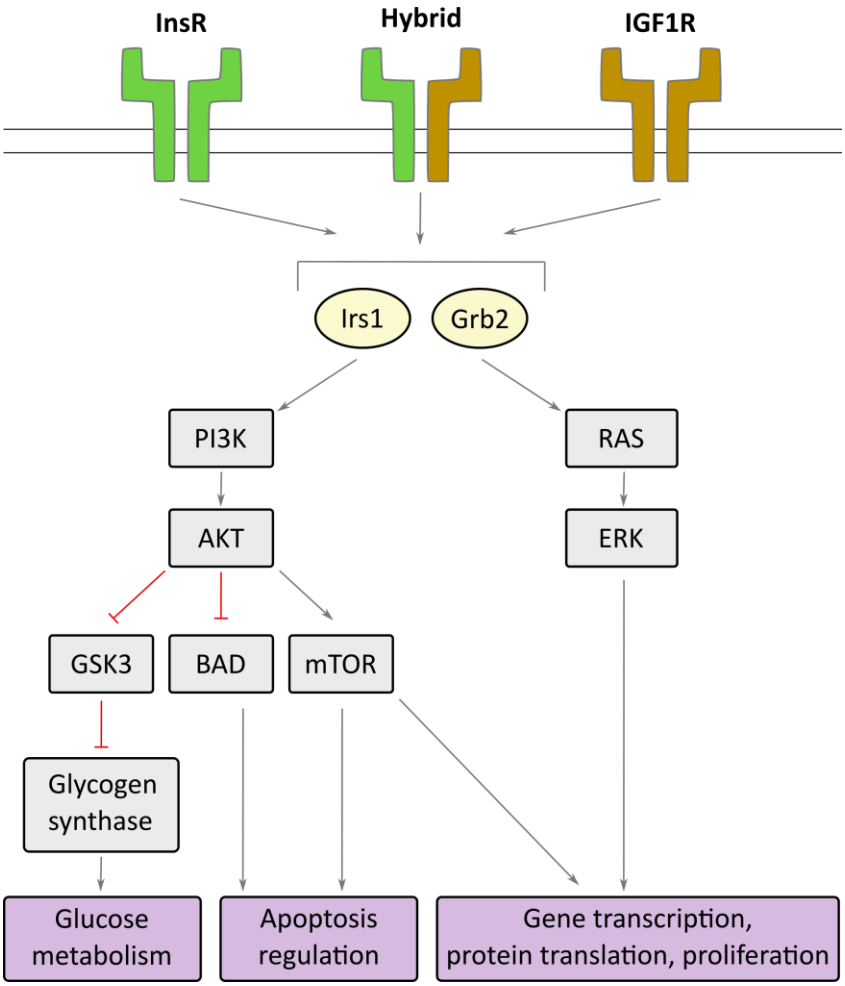

Figure 1-8: IGF1R signalling. The receptors for IGF1 and Insulin are evolutionarily conserved and share striking homology. As such, they share downstream signalling pathways and their receptors can heterodimerise. Through its adaptor proteins Irs1 and Grb2, IGF1R (and IR) activates the PI3K/AKT/mTOR and RAS/ERK pathways respectively to drive metabolism, growth, and survival signals. (Adapted from Huffman et al[160] and Tao et al[161]).

1.5 Epigenetics of early B cell development

1.5.1 Regulation of transcription

Expression of B-lineage genes and transcription factors required for early B cell development is regulated by several epigenetic mechanisms in order to maintain B-lineage commitment.

Histone Modifications

Predominant histone modifications associated with developing B cells are H3K4 (Histone 3, Lysine 4) and H3K27 methylation (Histone 3, Lysine 27). H3K4me1-3 are enriched over actively-transcribing genes, with H3K4me1 marking enhancers, H3K4me2 the 5' ends of genes, and H3K4me3 the gene's promoter[162,163]. Many methyltransferases and demethylases activate H3K4 methylation – such as the SET1A/B and Mixed-lineage leukemia (MLL) 1-3 methyltransferases, and the Lysine-specific histone demethylases (LSD) 1-2 and Jumonji AT-rich interactive domain-1 (JARID1) A-D demethylases[164,165,166]. In B cells for example, H3K4me1 has been shown to mark B-lineage specific genes, such as CD19, throughout their development[162], whilst EBF and FOXO1 facilitate the enrichment of H3K4me3 over the promotor of genes such as Pax5[163,167].

In opposition to H3K4 methylation, H3K27 methylation is a suppressive chromatin mark that can be found over both the promoter and body of the gene sequence itself[168,169]. In some circumstances, a gene locus can be bivalently marked with both active H3K4me3 and suppressive H3K27me3 as a "primed" expression state[168,169]. Trimethylation of H3K27 (H3K27me3) is mediated by the Polycomb repressive complex 2 (PRC2), which then recruits PRC1 for heterochromatic compaction of the target gene[170]. PRC2 is a multi-subunit complex, which contains a H3K27 methyltransferase subunit known as Enhancer-of-zest Homolog 2 (EZH2) to deposit the suppressive histone mark H3K27me3. Known H3K27 demethylases on the other hand include UTX/UTY (Ubiquitously transcribed tetratricopeptide repeat on chromosome X/Y) and Jumonji domain-containing protein D3 (JMJD3)[167].

As progenitor B cells develop, actively-transcribing genes will present with H3K4me3 and actively-suppressed genes will present with H3K27me3, and primed genes will present

with both H3K4me3 and H3K27me3[167,169]. In addition, H3K27me3 is also associated with the silencing of microRNA (miRNA) during lymphopoiesis in order to suppress lineage multipotency and drive commitment[171].

miRNA

miRNAs are small noncoding RNAs that, in their mature spliced form, have been shown to anneal to 3' Untranslated Region (UTR) of complimentary mRNA strands[172]. The binding of miRNA to its cognate mRNA results in its instability and/or inhibited translation. Thus, miRNAs function to regulate gene expression post-transcriptionally. In order to function however, pre-miRNA must first be spliced into its mature miRNA form by the RNase endoribonuclease DICER, then associate with the RNA-induced silencing complex (RISC)[173].

In mice, there are approximately 100 miRNAs expressed in the cells of bone marrow[174], and for progenitor B cells, these miRNAs help to drive lineage commitment and B cell maturation. Blocking pre-miRNA splicing by knockout of DICER in B-lineage cells leads to a block at the Pro-B cell stage[175]. More specifically, progenitor B cells differentially express miR-34a – which targets FOXP1 – during development. Like FOXO1, FOXP1 has been shown to upregulate RAG1/2 expression, and constitutive expression of miR-34a leads to a developmental block at the Pro-B cell stage[176]. Moreover, knockout of miR-17-92 – which targets PTEN – in developing B cells also results in a block at the Pro-B cell stage[177].

DNA Methylation

Methylation of DNA impacts on gene expression, and occurs at CpG sites throughout the genome. Dynamic regulation of DNA methylation is therefore observed throughout a

stem cell's development to its terminal differentiated cell state, as the switching on and off specific genes determines its identity[178]. DNA methyltransferases (DNMT) are responsible for methylating DNA, including of the daughter strands of DNA during each cell division[178,179], whilst demethylation occurs through a process of base excision repair via enzymes such as ten-eleven translocation methylcytosine dioxygenases (TET enzymes) and thymidine DNA gycosylase (TDG)[180]. Gene suppression in HSCs by DNA methylation at CpG sites must be selectively demethylated to allow gene expression as they commit down the B-lineage. For example, EBF facilitates chromatin remodelling and DNA demethylation of the gene coding for Igα (Mb1) – a subunit of the BCR – such that its expression can be induced by Pax5[181]. Consequently, progenitor B cells of EBF-deficient mice retain a hypermethylated Mb1 promoter[181,182].

1.5.2 Regulation of V(D)J recombination

Within the Ig_H and $Ig_{\kappa/\lambda}$ loci, there are many well-defined regulatory elements. They, along with epigenetic modifications, regulate V(D)J recombination through nuclear positioning and locus accessibility, and will be discussed further in this section.

Intronic Enhancer Eμ

Transcriptional enhancer elements within the Ig_H loci target gene segments for VDJ_H recombination. One of the first-described and best-studied Ig_H enhancer is the intronic enhancer Eμ, located in the intronic region 2kb downstream of J_H and upstream of C_H gene segments[183] (Figure 1-9). In lymphocytes, Eμ contributes to the relocation of sequestered Ig_H locus at the nuclear periphery to the active inner regions of the nucleus

via the 3' end[184,185]. Thus, the initial retained positioning of 5' V gene segments at the heterochromatic periphery in Pro-B cells is thought to contribute to the recombination of the 3'D and J gene segments prior to V gene recombination[184]. The Eμ DNA sequence contains DNA binding sites for many transcription factors, including EBF and Yin-Yang-1 (YY1), which facilitate in locus contraction, and deletion of Eμ leads to impairment of VDJ_H recombination and subsequent production of heavy chain[186,187]. Similar elements are found in the Igκ locus. Deletion of enhancers MiEκ and E3' for example leads to partial impairment in $VJ_κ$ recombination[188,189].

Intergenic control region 1

Located 2kb upstream of the D_H gene segments is the insulator intergenic control region 1 (IGCR1). Thus the D_H and J_H genes are flanked by the IGCR1 insulator and Eμ enhancer, with the V_H genes located separately 5' upstream of IGCR1[190] (Figure 1-9). The IGCR1 sequence contains DNA binding sites for the architectural and transcriptional repressor protein CCCTC binding factor (CTCF), known as CTCF binding elements (CBE). When CTCF binds to IGCR1, it restricts Eμ enhancer interactions to within the 3' region downstream of IGCR1 on the Ig_H locus[191]. Mutation of these CBE's leads to premature V_H-DJ_H recombination[192,193]. Similar elements are found in the Igκ locus. Deletion of the Igκ Sis silencer biases recombination in favour of Vκ genes that are more proximal to Jκ genes[194].

3' Regulatory region and CBE's

The 3' regulatory region (3'RR), as its name suggests, marks the 3' boundary of the Ig_H locus and serves as both an enhancer and architectural domain (Figure 1-9). It is made up of four DNase hypersensitivity sites (HS1-4) and is mostly involved in mature B cell functions such as CSR[195].

Further downstream of 3'RR are a cluster of CBE's defined by more hypersensitive sites (HS5-8)[196]. These CBE's allow CTCF to form insulator interactions with IGCR1 during D_H-J_H recombination, and binding sites for YY1 and cohesin proteins such as Rad21 implicate a structural complex that facilitates Ig_H DNA looping necessary for VDJ_H recombination[191,197].

Pax5-activated intergenic repeat elements

At the other end of the Ig_H loci, associated with the 5' distal V_H gene segments of the J558-interspersed 3609 family are 14 Pax5-activated intergenic repeat (PAIR) elements (Figure 1-9). Binding of Pax5 to PAIR elements during the Pro-B cell stage of development leads to antisense non-coding RNA transcription and compaction of the 2.5Mb V_H gene portion during V-DJ_H recombination. Thus, knockout of Pax5 in Pro-B cells leads decompaction of the 5' distal V_H gene segments and subsequent proximal V_H gene recombination bias[61]. Pax5 has also been shown to recruit RAG1/2 to its associated V-genes to facilitate V-DJ_H recombination[198].

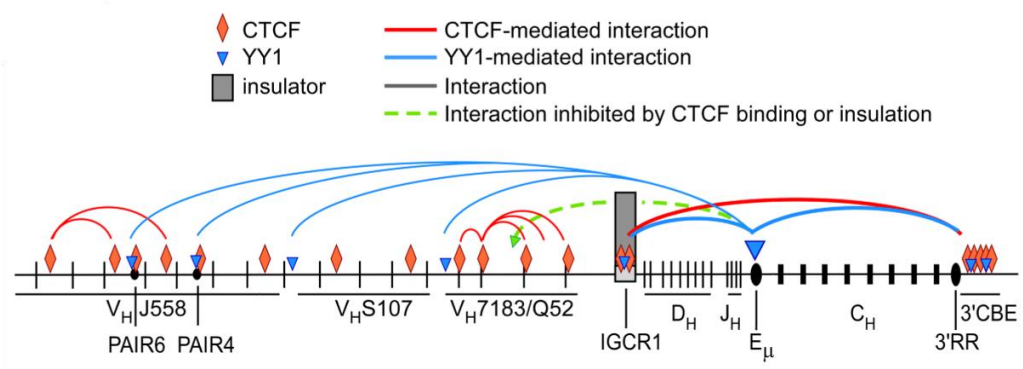

Figure 1-9: The Ig_H locus and its regulatory elements. Schematic representation of the Ig_H locus demonstrating how key regulatory elements (Eμ, IGCR1, 3'RR, 3'CBE, and PAIR elements) interact with the Ig_H locus via transcription factors (such as CTCF and YY1) to regulate VDJ_H recombination. When CTCF binds to IGCR1 during early B cell development, it insulates and inhibits Eμ enhancer interactions with 5' region upstream of IGCR1 (V genes), limiting Eμ interactions to within the 3' region downstream of IGCR1, thus preventing premature V-DJ_H recombination. The Iμ ncRNA is transcribed from the Eμ enhancer through

most of early B cell development, whilst antisense J558 V-gene transcripts and antisense intergenic transcription of lncRNA from PAIR elements (found amongst the 5' J558 V_H genes) are expressed specifically in Pro-B cells, suggestive of V_H and DJ_H gene segment convergence at transcription factories also associated with RAG1/2, thus facilitating V-DJ_H recombination. (Taken from Shih and Krangel[191]. Not to scale).

Epigenetics

Antisense intergenic transcription of long non-coding RNA (ncRNA) in the Ig_H V-region during VDJ_H recombination in Pro-B cells was first discovered by Bolland et al[199]. These long ncRNA's are transcribed at regulatory elements such as PAIR elements, and their direct functions remain elusive. However, their interspersed positioning throughout the Ig_H loci provide a suitable model for DNA looping of these actively-transcribing regions into a shared transcription factory. This is postulated to bring unrecombined V-gene segments into close proximity with the recombined DJ_H gene segment, thus facilitating in V-DJ_H recombination[200,201]. Evidence to support this can be found in the stage-specific production of J558 antisense transcripts and PAIR-derived ncRNA in Pro-B cells, together with almost continuous transcription of the Iμ transcript from Eμ, suggesting convergence of the V_H and DJ_H segments in transcription factories that are also associated with RAG1/2[199,202].

The regulatory elements of the Ig_H loci also have distinct B-lineage stage-specific epigenetic histone marks, which in turn have multiple functional roles during VDJ_H recombination. H3K4me3 histone modifications for example are associated with the transcription start sites (TSS) of actively-transcribing genes, including PAIR elements and Eμ, where lncRNA is transcribed. RAG2 is able to recombine genes associated with the H3K4me3 histone mark, and disruption of RAG2 association with histone by point mutation results in poorer efficiency of V(D)J recombination[200,203]. Other histone

modifications associated with Ig_H locus include inactive H3K9me/H3K27me3 markers, or active H3K9ac/H3K36me3, depending on the stage of recombination[204] and V-gene family[205]. The level of V_H gene-associated histone acetylation/methylation also correlates with its frequency of recombination[206]. More generally on the Ig_κ locus, signalling via IL7R maintains active suppression and compaction of the loci by H3K27me3, such that premature recombination does not take place in Pro-B cells[113].

DNA methylation at CpG is associated with the vast majority of the Ig_H locus in early progenitor B cells. DNase hypersensitivity sites of highly localised demethylated states are the exception, and can be found at regulatory regions such as Eμ and 3'RR, but also at promotor regions for DQ52 and DFL16.1 D_H gene segments. Demethylation patterns are stage-specific during B cell development, and are associated with accessibility, DNA interactions, and recombination[207]. Studies have shown that the de-novo DNA methyltransferase 3B (DNMT3B) is important in preventing Ig_κ recombination during heavy chain recombination by keeping the loci methylated during B cell development[208].

Local V_H chromatin states

It has recently been shown that the V genes in the Ig_H locus exist in one of three mutually-exclusive local chromatin states: architectural (A), enhancer (E), and background (Bg)[209]. A-states (defined by CTCF and Rad21 binding) and E-states (defined by Pax5, IRF4, YY1 binding, and H3K4me3) are found on actively-recombining V genes, whilst V genes with Bg-states (absent of either sets of A/E factors/markers) are less active. Interestingly, not only are the A and E chromatin states mutually exclusive, but they are also linked to the evolutionary background of the V gene families[209,210].

1.6 Ageing

As multicellular organisms age, there is progressive deterioration of physiological function as tissue homeostasis destabilises. Consequently, individuals can present with an array of chronic diseases – such as arthritis, diabetes (type 2), dementia, and cardiovascular disease – as well as many cancers[211]. The underlying mechanisms behind these seemingly unrelated diseases can be attributed to the established cellular hallmarks of ageing: genomic instability, telomere attrition, epigenetic alterations, loss of proteostasis, deregulated nutrient sensing, mitochondrial dysfunction, cellular senescence, stem cell exhaustion, and altered intercellular communication[212]. Genetic and environmental factors impact on an individual's susceptibility to the ageing hallmarks. As such, the ageing process results in a heterogeneous manifestation of these biological and clinical implications.

In mammals, ageing is associated with a redistribution of active euchromatin and inactive heterochromatin regions[213,214,215]. This coincides with alterations in DNA methylation patterns, in which global hypomethylation is observed in constitutive heterochromatic DNA (such as telomeres and repetitive DNA) whist DNA hypermethylation is acquired at CpG sites of promotor regions[216]. The repressive histone mark H3K9me3 is strongly associated with constitutive heterochromatic regions, so its observed redistribution with age also coincides with altered chromatin accessibility[215,217]. H3K27me3 on the other hand is a more dynamic repressive mark that is cell-type specific[218,219] and, in terms of ageing, shows contradictory patterns across model organisms. In *Drosophila* for instance, it has been postulated that ageing is associated with H3K27me3 accumulation, and that mutations in the H3K27

methyltransferase EZH2 extends lifespan[220]. Conversely, levels of H3K27me3 in *C. elegans* decrease with age, and loss of the H3K27 demethylase UTX1 in *C.elegans* extents lifespan[221]. Analysis of ENCODE data however would suggest that ageing in the human context is associated with an accumulation of H3K27me3 and thus, is consistent with the *Drosophila* model of ageing[222].

As well as localised age-associated histone repression, ageing is also associated with the active promotor-spanning H3K4me3 mark[223,224]. Like H3K27me3, this histone mark is dynamically induced leading to up/downregulation of several genes, and could therefore indicate aberrant age-associated cell activation that leads to other hallmarks of ageing, such as cell senescence[223,224].

Ageing is also strongly associated with mitochondrial dysfunction, both as a cause and consequence. Mitochondria are self-sustaining organelles with their own genome (mt-DNA) and protein synthesis. They play an essential role in metabolism, performing oxidative phosphorylation with metabolites to produce chemical energy and the reactive oxygen species (ROS) byproduct. Age-related cellular stress can increase the production and leakage of ROS into the cell, resulting in oxidative damage to macromolecules and DNA[225]. Additionally, cellular stress can trigger the release of mt-DNA from mitochondria which acts as a danger associated molecular pattern (DAMP) molecule to trigger the activation of caspase 1 and its downstream inflammatory cytokines, such as IL1β and TNFα[226,227]. Consequently, there is an increase in the level of mt-DNA found in blood circulation with age[228]. Aged liver and splenic cells have also been reported to have fewer mitochondria with reduced overall respiratory transport chain capacity[229,230]. These defects lead to reduced cellular metabolic output and ultimately cell exhaustion.

1.6.1 Growth hormone, IGF1, and insulin

Age-associated hormone-related changes such as menopause, andropause, and somatopause, is an indication that endocrine system dysfunction is contributing to this tissue homeostatic breakdown[231]. One such endocrine system that has been directly linked to ageing and longevity is the Growth Hormone (GH)/IGF1/Insulin axis. In aged humans (60+), serum levels of GH and IGF1 decline whilst insulin levels reciprocally increase[232,233]. This hormone instability subsequently coincides with insulin insensitivity that manifests as type 2 diabetes and growth-deficient diseases such as sarcopenia and osteoporosis[234,235].

Paradoxically, deletion of the IGF1R in simple model organisms *C. Elegans* and *Drosophila* has demonstrated an increase in lifespan[236,237]. But in more complex organisms such as mice the results are less conclusive, and dependent on strain and sex. For instance, heterozygous $IGF1R^{+/-}$ mice on a 129/J background have a 33% extended lifespan in females, but for males there is no significant difference[238]. Conversely, $IGF1R^{+/-}$ in the C57BL/6 strain showed no change in lifespan in either sex[239], but complete deletion of the adaptor protein $Irs1^{-/-}$ in C57BL/6 mice resulted in a 17% extended lifespan for females, but not males[240,241,242]. Targeted suppression of IGF1R signalling through complete knockouts also results in these mice being smaller in size. Interestingly, a knockout mouse model of Pappalysin-1 – an IGFBP4-specific protease – which therefore increases autocrine/paracrine IGF1 suppression by IGFBP4, was found to extend the lifespan of both male and female mice by 38%[242,243,244]. Moreover, targeted pharmacological inhibition of IGF1R in “middle-aged” 18 month old mice

resulted in a 9% extended lifespan in females[245], and calorie-restricted diets introduced around the same stage of life (to manually regulate IGF1/Insulin levels) have been shown to extend lifespan of both sexes in rodents, and even primates[246,247,248]. Thus, despite its complexities, it is evident that IGF1R signalling plays a role in the health and lifespan of an organism. However, it is possible that targeted suppression of IGF1R signalling – both biological and through human intervention – may be treating a symptom of ageing (i.e. growth dysregulation) rather than the underlying causes.

1.6.2 Aged immunity

There is growing concern for the health and wellbeing of our ever-ageing population. Studies have shown increased incidence of infections and poor effectiveness of flu vaccinations in elderly patients, with only 17-53% mounting an effective antibody response, as measured by seroconversion and seroprotection levels[249]. Notably, in the current global COVID-19 pandemic, approximately 90% of all deaths associated with COVID-19 infections in the UK have occurred in people over the age of 65 (data from Office of National Statistics (ONS), as of June 2020).

It is believed that senescence of immune cells – termed "immunosenescence" – plays a large part in the deterioration of an organism's immune surveillance. Age-associated involution of the thymus and reduced TCR diversity with age results in a depleted T cell output of limiting functional capacity[250,251]. Antibody repertoire diversity is also reduced, with a skewing of V-gene usage, an increase in self-recognition, and decrease in affinity to its cognate antigen[252,253,254,255,256]. Paradoxically, there are more circulating antibodies in the serum of aged individuals, but with lower affinities to their cognate

antigen[257,258]. There is also a reduction in switched memory B cells with age[259,260]. Combined, these changes reflect an age-associated reduction in the ability of mature B cells to undergo both class switch recombination (CSR) and somatic hypermutation (SHM), which is perhaps the result of reduced expression in CSR components such as E47 and activation-induced cytidine deaminase (AID)[261] and/or from reduced germinal centre formation with age[257].

Ageing is also associated with systemic and chronic low-grade inflammation, known as "inflammageing", caused by an increased presence of pro-inflammatory cytokines – such as TNFα, IL1, IL6, IL8, IFNα and IFNβ – in blood circulation[262]. The underlying causes of inflammageing are not fully understood, but are thought to be driven by senescent cells as they release DAMP (such as mt-DNA) and a cocktail of pro-inflammatory cytokines – such as IL1, IL6, IL8, IL13, IL18 – known as the Senescence Associated Secretory Phenotype (SASP)[262,263]. Immune cells are perpetually activated by these senescent cells, leading also to the disruption of complex tissue niches. In the contexts of B cells, ageing leads to the accumulation of a pro-inflammatory B cell subset known as age-associated B cells (ABCs). These quiescent cells express low-affinity IgM BCR and reduced IgD, whilst also releasing the inflammatory cytokines TNFα, IL4, and IL10[254,264]. Initially, these ABCs first appear in the periphery, but gradually build up in the bone marrow with age[264,265].

Disruption of the bone marrow niche with age consequently has detrimental effects on haematopoiesis[266]. HSC niches are broken down in ageing, exposing these otherwise quiescent and protected stem cells to growth and inflammatory mediators, thus contributing to stem cell exhaustion[267]. Alterations in bone marrow niche composition with age – both cellular and secretory factors – also plays a part in the observed myeloid

lineage bias[268,269] and, in the B cell niche, a reduction in progenitor B cell numbers and proportionally fewer Pre-B cells[133,270]. For example, there is an alteration in mesenchymal lineage commitment away from osteoblasts towards adipocytes[267,271], which in itself has its own complications regarding bone formation. But in the contexts of early B cell development, loss of osteoblasts as a supportive stromal niche with age also has detrimental consequences for Pro-B and Pre-B cell transition, as demonstrated by the ablation osx^{+} cells from the bone marrow[67]. Additionally, aged osteoblasts have been shown to have reduced responsiveness to IGF1[272,273] and thus themselves have intrinsic functional defects that would impact B lymphopoiesis.

In line with these deficiencies in osteoblasts, it is known that in mice there is an age-related reduction in the number and proportion of Pre-B cells[254,274,275]. A comprehensive study by *Koohy et al* explored the characteristics of aged Pro-B and Pre-B cells further, and has shed light on the intrinsic defects also present in the B-lineage with age[275]. Amongst their many findings, they found aged progenitor B cells had reduced expression of IGF1R, and its adaptor Irs1, at both the transcript and protein level. This reduction in expression was supported by the epigenetic profile of these genes, particularly at the Irs1 gene loci, which was less accessible, and had reduced H3K4me3 and increased H3K27me3 marker enrichment in aged Pro-B and Pre-B cells. It was therefore suggested that IGF1R signalling may be epigenetically suppressed in Pro-B and Pre-B cells, at the stage in development where it has been shown to be required for differentiation[67,84,]. This effect would be compounded by the reduced availability of IGF1 in circulation with age[232,233] (it is not known whether levels of IGF1 in the bone marrow declines with age), and the reduced number/functionality of the supportive IGF1-expressing osteoblast niche[272,273]. Impaired IGF1R signalling in aged Pro-B and Pre-B cells could be contributing

to their aged phenotype, both in terms of progenitor B cell development, but also in the diversity, affinity, and autoreactivity of BCR in the mature B cells they become. Thus, the role of IGF1R signalling in progenitor B cell development, and its dysregulation with age, is an exciting avenue for further research.

1.7 Hypothesis and aims

The ageing process is notoriously heterogeneous, but this thesis proposes that IGF1R signalling suppression in early B cell development is a common hallmark of ageing in all individuals. Intrinsic loss of IGF1R signalling, combined with transcriptomic dysregulation, in aged Pro-B and Pre-B cells is postulated to impede Pre-B cell progression and impact on BCR repertoire diversity in mice. Given the evolutionarily conserved role of IGF1R signalling, and its link to ageing, it is also postulated that human progenitor B cells will present with a similar suppression in IGF1R signalling.

In the following chapters, attempts will be made to answer the following questions:

1) Is suppression of IGF1R signalling in early B cell development a hallmark of ageing despite organism heterogeneity, and do these cells present with any of the other hallmarks of ageing?
2) What pathways are dysregulated at the transcript-level with age, and does this correlate with the downregulation of IGF1R signalling and Ig_H recombination?
3) Do aged progenitor B cells show reduced ability to differentiate in-vitro in the presence of IGF1? To what extent is this defect intrinsic to aged B cells, and/or regulated by H3K27me3?

4) Does IGF1 play a similar role in human progenitor B cell development, and is IGF1R signalling in these cells also suppressed with age?

2 MATERIALS & METHODS

2.1 Experimental

2.1.1 Bone marrow extraction from C57BL/6 mice

All mice used were of the C57BL/6 background, and all mice used were male. The following strains were used for the data in this thesis: wild-type (3 months and 20-27 months), CD45.1 and CD45.2 (mice used were on the CD45.2 background, unless stated). All mice were bred at the Biological Service Unit at the Babraham Institute under the project licence PPL 80/2529. Aged mice were only used if they showed no visible signs of tumour growth or enlarged spleen.

Mice were sacrificed by CO_2 asphyxiation and the bone marrow from both hind legs (femur and tibia) were extracted by flushing the central bone cavity with RPMI/5% FCS/24mM HEPES. This total bone marrow cell suspension was processed henceforth at 4^{o}C, including during centrifugation, to preserve sample integrity. Centrifugation steps were carried out at 400g unless otherwise stated. Cells were then washed in PBS, re-suspended in PBS/0.5% FCS/2mM EDTA (MACS buffer), and counted with a haemocytometer prior to further downstream sample preparation.

2.1.2 Flow cytometry analysis – general

Surface and viability staining

Cells were stained at a final concentration of 20 x 10^6 cells/mL in FACS buffer. Starting cell suspension was initially washed in FACS buffer, re-suspend in FACS buffer containing

anti-CD16/CD32 (1:400), transferred to a 5mL Falcon tube (BD Biosciences) or a V-bottom 96-well plate and left to incubate on ice for 15 minutes on ice. Prior to staining on cells, a master mix of fluorescently-conjugated antibodies/dyes were diluted to 2X final concentration in FACS buffer and added at 1:1 dilution to the cell suspension. Cells were incubated on ice in the dark for 1 hour.

Fixation/permeabilisation and intracellular staining

After surface staining, the cell-antibody solution was twice washed with FACS buffer then re-suspended in 100uL Cytofix/Cytoperm reagent (BD Biosciences, #554722) and incubated on ice in the dark for 20 minutes to fix and permeabilise the cells. Cells were then washed in 1X Perm/Wash buffer (BD, #554723). *Once fixed, spin cycles change from 400xg for 5 minutes to 800xg for 5 minutes at 4 degrees*. For permeabilization and intracellular staining, fluorescently-conjugated antibodies were diluted to 1X final concentration in 1X Perm/Wash buffer and used to re-suspend cells, which were then incubated on ice in the dark for 30-45 minutes. Cell-antibody solution was twice washed in 1X Perm/Wash buffer before being resuspended in FACS buffer to be run on a flow cytometer.

Compensation beads

UltraComp eBeads™ Compensation Beads (Invitrogen; #01-2222-41) were used as per manufacturer's instructions. For each single colour, in a 5mL Falcon tube, 50uL FACS buffer was added, followed by 1 drop of UltraComp eBeads (~50uL). 1uL of fluorescently-conjugated antibody was added to each individual tube containing beads and incubated on ice in the dark for 15 minutes. Once stained, the beads were washed with 1mL FACS buffer and re-suspended in 200uL FACS buffer. Cells were used for unstained and viability single colour controls.

Setting up the flow cytometer

LSRFortessa (BD Bioscieces), ZE5 Cell Analyzer (Bio-Rad), or Attune NxT (Invitrogen) Flow Cytometers were used to analyse cell samples. Flow cytometer voltages were set up using unstained and single colour-stained beads/cells. With the voltages set, the single colour controls were recorded and compensation calculated by the FACS Diva software prior to running samples. Sufficient events were recorded for each cell sample on a stopping gate of Lymphocytes (FSC-A vs SSC-A), single-cells 1 (FSC-A vs FSC-H), single-

cell 2 (SSC-A vs SSC-H) that stained negative for the Fixable Viability Dye (FVD). Once all samples had run successfully, FCS files were exported for further analysis in FlowJo (see "Computational" section for details).

2.1.3 Sorting progenitor B cells by FACS

Total murine bone marrow cell suspensions were depleted of committed cell lineages by magnetic cell sorting (MACS, Miltenyi Biotech). 25 million cells/mL in MACS buffer (PBS/0.5% FCS/2mM EDTA) were incubated with the following biotinylated antibodies on ice for 30 minutes: Ter119, Cd3e, Mac1/Cd11b, and Gr1/Ly-6G:

Antigen	**Conjugate**	**Clone**	**Dilution**	**Source**
Ter119	biotin	TER-119	1:400	Ebioscience
CD3e	biotin	eBio500A2	1:800	Ebioscience
Mac1 (CD11b)	biotin	M1/70	1:1600	Ebioscience
Gr1 (Ly-6G)	biotin	RB6-8C5	1:1600	Ebioscience

Table 2-1: MACS depletion for FACS. Biotinylated antibodies for MACS lineage depletion using magnetic streptavidin microbeads prior to FACS sort.

Cells were then washed and incubated with magnetic streptavidin microbeads (Miltenyi Biotech) on ice for a further 15 minutes at a concentration of 5uL/10^7 cells. After another wash and resuspension in 1mL MACS buffer, cells were put down an equilibrated LS column (Miltenyi Biotech) attached to a magnet. The depleted flow-through of unbound cells, enriched for the B cell lineage, were counted and resuspended at 20x10^6 cells/mL in FACS buffer (PBS/2.5% FCS/2mM EDTA) in preparation for flow cytometry staining. Depleted bone marrow cells were stained for flow cytometry as described in "Flow cytometry analysis – general" using the following antibodies/dyes:

Antigen	Conjugate	Clone	Dilution	Source
CD19	BV421	1D3	1:400	BD Biosciences
AA4.1 (CD93)	BV650	AA4.1	1:800	BD Biosciences
CD25	PEcy5	PC61.5	1:500	eBioscience
IgM	eFluor660	II/41	1:400	eBioscience
IL7Ra (CD127)	PE	eBioSB/199	1:400	eBioscience
CD43	PEcy7	S7	1:100	BD Biosciences
CD24 (HSA)	FITC	30F1	1:800	eBioscience
Fixable Viability Dye (FVD)	APCeFluor780	*N/A*	1:2000	eBioscience

Table 2-2: FACS antibody panel. Fluorescently-conjugated antibodies/dyes used to stain lineage-depleted bone marrow prior to FACS sort.

UltraComp eBeads™ (Invitrogen) were used for single colour compensation setup as described in "Flow cytometry analysis – general" (except for unstained and FVD single colour, where cells were used). After a wash and resuspension in FACS buffer, live singlet lymphocytes were sorted based on the following expression profiles:

Cell Population	Biomarker Expression
Pro-B (FrBC)	$CD19^{+}AA4.1^{+}CD25^{-}IgM^{-}IL7R\alpha^{+}CD43^{hi}CD24^{lo}$
Early Pre-B (FrC')	$CD19^{+}AA4.1^{+}CD25^{-}IgM^{-}IL7R\alpha^{+}CD43^{lo}CD24^{hi}$
Late Pre-B (FrD)	$CD19^{+}AA4.1^{+}CD25^{+}IgM^{-}$
Immature B (FrE)	$CD19^{+}AA4.1^{+}CD25^{-}IgM^{+}$

Table 2-3: Biomarker expression for progenitor B cell populations FACS sorted from lineage-depleted bone marrow.

Cells were sorted using a FACSAria Fusion (BD Biosciences) by a trained member of the Babraham Institute's Flow Cytometry Facility. All cells were collected in 2mL microtubes containing 2X DNA/RNA Shield buffer (Zymo, R1100-250) to lyse the cells immediately and preserve the genetic content. The sorted and lysed samples were then stored at -20^{o}C in 1X final concentration until processed later for DNA and RNA extraction (see "DNA and RNA extraction").

2.1.4 In-vivo BrdU cell cycle analysis

In-vivo labelling of mouse cells with BrdU using the BrdU-FITC Flow Kit (BD Biosciences, #559619) was carried out as per manufacturer's instructions. 200uL (2mg) solution of sterile BrdU in PBS was injected intraperitoneally into young and aged mice by a trained member of the Biological Service Unit at the Babraham Institute. After 1 hour, mice were sacrificed by CO_2 asphyxiation and the bone marrow extracted as described in "Bone marrow extraction from C57BL/6 mice". $5x10^6$ total bone marrow cells were taken from each mouse to be analysed by flow cytometry. Cells were first stained for surface markers (B220, CD19, IgM, IgD, CD43, CD25) and FVD in FACS buffer for 1 hour on ice, as described in "Flow cytometry analysis – general". They were then fixed and permeabilised as described in "Flow Cytometry Analysis – General", but were not stained intracellularly at this point. Instead, cells were resuspended in Freezing Medium (90% FCS/10%DMSO) and placed at -80^{o}C overnight. The following day, the cells were thawed, washed in 1X Perm/Wash buffer, and fixed/permeabilised again with Cytofix/Cytoperm reagent, this time for 5 minutes on ice. After washes in 1X Perm/Wash buffer, cells were resuspended in 100uL 300ug/mL DNase in PBS and incubated at 37^{o}C for 1 hour. Cells were again washed in 1X Perm/Wash buffer. For intracellular staining, fluorescently-conjugated antibodies were diluted to 1X final concentration in 1X Perm/Wash buffer and used to re-suspend cells, which were then incubated on ice in the dark for 30-45 minutes. Cell-antibody solution was twice washed in 1X Perm/Wash buffer then resuspended in 20uL 7AAD for 15 minutes on ice. Once staining was complete, cells were washed in 1X Perm/Wash buffer before being resuspened in FACS buffer to be run on a flow cytometer.

Antigen	Conjugate	Clone	Dilution	Source
B220	BUV395	RA3-6B2	1:200	BD Biosciences
CD19	BUV737	1D3	1:400	BD Biosciences
IgM	BV421	R6-60.2	1:50	BD Biosciences
IgM (intracellular)*	PE	Polyclonal	1:200	Jackson ImmunoResearch (115-116-075)
IgD	BV510	11-26c.2a	1:400	BioLegend
CD43	biotin	S7	1:200	BD Biosciences
α-biotin*	PEcy7	Polyclonal	1:500	BD Biosciences
CD25	BV785	PC61	1:200	BD Biosciences
BrdU*	FITC	3D4	1:400	BD Biosciences
7AAD**	7AAD	*N/A*	*N/A*	BD Biosciences
Fixable Viability Dye (FVD)	APCeFluor780	*N/A*	1:2000	eBioscience

*Table 2-4: BrdU flow antibody panel. Fluorescently-conjugated antibodies/dyes used to stain lineage-depleted bone marrow prior to BrdU flow cytometry analysis. *Added after fixation; **Added after intracellular stain.*

For single colour controls, either UltraComp eBeads™ (Invitrogen) were used (B220-BUV395, CD19-BUV737, IgM-BV421, IgD-BV510, BrdU-FITC) or cells (unstained, FVD-APCeFluor780, 7AAD, IgM-PE, CD25-BV785, CD43/α-biotin-PEcy7) and set-up as described in "Flow cytometry analysis – general". LSRFortessa (BD Bioscieces) flow cytometer was used.

2.1.5 In-vitro differentiation of murine bone marrow progenitors into B cells

Culture set-up

Total bone marrow cell suspensions from mice were depleted of committed cell lineages by magnetic cell sorting (MACS) as described in "Sorting progenitor B cells by FACS", with the additional depletion of B cells with biotinylated antibodies to both CD19 and B220:

Antigen	Conjugate	Clone	Dilution	Source
Ter119	biotin	TER-119	1:400	Ebioscience
CD3e	biotin	eBio500A2	1:800	Ebioscience
Mac1 (CD11b)	biotin	M1/70	1:1600	Ebioscience
Gr1 (Ly-6G)	biotin	RB6-8C5	1:1600	Ebioscience
CD19	biotin	1D3	1:400	Ebioscience
B220	biotin	RA3-6B2	1:200	Ebioscience

Table 2-5: MACS depletion for cell culture. Biotinylated antibodies for MACS lineage depletion using magnetic streptavidin microbeads prior to setting up in-vitro cultures.

After MACS depletion through an LS column, the remaining heterogeneous pool of cells were suspended at $0.125x10^6$ cells/mL in culture medium (IMDM, Invitrogen; 10% FCS stem-cell grade, Hyclone #SH30070.02E; 50U Penicillin/Streptomycin; $5.5x10^{-5}$M β-mercaptoethanol, Invitrogen) containing 1X final concentration of IL7 (10ng/mL, R&D Systems, 407-ML) and FLT3L (10ng/mL, R&D Systems, 427-FL). 2mL of this cell suspension was placed into each well of a 24-well plate, filling the outer wells with 2mL PBS. Cells were incubated in a 37°C, 5% CO2 humidified incubator for 4 days. On the 4th day, the top 1mL of culture medium was gently removed and discarded, taking care not to disturb the adherent/settled cells at the bottom of the well. In its place, fresh culture medium containing 2X final concentration of IL7 (20ng/mL) was added to the remaining 1mL of cell suspension in each well to make a final volume of 2mL and a 1:1 dilution of the freshly-added IL7. Cells were incubated in a 37°C, 5% CO2 humidified incubator for a further 4 days. On the 8th day, the process of medium replenishment as was carried out on the 4th day was repeated, this time adding 1mL fresh culture medium containing 2X final concentration of IGF1 (200ng/mL, R&D Systems, 791-MG) to the 1mL cells still in the well for a final volume of 2mL and 1X final concentration of IGF1 (100ng/mL). Cells were incubated in a 37°C, 5% CO2 humidified incubator for a further 4 days. On the 12th day, the process of medium replenishment was done exactly as was done on the 8th day: 1mL fresh culture medium containing 2X final concentration of IGF1 added to the 1mL cells still in the well for a final volume of 2mL. Cells were incubated in a 37°C, 5% CO2 humidified incubator for a further 3 days. On the 15th day, the process of medium replenishment was done exactly as was done on the 8th and 12th days: 1mL fresh culture medium containing 2X final concentration of IGF1 added to the 1mL cells still in the well

for a final volume of 2mL. Cells were incubated in a 37°C, 5% CO2 humidified incubator for a final 3 days. The 18th day marks the culture system's endpoint.

	Time point (Days)				
Condition	**0-4**	**4-8**	**8-12**	**12-15**	**15-18**
IGF1	IL7+FLT3L	IL7	IGF1	IGF1	IGF1

Table 2-6: Murine culture condition time points ("IGF1").

Flow cytometry analysis/sorts

For each of the culture timepoints (Day 0, 4, 8, 12, 15, and 18), non-adherent cells from chosen wells were extracted by pipette agitation and processed for flow cytometry analysis using the same processes described in "Flow cytometry analysis – general". In these experiments, 2 panels were used:

Antigen	**Conjugate**	**Clone**	**Dilution**	**Source**
B220	BUV395	RA3-6B2	1:200	BD Biosciences
CD19	BV605	1D3	1:400	BD Biosciences
IgM	eFluor660	II/41	1:400	eBioscience
IgM (intracellular)	eFluor450	eB121-15F9	1:400	BD Biosciences
Fixable Viability Dye (FVD)	APCeFluor780	*N/A*	1:2000	eBioscience

Table 2-7: Murine culture flow panel 1. Fluorescently-conjugated antibodies/dyes used to stain in-vitro cultured cells prior to flow cytometry analysis.

Antigen	**Conjugate**	**Clone**	**Dilution**	**Source**
B220	BUV395	RA3-6B2	1:200	BD Biosciences
CD19	BV605	1D3	1:400	BD Biosciences
IgM	eFluor660	II/41	1:400	eBioscience
IgM (intracellular)	FITC	II/41	1:400	eBioscience
IgK	BV421	187.1	1:400	BD Biosciences
IgD	BV786	11-26c.2a	1:400	BD Biosciences
Fixable Viability Dye (FVD)	APCeFluor780	*N/A*	1:2000	eBioscience

Table 2-8: Murine culture flow panel 2. Fluorescently-conjugated antibodies/dyes used to stain in-vitro cultured cells prior to flow cytometry analysis.

UltraComp eBeads™ (Invitrogen) and cells were used for single colour compensation setup as described in "Flow cytometry analysis – general". Cells were analysed using the LSRFortessa (BD Bioscieces).

Instances where cells were sorted by FACS for further downstream analysis in either VDJseq or RNAseq experiments, cells were stained with FVD-APCeFluor780 (1:2000, eBioscience #65-0865-14) and B220-BUV395 (1:200, BD Biosciences #563793), and $B220^{+}FVD^{-}$ singlet lymphocytes were collected. Cells were sorted using a FACSAria Fusion (BD Biosciences) by a trained member of the Babraham Institute's Flow Cytometry Facility. Cells were collected in 15mL Falcon tubes containing RPMI/5% FCS/24mM HEPES, then lysed in a 1:1 dilution of 2X DNA/RNA Shield. Samples were stored at -20^{o}C in 1X final concentration until processed later for DNA and RNA extraction (see "DNA and RNA extraction").

Alternative culture conditions

Different exogenous growth factor conditions were tested in addition to that using IGF1 as described in "Culture set-up", they were: i) BAFF included with IGF1 from days 12-18 ii) TSLP in place of IGF1 from days 8-18 iii) IL7 in place of IGF1 from day 8-12, followed by culture medium-only in place of IGF1 from days 12-18. In these alternative culture conditions, the same process for medium replenishment was carried out as described in "Culture set-up". 1mL fresh culture medium containing 2X final concentration of growth factor (BAFF: 40ng/mL, R&D Systems; TSLP: 40ng/mL, R&D Systems; IL7: 20ng/mL, R&D Systems) added to the 1mL cells still in the well for a final volume of 2mL and 1X final concentration of growth factor (BAFF: 20ng/mL, TSLP: 20ng/mL, IL7: 10ng/mL).

	Time point (Days)				
Condition	**0-4**	**4-8**	**8-12**	**12-15**	**15-18**
IGF1	IL7+FLT3L	IL7	IGF1	IGF1	IGF1
IGF1+BAFF	IL7+FLT3L	IL7	IGF1	IGF1+BAFF	IGF1+BAFF
TSLP	IL7+FLT3L	IL7	TSLP	TSLP	TSLP
Med	IL7+FLT3L	IL7	IL7	Med-only	Med-only

Table 2-9: Alternative murine culture condition time points.

Mixed chimeric cultures (young and aged)

Total bone marrow suspension from CD45.1$^+$ young (3 months) and CD45.2$^+$ aged (~24 months) C57BL/6 mice were lineage depleted of Ter119, Cd3e, Cd11b, Ly-6G, CD19 and B220-expressing cells by MACS depletion as described in "Culture set-up". After depletion, CD45.1$^+$ young and CD45.2$^+$ aged cells were mixed together at a 1:1 ratio before being suspended at 0.125x10^6 cells/mL in culture medium and placed into culture as described in "Culture set-up".

At day 0, 8, 15, and 18, non-adherent cells from chosen wells were extracted by pipette agitation and processed for flow cytometry analysis using the same processes described in "Flow cytometry analysis – general" using the following antibodies/dyes:

Antigen	Conjugate	Clone	Dilution	Source
B220	BUV395	RA3-6B2	1:200	BD Biosciences
CD19	BV605	1D3	1:400	BD Biosciences
CD45.1	PerCP-cy5.5	A20	1:400	eBioscience
CD45.2	FITC	104	1:400	BioLegend
IgM	eFluor660	II/41	1:400	eBioscience
IgM (intracellular)	eFluor450	eB121-15F9	1:400	BD Biosciences
Fixable Viability Dye (FVD)	APCeFluor780	*N/A*	1:2000	eBioscience

Table 2-10: Mixed murine culture flow panel. Fluorescently-conjugated antibodies/dyes used to stain mixed in-vitro cultured cells prior to flow cytometry analysis.

UltraComp eBeads™ (Invitrogen) and cells were used for single colour compensation setup as described in "Flow cytometry analysis – general". Cells were analysed using the LSRFortessa (BD Bioscieces).

Small molecule inhibition of JMJD3/Ezh2

Small molecule inhibitors for the H3K27 demethylase JMJD3 (GSK-J4[276]) and H3K27 methyltransferase Ezh2 (GSK-503[277]) were supplied by GSK collaborators, and stored as 10mM concentrations in 100% sterile DMSO (Dimethyl sulfoxide; Sigma Aldrich, #D2650). Final in-vitro working concentrations for each inhibitor were based on pIC50 values of H3K27me3 levels in different cell lines, as supplied by GSK collaborators, in a

final DMSO concentration of 0.1%. The inhibitors were not added to the cells in-vitro until the 8th day of the culture.

Total bone marrow suspension from young (3 months) and aged (~24 months) C57BL/6 mice were lineage depleted of Ter119, Cd3e, Cd11b, Ly-6G, CD19 and B220-expressing cells by MACS depletion and cultured as described in "Culture set-up" up to day 8. On the 8th day, 1mL fresh culture medium containing 2X final concentration of IGF1 and 2X final concentration of GSK-J4/GSK-503 in 0.2% DMSO were added to the 1mL cells still in the well for a final volume of 2mL and 1X final concentration of IGF1 and 1X final concentration GSK-J4/GSK-503 in 0.1% DMSO. On the subsequent 12th and 15th days, 1mL fresh culture medium containing 2X final concentration of IGF1 and 1X final concentration of GSK-J4/GSK-503 in 0.1% DMSO were added to the 1mL cells still in the well for a final volume of 2mL. Media supernatant was sampled at days 8, 12, and 15, and sent to the GSK collaborators to measure the concentration of GSK-J4/GSK-503 in-vitro. At day 18, non-adherent cells from chosen wells were extracted by pipette agitation and processed for flow cytometry analysis using the same processes described in "Flow cytometry analysis – general" using Panel 1. UltraComp eBeads™ (Invitrogen) and cells were used for single colour compensation setup as described in "Flow cytometry analysis – general". Cells were analysed using the ZE5 Cell Analyzer (Bio-Rad).

2.1.6 In-vitro differentiation of human bone marrow HSCs into B cells

This work was carried out as part of a 3-month position at the GSK labs in Stevenage, UK, under the supervision of Dr Clare Thomas and Dr David Tough.

Human CD34^{+} Bone Marrow was supplied by AllCells via Caltag Medsystems Ltd as a frozen stock containing ≥0.5x106 cells (ABM022F). Murine MS-5 cell line was supplied by DSMZ (ACC-441). Both human CD34^{+} bone marrow and murine MS-5 cells were cryogenically stored in liquid nitrogen until used.

Hybrid co-culturing of human CD34^{+} bone marrow cells on a confluent monolayer of cell cycle arrested MS-5 cells was performed as described by *Lee et al*[278], with some modifications. Frozen aliquots of MS-5 cells were thawed in a 37^{o}C water bath and

grown to confluence in culture medium (α-MEM, Millipore # SLM-021-B; 10% FCS ES-cell grade, Millipore #ES009-B; 100U Penicillin/ Streptomycin, Life Technologies #15140-122; 50mM 2-Mercaptoethanol, Gibco #31350010) in T175 flasks for 3-4 days. Once confluent, the culture medium was aspirated from the adherent cells, replaced with fresh culture medium containing 10ug/mL mitomycin C (Sigma, #M4287-2MG) and cells were the incubated in a 37°C, 5% CO2 humidified incubator for 3 hours. Whilst still adhered to the flask, MS-5 cells were washed three times in PBS, dissociated with a 5 minute incubation in 5mL TryPLE at 37^{o}C, and washed again in culture medium. MS-5 cell suspension was counted using a ViCell XR Cell viability analyser (Biomax 800741), diluted to 3x10^{5}cells/mL in culture medium, and 100uL was added to each well of flat-bottom 96-well plates for 30,000 cells per well (excluding the outer wells, which were filled with 200uL DPBS). Cells were left to incubate in a 37°C, 5% CO2 humidified incubator overnight. The following day, frozen aliquots of human CD34^{+} bone marrow cells were reconstituted as per the supplier's instructions. Cells were thawed in a 37^{o}C water bath, gently washed twice in 20mL culture medium, spinning at 200g for 15 minutes, and enumerating using Trypan Blue (Gibco) on a haemocytometer. Human CD34^{+} cells were resuspended at 3x10^{4} cells/mL in culture medium containing 2X final concentration of exogenous growth factors. 100uL of these human CD34^{+} cells were then pipetted onto the 100uL of MS-5 in the 96-well plates for a final volume of 200uL per well and 1X final concentration of growth factors, equating to 3000 human CD34^{+} cells on 30,000 murine MS-5 cells. Cells were incubated in a 37°C, 5% CO2 humidified incubator for 4 days. The media replenishment steps were the same as described in "In-vitro differentiation of murine bone marrow progenitors into B cells", whereby at days 4, 8, 12, and 15, 100uL of the 200uL were replaced with 100uL of fresh culture medium containing 2X final concentration of growth factors, and incubated further at 37°C, 5% CO2 in a humidified incubator. The 18th day marks the culture system's endpoint. The growth factors used in these culture systems were IL7 (R&D Systems #207-IL-025, 10ng/mL final), FLT3L (R&D Systems #308-FK-025, 10ng/ml final), IGF1 (R&D Systems #291-G1-200, 100ng/mL final) and BAFF (R&D Systems #7537-BF-025, 20ng/mL). 2 different culture system conditions using different combinations of these growth factors were performed:

	Time point (Days)				
Condition	**0-4**	**4-8**	**8-12**	**12-15**	**15-18**
IGF1	IL7+FLT3L	IL7	IGF1	IGF1+BAFF	IGF1+BAFF
IL7	IL7	IL7	IL7	IL7	IL7

Table 2-11: Human culture condition time points ("IGF1" or "IL7").

At day 8, 12, 15, and 18, non-adherent cells from chosen wells were extracted by pipette agitation and processed for flow cytometry analysis using the same processes described in "Flow Cytometry – General" using the following antibodies/dyes:

Antigen	**Conjugate**	**Clone**	**Dilution**	**Source**
CD19	PerCP-cy5.5	HIB19	1:50	BioLegend
CD34	BV421	581	1:100	BD Biosciences
CD38	PE	HIT2	1:50	eBioscience
IL7Ra (CD127)	BV605	A019D5	1:50	BioLegend
IgM	AlexaFluor488	MHM88	1:50	BioLegend
IgM (intracellular)	APC	MHM88	1:20	BioLegend
Fixable Viability Dye (FVD)	APCeFluor780	*N/A*	1:2000	eBioscience

Table 2-12: Human culture flow panel. Fluorescently-conjugated antibodies/dyes used to stain human in-vitro cultured cells prior to flow cytometry analysis.

UltraComp eBeads™ (Invitrogen) and cells were used for single colour compensation setup as described in "Flow cytometry analysis – general". Cells were analysed using the Attune NxT (Invitrogen).

In the instances where cells were sorted by FACS for further downstream analysis for RNAseq experiments, cells were stained with FVD-APCeFluor780 (1:2000, eBioscience #65-0865-14) and CD19-PerCPcy5.5 (1:50, BioLegend) and $CD19^{+}FVD^{-}$ singlet lymphocytes were collected. Cells were sorted using a FACSAria Fusion (BD Biosciences) by a trained user at GSK's R&D site in Stevenage, UK. Cells were collected in 15mL Falcon tubes containing 2X DNA/RNA Shield and final volume made to 1X with PBS post-sort. Samples were stored at -20^{o}C in 1X final concentration until processed later for DNA and RNA extraction (see "DNA and RNA extraction").

2.1.7 DNA and RNA extraction

Samples in which DNA and/or RNA was extracted from was done so using Zymo *Quick*-DNA/RNA Microprep Plus kit (D7005). This spin-column technique was carried out using the manufacturer's instructions. For samples preserved in DNA/RNA Shield, a 1:1 dilution in Lysis Buffer was done prior to adding to the column. When column-bound, RNA was treated with DNase (supplied in kit) for 15 minutes at room temperature.

2.1.8 DNA VDJseq

DNA VDJseq was carried out as described in *Chovanec et al*[279] following the "Low amount of starting material" steps, and illustrated in Figure 2-1. DNA was extracted from live FACS sorted B cells as described in "DNA and RNA extraction" and 0.5-1ug DNA was sonicated to an average of 500bp fragment size using the Covaris E220 ultrasonicator on the following settings: peak incident power (W): 105, duty factor: 5 %, cycles per burst: 200, treatment time (s): 80, temperature (°C): 7, water level: 6. Fragmented DNA was then end repaired and A-tailed (New England Biolabs, #E7442), then adaptors with a 12N UMI were ligated (New England Biolabs, #E7445):

Name	**Sequence (5'-3')**
P7 F1	ACACTCTTTCCCTACACGACGCTCTTCCGATCTNNNNNNNNNNNNGACTCG*T
P7 short R1	[Phos]CGAGTCNNNNNNNNNNNNAGATCGGAAGAG*C[spcC3]
P7 F2	ACACTCTTTCCCTACACGACGCTCTTCCGATCTNNNNNNNNNNNNCTGCTCC*T
P7 short R2	[Phos]GGAGCAGNNNNNNNNNNNNAGATCGGAAGAG*C[spcC3]

*Table 2-13: VDJseq adaptor ligation sequences. *= phosphorothioate bonds; [Phos]= phosphorylated; [spcC3]= carbon-3-spacer; N= UMI sequence (12N)*

DNA fragments were purified with 1X AMPure XP beads (Beckman Coulter, #A63881) as per manufacturer's instructions, primer extension was performed using J-specific biotinylated primers and the Vent (exo-) DNA polymerase (New England Biolabs, #M0257):

Name	Sequence (5'-3')
JH1 Rev Bio	[Biotin]AGCCAGCTTACCTGAGGAGAC
JH2 Rev Bio	[Biotin]GAGAGGTTGTAAGGACTCACCTG
JH3 Rev Bio	[Biotin]AGTTAGGACTCACCTGCAGAGAC
JH4 Rev Bio	[Biotin]AGGCCATTCTTACCTGAGGAG

Table 2-14: VDJseq biotinylated J-primer sequences.

Primer extension products were captured using 5uL of MyOne streptavidin T1 Dynabeads (Invitrogen, #65601) and left to incubate at room temperature on rotation overnight to allow binding of beads. Primer-bound beads were twice washed in B&W buffer (10mM Tris-HCl pH 7.5, 1mM EDTA, 2M NaCl; 0.05% Tween20) and once in EB buffer (Qiagen, #19086) before being resuspended in 10.5uL EB buffer. Using a Q5 high-fideity polymerase (New England Biolabs, #M0492S), DNA was amplified off of the beads (16-17 cycles) using the short form of the Illumina adaptors:

Name	Sequence (5'-3')
P7 short	ACACTCTTTCCCTACACGACGCTC*T
JH1 Rev Bio P5 short	GTGACTGGAGTTCAGACGTGTGCTCTTCCGATCT**CCCTGTGCCCCAGACATCGA*A**
JH2 Rev Bio P5 short	GTGACTGGAGTTCAGACGTGTGCTCTTCCGATCT**AGTGGTGCCTTGGCCCCAGTA*G**
JH3 Rev Bio P5 short	GTGACTGGAGTTCAGACGTGTGCTCTTCCGATCT**ACCAGAGTCCCTTGGCCCCAGTA*A**
JH4 Rev Bio P5 short	GTGACTGGAGTTCAGACGTGTGCTCTTCCGATCT**TGAGGTTCCTTGACCCCAGTAGTCCAT*A**

*Table 2-15: VDJseq P5 adaptor sequences. *= phosphorothioate bonds; bold= J-specific sequence*

Supernatant containing the amplified DNA was extracted on a magnetic column and purified with 1X AMPure XP beads. A second round PCR (5 cycles) with Q5 polymerase was performed using the Illumina flowcell primers to incorporate the flowcell-binding and library-barcoding sequences:

Name	Sequence (5'-3')
P5-U	AATGATACGGCGACCACCGAGATCTACACTCTTTCCCTACACGACGCTCTTCCGATCT
P7-I1	GATCGGAAGAGCACACGTCTGAACTCCAGTCAC**ATCACG**ATCTCGTATGCCGTCTTCTGCTTG
P7-I2	GATCGGAAGAGCACACGTCTGAACTCCAGTCAC**CGATGT**ATCTCGTATGCCGTCTTCTGCTTG
P7-I3	GATCGGAAGAGCACACGTCTGAACTCCAGTCAC**TTAGGC**ATCTCGTATGCCGTCTTCTGCTTG
P7-I4	GATCGGAAGAGCACACGTCTGAACTCCAGTCAC**TGACCA**ATCTCGTATGCCGTCTTCTGCTTG
P7-I5	GATCGGAAGAGCACACGTCTGAACTCCAGTCAC**ACAGTG**ATCTCGTATGCCGTCTTCTGCTTG
P7-I6	GATCGGAAGAGCACACGTCTGAACTCCAGTCAC**GCCAAT**ATCTCGTATGCCGTCTTCTGCTTG
P7-I7	GATCGGAAGAGCACACGTCTGAACTCCAGTCAC**CAGATC**ATCTCGTATGCCGTCTTCTGCTTG
P7-I8	GATCGGAAGAGCACACGTCTGAACTCCAGTCAC**ACTTGA**ATCTCGTATGCCGTCTTCTGCTTG
P7-I9	GATCGGAAGAGCACACGTCTGAACTCCAGTCAC**GATCAG**ATCTCGTATGCCGTCTTCTGCTTG
P7-I10	GATCGGAAGAGCACACGTCTGAACTCCAGTCAC**TAGCTT**ATCTCGTATGCCGTCTTCTGCTTG
P7-I11	GATCGGAAGAGCACACGTCTGAACTCCAGTCAC**GGCTAC**ATCTCGTATGCCGTCTTCTGCTTG
P7-I12	GATCGGAAGAGCACACGTCTGAACTCCAGTCAC**CTTGTA**ATCTCGTATGCCGTCTTCTGCTTG
P7-I13	GATCGGAAGAGCACACGTCTGAACTCCAGTCAC**AGTCAA**CAATCTCGTATGCCGTCTTCTGCTTG
P7-I14	GATCGGAAGAGCACACGTCTGAACTCCAGTCAC**AGTTCC**GTATCTCGTATGCCGTCTTCTGCTTG
P7-I15	GATCGGAAGAGCACACGTCTGAACTCCAGTCAC**ATGTCA**GAATCTCGTATGCCGTCTTCTGCTTG
P7-I16	GATCGGAAGAGCACACGTCTGAACTCCAGTCAC**CCGTCC**CGATCTCGTATGCCGTCTTCTGCTTG
P7-I18	GATCGGAAGAGCACACGTCTGAACTCCAGTCAC**GTCCGC**ACATCTCGTATGCCGTCTTCTGCTTG
P7-I19	GATCGGAAGAGCACACGTCTGAACTCCAGTCAC**GTGAAA**CGATCTCGTATGCCGTCTTCTGCTTG
P7-I20	GATCGGAAGAGCACACGTCTGAACTCCAGTCAC**GTGGCC**TTATCTCGTATGCCGTCTTCTGCTTG

Table 2-16: Illumina flowcell index primer sequences. Bold= library barcode index sequence.

The final library was twice purified in 1X AMPure XP beads and taken into “NGS quality control” prior to sequencing. VDJseq libraries were sequenced on a MiSeq 300bp Paired End run by a trained member of the Babraham Institute’s Sequencing Facility, and reads were processed and mapped using the BabrahamLinkON pipeline (see “VDJseq analysis” in the “Computational” section).

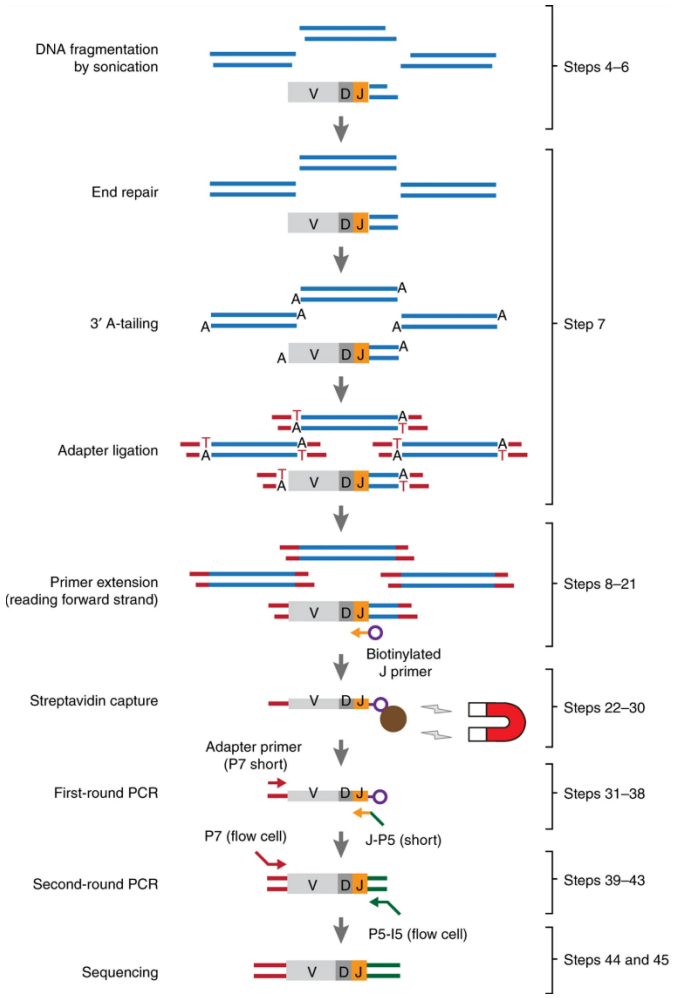

Figure 2-1: Schematic of VDJseq library preparation. Genomic DNA from FACS sorted progenitor B cells was sonicated to 500bp length. Fragmented DNA was then end repaired, A-tailed, and adaptor ligated. A single primer extension incorporates the biotinylated J-specific primer sequence, which is then captured by magnetic streptavidin T1 Dynabead. A first round of PCR is performed to amplify the captured VDJ-containing fragments, then a second round of PCR to incorporate the P5/P7 flowcell index sequences. The final library is then sequenced. (Taken from Chovanec et al[279]).

2.1.9 Bulk RNAseq

All bulk RNAseq libraries in this thesis were generated using the same methods. Total RNA was extracted from live FACS sorted B cells as described in "DNA and RNA extraction" and RNA Integrity Number (RIN) determined using a 2100 Bioanalyzer with a High Sensitivity RNA Pico kit (Agilent, 5067-1513) as per manufacturer's instructions. 10-500ng total RNA was then depleted of ribosomal RNA using the Ribo-Zero Gold rRNA

Removal Kit as per manufacturer's instructions (Illumina, now part of the TruSeq Stranded Total RNA Prep Gold kit, #20020598; no longer sold separately). RNAseq libraries were made from depleted RNA using either the NEBNext Ultra II Directional RNA Library Prep Kit for Illumina (New England Biolabs, #E7760) or TruSeq Stranded Total RNA Library Prep Gold (#20020598) as per manufacturer's instructions. In summary, rRNA-depleted RNA was chemically fragmented and primed, followed by reverse transcription for first strand synthesis, then second strand synthesis to generate cDNA fragments. These cDNA fragments were purified using AMPure XP beads before being end repaired and A-tailed, and the adaptors ligated. Another purification step with AMPure XP beads follows, then PCR amplification of adaptor-ligated cDNA fragments to incorporate the flowcell-binding and library-barcoding sequences (Table 2-16) to the final RNAseq library (PCR cycles vary based on starting RNA). Libraries were purified with AMPure XP beads and taken into "NGS quality control" prior to sequencing. Bulk RNAseq libraries were sequenced on a NextSeq500 HighOutput 75 bp Paired End run by a trained member of the Babraham Institute's Sequencing Facility, with an average sequencing depth of ~30 million reads per library. For processing of reads and downstream computational analysis, see "Bulk RNAseq analysis" of the "Computational" section.

2.1.10 Single-cell combinatorial indexing RNAseq (sciRNAseq)

A single-cell combinatorial indexing RNAseq (sciRNAseq) library was generated using the published protocol as described by *Cao et al*[280] and illustrated in Figure 2-2, with slight modifications.

Total bone marrow cell suspensions from 6 WT mice (3 young, ~3 months; 3 aged, ~24 months) were depleted of committed cell lineages by magnetic cell sorting (MACS) as described in "Sorting progenitor B cells by FACS", and $B220^{+}AA4.1^{+}IgD^{-}FVD^{-}$ live singlet lymphocytes were sorted using a FACSAria Fusion (BD Biosciences) by a trained member of the Babraham Institute's Flow Cytometry Facility using the following panel:

Antigen	Conjugate	Clone	Dilution	Source
B220	FITC	RA3-6B2	1:200	BD Biosciences
AA4.1 (CD93)	BV650	AA4.1	1:800	BD Biosciences
IgD	BV786	11-26c.2a	1:400	eBioscience
Fixable Viability Dye (FVD)	APCeFluor780	*N/A*	1:2000	eBioscience

Table 2-17: sciRNAseq FACS antibody panel. Fluorescently-conjugated antibodies/dyes used to stain lineage-depleted bone marrow prior to FACS sort.

Cells were collected in 15mL Falcon tubes containing RPMI/5% FCS/24mM HEPES, centrifuged at 400g for 5 minutes, then cell pellets were resuspended in 1mL chilled DPBS. 4mL 100% ice-cold methanol was slowly dripped onto the cell suspensions for a final volume of 5mL cells in 80% methanol (being sure to suspend the methanol and PBS together) to fix the cells. Cells were fixed on ice for at least 20 minutes. After fixation, cells were centrifuged at 800g for 5 minutes and washed twice in 1mL SSC-based Cell Wash Buffer (3X-SSC; 1% 20 U/µL SUPERase In RNase Inhibitor, Ambion; 1% 20mg/mL BSA, NEB) containing 1% Diethyl pyrocarbonate, with 800g centrifugation at 5 minutes in between each wash. A final wash in 1mL SSC-based Cell Wash Buffer without Diethyl pyrocarbonate was performed before cells were resuspended in 110uL PBS-based Cell wash Buffer (DPBS; 1% SUPERase In; 1% BSA). 10uL was taken for cell count by haemocytometer. Cells were diluted to $1x10^6$ cells/mL in PBS-based Cell Wash Buffer and 2uL (2000 cells) pipetted into V-bottom 96-well PCR plates (Eppendorf, #951020389) along with 0.25uL 10mM dNTP (one plate per mouse).

Wells were annotated based on the mouse from which their cell contents were derived from, in order to allow for organism-level barcoding during the first round of indexing.

The first round of sciRNAseq cell indexing occurs during in-situ first strand synthesis by reverse transcription (RT). 1uL of each 25uM indexed oligo-dT primer (containing a unique RT barcode and an 8N UMI) was added to their respective wells.

See Appendices *for all oligo-dT primer sequences and which mouse they were assigned to.*

Plates were incubated on a thermocycler at 55^{o}C for 5 minutes then immediately placed on ice. The SuperScript™ IV Reverse Transcriptase module (Invitrogen, #18090010; 1uL 5X buffer, 0.25uL 100mM DTT, 0.25 enzyme) and RNaseOUT™ Recombinant

Ribonuclease Inhibitor (Invitrogen, #10777019; 0.25uL) were added to each well and the plates were incubated for a further 10 minutes at 55^{o}C. 5uL of Stop Solution (40mM EDTA, Invitrogen #15575020; 1mM Spermidine, MPBio #19485201) was added to each well before all wells were pooled into 1 volume in a 5mL Falcon tube (BD Biosciences).

Based on their FSC/SSC profile, in-tact single cells were FACS sorted by a trained member of the Babraham Institute's Flow Cytometry Unit using a FACSAria Fusion (BD Biosciences) into fresh V-bottom 96-well PCR plates (100 events/well) containing 5uL Buffer EB (Qiagen). For second strand synthesis, the NEBNext® Ultra II Non-Directional RNA Second Strand Synthesis Module (NEB, #E6111L; 0.5uL buffer, 0.25uL enzyme) was added to each well and incubated on a thermocycler at 16^{o}C for 150 minutes, followed by 75^{o}C for 20 minutes. The cDNA was then tagmented with the addition of 5uL TD buffer and 0.5uL TDE1 enzyme (Illumina, #20034197) and 0.25uL of 20ng/uL genomic DNA (Promega, #G147A) at 55^{o}C for 5 minutes. The reaction was stopped by adding 12uL DNA Binding Buffer (Zymo, #D4003-1) to each well and incubated at room temperature for a further 5 minutes. cDNA fragments were purified with 36uL AMPure XP beads (Beckman Coulter, #A63881) per well, as per manufacturer's instructions, eluting in 16uL buffer EB (Qiagen) per well.

The second round of sciRNAseq cell indexing occurs during the PCR reaction to incorporate the Illumina flowcell sequences and barcodes. PCR reactions were set up such that each well of 16uL cDNA was given 20uL NEBNext High-Fidelity 2X PCR Master Mix (NEB, #M0541L), and a unique combination of P5 and P7 primers:

Name	Sequence (5'-3')
P5-1	AATGATACGGCGACCACCGAGATCTACAC**CTCCATCGAG**ACACTCTTTCCCTACACGACGCTCTTCCGATCT
P5-2	AATGATACGGCGACCACCGAGATCTACAC**TTGGTAGTCG**ACACTCTTTCCCTACACGACGCTCTTCCGATCT
P5-3	AATGATACGGCGACCACCGAGATCTACAC**GGCCGTCAAC**ACACTCTTTCCCTACACGACGCTCTTCCGATCT
P5-4	AATGATACGGCGACCACCGAGATCTACAC**CCTAGACGAG**ACACTCTTTCCCTACACGACGCTCTTCCGATCT
P5-5	AATGATACGGCGACCACCGAGATCTACAC**TCGTTAGAGC**ACACTCTTTCCCTACACGACGCTCTTCCGATCT
P5-6	AATGATACGGCGACCACCGAGATCTACAC**CGTTCTATCA**ACACTCTTTCCCTACACGACGCTCTTCCGATCT
P5-7	AATGATACGGCGACCACCGAGATCTACAC**CGGAATCTAA**ACACTCTTTCCCTACACGACGCTCTTCCGATCT
P5-8	AATGATACGGCGACCACCGAGATCTACAC**ATGACTGATC**ACACTCTTTCCCTACACGACGCTCTTCCGATCT
P5-9	AATGATACGGCGACCACCGAGATCTACAC**TCAATATCGA**ACACTCTTTCCCTACACGACGCTCTTCCGATCT
P5-10	AATGATACGGCGACCACCGAGATCTACAC**GTAGACCTGG**ACACTCTTTCCCTACACGACGCTCTTCCGATCT
P5-11	AATGATACGGCGACCACCGAGATCTACAC**TTATGACCAA**ACACTCTTTCCCTACACGACGCTCTTCCGATCT
P5-12	AATGATACGGCGACCACCGAGATCTACAC**TTGGTCCGTT**ACACTCTTTCCCTACACGACGCTCTTCCGATCT
P5-13	AATGATACGGCGACCACCGAGATCTACAC**GGTACGTTAA**ACACTCTTTCCCTACACGACGCTCTTCCGATCT
P5-14	AATGATACGGCGACCACCGAGATCTACAC**CAATGAGTCC**ACACTCTTTCCCTACACGACGCTCTTCCGATCT
P5-15	AATGATACGGCGACCACCGAGATCTACAC**GATGCAGTTC**ACACTCTTTCCCTACACGACGCTCTTCCGATCT
P5-16	AATGATACGGCGACCACCGAGATCTACAC**CCATCGTTCC**ACACTCTTTCCCTACACGACGCTCTTCCGATCT
P7-1	CAAGCAGAAGACGGCATACGAGAT**CCGAATCCGA**GTCTCGTGGGCTCGG
P7-2	CAAGCAGAAGACGGCATACGAGAT**ATAAGCCGGA**GTCTCGTGGGCTCGG
P7-3	CAAGCAGAAGACGGCATACGAGAT**CCGCAGCCGC**GTCTCGTGGGCTCGG
P7-4	CAAGCAGAAGACGGCATACGAGAT**TGCGCCTGGT**GTCTCGTGGGCTCGG
P7-5	CAAGCAGAAGACGGCATACGAGAT**AACGTAATCT**GTCTCGTGGGCTCGG
P7-6	CAAGCAGAAGACGGCATACGAGAT**ATTCTCCTCT**GTCTCGTGGGCTCGG
P7-7	CAAGCAGAAGACGGCATACGAGAT**ACCTAGTTAG**GTCTCGTGGGCTCGG
P7-8	CAAGCAGAAGACGGCATACGAGAT**ATAGGAGTAC**GTCTCGTGGGCTCGG
P7-9	CAAGCAGAAGACGGCATACGAGAT**GGTCGCTATG**GTCTCGTGGGCTCGG
P7-10	CAAGCAGAAGACGGCATACGAGAT**ATCCGTTAGC**GTCTCGTGGGCTCGG
P7-11	CAAGCAGAAGACGGCATACGAGAT**CTCTTAGCGG**GTCTCGTGGGCTCGG
P7-12	CAAGCAGAAGACGGCATACGAGAT**TGATTCAACT**GTCTCGTGGGCTCGG
P7-13	CAAGCAGAAGACGGCATACGAGAT**TTCGTTCCAT**GTCTCGTGGGCTCGG
P7-14	CAAGCAGAAGACGGCATACGAGAT**TACCTAATCA**GTCTCGTGGGCTCGG
P7-15	CAAGCAGAAGACGGCATACGAGAT**AACGGAACGC**GTCTCGTGGGCTCGG
P7-16	CAAGCAGAAGACGGCATACGAGAT**GATGCTACGA**GTCTCGTGGGCTCGG
P7-17	CAAGCAGAAGACGGCATACGAGAT**TTCGATAACC**GTCTCGTGGGCTCGG
P7-18	CAAGCAGAAGACGGCATACGAGAT**AACCTCAAGA**GTCTCGTGGGCTCGG
P7-19	CAAGCAGAAGACGGCATACGAGAT**CATACGATGC**GTCTCGTGGGCTCGG
P7-20	CAAGCAGAAGACGGCATACGAGAT**AAGCTGACCT**GTCTCGTGGGCTCGG
P7-21	CAAGCAGAAGACGGCATACGAGAT**TTATCGTATT**GTCTCGTGGGCTCGG
P7-22	CAAGCAGAAGACGGCATACGAGAT**AAGTCTAATA**GTCTCGTGGGCTCGG
P7-23	CAAGCAGAAGACGGCATACGAGAT**GTCGACGGAA**GTCTCGTGGGCTCGG
P7-24	CAAGCAGAAGACGGCATACGAGAT**ACTAATTGAG**GTCTCGTGGGCTCGG

Table 2-18: sciRNAseq PCR index primer sequences. Bold= barcode sequence in primer (see Table 2-19 and Table 2-20 for barcode sequences).

Name	Barcode
P5-1	CTCCATCGAG
P5-2	TTGGTAGTCG
P5-3	GGCCGTCAAC
P5-4	CCTAGACGAG
P5-5	TCGTTAGAGC
P5-6	CGTTCTATCA
P5-7	CGGAATCTAA
P5-8	ATGACTGATC
P5-9	TCAATATCGA
P5-10	GTAGACCTGG
P5-11	TTATGACCAA
P5-12	TTGGTCCGTT
P5-13	GGTACGTTAA
P5-14	CAATGAGTCC
P5-15	GATGCAGTTC
P5-16	CCATCGTTCC

Table 2-19: sciRNAseq P5 barcode sequences in reads. Sequence of P5 barcode in reads is the same as the sequence in the P5 primer sequence found in Table 2-18.

Name	Barcode*
P7-1	TCGGATTCGG
P7-2	TCCGGCTTAT
P7-3	GCGGCTGCGG
P7-4	ACCAGGCGCA
P7-5	AGATTACGTT
P7-6	AGAGGAGAAT
P7-7	CTAACTAGGT
P7-8	GTACTCCTAT
P7-9	CATAGCGACC
P7-10	GCTAACGGAT
P7-11	CCGCTAAGAG
P7-12	AGTTGAATCA
P7-13	ATGGAACGAA
P7-14	TGATTAGGTA
P7-15	GCGTTCCGTT
P7-16	TCGTAGCATC
P7-17	GGTTATCGAA
P7-18	TCTTGAGGTT
P7-19	GCATCGTATG
P7-20	AGGTCAGCTT
P7-21	AATACGATAA
P7-22	TATTAGACTT
P7-23	TTCCGTCGAC
P7-24	CTCAATTAGT

Table 2-20: sciRNAseq P7 barcode sequences in reads. Sequence of P7 barcode in reads is the reverse compliment of the P7 primer sequence found in Table 2-18.

With 16 different P5 primers and 24 different P7 primers, 384 unique combinations of P5-P7 primers were possible. In this experiment, 288 unique P5-P7 combinations were used (see Appendices). These PCR reactions were incubated on a thermocycler: 72°C for 5 minutes, 98°C for 30 seconds, 22 cycles of (98°C for 10 seconds, 66°C for 30 seconds, 72°C for 30 seconds) and a final 72°C for 5 minutes. The wells were pooled and the final sciRNAseq library was purified with 0.8X AMPure XP beads. DNA concentrations of the final library were determined by Qubit™ dsDNA HS Assay (Invitrogen, #Q32851), and sciRNAseq library-specific concentrations by KAPA Illumina SYBR Universal Library Quant Kit (Roche, #KK4824). The sciRNAseq library was sequenced on a NextSeq500 HighOutput 75 bp Single End by a trained member of the Babraham Institute's Sequencing Facility, with an asymmetrical cycle run (Read 1: 18 cycles, Read 2:52 cycles, Index 1: 10 cycles, Index 2: 10 cycles).

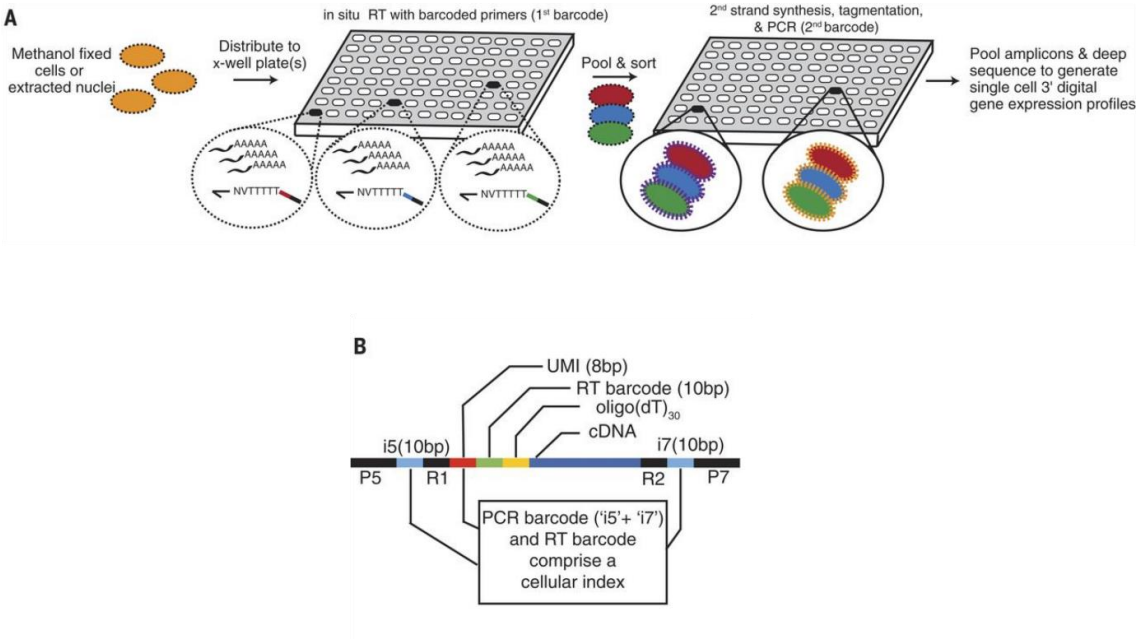

Figure 2-2: Schematic for sciRNAseq library preparation. (A) FACS sorted B220^{+}AA4.1^{+}IgD^{-} live singlet lymphocytes from 3 young and 3 aged mice were fixed in 80% methanol. Fixed cells were distributed across 96-well plates (2000 cells/well) for first strand synthesis (RT) and 1st round of barcode indexing. Cells from all mice were pooled, and in-tact singlet cells were FACS sorted into fresh 96-well plates (100 events/well) for tagmentation and PCR, where the 2nd round of barcode indexing occurs. The amplicons were pooled

and the final library is sequenced. (B) The final sciRNAseq library construct. The RT barcode (added during first strand synthesis) and P5/P7 barcode sequences (added during PCR) together make up the cellular index. (Taken from Cao et al[280]).

2.1.11 NGS quality control

Prior to Illumina sequencing, Next Generation Sequencing (NGS) libraries (RNAseq, sciRNAseq, VDJseq) were quality-assured by Qubit (Invitrogen, #Q32851), Bioanalyzer (Agilent, #5067-4626) and KAPA (Roche, #KK4824) quantitation, as per manufacturer's instructions. This provided accurate molar calculations of each NGS library for the aid of the trained personnel at the Babraham Institute's Sequencing Facility in their appropriate loading onto the Illumina sequencer.

2.2 Computational

2.2.1 Figures and statistics – general

GraphPad Prism (version 8.1.1), RStudio (version 1.1.463) and Microsoft Excel (Office 2016) was used to create plots, and its analytical tools were used to perform the statistical analyses.

2.2.2 Flow cytometry analysis

Exported .fcs files were loaded into FlowJo software (version 10.6.0) for visualisation. Manual gating was applied and replicated across samples in an experiment. Representative plots were exported for qualitative analysis. Population numbers/proportions were exported for quantitative analysis in GraphPad Prism and Excel.

2.2.3 Bulk RNAseq analysis

After sequencing, raw FastQ reads were quality and adaptor trimmed using TrimGalore and aligned by Hisat2[281] to the murine GRCm38 or human GRCh38 genome by a trained member of the Babraham Institute's Bioinformatics Department. The aligned .bam files were then loaded into Seqmonk for gene annotation and DESeq2[282] analysis using the RNAseq Quantitation Pipeline. Annotated and filtered gene lists were exported as log2 reads normalised to library size (per million reads) as a .txt file. Gene lists were then imported into GraphPad or RStudio (version 1.1.463) for creating plots.

TrimGalore: (https://www.bioinformatics.babraham.ac.uk/projects/trim_galore/)

Seqmonk: (https://www.bioinformatics.babraham.ac.uk/projects/seqmonk/)

Seqmonk RNAseq Quantitation Pipeline:

(https://www.bioinformatics.babraham.ac.uk/projects/seqmonk/Help/4%20Quantitation/4.3%20Pipelines/4.3.1%20RNA-Seq%20quantitation%20pipeline.html)

In some instances, DESeq2 was performed directly in RStudio with modifications to the code embedded in Seqmonk. These instances were when generating Shrunk Log2 Fold Change (LFC) values using the *lfcShrink* command (type= "normal"), or to include sex as a source of variation in the human samples using the *DESeqDataSetFromMatrix* command (design= ~ Sex+Age).

Gene Set Enrichment Analysis (GSEA)[283] was also performed on the DESeq2-filtered gene lists via the desktop application (version 4.0.3). Default parameters were retained, with some key details:

1) *C5.all.v7.1.symbols.gmt* used as gene set database;
2) *Mouse_ENSEMBL_Gene_ID_MSigDB.v7.0.chip/Human_ENSEMBL_Gene_MSigDB.v7.1.chip* used as chip platforms; "Signal2Noise" used for metric ranking; filtering for 15-500 gene enrichment per gene set.

Complete DESeq2 gene list datasets for the bulk RNAseq analyses performed can be found in the "Appendices".

2.2.4 VDJseq analysis

After sequencing, raw FastQ reads were processed through the BabrahamLinkON pipeline (https://github.com/peterch405/BabrahamLinkON). The pipeline is split into 3 stages: pre-cleaning (removes J-gene mispriming events, germline reads, and reads with low quality bases), deduplication (using 12N UMI), and assembly (using IgBlast[284] with the IMGT database). The output .tsv files of assembled VDJ reads were then analysed in RStudio, GraphPad Prism and Microsoft Excel to quantify and visualise results.

Complete filtered VDJseq V_H gene usage datasets for the analysis performed can be found in the "Appendices".

2.2.5 sciRNAseq analysis

The 384 (RT indexes) x 288 (PCR indexes) allows for single cells from all 6 mice to be barcoded from the single sciRNAseq library. After sequencing, 288 raw FastQ reads were processed through the sciRNAseq pipeline (https://github.com/cole-trapnell-lab/worm-rna/tree/master/primary_pipeline_scripts). In summary, the pipeline uses TrimGalore to trim adaptors, aligns reads to the GRCh38 genome using STAR (version 2.5), deduplicates reads based on 8N UMI and tagmentation site, then splits files into single-cells based on the 384 RT barcodes. The output of this pipeline is a sparse matrix of gene read counts for each of the single cells. The gene matrix was then imported into RStudio and processed through the SeuratR package (version 3.1.2) using the *Guided Clustering Tutorial* Vignette (https://satijalab.org/seurat/v3.1/pbmc3k_tutorial.html), filtering out single cells with <300 or >1500 reads, or <150 genes detected. For cell cycle regression, the "Alternative Workflow" of the *Cell-Cycle Scoring and Regression* Vignette was

followed (https://satijalab.org/seurat/v3.1/cell_cycle_vignette.html), using genes from GO Terms "Cell Cycle G1/S Phase Transition" and "Cell Cycle G2/M Phase Transition" for inputting S genes and G2M genes respectively (see Appendices for gene lists). UMAP clustering was performed on transformed data as part of this SeuratR pipeline (dims= 1:20, resolution= 0.8). Differential expression analysis comparing Young and Aged mice was performed as part of this SeuratR pipeline using the *FindMarkers* command.

Complete differentially-expressed gene list datasets from the SeuratR analysis performed for i) Cluster ID, and ii) Young versus Aged, can be found in the "Appendices".

3 DECONVOLUTING THE HETEROGENEITY OF AGEING IN EARLY B CELL DEVELOPMENT

3.1 Introduction

Individual organisms within a species age at different rates and with different clinical indications. This heterogeneity between individuals is even observed in the cellular niches of each tissue within an organism, all the way down to the single-cell. Understanding the ageing process, and elucidating the mechanisms involved, therefore requires a multi-layered approach when determining the changes that occur with age.

Within the cellular niche of the bone marrow, developing progenitor B cells rely on a stable microenvironment of growth factors and cell interactions to co-ordinate their differentiation. In healthy circumstances, it has been reported that IGF1, supplied by an osteoblast niche, supports the differentiation of Pro-B cells into Pre-B cells[84,285]. During this transition, the B cells undergo V-DJ_H recombination to produce a functioning Mu protein that forms part of the BCR.

As touched upon in the Introduction, the development of progenitor B cells is disrupted in ageing, and the findings from *Koohy et al* suggests an exciting mechanism involving the epigenetic suppression, and subsequent downregulation, of Irs1 in aged Pro-B and Pre-B cells[275]. Active suppression of the IGF1R signalling pathway at a stage when it is required for development could contribute to the ageing phenotype, and would fit with the vast literature linking IGF1R signalling to ageing in other tissues such as muscle and brain[286,287,288].

Evidence for the active suppression of IGF1R signalling in aged developing B cells is mounting, but the reasons for this remain broad and speculative[289]. One model that has

been reported in several different aged tissues and models is an upregulation of the Akt/PKB (protein kinase B) signalling pathway[290]. The significance to IGF1R signalling on Akt upregulation could lie in an established negative feedback mechanism following Akt overstimulation, whereby Irs1 is specifically targeted for inactivation[291,292]. Indeed, *Koohy et al* showed by KEGG pathway enrichment an upregulation of the PI3K-Akt signalling pathway in aged Pre-B cells[275].

It should be noted however that the heterogeneous nature of ageing exposes a limitation to the *Koohy et al* study: namely, that the authors pooled together the bone marrow of individual aged mice in order to "... minimize [the] confounding effects of heterogeneity". Doing so however means that they cannot definitively conclude for example that suppression of Irs1/IGF1R signalling is a hallmark of aged developing B cells in *all* individuals. Moreover, it is tempting also to hypothesise that the heterogeneity of aged phenotypes between individual organisms is the result of changes at the single-cell level to the composition of established cell populations. For example, several scRNAseq studies of ageing found a reduction of cells undergoing cell proliferation[293], and a study on aged HSC populations found changes in both cell cycle states and cell composition that impacted cell fate decisions[294], whilst a study looking at naïve/active $CD4^+$ T cells reported cell-to-cell transcriptional variability in the aged mice[295]. Ageing could also result in the diversion of a cell's development to an unconventional cell state that is not present in young, healthy individuals – as has been reported in B-cells from the spleen of aged mice[296]. In the case of progenitor B cells, the disruption of their bone marrow niche with age could lead to changes in the composition of transitioning progenitor cell states, or presence of new B-cell states entirely.

Another with regards to ageing heterogeneity is whether certain aged phenotypes correlate to a specific, often defective, functional output. For progenitor B cells, the functional output is successful and efficient V(D)J recombination of both heavy and light chain gene loci to produce a pool of mature naïve B-cells with a diverse repertoire of BCR's. Aged B cells have been associated with a decrease in antibody repertoire diversity, and an increased prevalence of auto-antibodies[297,298]. It would therefore be interesting to see if there is a correlation between antibody repertoire diversity and overall V_H-gene representation, and other definable age-associated characteristics.

To resolve the questions posed, my approach has been to extract progenitor B cell populations from the same individual young and aged mice, and for each individual to generate both transcriptomic and VDJ_H repertoire data from their Pro-B and Pre-B cell populations (using bulk RNAseq and DNA VDJseq techniques respectively). In doing so, perform pairwise comparisons that link transcriptomic variation to BCR repertoire diversity across the Pro-B to Pre-B cell transition. To support these studies, single-cell RNAseq has also been conducted on the progenitor B cells of different young and aged mice, to capture variation at the single-cell level. The aim of these multi-layered, multi-faceted datasets is to deconvolute the heterogeneity of ageing in early B-cell development, expose mechanisms of action, and determine the clinical implications.

3.2 Transcriptomic variation of Pre-B cells reveals age-associated clustering of mice

3.2.1 Young vs Aged Pro-B and Pre-B cells

From individual young and aged mice, Pro-B/FrBC ($CD19^+AA4.1^+CD25^-IgM^-IL7R\alpha^+CD43^{hi}CD24^{lo}$), Early Pre-B/FrC' ($CD19^+AA4.1^+CD25^-IgM^-IL7R\alpha^+CD43^{lo}CD24^{hi}$), Late Pre-B/FrD ($CD19^+AA4.1^+CD25^+IgM^-$), and Immature-B/FrE ($CD19^+AA4.1^+CD25^-IgM^+$) cells were sorted by FACS (Figure 3-1). To ensure sufficient coverage of aged heterogeneity, a total of 4 young and 12 aged mice were processed for this analysis. Of note, it was reported by *Koohy et al* that their FACS-sorted aged Pro-B cell fraction ($B220^+CD19^+CD43^+CD25^-IgM^-$) may have contained some mature B cell contaminant, owing to the presence of "upregulated" genes associated with mature-B cells, such as IgJ. To counter this, more progenitor B cell markers – such as the progenitor B cell-specific marker AA4.1 – were included in the defining of these cell populations.

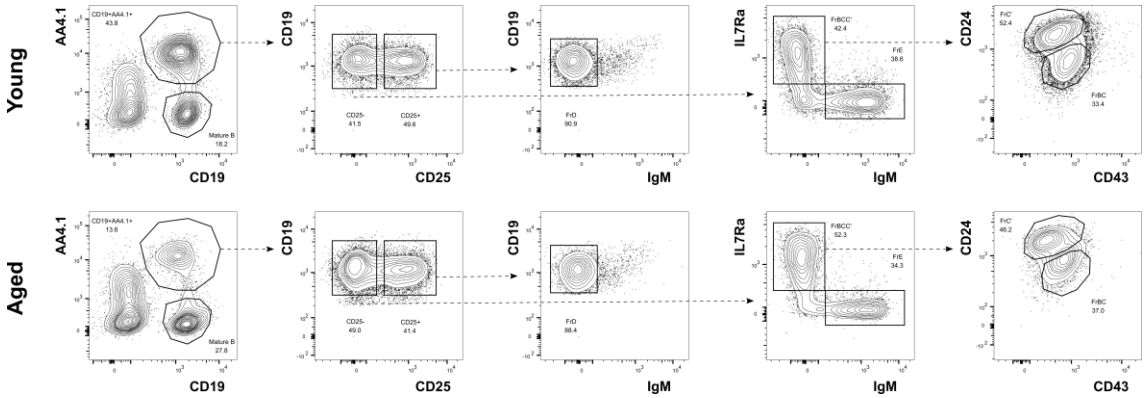

Figure 3-1: Sorting of progenitor B cells by FACS. Representative FACS plots showing the gating strategy to sort Pro-B (FrBC), Early Pre-B (FrC'), Late Pre-B (FrD), and Immature-B (FrE) from the total bone marrow of individual Young (n=4, top panel) and Aged (n=12, bottom panel) mice. All cells were gated for live singlet lymphocytes prior to this gating strategy.

For the Pro-B and Late Pre-B cells (herein named "Pre-B" cells, unless stated), RNA and DNA were extracted to generate RNAseq and VDJseq libraries respectively. Initial transcriptomic comparisons between Young (n=4) and Aged (n=12) mice by DESeq2 identified 916 differentially-expressed (DE) genes in the Pro-B cells (478 up, 438 down) and 1164 DE genes in the Pre-B cells (594 up, 570 down). *Koohy et al* detected only 136 DE genes in their aged Pro-B cells, and 55 DE genes in their aged Pre-B cells – with 29% (40/136) and 59% (33/56) of these genes also being detected in the respective aged Pro-B and Pre-B cell fractions of this study. The differences in DE gene detection could be the result of differences in the age of the mice used (19-22 months versus 24-27 months), the use of batch effect correction by *Koohy et al* (their batch effect between biological replicates was corrected using DESeq2), and/or differences in the potential for mature B cell contamination in the cell populations analysed (only 2/21 of the purported aberrantly-detected DE genes of aged Pro-B cells in *Koohy et al* were also detected in this study: *Igj and H2-DMb1*) – these features can contribute to the explaining of the mild overlap of 29% between the aged Pro-B cell DE genes. Nevertheless, there are obvious similarities between both studies in the DE genes that have the strongest p-value, such as *Rftn2*, *Plxna2*, and *Rnf125*. For some of these detected DE genes, there are no roles that have been defined for them in the regulation of normal early B cell development and so their differential expression in ageing is not immediately obvious.

Instead, the focus of this analysis will be on our current understandings of B cell development.

Of the 916 and 1164 DE genes of aged Pro-B and Pre-B cells respectively, 124 genes were differentially expressed in both cell populations versus their young counterparts. Strikingly, there was also a strong positive R^2 correlation (0.866) in the Log-fold change (LFC) in expression of the 124 DE genes between Pro-B and Pre-B cells. This demonstrates that the directionality and intensity of these 124 DE genes in ageing is maintained across the Pro-B and Pre-B cell stages (Figure 3-2).

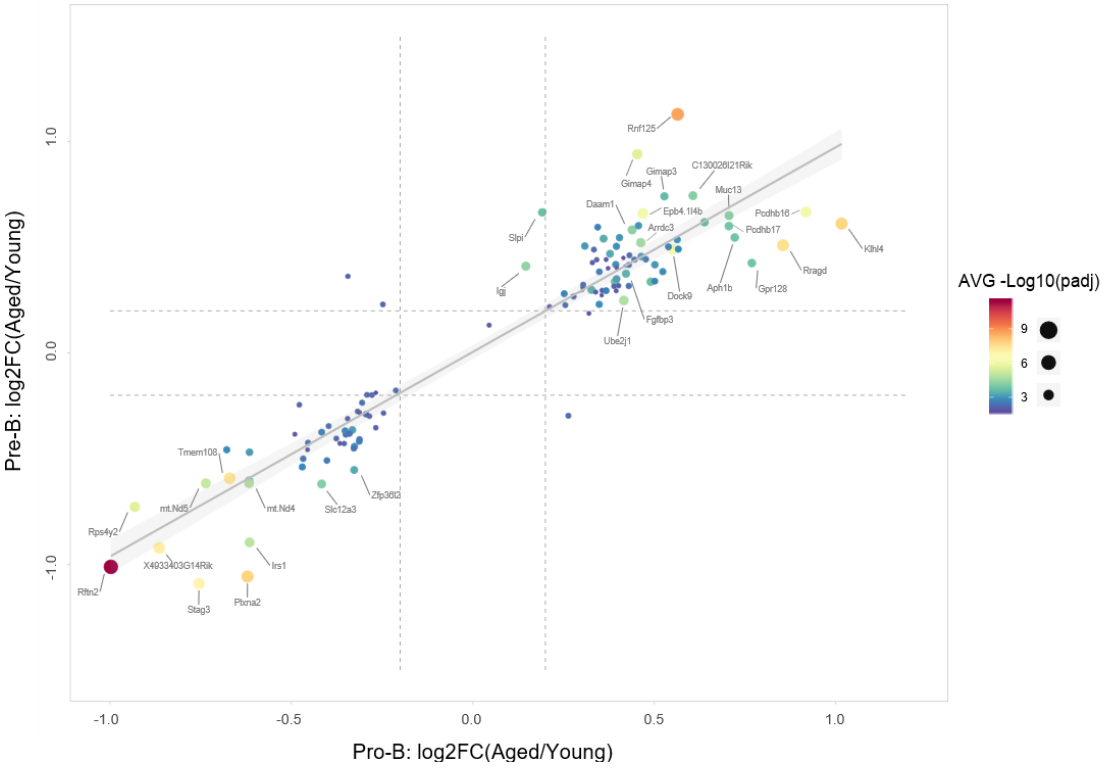

Figure 3-2: Log2 fold expression change in genes between the Aged and Young mice that were differentially expressed across the Pro-B and Pre-B cell stages. 124 genes were differentially expressed in both Pro-B (x-axis) and Pre-B (y-axis) cells of aged mice (R^2=0.866). Values below 0 are downregulated in ageing and values above 0 are upregulated in ageing. *The size and colour of each gene represents the average -Log10(padj) value for Pro-B and Pre-B cells (Aged/Young).*

Focussing on the genes with the largest LFC and strongest p-value reveal preliminary insights into potential pathways disrupted in these aged Pro-B and Pre-B cells. Members of the GIMAP family of immune-associated GTPases for example appear to be

upregulated in ageing. In particular, *GIMAP3* and *GIMAP4* are upregulated in both Pro-B and Pre-B cells (*GIMAP8* and *GIMAP's 6* and *7* are also DE in Pro-B and Pre-B cells respectively). Most of the literature on the GIMAP family have been conducted in T cells, but it would seem that they are involved in lymphocyte homeostasis, their expression is mediated by inflammation, and deficiency leads to inflammatory and autoimmune diseases[299,300].

The cell adhesion molecules *Pcdhb16* and *17* of the Protocadherin Beta Cluster family of genes are also upregulated across the Pro-B to Pre-B cell stages, suggesting more cell-cell interactions with age. On the other hand, there is a strikingly large number of mitochondrial genes coding for mitochondrial respiratory complexes that are significantly downregulated in ageing. Complex IV (*mt-Cyb*) along with 4 out of the 7 components for Complex I (*mt-Nd2, mt-Nd4, mt-Nd5, mt-Nd6*) are downregulated in both Pro-B and Pre-B cells, with a further 5th component of complex I (*mt-Nd1*) being downregulated in Pro-B cells only. There are even some genes known to play vital roles in Pro-B to Pre-B cell selection that are differentially expressed in these aged mice. For example, the RNA binding protein Zfp36l2 is known to promote progenitor B cell quiescence to facilitate in V(D)J recombination[301], and in aged Pro-B and Pre-B cells this gene's expression is downregulated. Reassuringly, and in line with the literature, Irs1 is also downregulated in aged Pro-B and Pre-B cells.

While this "bulk" style analysis comparing the Pro-B and Pre-B cells of all aged mice together against young shows dysregulation at the transcriptional level, it does not take into consideration the heterogeneity that exists between the individual aged mice. To this end, attempts to capture this transcriptomic variability were explored.

3.2.2 Hierarchical and K-means clustering on Transcriptomic Variability

To measure the transcriptomic variance of the Pro-B and Pre-B cell populations between all of the Young (n=4) and Aged (n=12) mice, a combination of clustering methods was applied. Hierarchical clustering was used to visualise the similarities of each individual, using a branching dendrogram, then cluster boundaries between the individual mice

were set by k-means. Through this method, the Pro-B cell populations did not show any discernible clustering, as indicated by the many levels of dendrogram branching and the split clustering of the young Pro-B cells (Figure 3-3). However, the Pre-B cells showed robust clustering of all the young individuals together with 4 out of the 12 aged (AD2, AD4, AD5, and AD7; coloured green), with the remaining 8 aged individuals forming their own separate cluster pairs of 4 each (AD1, AD3, AD6, AD9; coloured orange; AD8, AD10, AD11, AD12; coloured red). Visualising these clusters based on their principal components affirms the clustering classification of the aged mice by transcriptomic variance of their Pre-B cells. Doing so also reveals a level of transcriptomic similarity among the Pro-B cells of the young mice despite being unable to form their own distinct cluster when amongst the aged Pro-B cells. The positioning by both hierarchical cluster and principal component of the newly-established aged Pre-B cell clusters relative to young means that these 3 aged subgroups will hereafter be referred to as “Mild” (green), “Moderate” (orange), and “Severe” (red) to denote their degree of separation from the Young Pre-B cells. Given also that these Pro-B and Pre-B cells are derived from the same mice, the same subgroups can also be applied to the corresponding Pro-B cell populations.

Independent of one another, transcriptomic comparisons by DESeq2 were made between Young (n=4) and each of the 3 Aged subgroups (Mild n=4, Moderate n=4, Severe n=4). For the Pre-B cells, this lead to the generation of DE gene sizes that matched the anticipated severity of dysregulation: 148 DE genes for Mild (75 up, 73 down), 2561 DE genes for Moderate (1182 up, 1379 down), and 3596 DE genes for Severe (1770 up, 1826 down). On the other hand, when comparing Pro-B cells, the level of dysregulation in the Mild and Moderate subgroups was comparable, and it was the Severe subgroup that stood out as most dysregulated at this stage: 155 DE genes for Mild (88 up, 67 down), 143 DE genes for Moderate (78 up, 65 down), and 761 DE genes for Severe (400 up, 361 down). With the exception of Mild, based on the level of differential expression across the Pro-B and Pre-B cell stages, this data suggests that there is an age-associated dysfunction in the development of Pro-B cells transitioning into Pre-B cells.

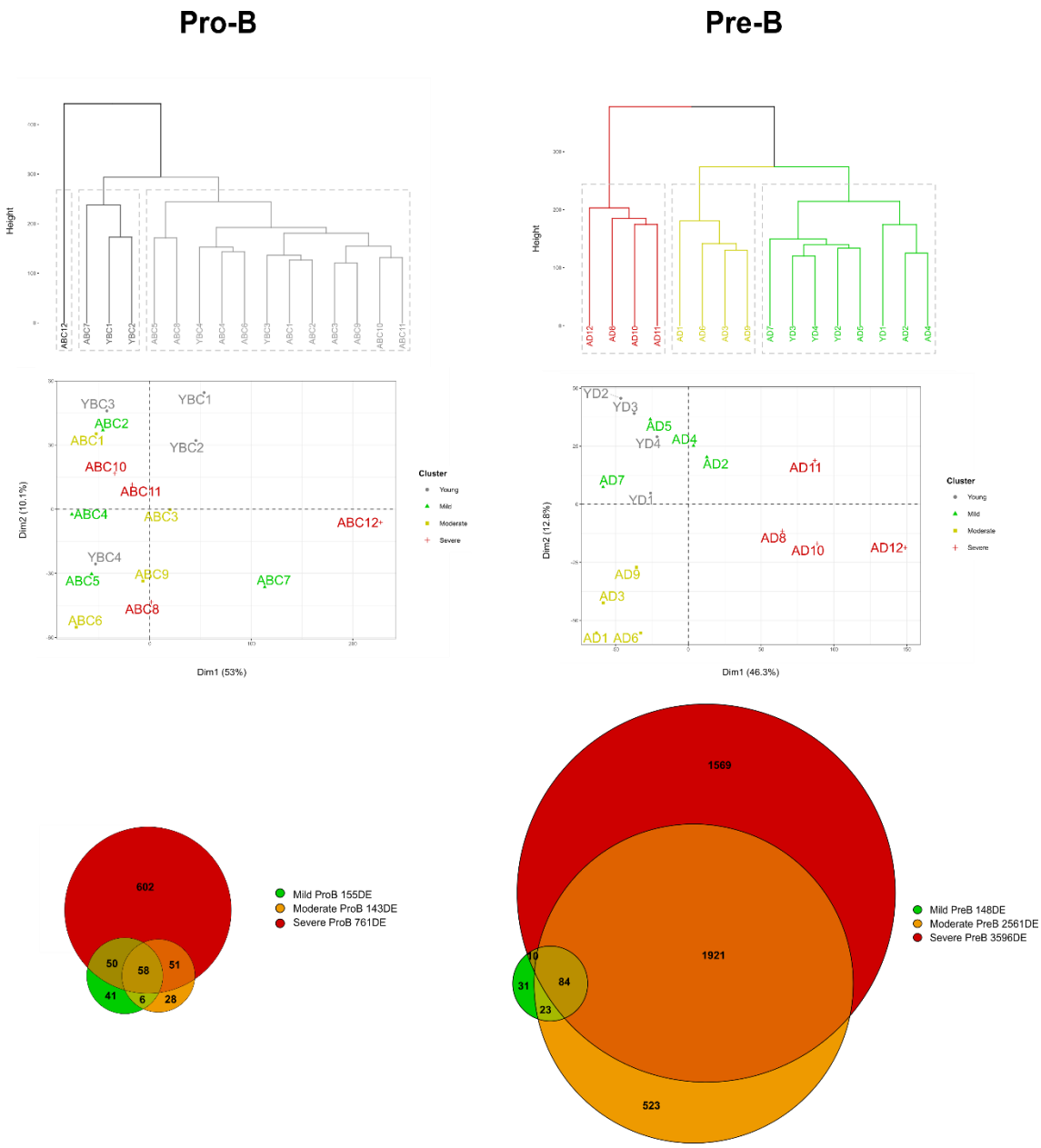

Figure 3-3: Clustering of individual Pro-B ("BC") and Pre-B ("D") cells based on transcriptomic variance. Clustering of Pre-B cells by hierarchical and k-means clustering (top panel) and PCA (middle panel) into Young (grey) and 3 distinct aged clusters: Mild (green), Moderate (orange), Severe (red). Corresponding Pro-B cells were subgrouped into the same clusters as their Pre-B cells. Each aged subgroup was compared to Young by DESEq2 and the results visualised by proportional Venn diagram (bottom panel) to determine aged subgroup similarities in DE genes.

With the aged heterogeneity captured and quantified, finding shared differential expression patterns between the aged subgroups in relation to the young group should reveal commonalities within the variability. For example, whilst the Severe mice possess 79% (602/761) DE genes for their Pro-B, and 44% (1571/3596) DE genes for their Pre-B

cells that are unique to this subgroup, the Moderate mice share 76% (109/143) DE genes for their Pro-B and 78% (2005/2561) DE genes for their Pre-B with these Severe mice. What this might indicate is a shared aged phenotype amongst the Moderate and Severe mice that is, as its name suggests, more “severe” in the Severe subgroup.

It is also important to deconvolute the genes that are differentially expressed in all aged mice from these aged subgroup overlaps; in particular, those genes that are differentially expressed in both their Pro-B and Pre-B cells. Identifying those key genes would support the possibility of their role in the dysregulation in Pro-B to Pre-B cell differentiation. For Pro-B cells, there are 58 DE genes shared amongst the 3 aged subgroups, and for Pre-B cells there are 84 DE genes (Figure 3-4).

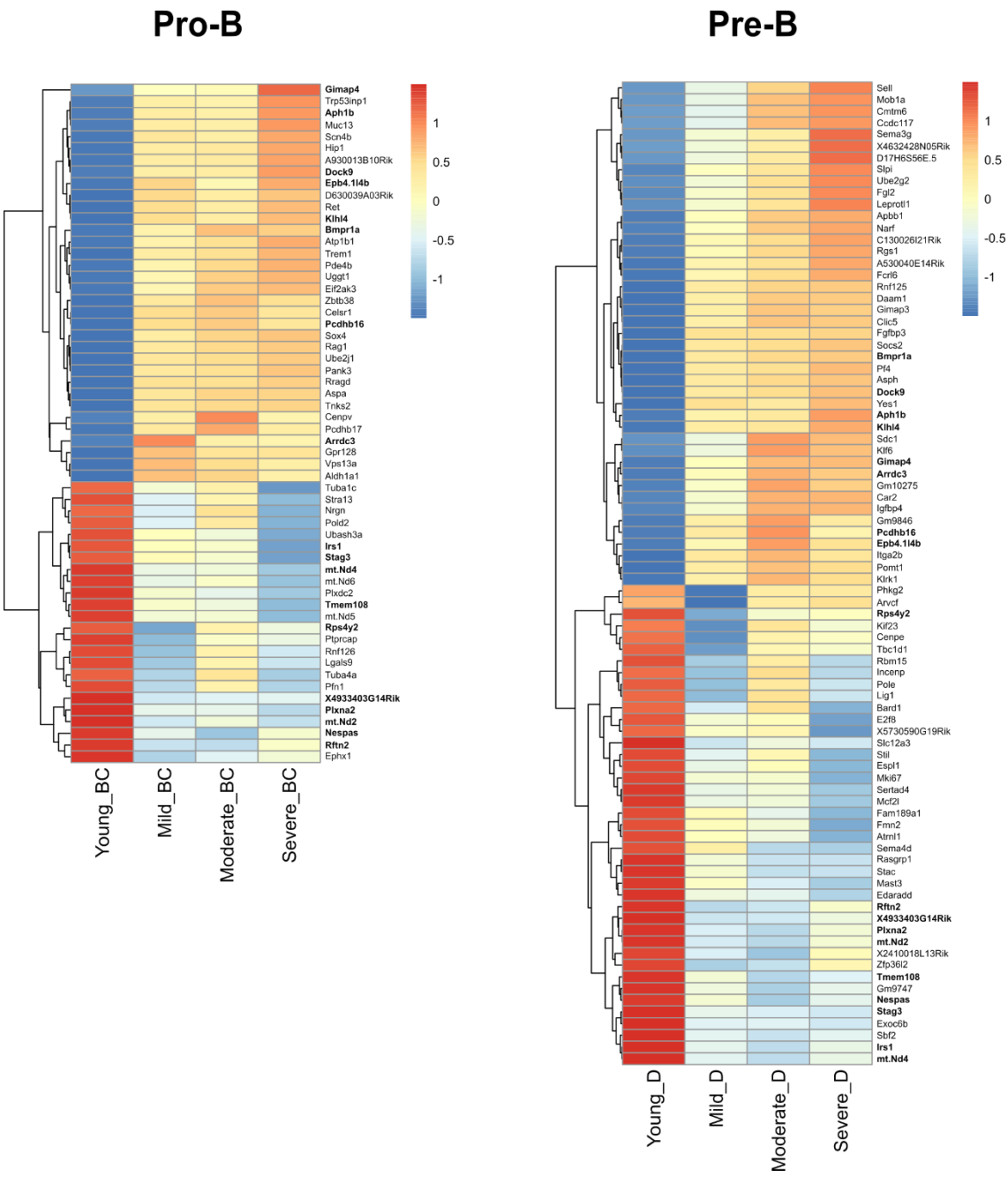

Figure 3-4: Genes that are differentially expressed in all aged Pro-B and Pre-B cells subgroups (Mild, Moderate, Severe). There are 58 genes differentially expressed in all aged Pro-B cell subgroups (left), and 84 genes differentially expressed in all aged Pre-B cells subgroups (right). 18 of these genes are differentially expressed in all Pro-B and Pre-B cell subgroups (highlighted bold).

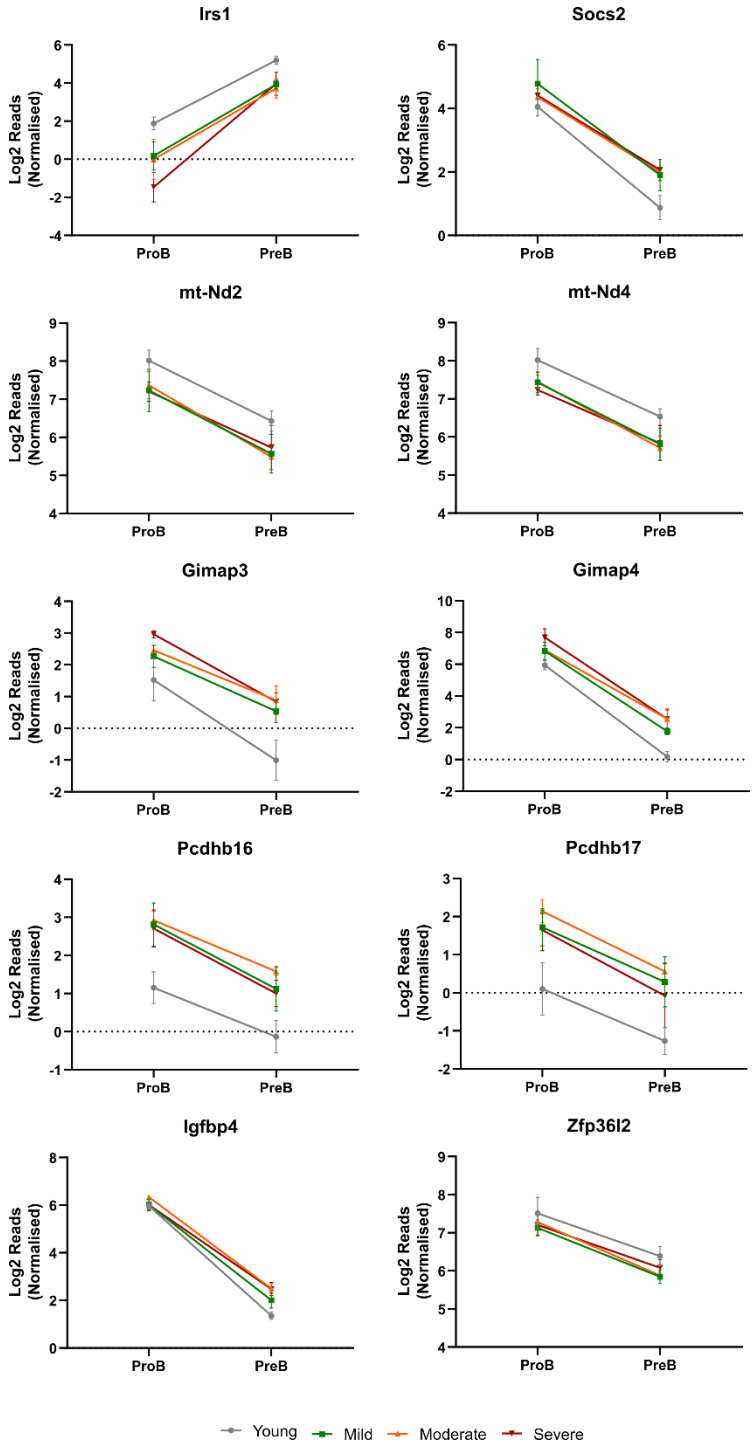

Figure 3-5: Genes of interest that are differentially expressed across the aged Pro-B to Pre-B cell stages. Irs1 is one of the 18 genes that are differentially expressed (downregulated) in all aged Pro-B ad Pre-B cell subgroups, along with mt-Nd2 (downregulated), mt-Nd4 (downregulated), the GTPase GIMAP4 (upregulated), and adhesion molecule Pcdhb16 (upregulated). GIMAP3 (upregulated) is also differentially expressed in all aged Pre-B cells but only the Severe Pro-B cells, and Pcdhb17 is upregulated in all except Severe Pre-B cells. Socs2 (upregulated), Igfbp4 (upregulated) and Zfp36l2 (downregulated) are only differentially expressed in the Pre-B subgroups. (Log2 reads per million reads).

Hierarchical clustering of these DE genes captures some interesting subgroup-specific expression dynamics. This is particularly prominent between the Pre-B cell groups. For example, there are genes which are up/down regulated to the same intensity across all aged Pre-B subgroups (e.g. *Stag3* and *Rnf125*), but there are also those genes that show a gradient of differential expression across the aged subgroups (e.g. *Fmn2* and *Sell*) (Figure 3-4). Perhaps the most pertinent finding from this analysis is the sustained presence of several DE genes that were identified in the previous analysis, prior to the introduction of subgrouping. These DE genes include *mt-Nd2, mt-Nd4, GIMAP3, GIMAP4, Pcdhb16, Pcdhb17, Zfp36l2, Igfbp4* and, crucially, *Irs1* (Figure 3-5). There are a total of 18 genes that are differentially expressed in all aged subgroups across both Pro-B and Pre-B cell stages (highlighted bold on the heatmaps). What this may suggest is that these 18 genes could be contributing to the core age-associated cellular defects that on early-onset produce a Mild phenotype, but which can eventually manifest into a Moderate or even Severe phenotype.

An effect of such a phenotype on progenitor B cells and their ability to differentiate efficiently may hinge on the suppression of its IGF1R signalling. As is evident from these results, not only is there a universal downregulation in Irs1 expression across all aged Pro-B and Pre-B cells, but so too is there an upregulation in the IGF1R suppressor *Socs2*[302,303] and the IGF1 binding protein *Igfbp4* – known to be expressed by senescent cells[304], prolong the half-life of IGF1, and inhibit its binding to IGF1R in lymphocytes[305] – in all aged Pre-B subgroups (Figure 3-5).

The comprehensive downregulation of *Irs1* in aged Pro-B and Pre-B cells, irrespective of heterogeneity, forms the basis for exploring cellular mechanisms that could be driving this suppression. As such, uncovering the biological pathways involving Irs1 that are dysregulated in these developing aged progenitor B cells could provide further insight into possible mechanisms at play in ageing.

3.2.3 Akt signalling: an Irs1-containing pathway that is upregulated in ageing

Enrichment of biological pathways dysregulated in aged Pro-B and Pre-B cells was achieved by Gene set enrichment analysis (GSEA) of Gene Ontology (GO) symbols. The initial aim using this method was to extract any pathways enriched across the Pro-B to Pre-B cell transition that involve Irs1. To this end, and to maximise all possible pathways enriched, all Young (n=4) and Aged (n=12) individuals were analysed using the 916 DE genes of the aged Pro-B, and a combined set of 4171 unique DE genes that are present in either the Mild, Moderate, or Severe subgroups of the aged Pre-B cells (Table 1). This analysis yielded only 2 out of 722 enriched GO symbols that were significant in the aged Pro-B cells (0.28%; p-value <0.05) versus 576 out of 2359 in the aged Pre-B cells (24.4%; p-value <0.05). Retaining all the enriched GO symbols (722 for Pro-B; 2359 for Pre-B) and filtering those that include Irs1, leave only 4 GO symbols that are enriched in both Pro-B and Pre-B cells. Of these, only 1 is statistically significant in the aged Pre-B cells: Protein Kinase B Signalling – also known as Akt.

	Pre-B (Young n=4, Aged n=12; 4171DE genes)				**Pro-B (Young n=4, Aged n=12; 916DE genes)**			
	SIZE	*NES*	*NOM p-val*	*FDR q-val*	*SIZE*	*NES*	*NOM p-val*	*FDR q-val*
LIPID CATABOLIC PROCESS	64	1.70	0.004	0.03	-----	--------	--------	--------
PROTEIN KINASE B SIGNALING	***59***	***1.46***	***0.04***	***0.13***	***20***	***1.14***	***0.30***	***0.69***
CAVEOLA	17	1.41	0.07	0.17	-----	--------	--------	--------
INSULIN SECRETION	46	-1.04	0.35	0.79	-----	--------	--------	--------
RESPONSE TO INSULIN	73	1.03	0.42	0.65	18	-0.83	0.63	1
RESPONSE TO PEPTIDE HORMONE	99	1.02	0.44	0.67	28	-0.78	0.73	1
MAMMARY GLAND DEVELOPMENT	32	0.90	0.62	0.83	-----	--------	--------	--------
CILIARY BASAL BODY	28	0.71	0.88	0.99	-----	--------	--------	--------
PROTEIN DOMAIN SPECIFIC BINDING	198	-0.84	0.93	1	46	-1.26	0.17	1
CELLULAR RESPONSE TO INSULIN STIMULUS	62	0.64	0.98	1	-----	--------	--------	--------
PROTEIN LOCALIZATION TO NUCLEUS	62	-0.70	0.98	1	-----	--------	--------	--------
INSULIN RECEPTOR SIGNALING PATHWAY	40	-0.61	0.99	1	-----	--------	--------	--------

Table 3-1: Irs1-containing GO symbols that were enriched in aged Pro-B and Pre-B cells by Gene Set Enrichment Analysis (GSEA). All unique DE genes from across the Mild, Moderate, and Severe Pre-B cell subgroup (4171), and the DE genes of the Aged Pro-B cells (916) were used to perform GSEA on GO symbols. This table shows the GSEA output for those enriched GSEA pathways that contain Irs1 in them, ranked on p-value. Size: number of genes from DE gene list that are in this pathway. NES: Normalised Enrichment Score. NOM p-val: Nominal p-value. FDR q-val: False Discovery Rate q-value. Empty rows: GO symbol not enriched.

Looking more closely at the *Protein Kinase B Signalling* GO symbol, of its 269 assigned genes, 20 were differentially expressed in the aged Pro-B cells (13 up; 8 down) and 59 were differentially expressed in the aged Pre-B cells (35 up; 24 down). Normalised Enrichment Scores (NES) of 1.14 and 1.46 respectively indicate that, overall, the Akt signalling pathway is upregulated in aged Pro-B and Pre-B cells. Contradictory to this trend however, is that signalling components upstream of Akt that are involved in the IGF1R signalling pathway appear to be downregulated. For example, as has already been established, *Irs1* is downregulated in all aged Pro-B and Pre-B cells, but *Igf1r* itself is also downregulated to a statistical significance in Moderate and Severe aged Pre-B cells, as is its adaptor protein *Grb2* (Figure 3-6). Such a trend would suggest that a negative feedback mechanism for Akt overstimulation may be operating in these aged progenitor B cells that could be supressing the IGF1R signalling pathway at the transcript (and potentially protein) level. Support for this claim could be in the sustained upregulation of known negative feedback regulators to other growth factor receptors, such as *Spry2* (for FGFR[306]) and *Pdcd6* (for VEGFR[307]), and the upregulation of miRNA's in the aged Pre-B cells of the *Koohy et al* study that are known to target *Irs1* (*miR-221/222*) and *Igf1r* (*Let-7f-2*) transcripts. Further still, the upregulation of genes involved in other known signalling pathways that utilise Akt could provide yet more insight into what mechanisms could be driving this proposed Akt overstimulation in ageing. These include genes involved in inflammation (*Il1b*), cell migration (*Ccl5*, *Cx3cr1*) and cell adhesion (*Itgb1*, *Itgb1bp1*). Interestingly, despite there being no known study to suggest that IGF1 is expressed by B cells, *Igf1* was transcriptionally upregulated in Severe aged Pre-B cells. Although, given that the expression levels are low, and only significant in the most severe aged Pre-B subgroup, expression at the protein level would be unlikely, but this should validated.

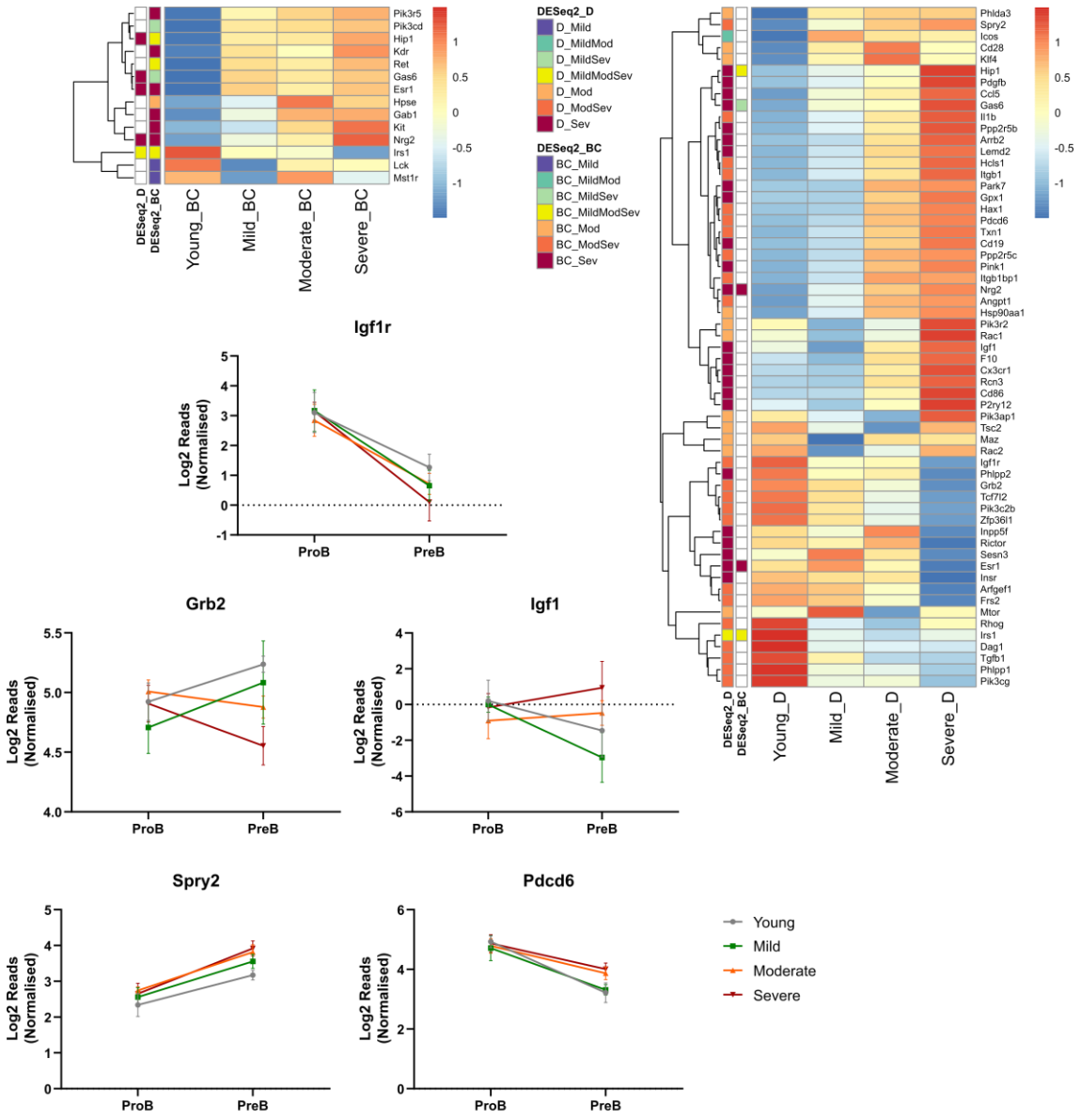

	Pre-B *(Koohy et al 2018)*		
	Log2 Fold Change (Aged/Young)	*p-val*	*FDR (padj)*
Let-7f-2	0.512	0.002	0.023
miR-222	0.539	0.001	0.019
miR-221	0.621	0.0001	0.003

Figure 3-6: Enrichment of the Protein Kinase B (PKB) Signalling Pathway across aged Pro-B and Pre-B cells. DE genes that were enriched for the PKB pathway in aged Pro-B (left heatmap) and Pre-B (right heatmap) cells, split by subgroup (Mild, Moderate, Severe) and normalised by z-score for each gene. Each gene is annotated to show which aged Pro-B or Pre-B subgroups have this gene differentially expressed versus Young by DESeq2. Gene expression in Pro-B and Pre-B cells of 5 genes from these heatmaps plotted together: Igf1r, Grb2, Igf1, Spry2, and Pdcd6. Igf1r and its adapter protein Grb2 are downregulated in Moderate and Severe Pre-B cells, and the PKB negative feedback regulators Spry2 and Pdcd6 are upregulated in Moderate and Severe Pre-B cells. Igf1 appears to be upregulated at low levels in Severe

Pre-B cells only. Extraction of short RNAseq data from the aged Pro-B ad Pre-B cells of Koohy et al for DE miRNA that are in the PKB GO symbol are presented in the table (bottom). (Log2 reads per million reads).

3.2.4 Common pathway dysregulation amongst the subgroups of aged Pro-B and Pre-B cells

To determine what biological pathways are dysregulated amongst the aged subgroups, and across the Pro-B and Pre-B cell stages, GSEA was re-applied independently to each Mild, Moderate, and Severe subgroup using their own DE gene sets versus Young (Figure 3-7). For Pro-B cells, this resulted in 2/63 (Mild; 155 DE genes), 5/53 (Moderate; 143 DE genes), and 16/647 (Severe; 761 DE genes) of the GO symbols enriched for in each aged subgroup reaching statistical significance (p-value <0.05). For Pre-B cells, there were 6/27 (Mild; 148 DE genes), 324/1701 (Moderate; 2561 DE genes), and 566/2183 (Severe; 3596 DE genes) statistically significant GO symbols enriched (p-value <0.05). When comparing between the aged subgroups of these Pro-B or Pre-B cells, enriched GO symbols were retained if they reached statistical significance in at least 1 of the 3 aged subgroups. This leaves the aged Pro-B cell subgroups with only 23 (22 up, 1 down) uniquely-enriched GO symbols, versus 651 (551 up, 99 down) between the aged Pre-B cell subgroups, indicative of increased biological dysregulation during Pro-B to Pre-B cell development in ageing.

Strikingly, there was also robust overlap in the enriched GO symbols shared between the subgroups of both aged Pro-B and Pre-B cells, suggesting that, amongst the heterogeneity, there could be common age-related pathways that are dysregulated.

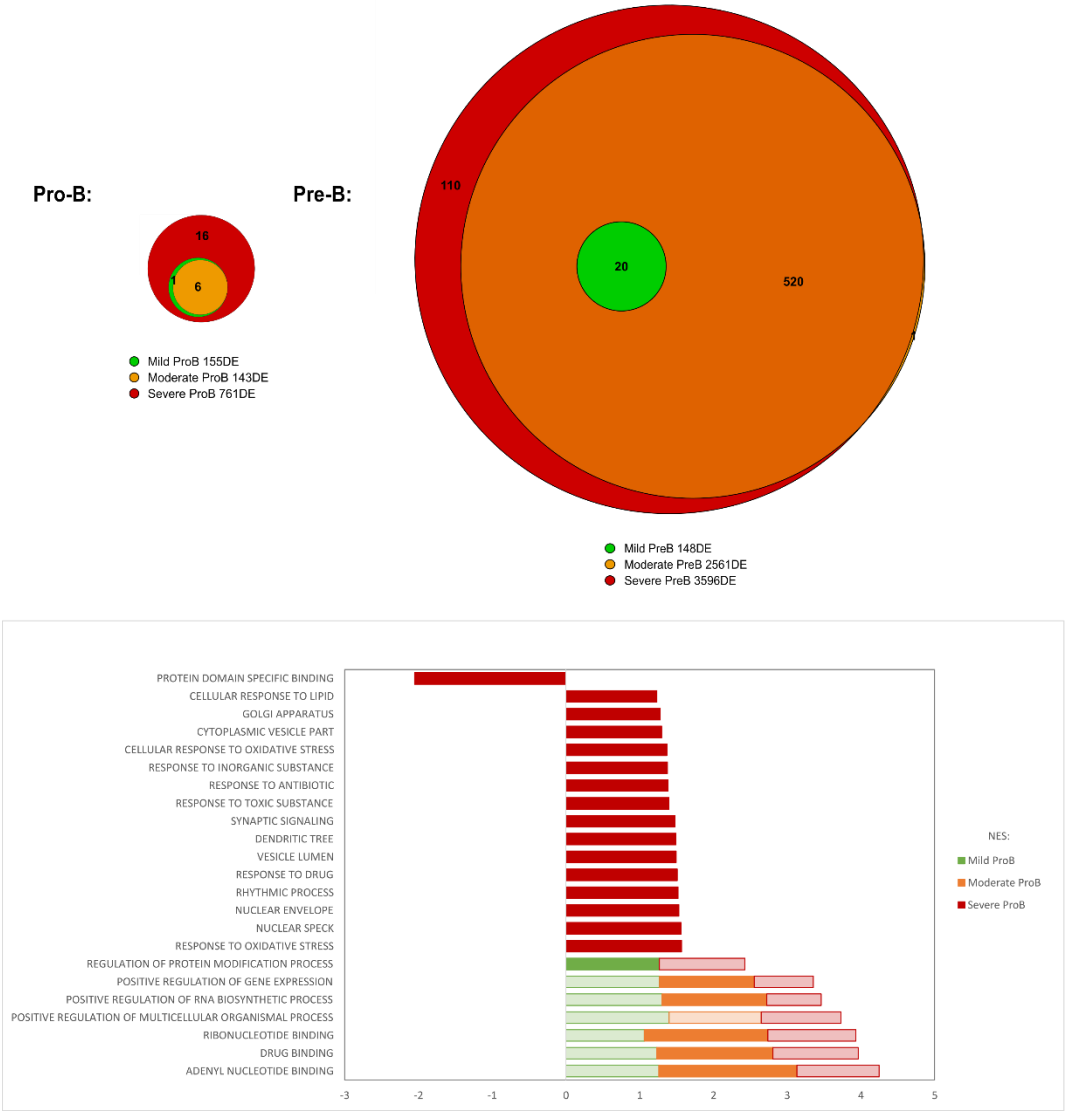

Figure 3-7: All GO symbols enriched by GSEA in aged Pro-B and Pre-B cell subgroups. Pathway enrichment performed on all aged Pro-B and Pre-B subgroups (Mild, Moderate, Severe) using their individual DE gene lists. Shared GO symbols were retained if they reached significance in at least one of the 3 aged subgroups (p-val <0.05). Pro-B cells had a total of 23 GO symbols across the aged subgroups after this filtering method (Venn, left), versus 651 for aged Pre-B cells (Venn, right). The 23 GO symbols of Pro-B cells were further visualised by Normlised Enrichment Score (NES; barplot). Positive: upregulated; Negative: downregulated; Opaque: p-val <0.05; Transparent: p-val >0.05.

From the 23 uniquely-enriched GO symbols of the aged Pro-B cell subgroups, there were no clear or specific pathways of dysregulation, since the GO symbols captured were still very broad (such as *Positive Regulation of Gene Expression*). It is feasible that the potential pathways of interest in these aged Pro-B cells remained below the statistical thresholds (p-value <0.05 in at least 1 of the 3 aged Pro-B subgroups). Additionally,

interpreting the aged Pro-B cell data this way, independently of the aged Pre-B cell data, does not capture pathways that are dysregulated *across* the 2 cell stages. To this end, comparisons were made between the enriched GO symbols of aged Pro-B and Pre-B cells together, as doing so would resolve both of these issues – by uncovering GO symbols that are enriched in both Pro-B and Pre-B cells, but which only have to be statistically significant in 1 of these cell types.

Since there was a robust overlap in GO symbol enrichment, all aged Pro-B cells (n=12) were analysed together again (as done previously in 3.2.3), and compared to the 3 aged Pre-B subgroups (Mild n=4; Moderate n=4; Severe n=4). As expected, this resulted in an increase from 23 to 279 in GO symbols enriched for in aged Pro-B that are also enriched, and statistically significant (p-value <0.05), in aged Pre-B cells. Overall, across both Pro-B and Pre-B cell stages, there were considerably more pathways that were upregulated in ageing than there were downregulated.

20 out of the 651 unique GO symbols enriched across the aged Pro-B and Pre-B cells were shared between all subgroups and cell stages (16 up, 4 down; Figure 3-8). Looking at these GO symbols for common dysregulated pathways once again reveals GO symbols with fairly broad scope – for example, *Protein Phosphorylation*. However, within this small but broad collection of GO symbols were some that can be attributed to the same biological mechanism or pathway. For example, 4 of these GO symbols are involved in cell cycle – *Cell Cycle*, *Cell Cycle Process*, *Mitotic Cell Cycle*, and *Regulation of Cell Cycle* – and appear to be downregulated in the aged Pre-B cells. There are also a collective of upregulated GO symbols that could point to signalling pathways that utilise downstream Akt effector functions – such as *Locomotion* (i.e. cell motility), *Regulation of Immune System Process*, and *Biological Adhesion*. Combined upregulation of multiple signalling pathways that all activate Akt could provide an explanation for the enriched upregulation of the *Protein Kinase B Signalling* GO symbol in these aged Pro-B and Pre-B cells.

More refined evidence to support the upregulation of these Akt signalling pathways in ageing can be found in the remaining 631 GO symbols shared between aged Pro-B and the Moderate and Severe aged Pre-B cells. Amongst the top-10 ranked upregulated GO symbols in this overlap are *Inflammatory Response* and *Leukocyte Migration*, both of which utilise Akt signalling. The recurrence also of cell cycle downregulation in this

overlap of Pro-B and Pre-B cells, in the form of the GO symbol for *Cell Division*, strengthens the idea that aged progenitor B cells are less proliferative. Furthermore, the most enriched GO symbols present in just the Moderate and Severe aged Pre-B cells still show an overrepresentation of upregulated inflammatory and cell migratory signals, and downregulation of cell cycle (cytokinesis) pathways.

Interestingly, another top-ranked GO symbol that is enriched across the aged Pro-B and Pre-B (Moderate and Severe) cells is the downregulation of the GO symbol for *Regulation of Gene Expression Epigenetic*. *Koohy et al* concluded that, in aged Pre-B cells, *Irs1* is epigenetically suppressed by Polycomb-driven H3K27 tri-methylation at its gene promoter. The enrichment therefore of relevant epigenetic GO symbols amongst the aged subgroups could provide transcriptomic evidence that supports these findings. Sure enough, one of the most enriched GO symbols, present only in the Moderate and Severe aged Pre-B cells, is the downregulation of *Histone Methyltransferase Complex*, which will now be explored further alongside other top-ranking enriched GO symbols.

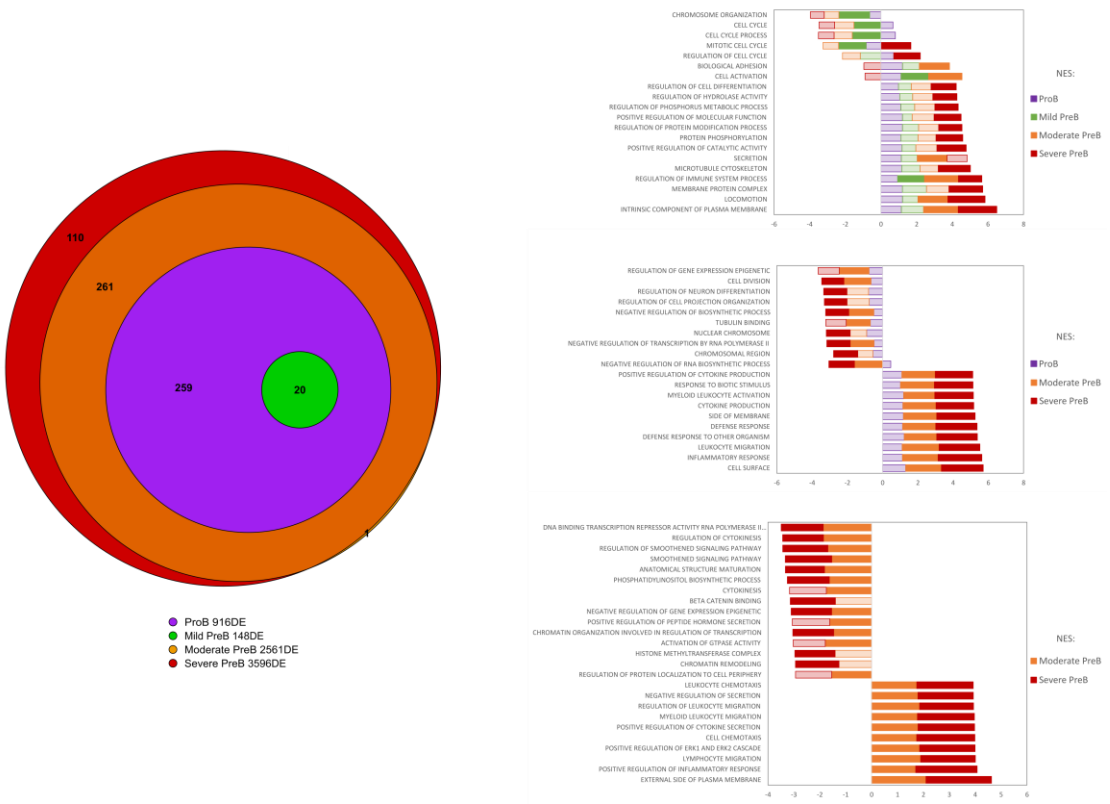

Figure 3-8: Shared GO symbols enriched by GSEA in all aged Pro-B cells versus aged Pre-B cell subgroups. Pathway enrichment performed on all aged Pro-B cells (Aged) and Pre-B subgroups (Mild, Moderate, Severe) using their individual DE gene lists. Shared GO symbols were retained if they reached significance in at least one of the 4 aged subgroups (p-val <0.05). The 20 GO symbols enriched in aged Pro-B and all 3

aged Pre-B subgroups were visualised by Normalised Enrichment Score (NES; top barplot). The most positively and negatively enriched GO symbols (cumulative NES) shared between the Pro-B and Moderate and Severe Pre-B only (middle barplot), and between the Moderate and Severe Pre-B only (bottom barplot), are also plotted. Positive: upregulated; Negative: downregulated; Opaque: p-val <0.05; Transparent: p-val >0.05.

3.2.5 Exploring key pathways dysregulated across ageing Pro-B and Pre-B cells

Looking at the GSEA shared between the different aged Pro-B and Pre-B subgroups has revealed several interesting dysregulated pathways that overlap in both signalling and effector mechanism. Better understanding of the dynamics of these dysregulated pathways in aged Pro-B and/or Pre-B cells could determine the mechanism for their ageing phenotypes, and expose any connections they may have to the suppression of their vital IGF1R signal.

3.2.5.1 Leukocyte Migration (Pro-B, Moderate and Severe Pre-B)

Migration of progenitor B cells has a strong influence on their ability to differentiate. In normal circumstances, Pro-B cells are exposed to cell-cell interactions with the bone marrow niche, whereas Pre-B cells must detach themselves from cell-cell interactions in order to progress. The fact therefore that the aged Pre-B cells display upregulation of several cell adhesion molecules is suggestive of cellular interactions that could interfere in its normal development. Adhesion molecules *Sell* and *Itga2b* of the *Leukocyte Migration* GO symbol for example are strongly upregulated in all aged Pre-B subgroups (Figure 3-9). There are also other cell adhesion molecules not part of this GO symbol that support this idea. The protoocadherin proteins *Pcdhb16 and 17* for example are strongly upregulated in all aged Pro-B and Pre-B subgroups, as identified in earlier analysis (Figure 3-5).

Also of note in the upregulated *Leukocyte Migration* GO symbol is the presence of an array of both chemokines and chemokine receptors. Whilst most are very low-

expressing, they are still differentially increased in expression in the aged Pro-B and/or Pre-B cells. The higher-expressing of the chemokines are Ccl6 and Ccl9, which are upregulated in Moderate and Severe aged Pre-B cells. Interestingly, Ccl9 has been linked to bone resorption, and its upregulation in aged Pre-B cells could therefore be contributing to another established age-associated phenomena in osteoporosis[308]. The more highly expressing chemokine receptors are Cxcr5 in aged Pro-B and Ccr2 in Moderate and Severe aged Pre-B subgroups. Cxcr5 is receptor for B-cell chemoattractant CXCL13, and Ccr2 is for the monocyte chemoattractant MCP1. The upregulation of both of these receptors in ageing perhaps suggests an inflammatory environment that these aged progenitor B cells are responding to.

Furthermore, it could even be that the increased presence of cell-cell interaction and/or increased cell motility as a result of chemoattraction in these aged Pre-B cells is contributing an overstimulation in its Akt pathway. Evidence to suggest this lies in the presence of upregulated integrin molecules (*Itgb1*), chemokines (*Ccl5*), and chemokine receptors (*Cx3cr1*) in both the *Leukocyte Migration* and *Protein Kinase B Signalling* upregulated GO symbols.

	Leukocyte Migration (488 Genes)			
	NES	*NOM p-val*	*FDR q-val*	*# Genes in PKB*
Pro-B	1.11	0.308	0.645	1 (4.4%)
Moderate Pre-B	2.09	<0.0001	0.0005	6 (8.0%)
Severe Pre-B	2.32	<0.0001	<0.0001	9 (9.0%)

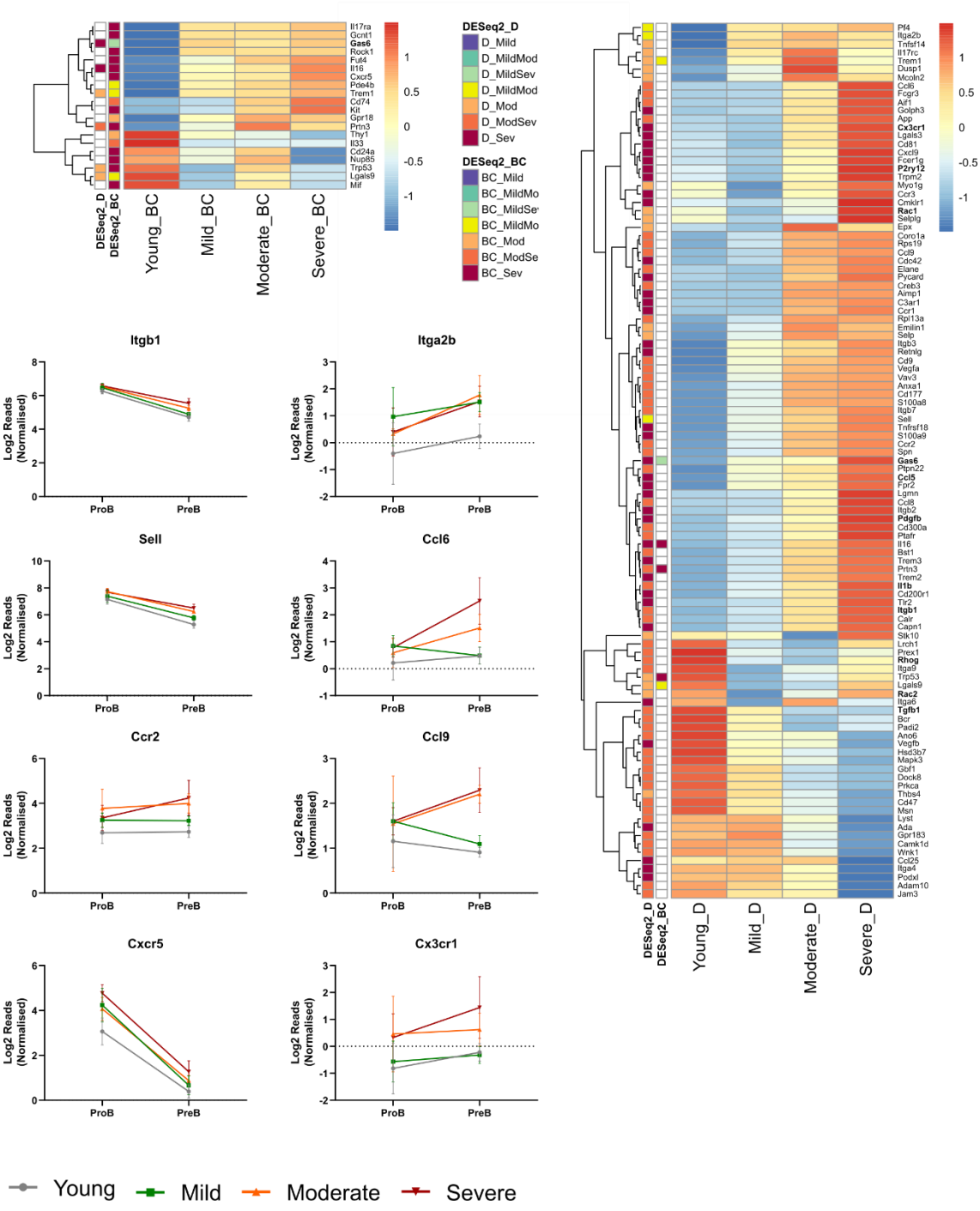

Figure 3-9: Breakdown of the DE genes involved in enrichment of the Leukocyte Migration GO symbol. Summary of the output statistics of the GSEA (table, top; "# Genes in PKB" are the DE genes enriched in Leukocyte Migration that are also enriched in the PKB Signalling GO symbol). DE genes that were enriched for the PKB pathway in aged Pro-B (left heatmap) and Pre-B (right heatmap) cells, split by subgroup (Mild, Moderate, Severe) and normalised by z-score for each gene. Each gene is annotated to show which aged

Pro-B or Pre-B subgroups have this gene differentially expressed versus Young by DESeq2. Genes that are also enriched in the PKB Signalling GO symbol are highlighted bold. 8 genes from these heatmaps looked at in more detail: Itgb1, Itga2b, Sell (adhesion molecules); Ccl6, Ccl9 (chemokines); Ccr2, Cxcr5, Cx3cr1 (chemokine receptors). (Log2 reads per million reads).

3.2.5.2 Inflammatory Response (Pro-B, Moderate and Severe Pre-B)

Inflammageing is a well-established characteristic of ageing tissue[309,310], and so the strong enrichment of an upregulated *Inflammatory Response* GO symbol in these aged Pro-B and Pre-B cells would be consistent with the literature. An inflammatory environment would also tie in with the increased *Leukocyte Migration* observed, as the aged cells respond to chemoattraction and engage in cell motility. What might be driving this inflammatory response in these aged Pro-B and Pre-B cells could be inferred from the genes upregulated in this GO symbol (Figure 3-10). In Pro-B cells for example, there is a robust increase in the expression of the pro-inflammatory receptor *Trem1*, which is known to amplify immune responses and, in the context of ageing, has been shown to upregulate on a diminished DNA damage response[311]. There are also several genes associated with IL1B response that are upregulated across the Pro-B and Pre-B cells stages. For example, in aged Pro-B (Severe) and Pre-B (Moderate and Severe) cells, Cathepsin S (*Ctss*) is upregulated, which is known to increase expression of IL1B. Sure enough, the expression of *Il1b* is also upregulated to a statistical significance in Moderate and Severe aged Pre-B (albeit at low-levels). The additional upregulation of Caspase 1 (*Casp1*) in Moderate and Severe aged Pre-B cells means that any IL1B protein being expressed in these cells will be proteolytically cleaved into its active form[312]. Thus these cells will be actively engaging in an inflammatory response. Of note, *Il1b* is an upregulated gene that is also enriched in the *Protein Kinase B Signalling* GO symbol. Given also that inflammatory responses frequently utilise Akt for its downstream effects, it would be sensible to suggest that, as with *Leukocyte Migration*, the upregulated *Inflammatory Response* and *Protein Kinase B Signalling* are interlinked.

	Inflammatory Response (696 Genes)			
	NES	*NOM p-val*	*FDR q-val*	*# Genes in PKB*
Pro-B	1.13	0.314	0.677	3 (9.4%)
Moderate Pre-B	2.02	<0.0001	0.002	5 (6.0%)
Severe Pre-B	2.48	<0.0001	<0.0001	10 (7.4%)

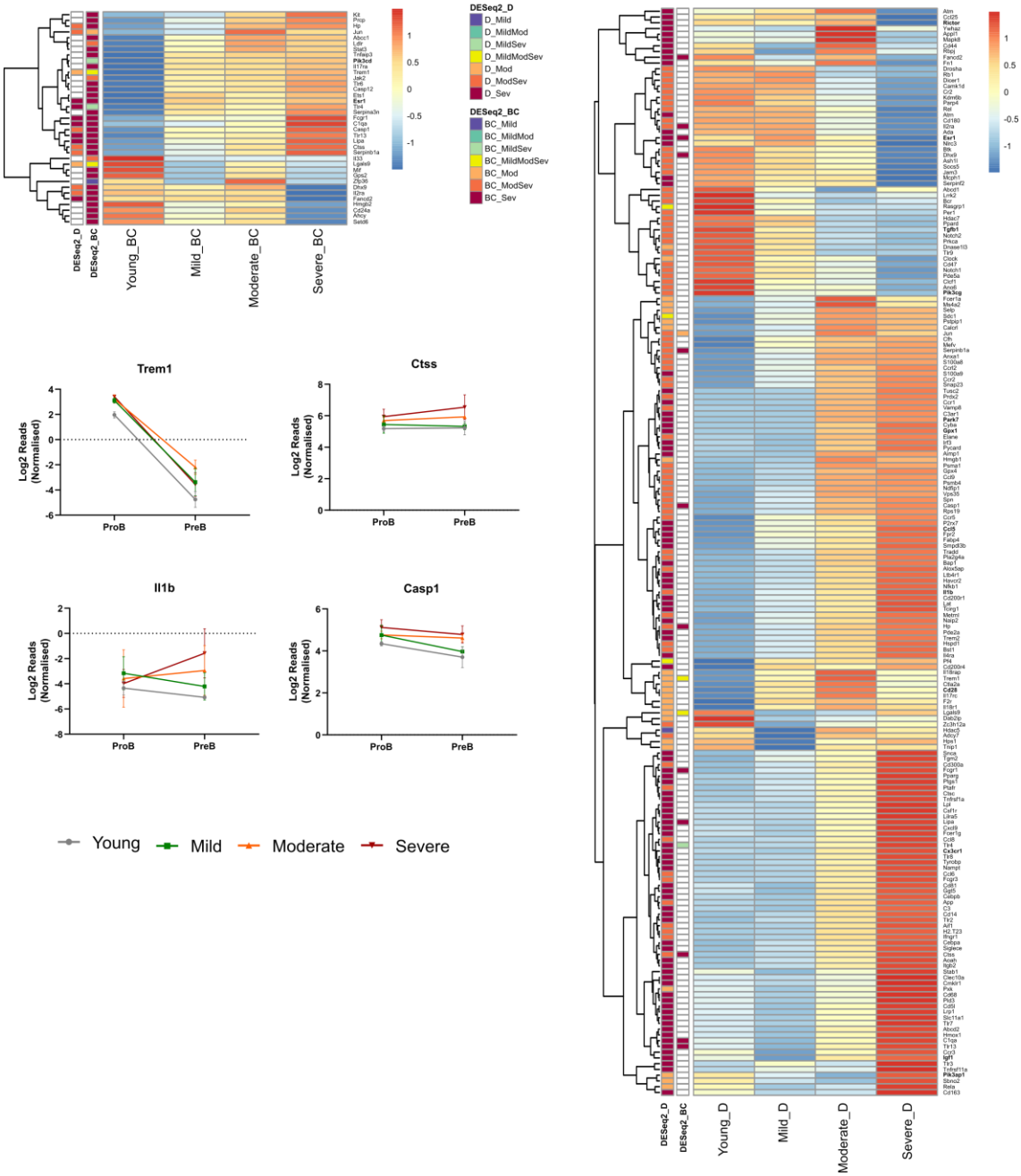

Figure 3-10: Breakdown of the DE genes involved in enrichment of the Inflammatory Response GO symbol. Summary of the output statistics of the GSEA (table, top; "# Genes in PKB" are the DE genes enriched in Inflammatory Response that are also enriched in the PKB Signalling GO symbol). DE genes that were enriched for the PKB pathway in aged Pro-B (left heatmap) and Pre-B (right heatmap) cells, split by subgroup (Mild, Moderate, Severe) and normalised by z-score for each gene. Each gene is annotated to show which aged Pro-B or Pre-B subgroups have this gene differentially expressed versus Young by DESeq2. Genes that are also enriched in the PKB Signalling GO symbol are highlighted bold. 4 genes from these

heatmaps looked at in more detail: Trem1; Ctss, Casp1, Il1b (all linked to Il1b signalling). (Log2 reads per million reads)

3.2.5.3 Cell Division (Pro-B, Moderate and Severe Pre-B)

From the enrichment of the *Cell* Division GO symbol, it would suggest that both Pro-B and Pre-B cells have a downregulation of cell cycle gene expression in ageing (Figure 3-11). However, for Pro-B cells this downregulation is more strongly associated with the Severe subgroup, suggesting a more reduced proliferative capacity of these particular aged cells. Instead, the presence of certain groups of cell cycle genes in the *Cell Division* GO symbol that are differentially expressed across the Pro-B and Pre-B cell stages could be more indicative of a disruption to certain stages of cell cycle progression in these aged cells. For example, the Centromere proteins *Cenpv* and *Cenpe* of the kinetochore complex are differentially upregulated in ageing, with *Cenpv* upregulated at the Pro-B cell stage and *Cenpe* upregulated at the Pre-B cell stage, which could suggest dysregulation of cytokinesis. Additionally, and perhaps surprisingly, there are some genes more commonly associated with asymmetric cell division (meiosis), such as *Stag3* and *Fmn2*, which are strongly downregulated across the Pro-B and Pre-B cell stages in ageing. However given that progenitor B cells do not undergo meiosis, the differential expression of these genes could be through other unknown functions that may or may not be involved in cell division.

As well as cytokinesis, there is evidence to suggest that progression to S-phase is also impacted. For example, there is a distinct shift in cyclin D expression in these aged Pro-B and Pre-B cells, as evident from the upregulation of *Ccnd2* (significant in Severe Pro-B and Mild Pre-B only) and downregulation of *Ccnd3* (significant in Mild Pro-B, and Moderate and Severe Pre-B only). Given the antagonistic nature of cyclin D2 and cyclin D3, this would suggest a change in cell cycle dynamics in the aged Pro-B and Pre-B cells.

	Cell Division (593 Genes)			
	NES	*NOM p-val*	*FDR q-val*	*# Genes in PKB*
Pro-B	-0.67	0.887	1.0	1 (2.9%)
Moderate Pre-B	-1.53	<0.0001	0.468	4 (4.3%)
Severe Pre-B	-1.26	0.055	0.619	5 (3.75%)

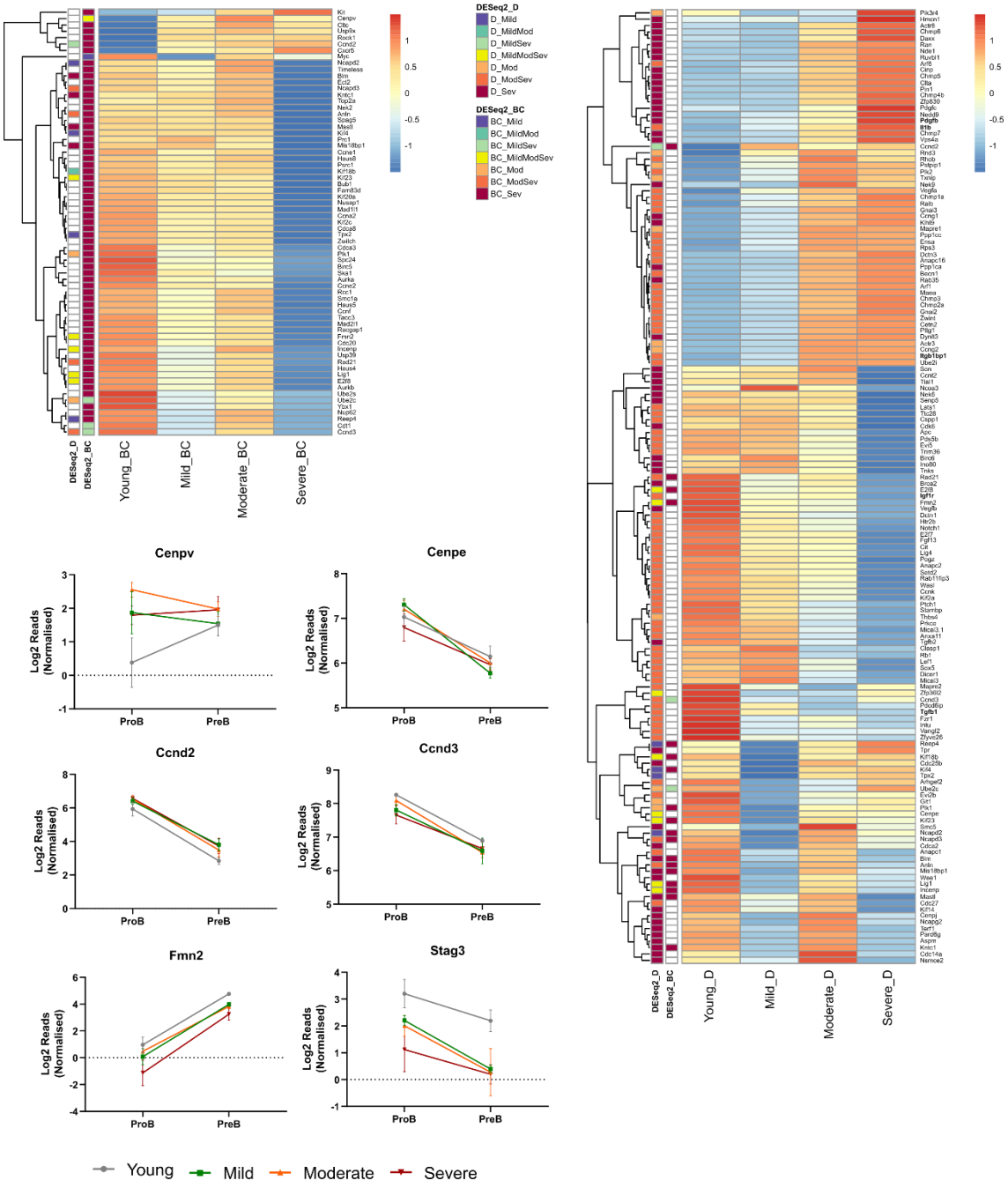

Figure 3-11: Breakdown of the DE genes involved in enrichment of the Cell Division GO symbol. Summary of the output statistics of the GSEA (table, top; "# Genes in PKB" are the DE genes enriched in Cell Division that are also enriched in the PKB Signalling GO symbol). DE genes that were enriched for the PKB pathway in aged Pro-B (left heatmap) and Pre-B (right heatmap) cells, split by subgroup (Mild, Moderate, Severe) and normalised by z-score for each gene. Each gene is annotated to show which aged Pro-B or Pre-B subgroups have this gene differentially expressed versus Young by DESeq2. Genes that are also enriched in the PKB Signalling GO symbol are highlighted bold. 4 genes from these heatmaps looked at in more

detail: Cenpv, Cenpe (centromere proteins); Ccnd2, Ccnd3 (cyclins). An additional 2 DE genes not enriched in this GO symbol but which have a role in cell division are also shown: Fmn2 (downregulated in Severe Pro-B and all aged Pre-B), Stag3 (downregulated in all aged Pro-B ad Pre-B subgroups). (Log2 reads per million reads)

3.2.5.4 Histone Methyltransferase Complex (Moderate and Severe Pre-B)

Changes in the expression of certain epigenetic regulators in aged Pro-B and Pre-B cells could have lasting implications to their cellular function. The enriched downregulation of the *Regulation of Gene Expression Epigenetic* GO symbol in both aged Pro-B and Pre-B (Moderate and Severe) cells, and of the *Histone Methyltransferase Complex* in aged Pre-B cells (Moderate and Severe), could point to such a mechanism (Figure 3-12). For example, the upregulation of the H3K4 demethylase *Kdm5a* in aged Pro-B cells (significant only in Severe) could prevent the active H3K4me3 mark from being retained on some genes, thereby negatively impacting its expression. Perhaps more relevant to the development of progenitor B cells however is the differential expression in the H3K27 demethylase *Kdm6b* (also known as *JMJD3*) and the H3K27 methyltransferase *Ezh2*. In normal circumstances, *Kdm6b* expression is increased by a log2-fold on differentiation from Pro-B to Pre-B cell, while *Ezh2* expression remains relatively unchanged. In ageing, this increased expression in *Kdm6b* is either retained (Mild), reduced (Moderate), or lost (Severe), without a comparative change in expression to *Ezh2* (Severe aged mice are the only aged subgroup with differential expression of *Ezh2,* and even then *Ezh2* is downregulated by less than 1.2-fold compared to *Kdm6b* downregulation of over 2.6-fold).

These changes in expression dynamics to *Kdm6b:Ezh2* could alter the epigenetic landscape, with an increase in H3K27me3 suppression. Such a shift would therefore fit the findings from *Koohy et al*, which found an increase in H3K27me3 over the *Irs1* promotor of aged Pre-B cells, thereby supressing its gene's expression.

	Histone Methyltransferase Complex (89 Genes)		
	NES	*NOM p-val*	*FDR q-val*
Moderate Pre-B	-1.41	0.063	0.573
Severe Pre-B	-1.55	0.020	0.647

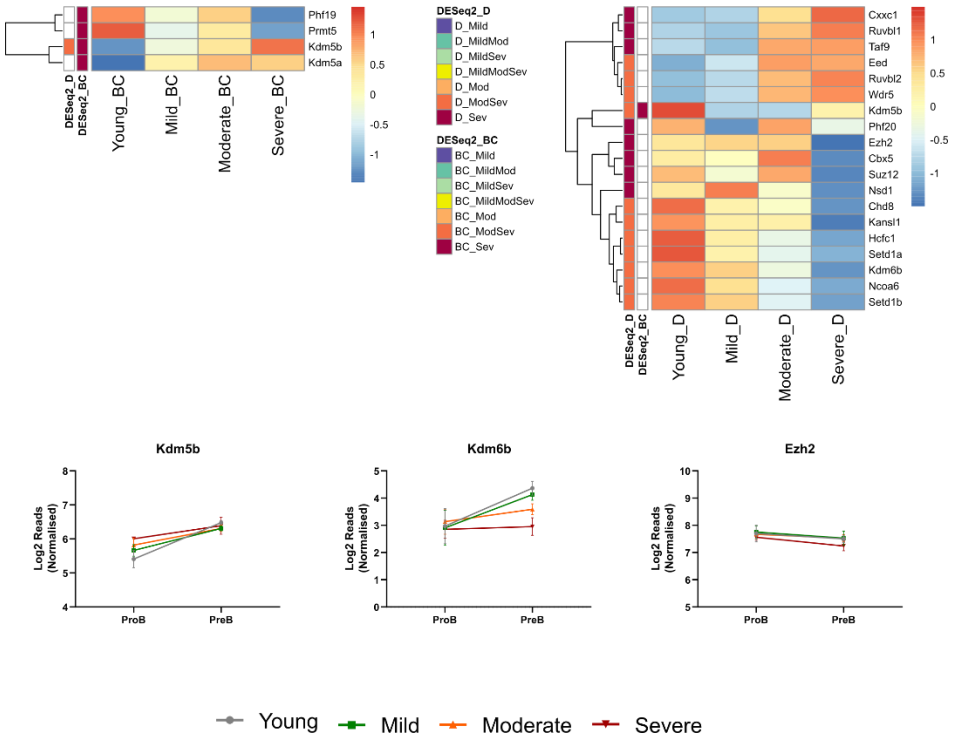

Figure 3-12: Breakdown of the DE genes involved in enrichment of the Histone Methyltransferase Complex GO symbol. Summary of the output statistics of the GSEA (table, top). DE genes that were enriched for the PKB pathway in aged Pro-B (left heatmap) and Pre-B (right heatmap) cells, split by subgroup (Mild, Moderate, Severe) and normalised by z-score for each gene. Each gene is annotated to show which aged Pro-B or Pre-B subgroups have this gene differentially expressed versus Young by DESeq2. Three genes from these heatmaps looked at in more detail: Kdm5b (H3K4 demethylase), Kdm6b (H3K27 demethylase), Ezh2 (H3k27 methyltransferase). (Log2 reads per million reads).

Exploration of these select GSEA pathways represents a snapshot of the global transcriptomic landscape in the aged Pro-B and Pre-B cells. From this snapshot, all of the dysregulated pathways can be linked back to an age-associated IGF1R suppression, either directly or indirectly. *Leukocyte Migration* and *Inflammatory Response* upregulation could be involved in the observed upregulation in *Protein Kinase B Signalling*. Such aberrant overstimulation of the Akt pathway can lead to a negative feedback suppression of Irs1 both transcriptionally by means of miRNA expression, and at the protein level through inactivating phosphorylation. Similarly, sustained downregulation of the H3K27 demethylase *JMJD3* of the *Histone Methyltransferase*

Complex across the Pro-B to Pre-B cell transition with age could be impacting the dynamic process of *Irs1* regulation through histone modifications. The resultant suppression/desensitisation of IGF1R signalling of aged Pro-B and Pre-B cells could have an impact on cell proliferation, and so explain some of the observed downregulations in *Cell Division*.

Furthermore, it would appear that the initial age-associated transcriptomic heterogeneity unearthed through this analysis is more indicative of progressive dysregulation of the same, interconnected biological pathways. Whether or not these transcriptomic differences translate to a comparative functional defect remains to be seen.

3.3 Correlations of aged subgrouping to other phenotypic characteristics

3.3.1 Retrospective meta-analysis reveals striking subgroup-specific trends

Subgrouping of these individual aged mice has been achieved exclusively through the transcriptomic variances of their Pre-B cell populations. Such subgrouping was not resolved from measuring the transcriptomic variances of their respective Pro-B cell populations. However, other heterogeneous age-related characteristics displayed between these mice may now be resolvable under this newfound subgrouping.

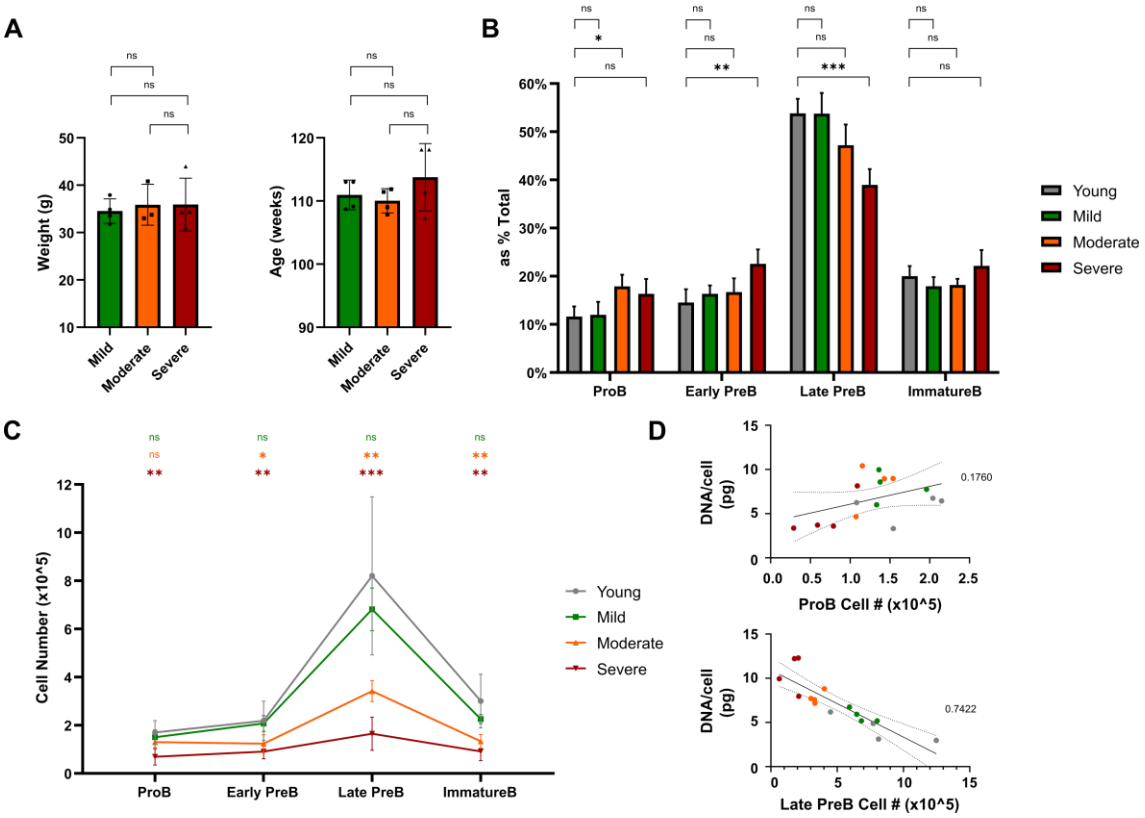

Figure 3-13: Retrospective analysis of other measurable characteristics based on aged subgroups. (A) There were no statistical differences in the weight or age of the aged mice, however the Severe subgroup does contain the 2 oldest mice. (B) Proportion of progenitor B cells Pro-B to Immature B cells shows a subgroup-specific skewed over-representation of Pro-B and Early B cells at the expense on their Late Pre-B cells. (C) Absolute cell numbers for all progenitor B cell populations decrease in a subgroup-dependant manner, but only reaching statistical significance versus Young in the Severe subgroup (except for the Late Pre-B cells where Moderate are also statistically reduced versus Young). (D) A correlation arises between the Pro-B and Late Pre-B cell stages of development between the total number of cells and the DNA content per cell (R^2=0.7422). This correlation follows the same subgroup-dependant trends. (Statistics by one-way ANOVA). Colour of dot indicates subgroup (grey=Young, green=Mild, orange=Moderate, red=Severe).

Macroscopically at the organism level, there were no differences in the ages or weight of the aged mice within each subgroup (mean: 112 weeks; 35.7g; Figure 3-13). However, at the cellular level, there was a subgroup-specific shift in the proportional representation of each progenitor cell population. Here, the cell proportions of the Mild mice were comparable to the Young mice, while the Moderate and Severe mice had an increased representation of Pro-B (significant in the Moderate) and Early Pre-B (significant in the Severe) cells, with a corresponding decrease in their Late Pre-B cell proportions. Such a shift is indicative of a blockage, or slowing down, of differentiation

from the Pro-B to Pre-B cell stage. When looking at the absolute number of cells from the bone marrow of each mouse, we again we see a subgroup-specific reduction in the number both Late Pre-B cells, and even their successive Immature-B cells (significant in Moderate and Severe aged). There is even a modest, but non-significant reduction detected in the number of Early Pre-B cells of Moderate, that is significant in Severe mice.

Further evidence to suggest this age-related defect is taking hold in the Pro-B to Pre-B cell transition can be found in the amount of DNA extracted from each cell population. There was a striking correlation observed amongst the Late Pre-B cell, between their total number of cells per mouse and the amount of DNA obtained from that cell population, that was not detected in the Pro-B cells (R^2: Pro-B=0.1760; Late Pre-B=0.7422). A relationship in which the mice with fewer Late Pre-B cells (disproportionately, the aged subgroups) have more DNA content would suggest an accumulation of cells that have undergone DNA replication (S-phase) and are awaiting cytokinesis (G2/M-checkpoint). Such an accumulation fits with the transcriptomic findings of dysregulation in the cell cycle of these aged Pre-B cells, in particular their *Cell Division*.

3.3.2 Modest but significant reduction in V-DJ_H recombination in aged Pre-B cells

As described in *Section 3.2.1*, DNA extracted from the Pro-B and Late Pre-B cell populations of these Young (n=4) and Aged (n=12) mice was used to create VDJseq libraries of the recombination events between V, D, ad J gene segments of their Ig_H locus. It is during the transition between these 2 stages that progenitor B cells undergo V-DJ_H recombination in search of a functional V-gene segment to complete the VDJ gene coding for heavy chain protein Mu. Therefore, the ratio of VDJ:DJ reads generated in these VDJseq libraries will represent this recombination event through increased ratio of VDJ reads from Pro-B to Pre-B cell. This marked increase in ratio of VDJ reads from Pro-B to Pre-B cell is observed in Young and Aged cells (average ~0.7x to ~3x VDJ:DJ for Young Pro-B and Pre-B cells respectively), with the ratio at the Pro-B cell stage being

comparable. However, there appears to be a modest, albeit significant, subgroup-specific reduction in the overall representation of VDJ reads relative to DJ reads in the aged Pre-B cells (Figure 3-14). This may suggest an increased number of individual aged Pre-B cells within the overall cell population that have not yet undergone V-DJ_H recombination, or have only V-DJ_H recombined 1 of their 2 alleles.

The efficiency of recombining a functional V-gene segment (i.e. its coding region has an open reading frame without a stop codon, and no defect in the splicing sites, recombination signals and/or regulatory elements) through the V-DJ_H recombination process is also improved through normal Pro-B to Pre-B cell differentiation (average ~28% vs ~72% functional V-gene for Young Pro-B and Pre-B cells respectively), and this dynamic is again seen in the aged progenitor cells. The only aged difference was found in the Severe Pro-B cells having proportionally more Nonfunctional V-gene recombination events versus Young Pro-B cells, but by the Pre-B cell stage this difference is alleviated such that all aged Pre-B cells have the same recombination efficiency once a V-gene has been paired (Figure 3-14).

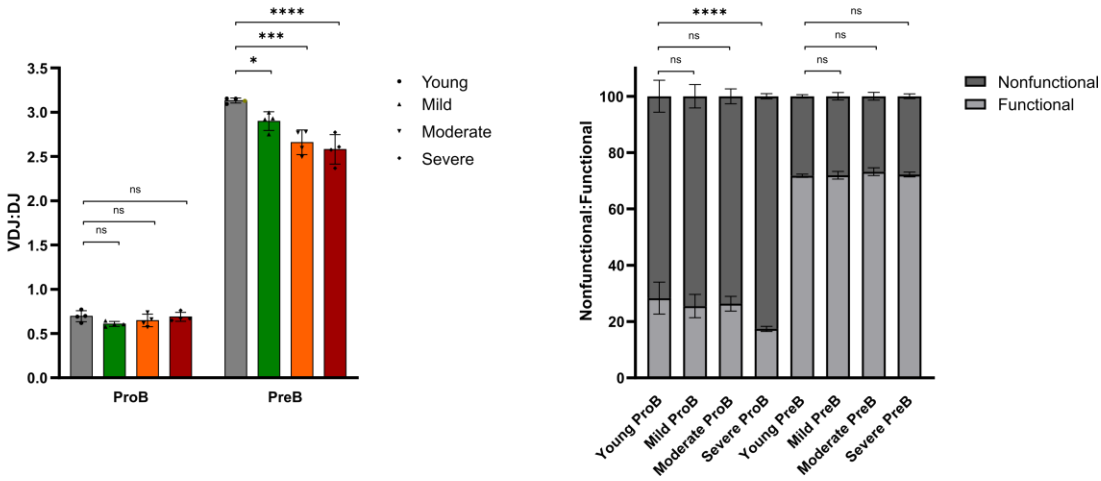

Figure 3-14: Aged subgroup-dependant changes in V-DJ_H recombination efficiency. Aged cells show a shift in more VDJ reads versus DJ reads from the Pro-B to Pre-B cell stages, but a subgroup-dependant decrease in the proportions of VDJ reads in their Pre-B cells (left graph). Of these VDJ reads, the Pro-B cells of the Severe subgroup appear to recombine using fewer functional V-genes, but are able to recover this deficit by the Pre-B cell stage where all aged Pre-B cells show comparable levels of functional V-gene recombination. (Statistics by one-way ANOVA).

3.3.3 Greater 7183/Q52 and reduced J558 V-gene usage in an age-related Ig_H 3'-5' skew

Successful V-DJ_H recombination during the Pro-B and Pre-B cell stages can occur using 1 of a possible 110 functional V-genes in mice[313]. Therefore, in addition to these aged progenitor B cell possibly undergoing slower V-DJ_H recombination, they could also be recombining these different functional V-genes at different frequencies compared to Young that would lead to a skewed repertoire. To measure this, all of the functional VDJ reads for each Pro-B and Pre-B cell population from each mouse were mapped to their respective V-gene on the Ig_H locus. However, Pro-B cells inherently have less functional VDJ reads per cell population, and so the total number of VDJ reads available per individual mouse were significantly less than for their respective Pre-B cell populations (~4-fold difference, Figure 3-15). To accommodate this difference in gene coverage, filtering methods were in place to remove V-genes will low reads (at least 1 read in 3 out of 4 young Pro-B cells) or which represented a low proportion of the overall V-gene repertoire (>0.25% in the average of young Pro-B cells). This left a total of 71 functional V-genes that were compared between the Young and Aged Pro-B and Pre-B cells. One of the Pro-B cell VDJseq libraries of the Severe aged subgroup had a very low coverage of these 71 V-genes (544 VDJ reads), with only 11 of the 71 genes having more than 1 VDJ read mapped to it. As a result, this aged mouse was left out of the analysis (Pro-B and Pre-B cells).

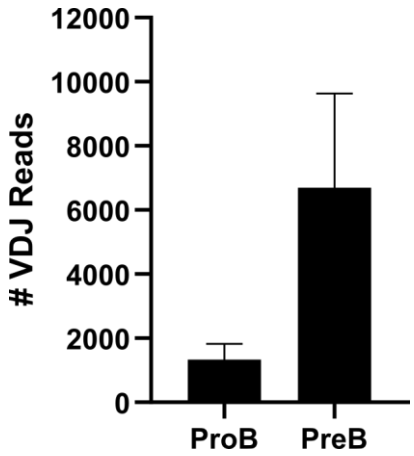

Figure 3-15: Unique VDJ_H reads per mouse (Young and Aged) in the Pro-B cells versus Pre-B cells. Compared to Pre-B cells, Pro-B cells have per mouse: i) fewer cells; ii) fewer total VDJ reads; iii) fewer functional VDJ reads. These differences accumulate into a comparative deficit in available VDJ reads per mouse in the Pro-B cells to map to the Ig_H locus.

Aged Pro-B cells were treated as one group (n=11) whilst the aged Pre-B cells were separated into their subgroups (Mild, n=4; Moderate, n=4; Severe, n=3) and compared against Young (n=4). V-gene usage was presented as a percentage of the overall representation for each V-gene across the whole Ig_H locus (Figure 3-16A). Log-fold differences in the mean averages of V-gene usage for aged mice versus young demonstrate that there is an overall shift in the representation of V-genes across the Ig_H locus in both Pro-B and Pre-B cells, with more 3'-proximal V-genes being used more in ageing than the distal 5' V-genes. This repertoire shift shows levels of subgroup-dependency at the Pre-B cell stage, as the Mild aged mice show the mildest version of the overall skewing. Statistical analysis of each V-gene reveals *J558.42.132* to be the only significant hit in the Pro-B cell stage, with a lower representation in the aged mice (highlighted, Figure 3-16A). However, the discrepant use of this V-gene is corrected by the Pre-B cell stage, as aged mice from all subgroups are comparable to Young Pre-B cell *J558.42.132* usage.

On the other hand, the usage in 17 of these 71 V-genes was statistically different between the Pre-B cells of aged and young mice (highlighted, Figure 3-16A), all of which (with the exception of *SM7-3-54*) falling in either the 3'-proximal 7183/Q52 family (4/17) or the distal 5' J558 family (12/17). In line with the overall repertoire skew, the representation of the 7183/Q52/SM7 V-genes increase in the aged Pre-B cells whereas the J558 genes decrease (with the exception of *J558.22.112*, which increases in ageing).

To capture to general changes in V-gene usage across the Ig_H locus, V-genes were grouped together based on their geographical positioning to the 3' region and thus, to the DJ_H gene segments[313] (Figure 3-16B). This confirmed that there is a statistical increase in the usage of "Proximal" V-genes in aged Pro-B and Pre-B cells, with a reciprocal decrease in the usage of "Distal" V-genes.

Interestingly, even within this pan-aged, Ig_H locus-wide trend there are aged subgroup differences in the individual V-genes used. For example, there are some V-genes that

are differentially misrepresented in the subset of the aged mice (*J558.12.102* down more in Mild-only than Moderate and Severe; *SM7.3.64,* of the Middle family, up in Moderate-only; *J558.6.96* statistically down in Moderate-only, *7183.20.37* up in Mild and Severe only), but mostly there are subgroup differences in the proportional misrepresentation of certain V-genes (*Q52.2.4* and *7183.4* up most in Severe; *J558.9.99*, *J558.52.145*, *J558.72.173* and *J558.81.187, J558.84.190* down most in Severe). Lastly, it is noticeable that there are subgroup differences in the V-genes contributing to the overall 3' V-gene bias: as in the Moderate and Severe subgroups these are the V-genes *Q52.2.4* and *7183.4.6* (and *Q52.3.8* for Moderate) whereas for the Mild subgroup it is the more 3'distal *7183.20.37* V-gene (Figure 3-16A).

Overall, in the contexts of V-DJ_H V-gene usage in these aged Pre-B cells, a change in repertoire diversity was observed in all aged subgroups, albeit at different intensities. Such limitations to their repertoire is likely to contribute to the age-associated defects in their mature B cell functions when mounting an immune response. Whether nuanced differences in individual V-gene usage observed between the aged subgroups has any further functional significance, remains to be determined.

This comprehensive analysis of the same individual Young (n=4) and Aged (n=12) mice has allowed for the transcriptomic heterogeneity of Pro-B and Pre-B cells to be categorised, interrogated, and linked back to functional output (in the form of cell numbers, V-DJ_H recombination efficiency, and resultant VDJ_H repertoire diversity). All of this analysis was conducted on the overall Pro-B and Pre-B cell populations. The heterogeneity captured between these individual aged Pro-B and Pre-B cells could therefore either be the result of differences between their overall cell populations, or changes in the composition of the single-cells that make up these populations.

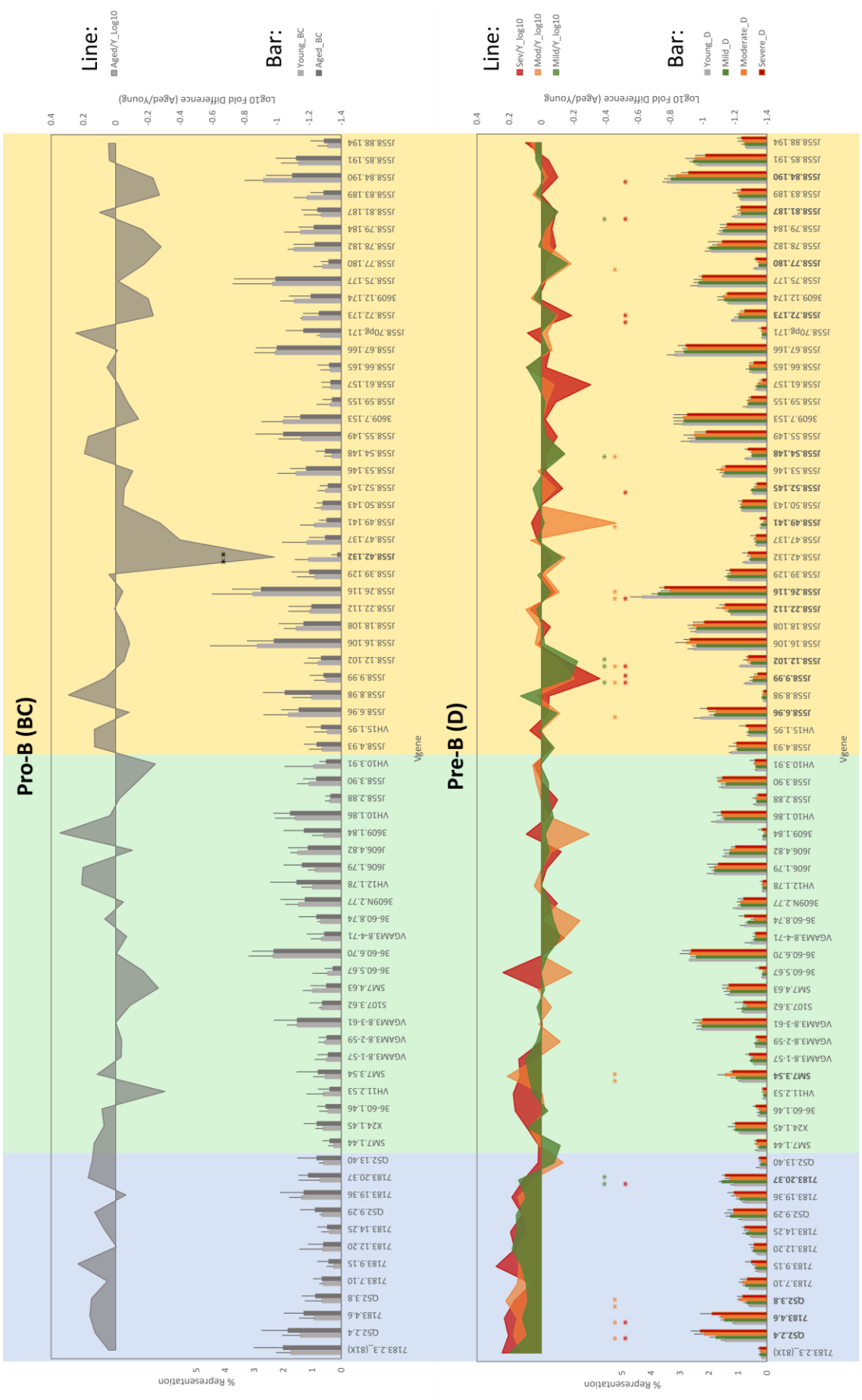
Pro-B (BC)
Pre-B (D)
Line:
Aged/Y_log10
Bar:
Young_BC
Aged_BC
Sev/Y_log10
Mod/Y_log10
Mild/Y_log10
Young_D
Mild_D
Moderate_D
Severe_D
Log10 Fold Difference (Aged/Young)
% Representation
Vgene

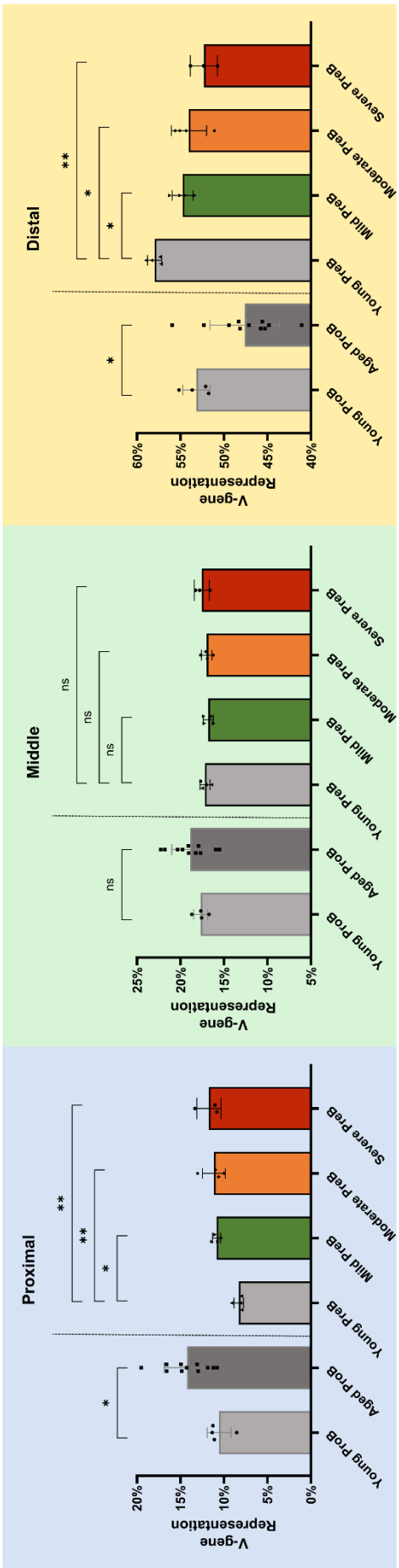
Distal
Middle
Proximal
V-gene Representation
Severe PreB
Moderate PreB
Mild PreB
Young PreB
Aged ProB
Young ProB
ns
*
**

Figure 3-16: V-gene usage across the Ig_H locus of Pro-B and Pre-B cells. (A) 71 functional V-genes compared between Young and Aged Pro-B (top) and Pre-B (bottom) cells. Aged Pro-B cells (n=11, dark grey) compared against Young Pro-B cells (n=4, light grey). Aged Pre-B cells (Mild, n=4, green; Moderate, n=4, orange; Severe, n=3, red) compared against Young Pre-B cells (n=4, light grey). Average % representation of each V-gene displayed as barplot (primary yaxis), with the Aged/Young log-fold differences in the average % representation of each V-gene plotted as a line above each barplot (secondary y-axis). Statistically different V-genes highlighted bold (Pro-B=1; Pre-B=17) and shaded out across both Pro-B and Pre-B plots. Colour of shading represents either V-gene family (blue=7183/Q52; green=SM7; yellow=J558), or the V-gene significant in Pro-B cells (orange=J558.42.132). (B) Summary of the V-gene usage based position to the 3' end of locus: "Proximal" (blue), "Middle" (green), "Distal" (yellow). Colour of group corresponds to colour of highlighted region in (a). (Statistical analysis: t-test Pro-B; one-way ANOVA Pre-B; pval <0.05).

3.4 Heterogeneity of ageing at the single-cell level

3.4.1 Optimisations and QC of the sci-RNAseq library

Resolving transcriptomic differences in progenitor B cells at the single-cell level would clarify if the observed defects in Pro-B to Pre-B cell development from *Section 3.3* affect the entire cell population, or just a subset of cells (and of varying proportions within each aged mouse). To achieve this, a single-cell RNA sequencing technique known as sciRNAseq (single-cell combinatorial indexing) created by *Cao et al*[280] was performed on a FACS-sorted pool of progenitor B cells ($B220^+AA4.1^+IgD^-$) from both Young (n=3) and Aged (n=3) mice. sciRNAseq is an *in-situ* plate-based technique which, through the libraries preparation, incorporates a series of indexes onto poly-adenylated mRNA of methanol-fixed cells. Single cells from the final indexed library can then be computationally identified. Through this technique, it is therefore possible to separately index cell populations from individual young and aged mice before incorporating them all into a single sciRNAseq library.

A modification to the published protocol was necessary in order for it to work on B-cells. After cell fixation in 80% methanol, but prior to reverse transcription, a series of washes are carried out in a PBS-based buffer. Despite this wash buffer containing a cocktail of

RNase inhibitors (including the potent and irreversible RNase deactivator DepC), the total RNA of B-cells was still definitively degraded (Figure 3-17). A test adopting the published technique[314] of replacing PBS with the higher-salt content of 3X-SSC during the washing steps preserved the integrity of total RNA in B-cells, at the expense of some cell loss.

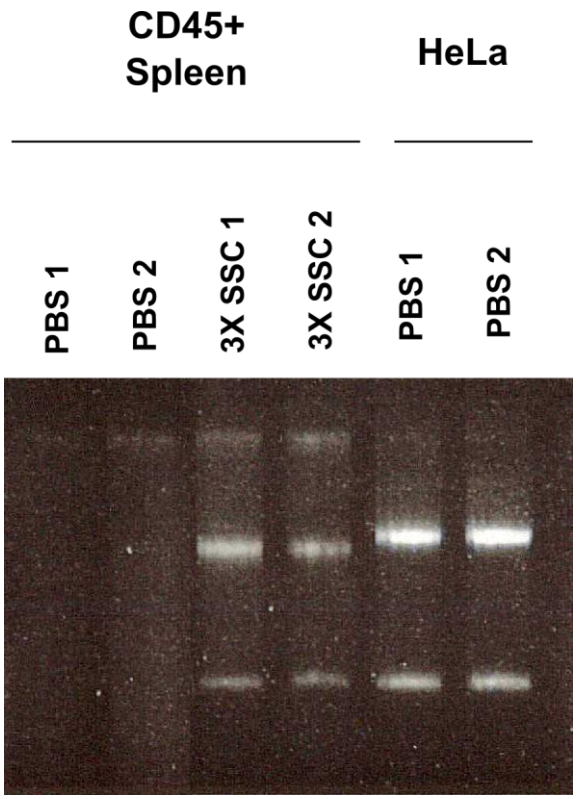

Figure 3-17: Modifying wash buffer from PBS to 3X SSC to retain RNA integrity of B cells. Total RNA of methanol-fixed CD45$^+$ splenic cells degrades during the sciRNAseq wash step described in the methods. Replacing the PBS with 3X SSC in the wash buffer retains the integrity of the total RNA. HeLa used as a comparator as these were used in sciRNAseq optimisations by Cao et al. 2 replicates for each condition shown.

In this study, a pool of B220$^+$AA4.1$^+$IgD$^-$ progenitor B cells were extracted from 3 young (cell counts: Young1=2.5x10^6, Young2=2.8x10^6, Young3=3.2x10^6) and 3 aged (cell counts: Aged1=1.7x10^6, Aged2=1.4x10^6, Aged3=0.54x10^6) mice, and the adapted 3X-SSC wash buffer was used after cell fixation (cell counts: Young1=1.25x10^5, Young2=1.1x10^5, Young3=3.75x10^5, Aged1=0.65x10^5, Aged2=0.85x10^5, Aged3=0.6x10^5). Cells from individual mice were separately barcoded at the 1st round of indexing, before being pooled together into one sciRNAseq library that underwent another round of indexing.

From this 2nd and final round of indexing, there was a total of 288 wells with a maximum of 100 cells per well (young and aged, mixed). The final sequenced library consisted of 15,989 cells (11,427 young, 4,562 aged) at a sequencing depth of ~10,000 reads per cell, and a deduplication rate of 93.9%. This output is consistent with a comparative study conducted by *Cao et al*, where 50-80% cell recovery is expected from a sciRNAseq library, with a sequencing depth of ~20,000 reads per cell, and deduplication rate of ~80% - slightly more optimal numbers obtained with their cell type (*C.elegans*). Of note, there was a marked difference in the ratio of intronic reads between my final sciRNAseq library and that of *Cao et al* (45%; versus only 2.13%). This would indicate a bias in my library towards nuclear RNA that has perhaps come about as a result of the necessary changes made to the wash buffer components (a more aggressive high-salt 3X-SSC buffer) – which could have feasibly washed away some cytosolic RNA from the cells in the process (Figure 3-18).

In any case, when comparing the number of unique UMI reads and Genes detected in the final library of *Cao et al* against my own, there were reassuring parallels (Figure 3-18). As such, this sciRNAseq library of young and aged progenitor B cells passed all quality controls, and is sufficient to analyse for biological signatures.

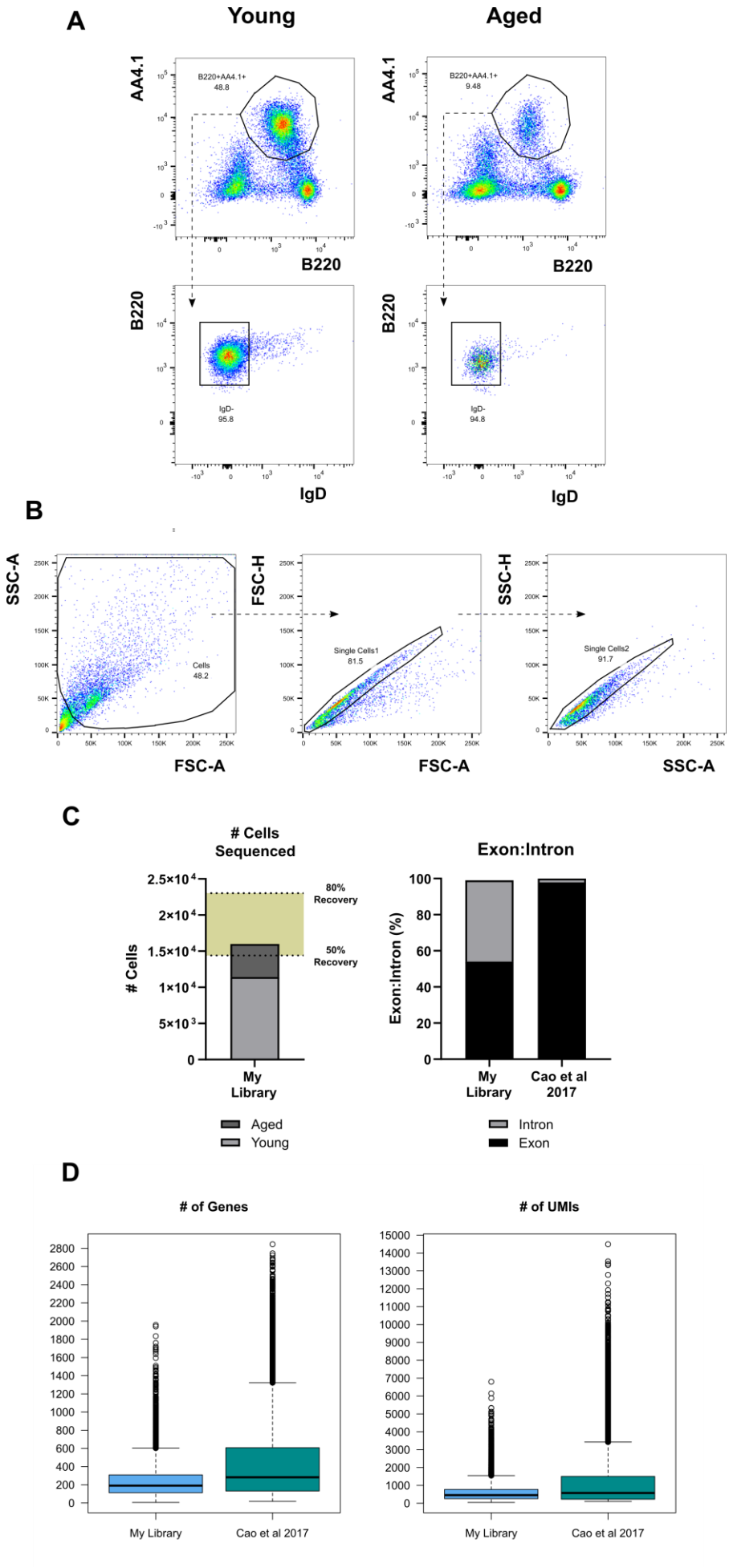
A
Young
Aged
AA4.1
B220+AA4.1+
48.8
B220
B220
IgD-
95.8
IgD
B220+AA4.1+
9.48
IgD-
94.8
B
SSC-A
FSC-A
Cells
48.2
FSC-H
Single Cells1
81.5
SSC-H
Single Cells2
91.7
C
Cells Sequenced
Cells
80% Recovery
50% Recovery
My Library
Aged
Young
Exon:Intron
Exon:Intron (%)
My Library
Cao et al 2017
Intron
Exon
D
# of Genes
# of UMIs
My Library
Cao et al 2017

Figure 3-18: Generation of the sciRNAseq library. (A) Representative FACS plots for the sorting of B220^{+}AA4.1^{+}IgD^{-} B cell progenitors from the bone marrow of young (n=3) and aged (n=3) mice for the final sciRNAseq llibrary. All cells were gated for live singlet lymphocytes prior to this gating strategy. (B) Representative FACS plots for the sorting of in-tact single cells into individual wells after in-situ first-strand synthesis as part of the sciRNAseq library preparation. (C) Total number of cells sequenced from the young (n=3) and aged (n=3) mice. (D) Ratio of Exon:Intron reads from the total sciRNAseq library, compared to Cao et al. (E) Total number of unique UMI reads and genes detected per cell in the final sciRNAseq library, versus a library generated by Cao et al with C.Elegans. (Medians – number of genes: My Library=191, Cao et al=285; median number of UMIs: My Library=454, Cao et al=575).

3.4.2 Clustering analysis (UMAP) to identify cell populations

Cells with between 300-1500 reads and <150 genes detected were taken into the downstream SeuratR analysis to remove low-expressing cells, potential doublets, and cells with poor gene coverage. The final cell distribution of read coverage and genes detected (and its expected positive correlation) is consistent across the individual mice within the sciRNAseq library (Figure 3-19). When exploring which genes contribute the most variance amongst the cells of young and aged mice, there were some similarities – for example *Sdk2*, *Parn*, *Fndc1*. However, the strong presence of *Iga* and *Igj* genes in the aged cells gives early implications that there are some mature B cell contaminants present within this B220^{+}AA4.1^{+}IgD^{-} cell fraction (Figure 3-19).

Prior to analysis, the difference in expression between S-phase and G2M genes was regressed out of the total sciRNAseq library (young and aged cells together), such that the differential gene expression used to define cell clusters would only consider cell cycle genes that are distinctly different between different cells. This modified version of cell cycle regression therefore preserves the different bursts of proliferation characteristic of normal progenitor B cell development (i.e. during Pro-B to Pre-B cell differentiation), whilst removing cell cycle differences that could occur within established cell populations. The remaining variances in gene expression within the total sciRNAseq library was quantified by principal component analysis, with many B-cell specific genes (such as *Cd19*, *Vpreb*, *Ighm*, *Igkc*) and cell cycle genes (such as *Cdkn2c*, *Top2a*, *Cenpf*, and *Mki67*) contributing the most variance (Figure 3-19).

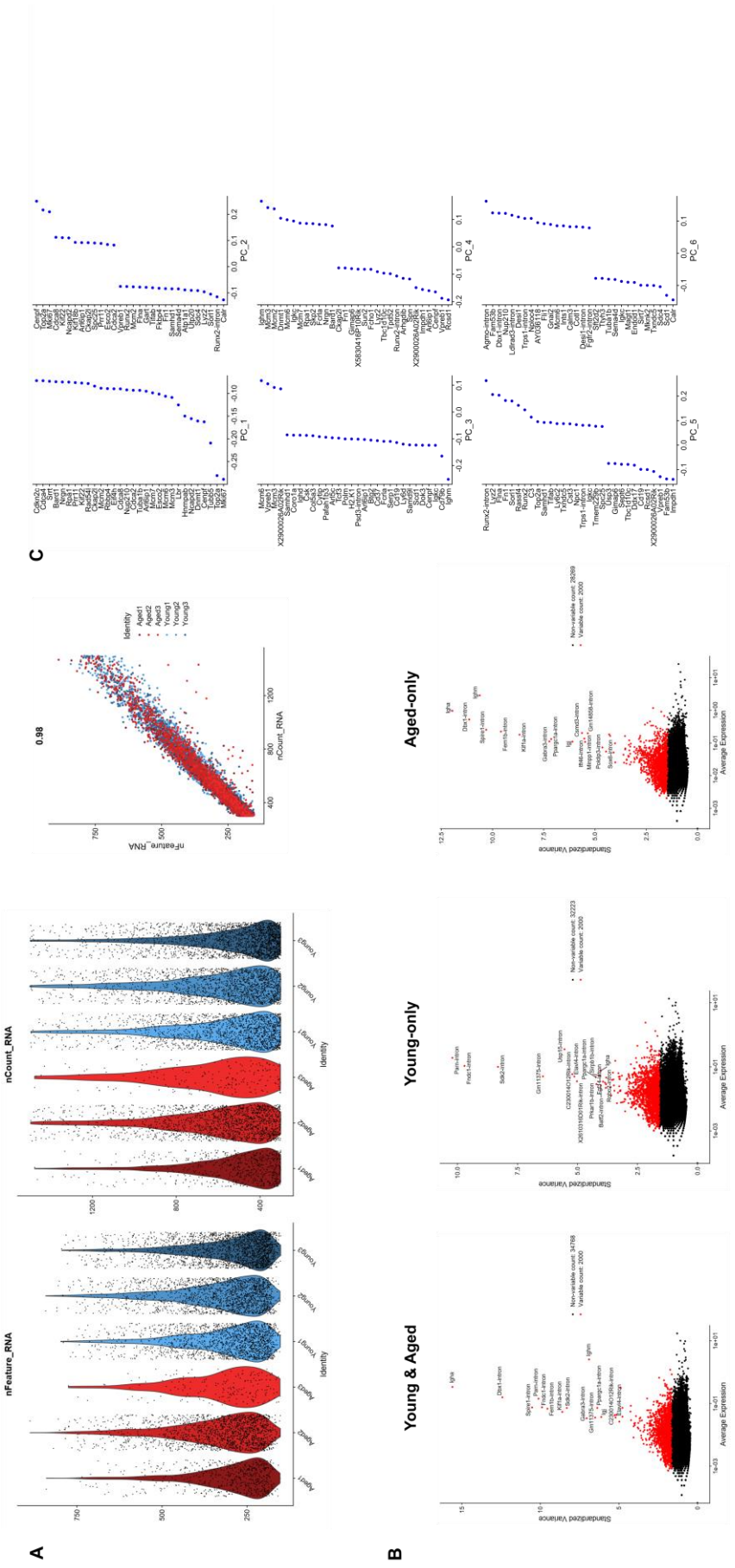
A
nFeature_RNA
nCount_RNA
Identity
B
Young & Aged
Young-only
Aged-only
Standardized Variance
Average Expression
C
PC_1
PC_2
PC_3
PC_4
PC_5
PC_6

Figure 3-19: Processing of sciRNAseq library through the SeuratR pipeline. (A) Total number of unique UMI reads and genes detected per cell after filtering the sciRNAseq library for cells with between 300-1500 reads and <150 genes, split into the individual young (n=3) and aged (n=3) mice. (B) The genes contributing the most variance between the cells in the sciRNAseq library when looking at i) Young and Aged together ii) Young-only iii) Aged-only. (C) Principal Component (PC) loadings of the top 6 PCs, in the total sciRNAseq library (Young and Aged) after regression of cell cycle genes.

These principal components were then used to generate 9 distinct cell clusters that were visualised using the dimension reduction technique UMAP (Uniform Manifold Approximation and Projection). Clusters were renamed based on gene expression patterns – with the guidance of the literature classifications, my own bulk RNAseq data from Pro-B and Pre-B cells, and confirmed using the online tool ImmGen (Figure 3-20, https://immgen.org). Genes with the suffix "-intron" represent reads that mapped to intronic regions.

5 of the 9 clusters generated in this analysis accounted for the Pro-B, Pre-B – split into "Cycling Early", "Resting Late", and "Transitioning Late" Pre-B) – and Immature-B cell populations expected in a $B220^{+}AA4.1^{+}IgD^{-}$ cell niche. Expression of the surrogate light chain *Vpreb1* together with *Rag1* and *Dntt* (terminal deoxynucleotide transferase – TdT) defined the Pro-B cell population that was actively engaging in V-DJ_H recombination. The Pre-B cell clusters all shared the expression of the transcription factor *Bach2*, but the differential expression of other genes provided the distinction into the 3 clusters identified. The "Cycling Early" Pre-B cell clusters expressed cell cycle genes – such as *Mki67*, *Cenpf*, and *Top2a* – along with the known Early Pre-B cell marker *Cd24a*. The 2 Late Pre-B cell populations "Resting" and "Transitioning" were defined by the switching-off of these cell cycle genes, and re-expression of *Rag1*. However, the difference between these 2 clusters lies in the expression of genes such as *Cd79b*, *Serinc5*, and *H2-K1* in the "Transitioning" Late Pre-B cell cluster – named so because of its expression of *Cd79b*, which codes for the BCR component Igα. Finally, the expression of B-cell specific transcription factor *Ikzf3* – also known as AIOLOS – along with increasing expression of *Igkc* gave rise to the Immature B cell population. Its unique expression of *Scd1* was also consistent with ImmGen data. When comparing the levels of *Ighm* gene for the heavy

chain protein Mu, there was an increased expression across these newly-defined clusters, adding validity to this manual classification.

Surprisingly, 3 of the 9 clusters appear to be other B cell subsets that would not have been expected in this $B220^{+}AA4.1^{+}IgD^{-}$ cell niche. Despite the removal of IgD-expressing cells, and positive selection with the progenitor B cell marker AA4.1, there still remains a contamination of mature B cells within this cellular niche (as defined by the expression of *Igj* and *Igha*). There were also cells precursor to Pro-B cells in this $B220^{+}AA4.1^{+}IgD^{-}$ cell fraction. PrePro-B cells (defined by *Bcl2*, *Runx2*, and *Mpeg1*) and even CLPs (defined by *Ccr2*, *Fn1*, and *Mpeg1*) appear to have unexpectedly contaminated the niche.

The final cluster yet to be assigned did not seem to fit any classifications of known B cell populations from the literature, and was defined by its expression of *Agmo* (involved in lipid metabolism) and *Dbx1* (involved in neural development) – neither of which have been shown to be expressed in B-cells. However, based on the fact that these cells express *Ighm*, it must be assumed that they are of the B-lineage. As such, they have been named “Other”.

It should be stressed at this point that the classifications of progenitor B cell populations through this sciRNAseq experiment do not necessarily correspond to the same cell populations defined in the previous experiment, as those FACS-sorted Pro-B ($CD19^{+}AA4.1^{+}CD25^{-}IgM^{-}IL7R\alpha^{+}CD43^{hi}CD24^{lo}$) and Late Pre-B ($CD19^{+}AA4.1^{+}CD25^{+}IgM^{-}$) cell fractions may instead represent a population of cells that overlap the cluster boundaries assigned through this analysis by transcriptome. The fact also that this single-cell library is biased towards reads mapping to intronic regions would suggest a more nascent transcriptome, which would therefore be capturing different gene expression dynamics to that of the bulk RNAseq libraries described previously.

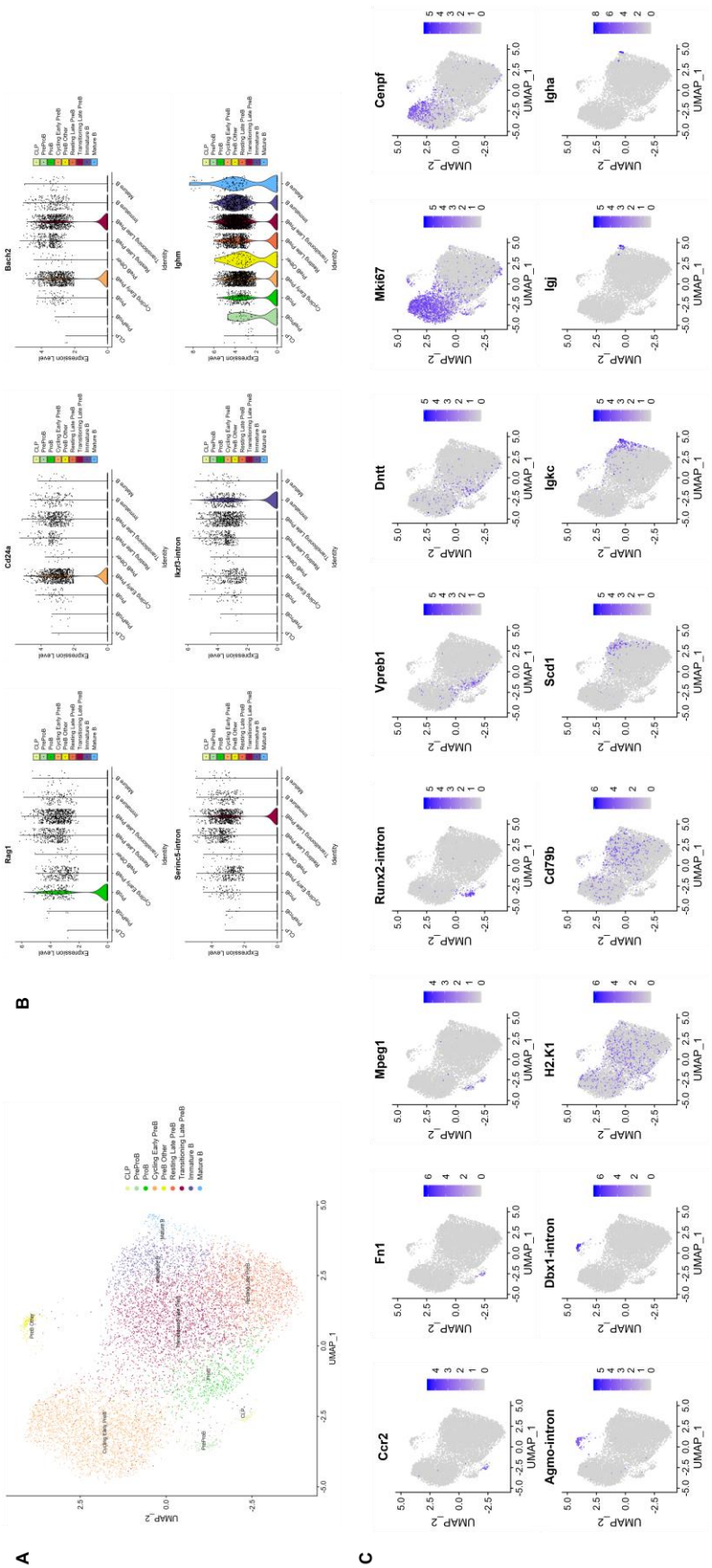
A
B
C
UMAP_1
UMAP_2
Expression Level
Identity
CLP
PreProB
ProB
Cycling Early ProB
ProB Other
Resting Late ProB
Transitioning Late ProB
Immature B
Mature B
Bach2
Igllm
Cd24a
Ikzf3-intron
Rag1
Serinc5-intron
Cenpf
Igha
Mki67
Igj
Dntt
Igkc
Vpreb1
Scd1
Runx2-intron
Cd79b
Mpeg1
H2.K1
Fn1
Dbx1-intron
Ccr2
Agmo-intron

Figure 3-20: Classification of cell clusters based on gene expression profiles. (A) UMAP visualisation of the total sciRNAseq library (Young and Aged cells) with the 9 defined clusters renamed to B-cell subsets. (B) Violin plots of key genes that helped with renaming of the cell clusters to known B-cell subsets. (C) Expression levels of key genes that defined each cell cluster: CLP (Ccr2, Fn1, Mpeg1), PrePro-B (Mpeg1, Runx2), Pro-B (Vpreb1, Dntt), Cycling Early Pre-B (Mki67, Cenpf), Pre-B Other (Agmo, Dbx1), Transitional Pre-B (H2-K1, Cd79b), Immature B (Igkc), Mature B (Igj, Iga).

3.4.3 Young versus Aged at the single-cell level

With the cell clusters of the whole sciRNAseq library identified, comparisons were then made between the Young (n=3) and Aged (n=3) mice. By comparing both the proportions of each cell population and the expression of genes within each population, conclusions can be drawn as to what extent the aged differences at the single cell level could be driving the observed heterogeneity at the organism level.

All clustered cell populations were present in both Young and Aged mice. Thus, there were no sub-populations of cells exclusively arising in the aged $B220^{+}AA4.1^{+}IgD^{-}$ niche that would be suggestive of aged heterogeneity at the single-cell level within defined cell populations (Figure 3-21). However, there are differences at the organism level in the proportion of each cell population. For example; the “Other” cell population is represented more in Young 1 and Aged 2, whilst the PrePro-B cell population is greater in Aged 3. There also appears to be an overall increase in mature B cell contamination in all of the Aged mice, but Aged 3 has a far greater proportion in its niche.

When looking at the other cell populations, there appears to be an age-associated trend towards less Cycling Early Pre-B cells and more Resting Late Pre-B cells, as well as a reduction in Immature B cells in these aged mice. However, the small sample size (n=3) means there is no statistical significance. The clustering of Pre-B cells on cell cycle state therefore makes it possible to show that there does appear to be a reduced capacity for the aged Pre-B cells to undergo cell division – a finding which is consistent with the results of the bulk RNAseq analysis on their FACS-defined Late Pre-B cell population.

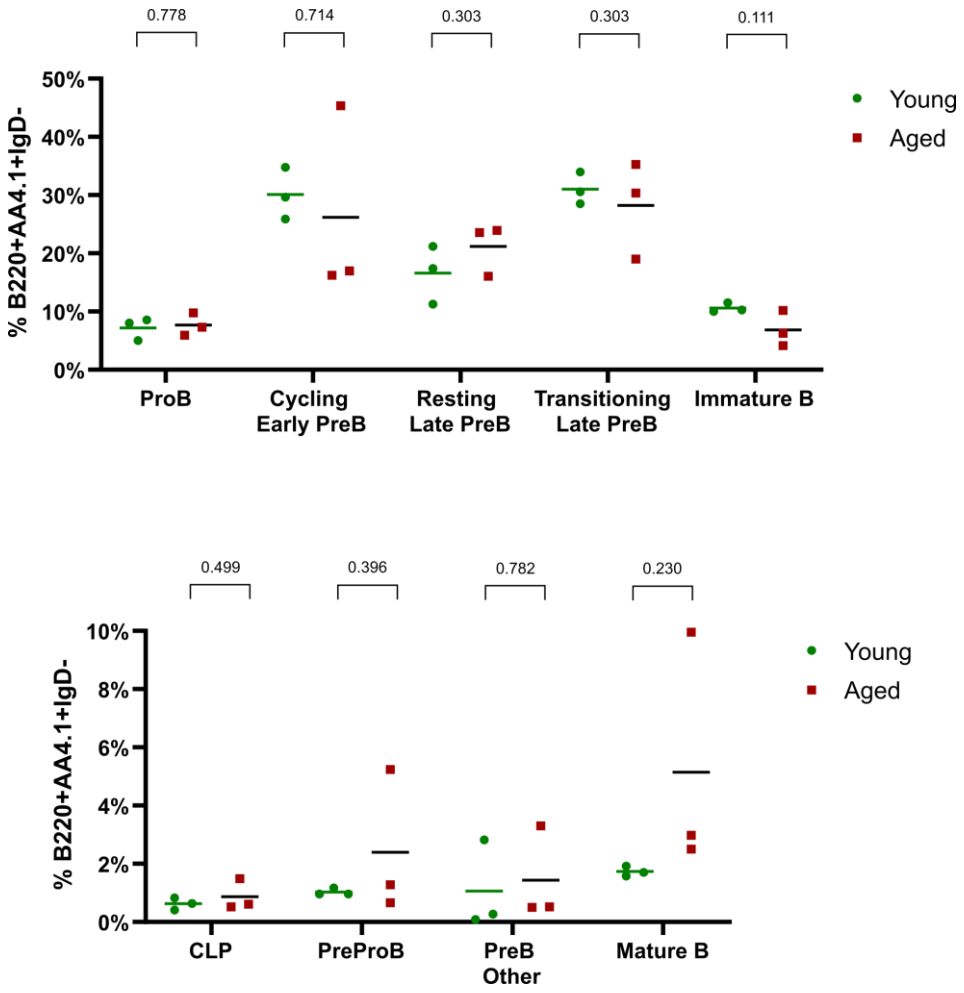

Figure 3-21: Proportions of each cell cluster in young (n=3) and aged (n=3) mice, as % of all cells in the B220⁺AA4.1⁺IgD⁻ population. Graphs split into cells expected to be in this cell population (top) and the rest (bottom). Statistical analysis: t-test, pval <0.05.

Differential gene expression analysis was conducted on the cell clusters of Young and Aged mice using the Wilcoxon rank sum test (Figure 3-22).

Through this analysis, many genes were differentially expressed to varying statistical significance across the cell types. Some genes were significant (FDR padj <0.05) in all cell types such as *Yam1*, *Cdk8-intron*, and *Cmss1-intron*. *Yam1* is a long noncoding RNA found in the nucleus that has been shown to associate with YY1 in myocytes to upregulate miRNA transcription networks[315]. *Cdk8* is a kinase that regulates cell cycle, while *Cmss1* is an RNA binding protein that binds poly-adenylated RNA and has been shown in yeast to counter an induced cell cycle arrest[316]. None of these genes have been characterised in normal early B cell development, nor are they found to be differentially expressed in the aged Pro-B and Pre-B cells through bulk RNAseq. As such, any age-

related transcriptomic dysregulation observed in this nascent RNA transcriptome would appear to be corrected for post-transcriptionally since there is no dysregulation in the bulk RNAseq data.

Some interesting DE gene hits came out of this analysis that were also consistent with the results of *Sections 3.2 and 3.3*. For example, aged cells in the Cycling Pre-B cell cluster show statistical upregulation of an interleukin-1 receptor accessory protein *Il1rapl1*. Paradoxically, expression of this gene has only been reported in neural cells, however this aberrant expression in aged Pre-B cells could suggest a more general upregulation of the inflammatory IL1B pathway, as also observed in the bulk RNAseq data of aged Pro-B and Pre-B cells. Additionally, *Ighm* expression in reduced in these aged Cycling Pre-B cells, which carries over into the Transitional Pre-B cell cluster. This is suggestive of reduced V-DJ_H recombination events in the aged Pre-B cell populations as they differentiate from Pro-B cells, as was also seen in the bulk VDJseq analysis. The fact that these aged Transitional Pre-B cells also have an increased expression of *Rag1* could indicate that more of these aged Pre-B cells are still in the process of recombining either their heavy or light chain, relative to young cells at the same stage.

Across the Pre-B cell clusters, many of the statistically upregulated genes in ageing can be linked back to cell signal transduction, such as *Strn3*, *Dgkd* and *Mctp2* in the Resting Pre-B; or *Gng2* and *Sh3kbp1* in the Transitional Pre-B cells. *Sh3kbp1* was of particular interest, since it is a kinase-binding adaptor protein for EGFR signalling whose function is inhibited by the negative feedback regulator Spry2, and so could tie in with the overstimulation of the Akt signalling pathway also observed in the bulk RNAseq analysis.

Two of the most statistically upregulated genes in aged Transitional Pre-B cells were genes involved in polycomb repressor complex (PRC) functions – *Tug1* (a lncRNA) and *Epc2* (Enhancer of Polycomb Homolog 1). Upregulation of the PRC2 complex in these aged Pre-B cells would fit with the understanding that *Irs1* may be actively suppressed epigenetically by H3K27me3; as reported by *Koohy et al*.

Across all of the cell clusters, there was a strong representation of downregulated mitochondrial genes in the aged cells. The most prominent downregulated mitochondrial genes were *mt-Rnr1* and *mt-Rnr2* coding for 12S and 16S ribosomal RNA respectively. However, across the Pre-B cell stages there was an additional

downregulation of *mt-Cytb* (in Cycling, Transitional, and Resting Pre-B cells) and *mt-Nd4* (in Cycling and Transitional Pre-B cells) coding for respiratory complex proteins. Such downregulation of mitochondrial genes, especially those coding for the respiratory complex, replicates the findings of the bulk RNAseq data.

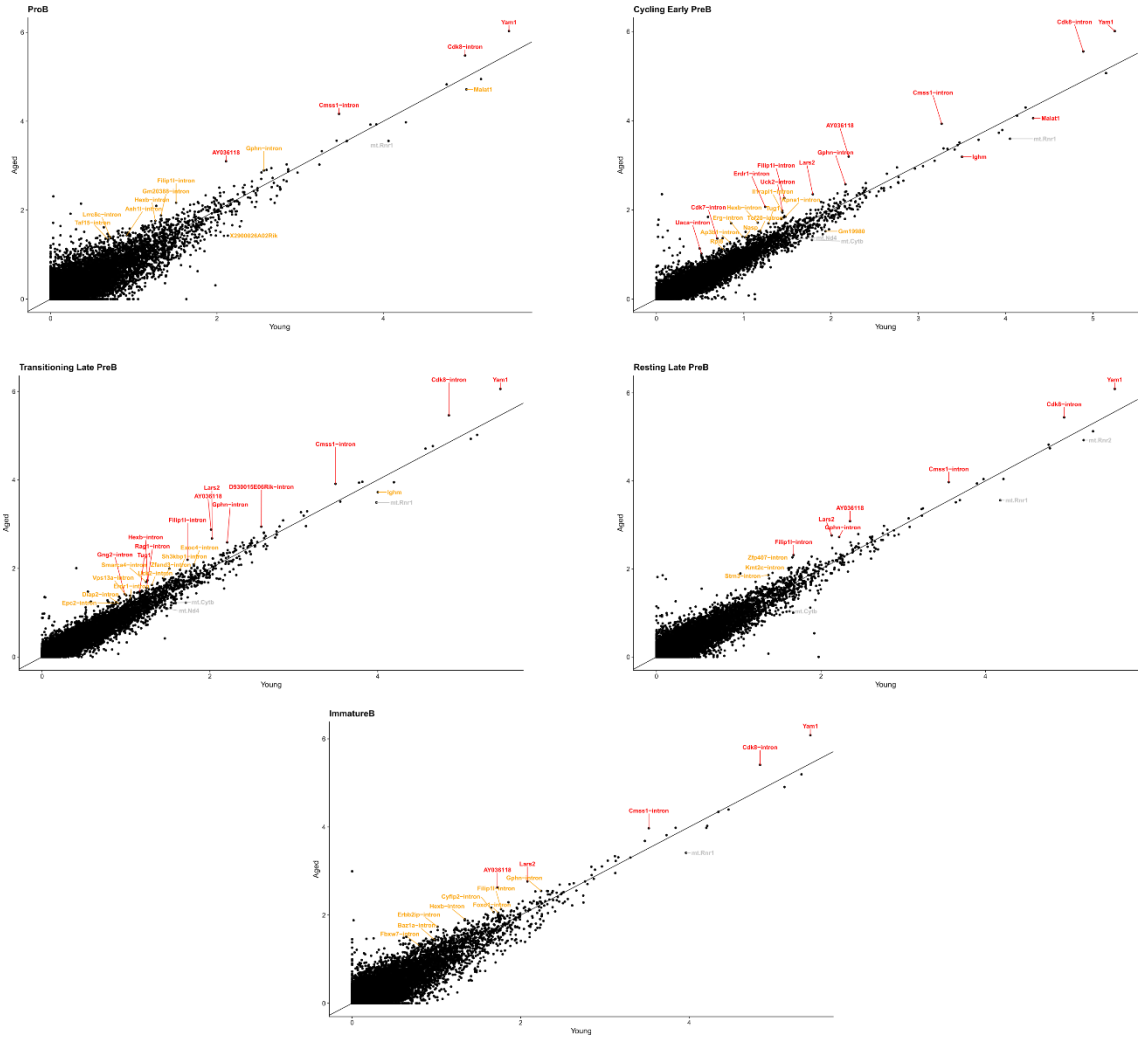

Figure 3-22: DE genes in the aged progenitor B cell clusters. Scatterplot of the average log1p gene expression between young (n=3) and aged (n=3) mice for Pro-B, Cycling Early Pre-B, Transitioning Late Pre-B, Resting Late Pre-B, and Immature B cell clusters. Differential gene expression analysis on each cluster (Pro-B: 70 DE p-val <0.05, 4 DE FDR padj <0.05; Cycling Early Pre-B: 89 DE p-val <0.05, 13 DE FDR padj <0.05; Transitioning Late Pre-B: 54 DE p-val <0.05, 12 DE FDR padj <0.05; Resting Late Pre-B 41 DE p-val <0.05, 7 DE padj <0.05; Immature B 68 DE p-val <0.05, 5 DE padj <0.05). All statistically significant DE genes by FDR padj are shown (red), as well as the next 10 most significant p-value genes (orange) and all significant mt-genes (grey; p-val +/- FDR padj).

This exploration of transcriptomic differences at the single cell level has shown that, while there are differences between the aged mice in the representation of each B cell population, biological differences, and therefore heterogeneity, are still constrained to their analogous cell populations. As such, better conclusions can be drawn about age-related differences using the bulk RNAseq data, since it has ~10^4-fold deeper sequencing resolution. However, this work does show that despite the stringent selection for desired progenitor B cells by FACS ($B220^+AA4.1^+IgD^-$), there was still a small level of cell contamination. This is something to consider when interpreting the data from *Section 3.2* as this bulk RNAseq was conducted on cells that were FACS-sorted to a similar level of purity.

As for the "Pre-B Other" cell cluster to come from this analysis, its lack of classification in the literature could suggest a possible unknown rare cell state within the progenitor B cell niche. However, it was only represented in 2 out of the 6 mice analysed and so could instead be either contamination or technical artefact. Further interrogation into the existence of this cell cluster may be a possible next step of research.

3.5 Discussion

Exploration into the transcriptomic heterogeneity of aged progenitor B cells was achieved in this chapter, both at the single-cell and cell population level. Through these two approaches, it was found that heterogeneity lay at the cell population level, which was explored to a greater sequencing depth in Pro-B and Pre-B cell populations.

This chapter successfully demonstrated an unbiased approach in handling the biological heterogeneity of ageing in the context of developing progenitor B cells. Through the subgrouped analysis of aged mice based on their Pre-B cell transcriptomes, it has been possible to show progressive dysregulation of biological pathways associated with inflammation, cell migration and cell adhesion, across the Pro-B to Pre-B cell transition. Upregulation of these signalling pathways is suggestive of aberrant progenitor B cell response to a disrupted external microenvironment[266,317,318].

The progressive transcriptomic dysregulation observed appears to have a negative causal effect on the differentiation of Pro-B cells at the population-level as they undergo V-DJ_H recombination (reduced VDJ_H:DJ_H of aged Pre-B cells, with a differential 3'-proximal>5'-distal V-gene usage) to become Pre-B cells, which must also undergo a proliferative burst. Such actions require large amounts of energy, and so an aged reduction in mitochondrial output due to a decrease in the presence/expression of mitochondrial genes reported throughout the developmental stages would limited these functions. Impaired mitochondrial respiratory capacity in aged leukocytes is well-documented[319,320], and normal progenitor B cells are known to undergo a shift from glycolysis to oxidative phosphorylation at the Pro-B to Pre-B cell stages[321,322] . Validation experiments using Seahorse or MitoTracker technology could be used to confirm if there is indeed a decrease in oxidative phosphorylation in the aged Pre-B cells, and whether this is due to a decrease in mitochondrial output (as a result of decreased gene expression) or decrease in mitochondrial mass (as a result of decreased biogenesis).

The metabolic pathway is regulated predominantly through cell surface receptor signalling via mTOR. In developing B cells, cell growth has conventionally been credited to IL7R and preBCR signalling, resulting also in the proliferation and differentiation of Pro-B cells and Pre-B cells[323,324]. However, there is growing evidence to support the more widely recognised mTOR-activating IGFR signalling pathway as playing a key role in murine Pro-B to Pre-B cell development[133,285,325,326]. My work showing a comprehensive decrease in *Irs1* gene expression in all aged Pro-B and Pre-B cells irrespective of heterogeneity adds weight to the hypothesis that defects in development at this stage are the result of supressed IGF1R signalling. It was also found that *Grb2* is transcriptionally downregulated in aged Pre-B cells, and given that Grb2 protein plays a role in BCR signalling through interactions with BLNK/SLP65 could also suggest a suppression of preBCR signalling at the Pre-B cell stage[327,328]. To confirm that the phenotype in aged progenitor B cells is IGF1R mediated, an IGF1R/Irs1 conditional KO mouse models could be generated and characterised to see if transgenic mice with B-cell specific loss will lead to an early-onset aged phenotype. In conjunction with this animal model, an *in-vitro* model system for differentiating progenitor B cells in the presence of exogenous IGF1 could also be used to compare the efficiency of young and

aged cells in a more controlled environment, for example to distinguish intrinsic from extrinsic defects.

In this chapter, compelling evidence supporting a multi-layered mechanism of suppression for *Irs1* has been shown that could be targeting at the gene expression, post-transcriptional, and protein level. The reduced expression of the H3K27 demethylase protein JMJD3 in aged Pre-B cells is consistent with the observed increase in H3K27me3 enrichment over the *Irs1* promoter, thereby supressing the gene's expression[275]. Additionally, the robust upregulation of *Soc2* gene expression in all of the aged Pre-B cells of this study provides another layer of IGF1R (and IL7R) signal suppression beyond the transcript level. *Koohy et al* have also shown in aged Pre-B cells an increase in the expression of miRNA's *miR-221*, *miR-222*, that target *Irs1* transcripts for degradation, providing more regulation at the post-transcriptional level[275] . At the protein level, Irs1 can be phosphorylated by different Serine/Threonine kinases (e.g. mTOR, S6K1, ERK, GSK3) at residues that can either activate (e.g. Ser-302) or inactivate (e.g. Ser-307)[292,329]. Irs1 inactivation via this process is part of a negative feedback mechanism that derives from the overstimulation of AKT signalling. Many metabolic disorders are characterised by the desensitisation of insulin signalling as a result of AKT overstimulation, which can be brought about by inflammatory mediators, such as TNFα[330,331]. I propose that a similar mechanism of Irs1 suppression is taking place in these aged Pro-B ad Pre-B cells, whereby unwanted overstimulation of the AKT signalling pathway by inflammatory mediators, cell migration signals, and cell adhesion, are driving targeted inactivation/suppression of Irs1 at the gene expression, post-transcriptional, and protein level. Whether all of these regulatory processes targeting Irs1 can be linked to this same negative feedback mechanism remains to be determined, although studies have shown downregulation of JMJD3 to be linked to insulin insensitivity, and *miR-221*, *miR-222* upregulation to AKT activation[332].

While this work suggests a plausible model, it is based on transcriptomic analysis alone, and so as such remains speculative. Validation experiments would need to be done on the protein levels of genes of interest to see if they reflect the transcript expression (e.g. Socs2, IGFBP4, Grb2, JMJD3/Kdm6b, Ezh2). Similarly, looking at the level of phosphorylation of certain proteins (and in some cases at different amino acid residues) would elucidate the validity of the proposed negative feedback inactivation of Irs1

protein – for example, Akt, mTOR, S6K1, GSK3 and Irs1 (Ser-302 versus Ser-307). Explorations should also be made in determining what inflammatory mediators, if any, are present within the bone marrow of the aged mice. An interesting candidate would be TNFα, since it has already been strongly linked inflammaging[333,334], Irs1 inactivation via negative feedback[330,331], and to the induction of the Il1b pathway (components of which had a recurring presence in my data)[335]. Other studies have also shown that blocking TNFα triggers a reduction in the expression of adhesion molecules and VEGF[336,337].

Prior however to the validation of a model hypothesis to age-impaired B cell development that revolves around Irs1/IGF1R signalling, it seemed appropriate first to confirm that desensitisation to IGF1 in fact is responsible for the aged phenotype of defective Pro-B to Pre-B differentiation. As you will encounter in the next chapter, the decision was made to create an *in-vitro* model system of progenitor B cell development that uses IGF1 to drive Pro-B to Pre-B cell differentiation. Doing so therefore not only allowed me to validate the impact of IGF1 on young and aged B cell development, but also provided a controlled platform for which hypothesised mechanisms driving the ageing phenotype could be explored either as part of this thesis, or for future experiments to come. In the case of Irs1 suppression, these functional experiments include, but are not limited to, the use of siRNA's or LNA's (complementary to miRNA's such as *miR-221/222*) or small molecule inhibitors (for example, to Socs2, JMJD3, or Ezh2).

Second to the robust connection to IGF1R suppression was the recurrence in these datasets of evidence which suggests defects in cell division in these aged Pro-B and Pre-B cells. As such, this too was explored in more detail in the next chapter.

To conclude, IGF1R suppression during aged Pro-B to Pre-B cell provides is a neat model that ties together many of the age-associated observations, including reductions in cell division, differentiation, and mitochondrial transcripts. The next chapter will look to take some of these observations further and attempt to validate them through functional experiments.

4 Creation of an in-vitro System for B cell Development to Explore Aged Defects

4.1 Introduction

A stable bone marrow microenvironment is essential for normal progenitor B cell development. Commitment down the B-lineage from haematopoietic progenitors, regulation of cell proliferation, and controlled differentiation through the different B cell subsets, all rely on growth factors and stromal cell interactions in different combinations at particular stages. IL7, the master regulator of progenitor B cell proliferation and differentiation in mice, drives differentiation of the earliest B cell progenitors (PrePro-B cells) which also require other factors including SCF and FLT3-L[72,75]. IL7 has also been shown to work with CXCL12, IGF1 and the pre-BCR to drive differentiation at the Pro-B and Pre-B cell stages[69,122,134]. On its own, IL7 is able to proliferate and maintain cells at the Pro-B cell stage[99]. An alternative factor termed Thymic Stromal Lymphopoietin (TSLP), whose receptor TSLPR pairs with IL7Rα, works in a similar fashion to IL7, and has been shown to selectively proliferate pre-BCR^{+} Pre-B cells[70,338]. However, knockout studies of TSLPR demonstrate the redundant role of TSLP signalling in early B cell development[339], whereas knockout of IL7/IL7R results in a near complete block in development at the Pro-B cell stage[340,341]. Collectively, these studies demonstrate the pivotal role of IL7 in early B cell development, with the combination of other factors that complete the microenvironment facilitating at different stages of early B cell development.

It is proximity to, and interactions with, different supportive stromal cells within the bone marrow niche that provide these developing B cells with the right combination of factors to either commit, proliferate, or differentiate. Stromal cells of the mesenchymal linage known to support different stages of progenitor B cell development include $LepR^+$ cells, CXCL12-abundant reticular (CAR) cells, and osx^+ osteoblasts[64,342]. These supportive cells express factors such as SCF, IL7, CXCL12 and IGF1 at different levels, and so therefore support different stages of development. For example, osx^+ osteoblasts express IGF1 for autocrine differentiation into osteocytes, however selective inhibition of IGF1 production from these osx^+ cells also leads to a reduction in Pro-B to Pre-B cell development in the bone marrow[67,147].

Attempts have been made to support the development of primary progenitor B cells in-vitro by mimicking this complex bone marrow microenvironment. One must consider many aspects, such as the starting primary cell population to initiate the culture, whether to include a supportive stromal cell line, and what exogenous growth factors to use in order to coordinate the appropriate effector cell fate decision. For example, *Cho et al*[343] start with murine embryonic stem cells on an OP9 stromal layer, and with the knowledge that OP9 cells produce IL7 and SCF, exogenously add FLT3-L in order to enhance the commitment of these stem cells down the B-lineage. In the *Vosshenrich et al* study[338], where they were exploring the role of TSLP in selectively proliferating pre-BCR^+ Pre-B cells, $CD19^+CD43^+$ Pro-B cells were cultured on an NIH3T3 stromal layer with exogenous IL7 or TSLP added to drive the production of IgM^+ cells in-vitro. *Landreth et al*[326] on the other hand depleted both adherent and $B220^+$ cells from total bone marrow suspension, culturing them on the IGF1-producing S17 cell line, with a supplement of exogenous IL7 in order to drive differentiation of these non-B cells into cytoplasmic Mu-expressing B cells. In similar fashion, *Holl et al*[344] depleted the adherent cells from a total bone marrow suspension, but retained the in-vivo derived B cells in the culture, and in the absence of any form of supportive stromal layer, adding first IL7 to proliferate the pro-B cells before adding BAFF to enrich for the IgM^+ cells in the culture. What has not yet been demonstrated in the literature however is an in-vitro system that can take primary $B220^-$ bone marrow progenitors and differentiate them into $B220^+IgM^+$ B cells – a testament to the complexity of this bone marrow niche in-vivo. Additionally, those systems that claim to produce IgM^+ B cells in-vitro appear to present a reduced antibody

repertoire diversity, or an overrepresentation of autoantibodies. The ability to harness a system that can derive all stages of B cell development in a more controlled in-vitro environment would be valuable in understanding what cells and factors are required for optimal development.

In ageing, the bone marrow microenvironment is disrupted, resulting in impaired B cell development[268,269]. There are changes in stromal cell composition resulting in mesenchymal progenitor cell differentiation favouring the adipolineage over the osteolineage[266,271]. There is also reduced production/release of (and response to) key growth factors from these aged stromal cells, such as IGF1 from aged osteoprogenitors[272,325], as well as the aberrant presence inflammatory cytokines such as TNFα produced by age-associated B cells (ABCs)[345]. All of these changes could be contributing to the aged defects in progenitor B cell development.

Such disruption to the bone marrow niche is supported in the findings from Chapter 3, which demonstrate transcriptional upregulation in inflammation, cell migration and cell adhesion in aged Pro-B and Pre-B cells, suggestive of response to external environment. From these results, the most apparent functional outcomes to the disruption of B cell development are reduced cell division and impaired VDJ_H recombination dynamics (reduced V-DJ_H recombination and overall V-gene usage), manifesting as a reduced Pro-B to Pre-B cell transition. It was also hypothesised that these aged defects could be caused by the suppression of IGF1R signalling through downregulation of its adaptor Irs1. By differentiating aged progenitor B cells in an in-vitro setting away from its disrupted microenvironment, and in the presence of exogenous IGF1 in excess, one would be able to determine the contribution of defective IGF1R signalling to the aged defected observed in-vivo.

This chapter therefore will predominantly explore the creation of an in-vitro culture system for differentiating young and aged progenitor B cells with IGF1, and then utilising this system to validate findings from Chapter 3. I will begin however with an in-vivo experiment to investigate the changes in cell cycle progression in aged progenitor B cells, since the findings from Chapter 3 were suggestive of reduced cell division with age.

4.2 Reduction in aged Pro-B and Pre-B cells entering S-phase

In Chapter 3, I demonstrated a decrease in absolute numbers of progenitor B cells in the bone marrow of aged mice, resulting also in a reduced proportion of the $CD25^+$ Late Pre-B cells. I also showed by GSEA the enriched downregulation of several GO symbols associated with cell cycle, such as *Cell Division*. Combined with the surprising finding that these aged $CD25^+$ Late Pre-B cells also possessed more quantifiable DNA per cell than their young counterparts lead to the hypothesis that these aged cells may be stuck at the G2M checkpoint of cell cycle, awaiting cytokinesis.

To follow up these findings, in-vivo BrdU analysis was conducted to capture the real-time cell cycle stages of progenitor B cells in their bone marrow environments. Pro-B ($B220^+CD19^+IgD^-CD25^-IgM^-CD43^+$ small), Early Pre-B ($B220^+CD19^+IgD^-CD25^-IgM^-CD43^+$ large), Late Pre-B ($B220^+CD19^+IgD^-$ $CD25^+IgM^-$), and Immature B ($B220^+CD19^+IgD^-$ $CD25^+IgM^+$) cells from young (3 months; n=6) and aged (~24 months; n=8) WT mice were analysed. There were some subtle differences in the classification of the progenitor B cell populations compared to those defined in Chapter 3 (Pro-B: $CD19^+AA4.1^+CD25^-IgM^-$ $IL7R\alpha^+CD43^{hi}CD24^{lo}$ versus $IgD^-B220^+CD25^-IgM^-CD19^+CD43^+$small; Early Pre-B: $CD19^+AA4.1^+CD25^-IgM^-IL7R\alpha^+CD43^{lo}CD24^{hi}$ versus $IgD^-B220^+CD25^-IgM^-$ $CD19^+CD43^+$large; Late Pre-B $CD19^+AA4.1^+CD25^+IgM^-$ versus $IgD^-B220^+CD25^+IgM^-$; Immature B: $CD19^+AA4.1^+CD25^-IgM^+$ versus $IgD^-B220^+CD25^-IgM^+$). Despite this, the reduction in the proportions of Late Pre-B cells in ageing was still observed (Figure 4-1).

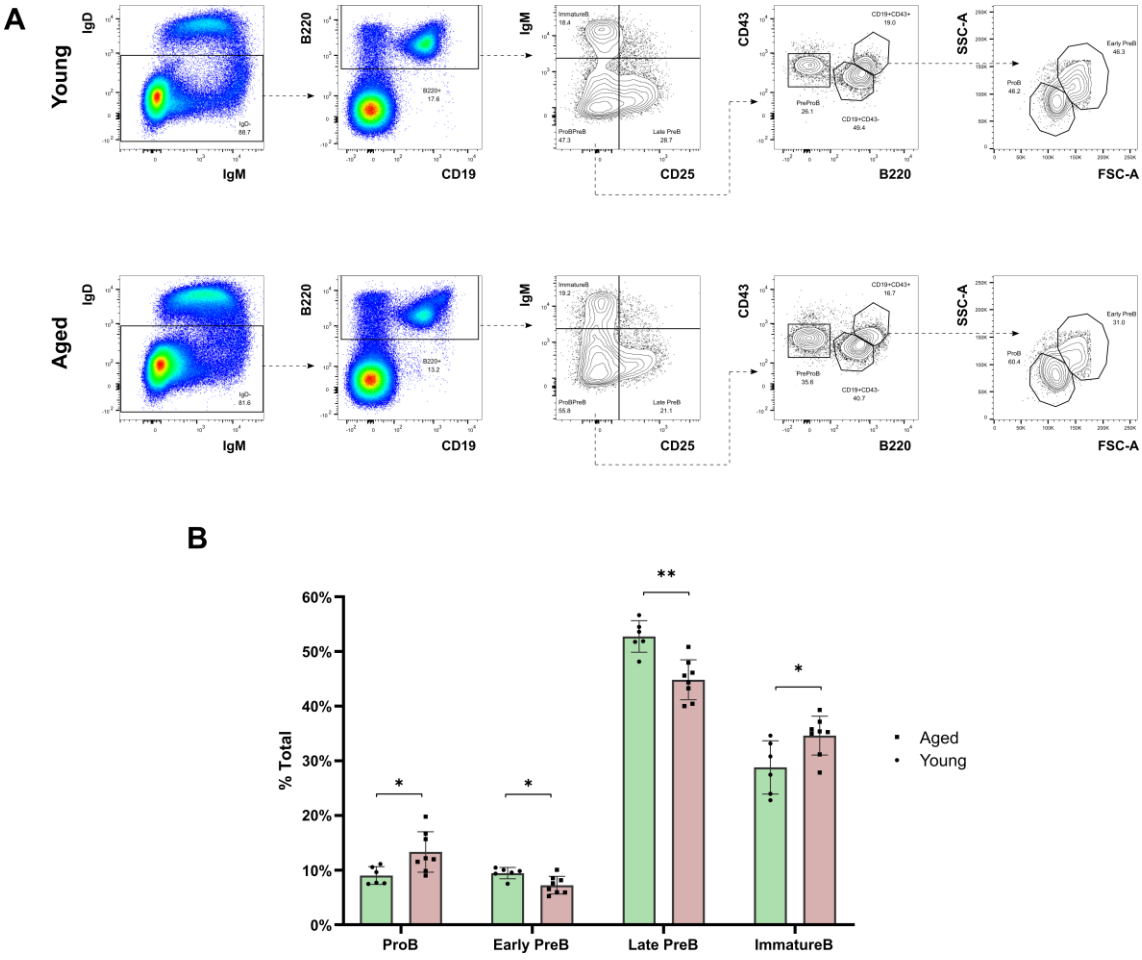

Figure 4-1: Gating strategy for progenitor B cell populations. (A) FACS plots showing the classification of Pro-B ($IgD^-B220^+CD25^-IgM^-CD19^+CD43^+$small), Early Pre-B ($IgD^-B220^+CD25^-IgM^-CD19^+CD43^+$large), Late Pre-B ($IgD^-B220^+CD25^+IgM^-$) and immature B ($IgD^-B220^+CD25^-IgM^+$) for young (top panel) and aged (bottom panel) mice, to be used for cell cycle analysis. All cells were gated for live singlet lymphocytes prior to this gating strategy. (B) Proportions of each B cell population as a percent of total (Young n=6, Aged n=8; padj <0.05, multiple t-test with FDR correction).

For each of the Pro-B, Early Pre-B, Late Pre-B, and Immature B cell populations, cell cycle stages were classified for each cell based on the incorporation of BrdU and/or 7AAD into their DNA (Figure 4-2). 7AAD stains all DNA, and so will resolve the G0 and G2M stage cells based on DNA quantity, whereas BrdU can only incorporate into actively replicating DNA, thereby revealing cells in S-phase. Through this separation, the expected burst of proliferation characteristic of the cycling Early Pre-B cells is captured, with >80% of these cells actively in S-phase (Figure 4-2).

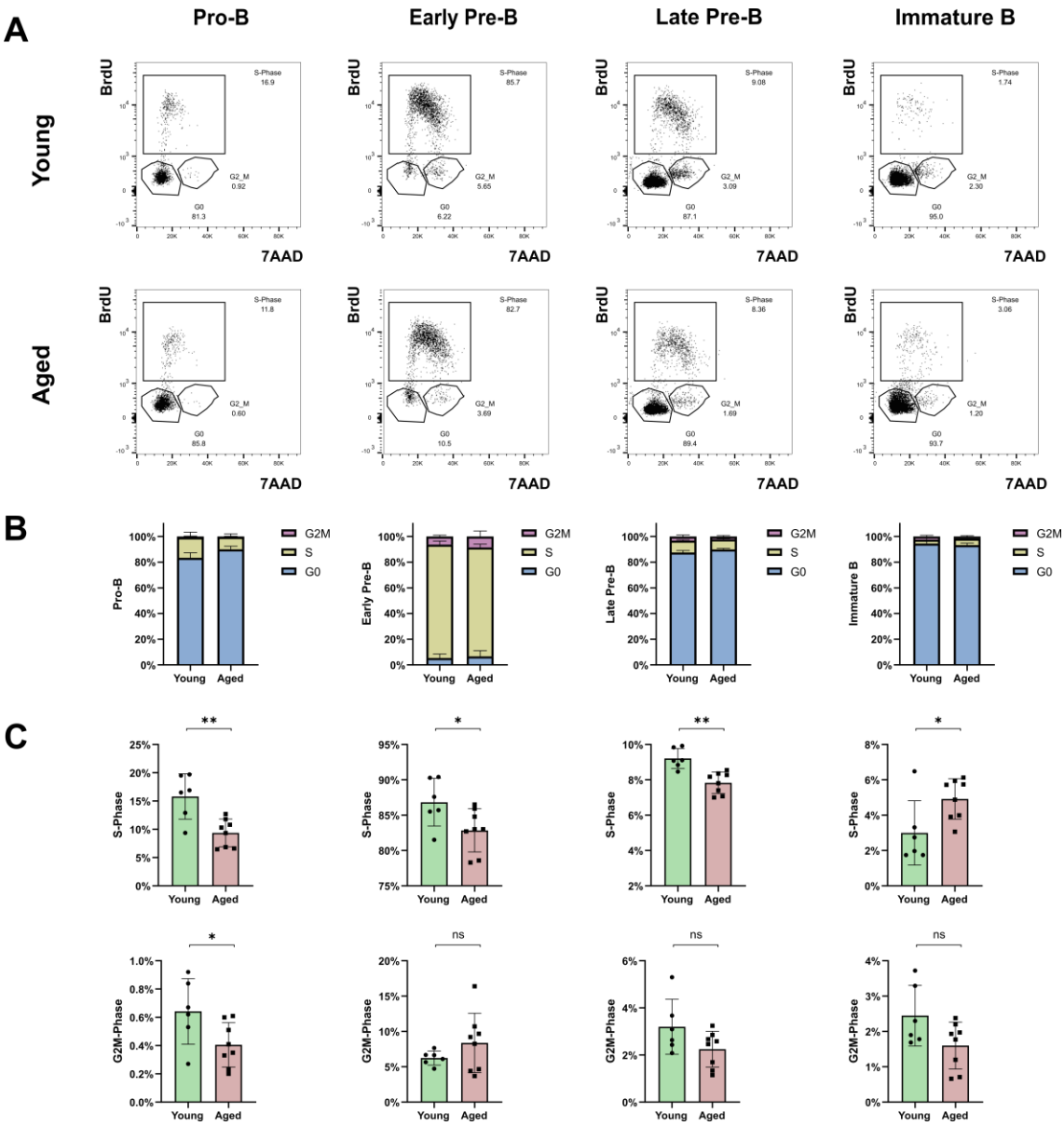

Figure 4-2: Cell cycle analysis of progenitor B cell populations. (A) Gating strategy for classification of G0, S, and G2M phases of cell cycle based on BrdU and 7AAD staining for each progenitor B cell population of young (top panel) and aged (bottom panel) mice. (B) 100% stacked barplots summarising the proportional breakdown of cell cycle stages for each cell population. (C) Young and aged comparisons in the proportion of S-phase (top panel) and G2M-phase (bottom panel) cells for each cell population (Young n=6, Aged n=8; pval <0.05, unpaired t-test).

Across the Pro-B, Early Pre-B, and Late Pre-B cell populations, there was a mild but significant reduction in the proportion of aged cells in S-phase, consistent with the hypothesis that aged Pro-B and Pre-B cells are less proliferative. Interestingly, there was also a mild but significant increase in the proportion of Immature B cells in S-phase in the aged group, perhaps indicative of premature stimulation in the aged bone marrow.

It can therefore be concluded that aged cells have a reduced capacity to engage in cell cycle through the Pro-B and Pre-B cell stages, as indicated also in Chapter 3. On the other hand, it was also anticipated that the aged Late Pre-B cells would have more cells in G2M-phase, since aged cells possessed more DNA per cell when compared to the young Pre-B cells and so would suggest DNA replication (S-phase) without cell division. However, there was no difference between young and aged mice in the proportions of cells in G2M in this cell population. For the other progenitor B cell populations, the only statistical difference between young and aged was in the Pro-B cells, which had larger proportion of cells in G2M in young. The contradictory measurements in the DNA content of aged Late Pre-B cells means that experimentally this will need to be explored further.

4.3 Creation of an in-vitro system for differentiating B cells

As mentioned in the chapter's *Introduction*, several in-vitro systems for differentiating progenitor B cells exist in the literature. However, none have succeeded in developing a system which can differentiate a starting $B220^-$ haematopoietic progenitor population into IgM^+ B cells. In such a system, all B cells and their V(D)J recombination events will have occurred in-vitro as a result of the culture conditions (i.e. stromal cell and exogenous growth factors) and so this presents the opportunity to better interrogate the dynamics of B cell development. I present here the creation of this system, which was essentially designed by combining and optimising the methods and findings from the independent studies referenced in the *Introduction*[346,343,338,326,344]. Given also its purposes for this project were to elucidate the role of IGF1R signalling in young and aged B cell development, the system in question has been designed to be IGF1-focussed.

In summary, bone marrow cell suspension is depleted of most committed haematopoietic lineages (B cells: $CD19^+$ and $B220^+$; T cells: CD3e; Macrophages: CD11b; Granulocytes: Gr-1; Red Blood Cells: Ter119) and the remaining heterogeneous pool of haematopoietic progenitors and endogenous stromal cells are used as the starting cell population to culture. The culture lasts 18 days, during which time cells are exposed to different exogenous growth factors in order to drive the necessary developmental cell

fate decisions. Initially, the $B220^-$ cells are exposed to IL7 with FLT3L for 4 days in order to drive commitment down the B-lineage. Then more IL7 is provided, this time on its own, for a further 4 days to maintain B cell differentiation and proliferation. Finally, cells are exposed to IGF1 for 10 days over a series of 3 media replenishments until the in-vitro derived $B220^+$ cells express IgM on their surface (Figure 4-3). The 5 media replenishments in total over the course of the 18 day culture are achieved by removing half of the cell medium and replacing with fresh medium containing the exogenous growth factors at twice their final concentration.

Over the course of the optimisation process, incremental changes were made to reach the final culture conditions. For example, 6-well plates were initially used, but it was found that as the cell numbers increased through the culture, they were exposed to a "vortex effect" within each well. Therefore, cells are cultured in 24-well plates where they remain undisturbed in suspension for the duration of the culture. The length of IGF1 exposure was initially 7 days, but extension to 10 days was found to give better enrichment of IgM^+ cells. When determining the starting cell population, a reductionist approach was adopted, whereby cultures were first trialled with lineage-depleted bone marrow cells that still contained the B-lineage ($B220^+CD19^+$), then without $CD19^+$ cells ($B220^+CD19^-$), until finally settling with no B cells ($B220^-CD19^-$) as there was no difference in IgM^+ generation (data not shown).

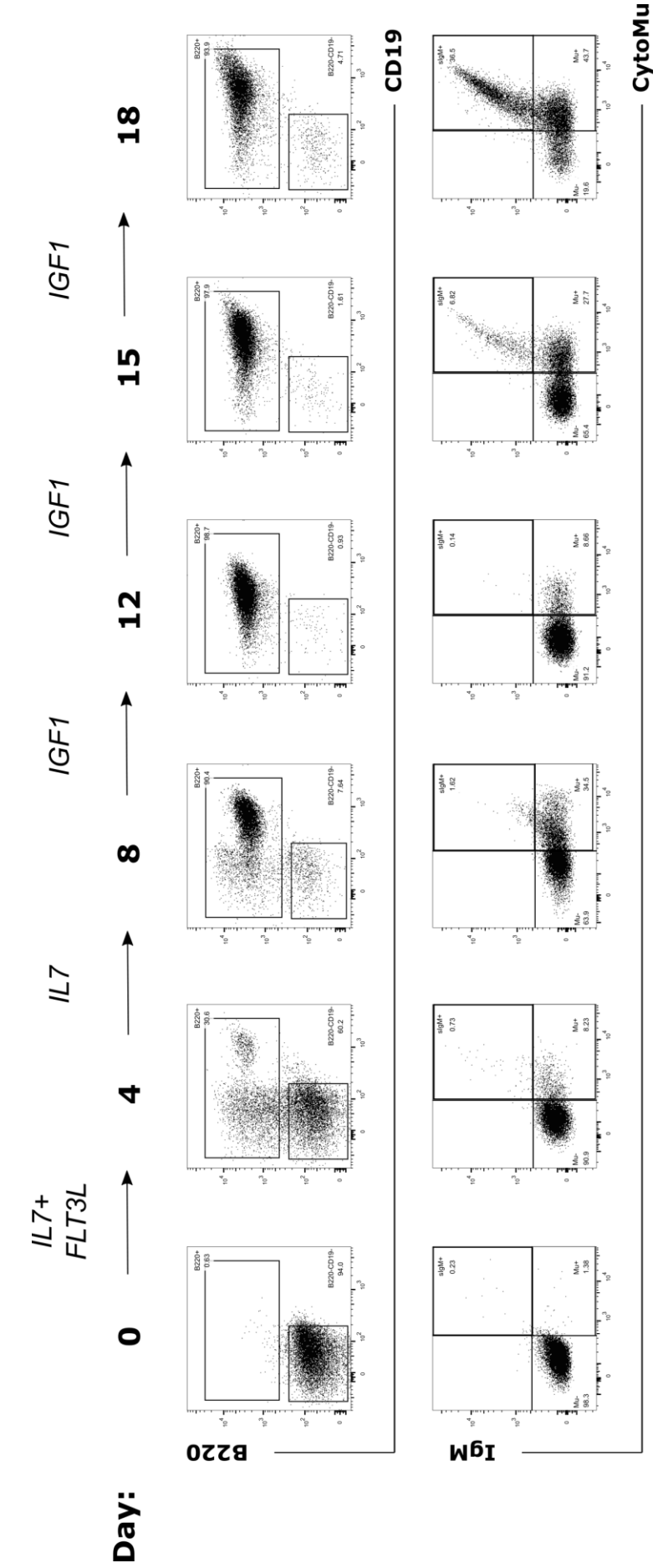
Day:
0
4
8
12
15
18
IL7+
FLT3L
IL7
IGF1
IGF1
IGF1
B220
CD19
IgM
CytoMu

Figure 4-3: In-vitro culture system schematic. Lineage-depleted bone marrow cells from young (3 months) mice that do not contain B cells (B220/CD19) and have therefore not undergone VDJ_H recombination (CytoMu/IgM) are used as the starting cell population. Cell are differentiated into B cells ($B220^+CD19^+$) and undergo VDJ_H recombination ($CytoMu^+/IgM^+$) over the course of the 18 day culture when exposed to IL7, FLT3L, and IGF1. FACS plots represent cells at each timepoint (day 0, 4, 8, 12, 15, 18). All cells were gated for live singlet lymphocytes prior to this gating strategy.

The final culture dynamics sees a pool of non-B cells at day 0 differentiate into $B220^+$ cells by day 8 (mean: 90.5%) in the presence of IL7 (and FLT3L), with approximately one third of these $B220^+$ cells expressing cytoplasmic Mu (mean: 31.9%, $0.95x10^6$ cells) (Figure 4-4). These $B220^+$ cells proliferate to confluence from day 8-12 with the addition of IGF1. Interestingly from days 8-12, as the $B220^+$ cell numbers more than doubles ($2.98x10^6$ cells to $7.03x10^6$ cells), the number of cytoplasmic Mu^+ cells conversely halves ($0.95x10^6$ cells to $0.49x10^6$ cells), resulting in a cumulative 4-fold reduction in the proportion of $B220^+$ cells that express cytoplasmic Mu (31.9% to 7.16%). Cells are exposed to further IGF1 from days 12-18 (with a replenishment of medium at day 15), during which time the total $B220^+$ cell population declines (due to cell death), and IgM^+ cells are produced. The end result is by day 18, on average ~40% of the remaining $B220^+$ cells are cytoplasmic Mu^+ and ~20% are IgM^+, translating to ~60% of $B220^+$ cells that have undergone V(D)J recombination in-vitro. Recombination status of the Ig_H locus was confirmed by DNA VDJseq, comparing the percent of VDJ_H reads from all VDJ_H and DJ_H reads in all the $B220^+$ cells generated at each timepoint measured. Increased functional V-gene recombination (functional if coding region has an open reading frame without a stop codon, no defect in the splicing sites, recombination signals and/or regulatory elements) from days 12-18 reflected the increased proportions of cytoplasmic Mu and surface IgM expression seen at the same timepoints (Figure 4-4).

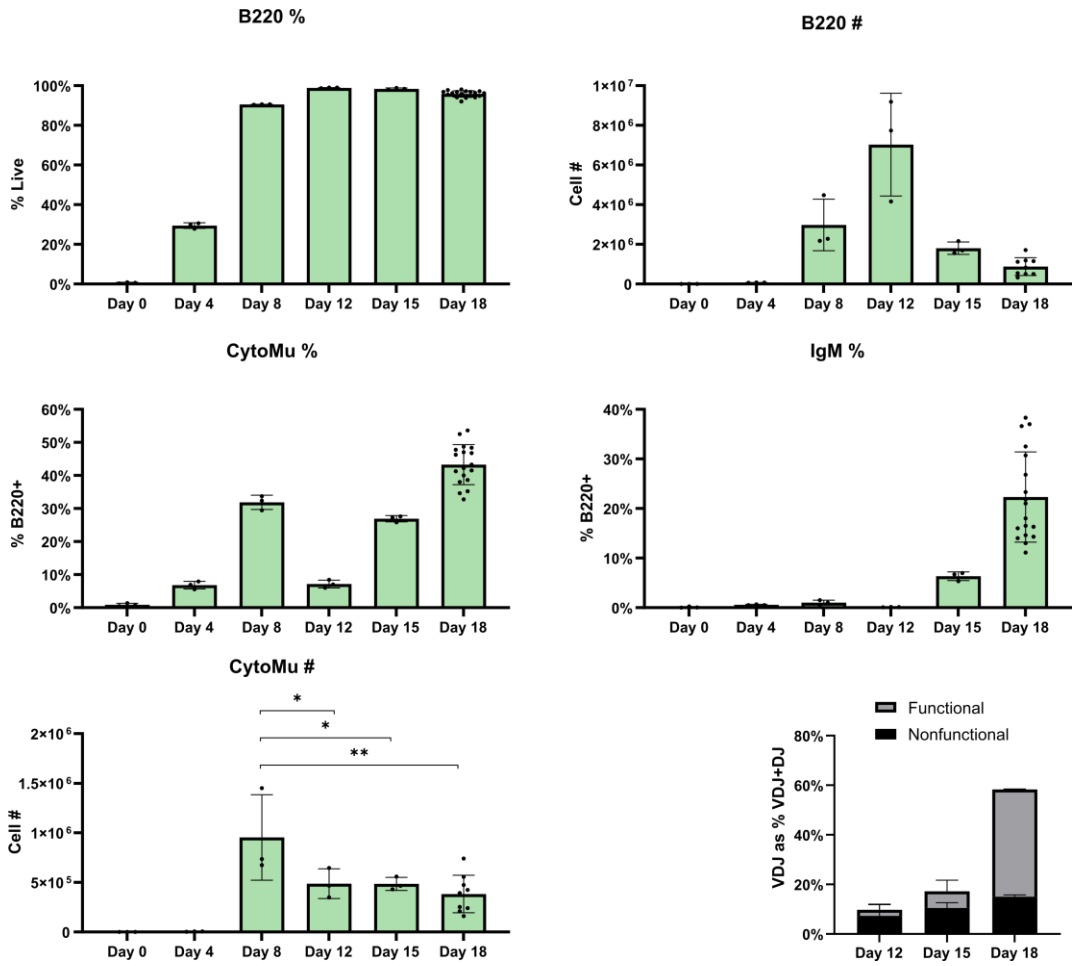

Figure 4-4: Summary of the in-vitro growth dynamics for cells from young (3 months) mice. Lineage-depleted bone marrow cells were exposed to the culture conditions shown in Figure 4-3. Once cells differentiate into B220⁺ B cells, they remain the dominant cell type for the duration of the culture (top left). The largest proliferative burst of B220⁺ cells is seen from day 8-12, after which point cell numbers decline (top right). Cytoplasmic Mu⁺ cells are first detected at day 8, but it is not until days 15-18 that IgM⁺ cells are produced. All cells were gated for live singlet lymphocytes prior to this gating strategy. VDJ_H recombination status of the Ig_H locus by VDJseq (% VDJ reads from all recombination events in B220⁺ cells, bottom right) reflect the levels of heavy chain protein expression from day 12-18. (Cell numbers are per well; Day 0-15 n=3, Day 18 n=18, VDJseq n=2; statistics by one-way ANOVA).

It was reported by *Holl et al* in their culture that exposure to the B cell survival factor BAFF permitted differentiation into IgM⁺ cells in-vitro. However, the inclusion of BAFF with IGF1 from Days 12-18 in my cultures showed no additional improvements to the enrichment of either cytoplasmic Mu or IgM⁺ cells at the day 18 timepoint (Figure 4-5).

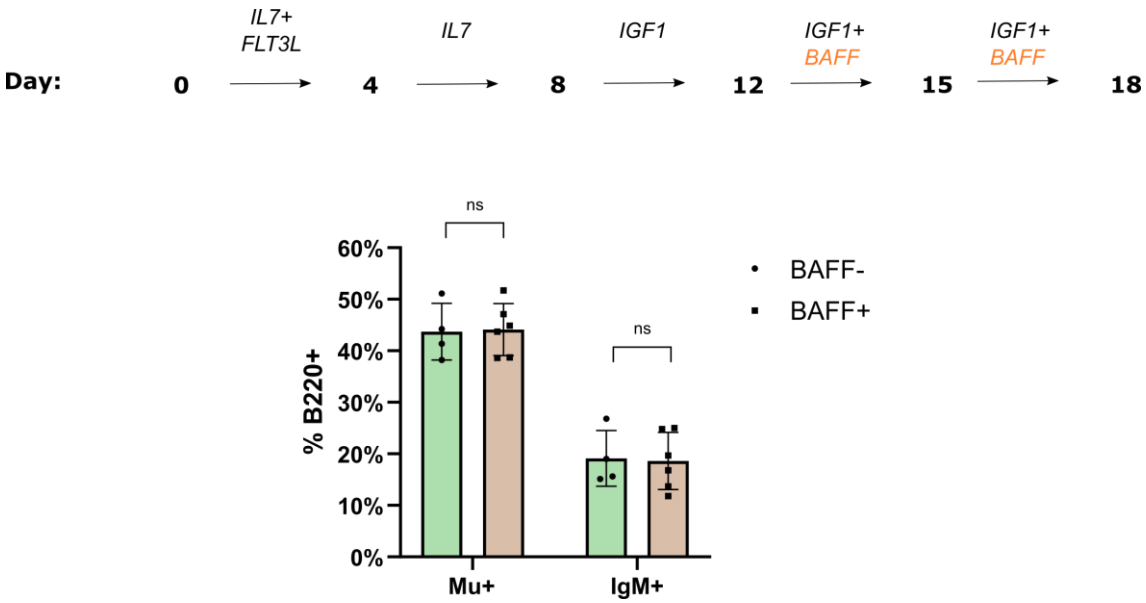

Figure 4-5: Inclusion of BAFF with IGF1 from days 12-18 did not provide any additional improvements to the proportion of live B220⁺ cells that express either cytoplasmic Mu or surface IgM. (BAFF- n=4, BAFF+ n=6; pval <0.05, unpaired t-test).

Alternative techniques for generating IgM⁺ cells in-vitro include using TSLP[338,346] or starving B cells of growth factors by replenishing the cells with media lacking additional exogenous factors[347]. Comparisons were therefore made between the use of IGF1 and these other 2 methods – herein named "TSLP" and Medium-only ("Med") – to see which method gave the best enrichment of B cells expressing either cytoplasmic Mu or surface IgM⁺ B cells (Figure 4-6). While there were no differences between the TSLP and Medium-only ("Med") conditions in generating these later-stage B cell subsets, exposure to IGF1 showed a significant increase in the proportions of both cytoplasmic Mu and surface IgM-expressing B cells by day 18.

Looking again at the recombination status of the Ig_H locus (percent VDJ_H reads from VDJ_H and DJ_H recombination events) from the B220⁺ cells generated at day 18 shows that this superior V-DJ_H recombination in IGF1 versus Med conditions is also through functional recombination events (in-vitro IGF1: 58.9% VDJ_H, 74.2% functional V-gene; in-vitro Med: 35.7% VDJ:DJ, 53.0% functional V-gene). When also compared against in-vivo derived Late Pre-B cells (from Chapter 3) – a population that is biased towards cytoplasmic Mu⁺ cell status – the recombination efficiency of the in-vitro IGF1-exposed B220⁺ cells is reaching the frequency found in bone marrow (in-vivo Late Pre-B: 75.8% VDJ_H, 71.8%

functional V-gene). What this therefore demonstrates is that IGF1 plays a key role in the differentiation of progenitor B cells that begins at the V-DJ_H recombination stage of Pro-B to Pre-B cell development.

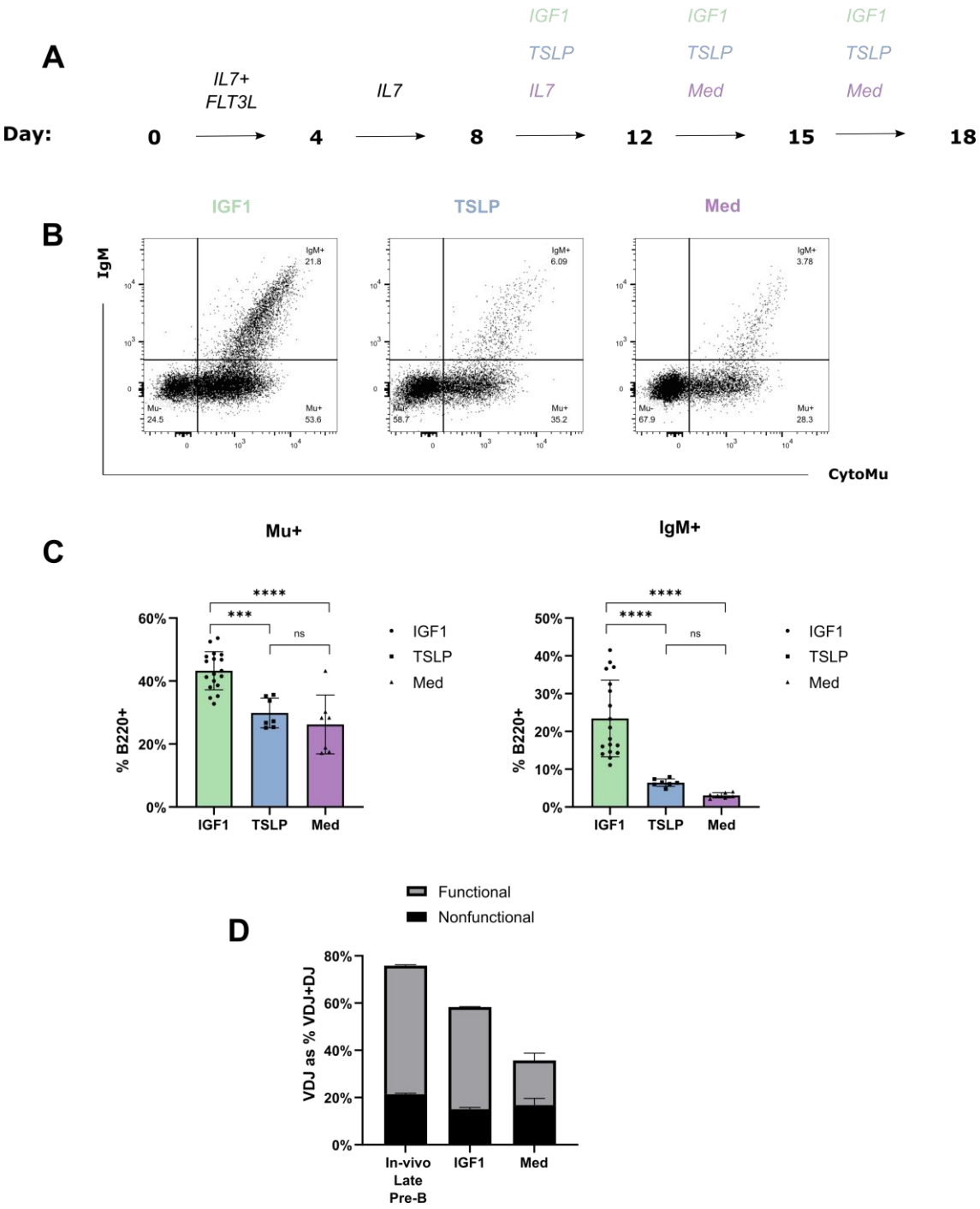

Figure 4-6: Comparisons of IGF1 with TSLP and Medium-only conditions. (A) Cells from young (3 months) mice were differentiated with IL7 (and FLT3L) for days 0-8, then either exposed to IGF1, TSLP, or more IL7 for days 8-12, followed by either IGF1, TSLP or medium without any additional growth factors (Medium-only; Med) respectively for days 12-18. (B) Representative FACS plots from day 18 showing the proportion

of B220$^+$ cells expressing cytoplasmic Mu or surface IgM across the 3 different conditions: i) IGF1 ii) TSLP iii) Med. All cells were gated for live singlet lymphocytes prior to this gating strategy. (C) B220$^+$ cells exposed to the IGF1 condition had proportionally more cytoplasmic Mu (left) and surface IgM (right) expression at day 18 compared to the TSLP and Med conditions. (D) VDJ$_H$ recombination status of the Ig$_H$ locus by VDJseq show cells grown in IGF1 to recombine more functional V-genes compared to Med condition, but less than in-vivo Late Pre-B cells (CD19$^+$AA4.1$^+$CD25$^+$IgM$^-$). (FACS analysis: IGF1 n=18, TSLP n=7, Med n=7; padj <0.05, one-way ANOVA. VDJseq analysis: Late Pre-B n=4, IGF1 n=2, Med n=2)

Further interrogation of the IgM$^+$ B cell populations generated after exposure to IGF1 revealed that over 80% also express the light chain protein Igκ, and thus have undergone all stages of V(D)J recombination in-vitro (Figure 4-7). However there was an additional unexpected finding that a third of these IgM$^+$ cells (36.7% average) also co-express IgD – indicative of a mature naïve B cell subset. It can be concluded therefore that this in-vitro culture system can generate all stages of B cell development from a starting population of non-B cells.

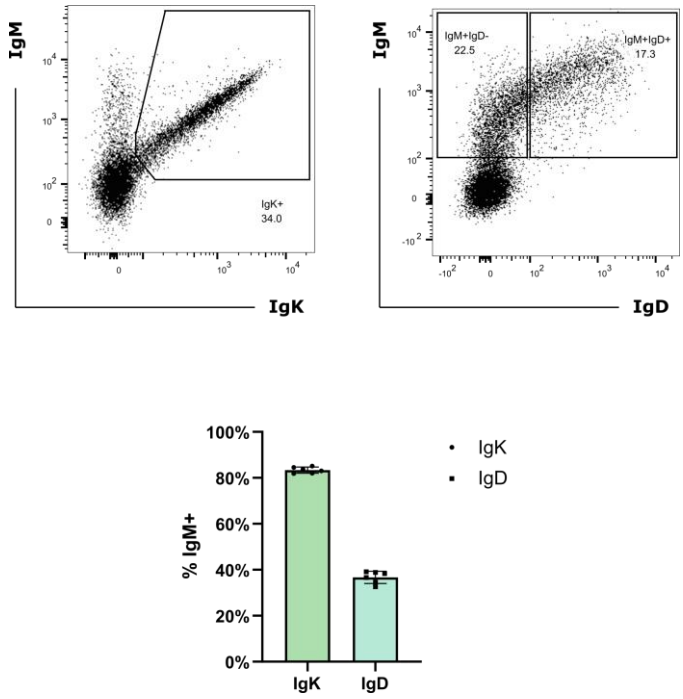

Figure 4-7: Expression of Igκ and IgD at day 18 when exposed to IGF1. (A) Representative FACS plots of B220$^+$ cells from young (3 months) mice. All cells were gated for live singlet lymphocytes prior to this gating strategy. (B) Quantifications for the proportion of B220$^+$IgM$^+$ cells that express either Igκ or IgD (n=6).

4.4 Impairments in aged B cell development in response to IGF1

Following establishment and characterisation of an in-vitro system for early B cell development, functional experiments exploring the biology of aged progenitor B cell development were performed. Bone marrow from aged mice were this analysed in this in-vitro system. Through the course of the 18 day culture, aged (21-26 months) WT mice follow the same developmental trajectory as young (3 months) mice (Figure 4-8). Lineage-depleted bone marrow cells differentiate into $B220^{+}$ B cells and then express cytoplasmic Mu and surface IgM when exposed to IGF1. However, it should be noted that the aged starting population of $B220^{-}$ cells had a very weak stain for IgM by flow cytometry that was not present in the young (Figure 4-9 and Figure 4-10). Given also that this cell population is not thought to be of the B cell lineage, this aberrant IgM stain is more likely to be from "natural IgM" bound to the surface of these cells, rather than expressed on their cell surface[348], which is known to increase with age[258]. In any case, this aged difference is lost through the culture as the cells propagate (Figure 4-10).

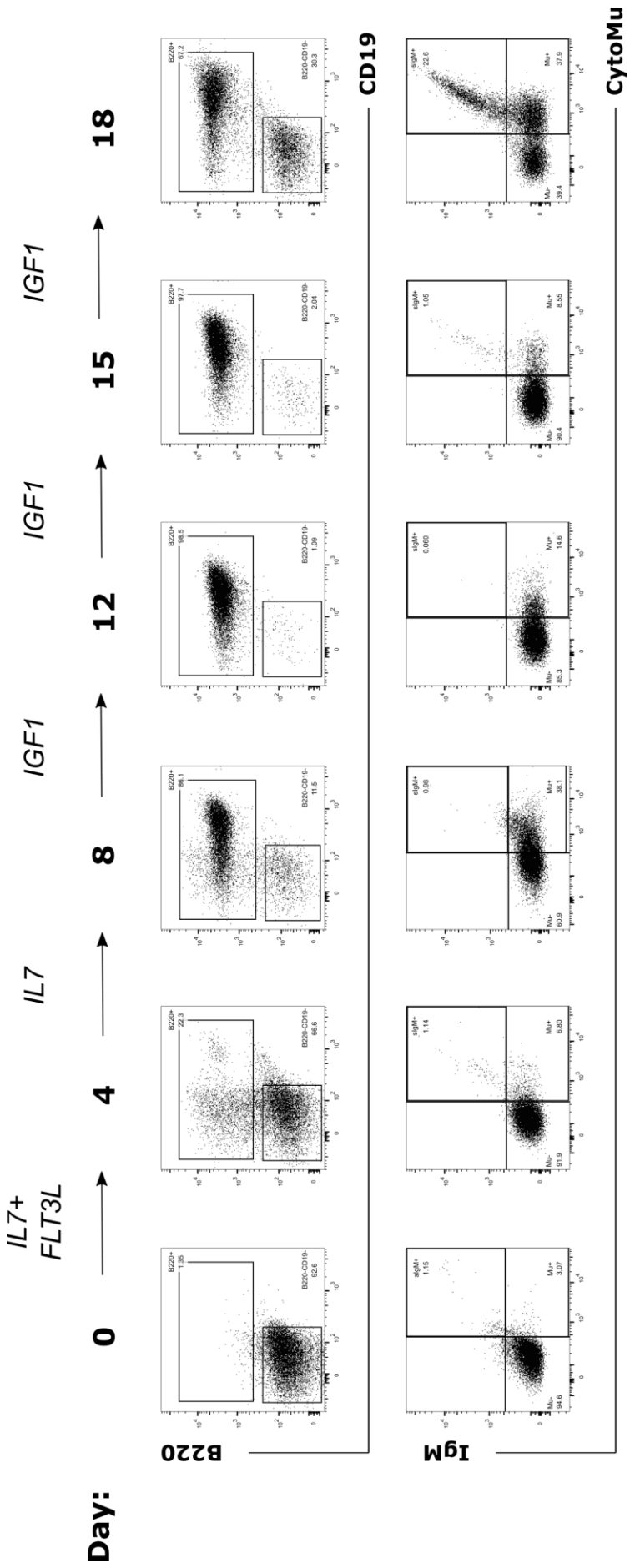
Day:
0
4
8
12
15
18
IL7+
FLT3L
IL7
IGF1
IGF1
IGF1
B220
IgM
CD19
CytoMu

Figure 4-8: In-vitro culture system schematic for aged cells. As with Figure 4-3, lineage-depleted bone marrow cells from aged (21-26 months) mice that do not contain B cells (B220/CD19) and have therefore not undergone VDJ_H recombination (CytoMu/IgM) are used as the starting cell population. Cells are differentiated into B cells ($B220^+CD19^+$) and undergo VDJ_H recombination ($CytoMu^+/IgM^+$) over the course of the 18 day culture when exposed to IL7, FLT3L, and IGF1. FACS plots represent cells at each timepoint (day 0, 4, 8, 12, 15, 18). All cells were gated for live singlet lymphocytes prior to this gating strategy.

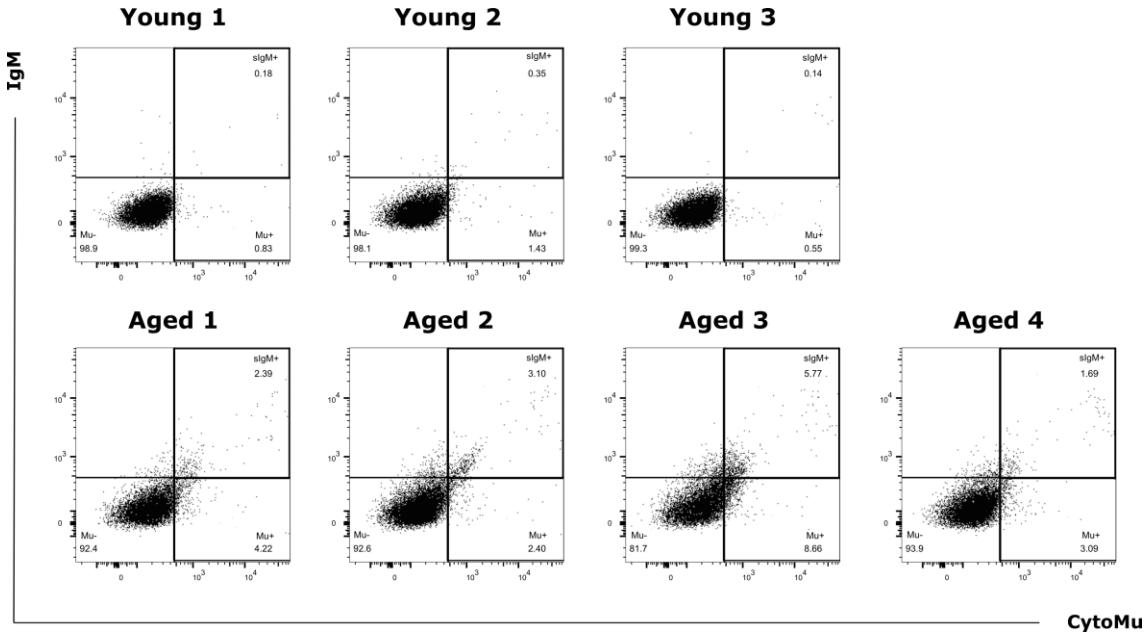

Figure 4-9: Low-level IgM staining on lineage-depleted aged bone marrow cells. Representative FACS plots show the presence of cytoplasmic Mu or surface IgM on the starting cell culture population of lineage-depleted bone marrow cells ($B220^-CD19^-CD3e^-CD11b^-Gr1^-Ter119^-$) of young (top panel) and aged (bottom panel) mice at day 0. All cells were gated for live singlet lymphocytes prior to this gating strategy.

There were also some notable differences in the growth/selection dynamics of aged cells compared to young as they progressed through the culture. For example, aged $B220^-$ cells appear to be less efficient at differentiating into $B220^+$ cells when exposed to IL7 and FLT3L (days 0-8), although this is rectified when the cells reach confluence at day 12 (Figure 4-10). However, the difference is again reinstated during the IGF1-driven selection process to day 18, as there is a reduction in both the number and proportions of $B220^+$ cells in the aged culture versus young (Young vs Aged mean: 95.8% vs 81.9% $B220^+$; ~0.5-1.5x10^6 cells vs ~0.12-0.75x10^6 cells). Interestingly, cytoplasmic Mu production in these aged cells when exposed to IL7 (day 8) is comparable to young, as

opposed to in IGF1 (day 18) where there is ~25% reduction in cytoplasmic Mu^+ (Young: 43.26%, Aged: 30.58%; mean) and ~50% reduction in surface IgM^+ cells (Young: 22.32%, Aged: 13.07%; mean) (Figure 4-10). These dynamics suggest that aged progenitor B cells have a reduced capacity to differentiate in response to IGF1. In support, when aged cells were cultured in TSLP and Medium-only conditions (as described in Figure 4-6A), the aged reduction in cytoplasmic Mu and surface IgM expressing cells at day 18 compared to young was greater when cells were exposed to IGF1 (Figure 4-11).

The IGF1-dependent defects in aged B cell development observed through this in-vitro culture effectively recapitulate the defects observed in-vivo of impaired V-DJ_H recombination and reduced Pro-B to Pre-B cell transition. What is perhaps most surprising about these findings is that the aged desensitisation to IGF1 response that leads to impaired early B cell development arises from haematopoietic progenitors that have not yet committed down the B-lineage, and thus the aged defect appears to persist as cells differentiate.

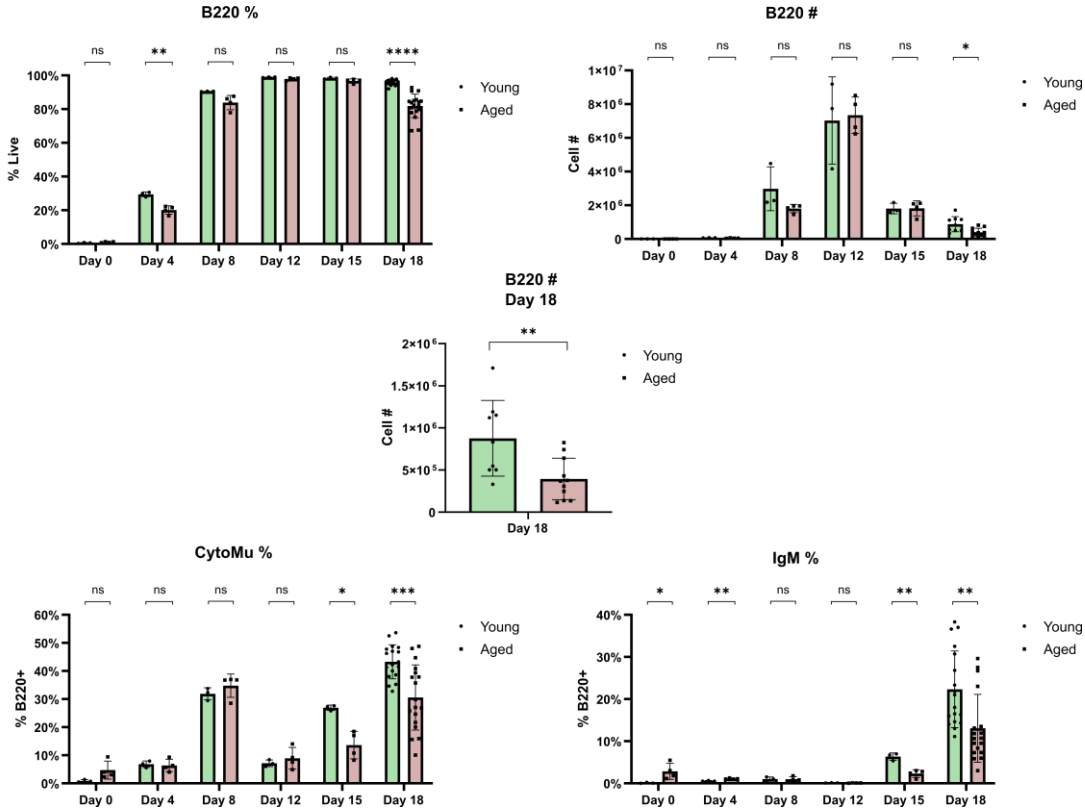

Figure 4-10: Comparative summary of the in-vitro growth dynamics for cells from young (3 months) and aged (21-26 months) mice. Aged cells show reduced $B220^+$ proportions at day 4 and 18 (top left), but only show statistically significant reductions in $B220^+$ numbers at day 18 (top right, and centre). Cytoplasmic

Mu expression is comparable at day 8, but is reduced in aged cells from days 15-18 (bottom left). The higher IgM⁺ proportions in aged cells at day 0 reflect the low-level staining of Figure 4-9. Despite this, aged cells have reduced proportions of IgM⁺ cells from days 15-18 (bottom right). (Young: days 0-15 n=3; Aged: days 0-15 n=4; Young: day 18 n=18; Aged: day 18 n=18; padj <0.05, multiple t-test with FDR correction. B220⁺ numbers day 18: Young n=9, Aged n=11; pval <0.05 unpaired t-test).

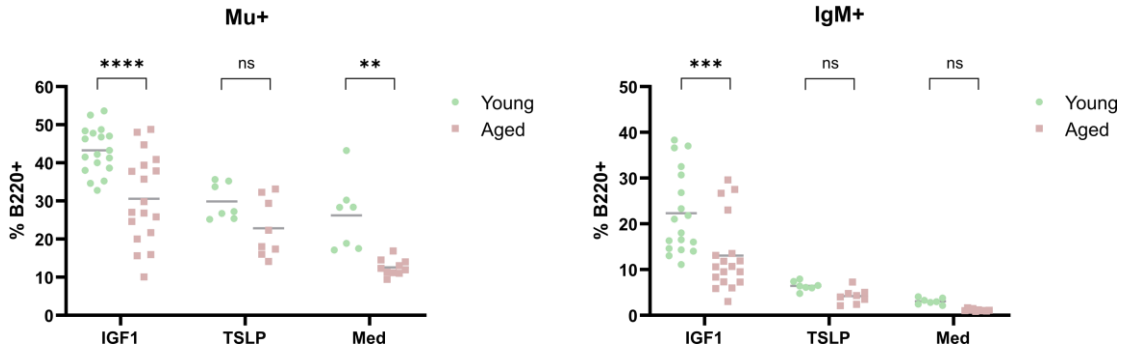

Figure 4-11: Aged reductions in cytoplasmic Mu and surface IgM expressing cells in IGF1 versus TSLP and Medium-only conditions. Aged B220⁺ cells at day 18 show reduced proportions that express cytoplasmic Mu and surface IgM, with the most prominent reductions when exposed to IGF1 (IGF1: Young n=18, Aged n=18; TSLP: Young n=7, Aged n=8; Med: Young n=7, Aged n=8; padj <0.05, two-way ANOVA).

Although aged progenitor B cells display a reduced capacity to differentiate in-vitro, they still produce IgM⁺ cells. Of these IgM⁺ cells, the proportion that also express Igκ at day 18 is comparable to young, suggesting that aged B cells can sufficiently $VJ_κ$ recombine and pair with heavy chain protein to produce the complete BCR. On the other hand, there was a reduction in the proportion of IgM⁺ cells that co-express IgD, demonstrating that there may also be age-related defects in the maturation of B cells into their mature form (Figure 4-12). Whether these further defects in B cell maturation are IGF1-dependant required further investigation.

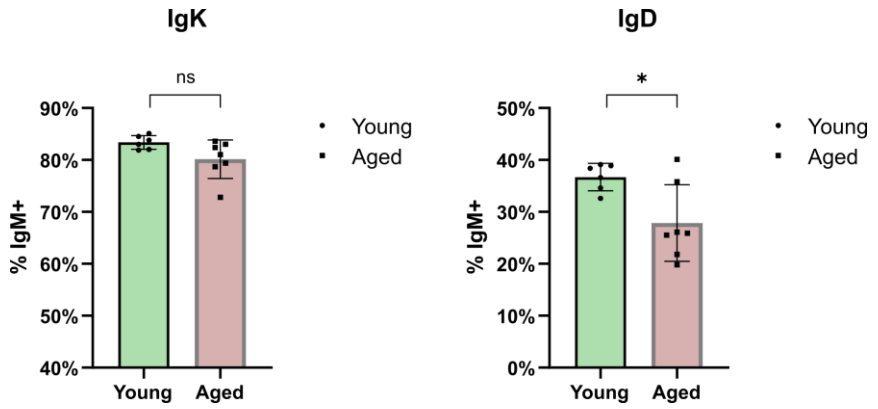

Figure 4-12: Comparative expression of Igκ and IgD in young and aged B220$^+$IgM$^+$ cells at day 18 when exposed to IGF1. There is no difference in the proportion of Igκ cells, but an aged reduction was seen in the proportions of IgD$^+$ cells (Young n=6, Aged n=7; pval <0.05 unpaired t-test).

Further interrogation of the Ig_H locus recombination status by DNA VDJseq affirms the observations that aged B cells have reduced V-DJ_H recombination capacity in-vitro. Percentage of VDJ_H reads in young and aged B220$^+$ at day 18 revealed that the greater proportion of V-DJ_H recombination events in young versus aged were of functional V-genes (Figure 4-13).

It was established in Chapter 3 that there is an age-associated shift in the usage of functional V-genes across the Ig_H locus of aged Pre-B cells derived in-vivo, manifesting into an overall over-representation of the 3'-proximal Q52/7183 V-gene families, to the detriment to the distal 5' J558/3609 V gene families. Important biological insights surrounding the impact of IGF1 on repertoire diversity could therefore be elucidated by comparing the V-gene usage of young and aged B220$^+$ cells cultured in the presence or absence of IGF1 in-vitro with that of these in-vivo derived Pre-B cells. However, there appears to be an inherently reduced repertoire diversity in cells that undergo V-DJ_H recombination in-vitro, which unfortunately also presents as an overall over-representation of the 3'-proximal Q52/7183 V-gene families, at the detriment to the distal 5' J558/3609 V gene families (Figure 4-13). This confounding in-vitro repertoire skewing therefore impedes the biological conclusions that can be drawn when comparing the V-gene usage of young and aged cells.

Nevertheless, when comparing the V-DJ_H repertoires of young B220$^+$ cells cultured in either the IGF1 or the Medium-only conditions, there still appears to be differences in

V-genes used, such that the cells cultured in IGF1 use the 3'-proximal Q52/7183 V-genes less frequently than if they were cultured in the absence of IGF1, to the benefit of the "Middle" families (i.e. all except J558, 3609, 7183, and Q52; as defined by *Johnston et al*[313]) and, to a lesser extent, the distal 5' J558/3609 families (Figure 4-13). This difference in repertoire diversity may demonstrate a positive impact of IGF1 on repertoire diversity, irrespective of the inherent in-vitro biases. Furthermore, preliminary data comparing the V-DJ_H repertoires of young and aged $B220^+$ cells cultured in IGF1 aim to investigate whether there is age-associated over-representation of the 3'-proximal Q52/7183 V-gene families, to the detriment to the distal 5' J558/3609 V gene families. Preliminary interpretations suggest that aged cells exposed to IGF1 potentially have a greater proportion of 3' proximal V-genes used and less distal 5' V-genes, as seen also with in-vivo Late Pre-B cells. However, with only 2 biological replicates examined, more repeat experiments will be need to be carried out if any robust conclusions are to be drawn.

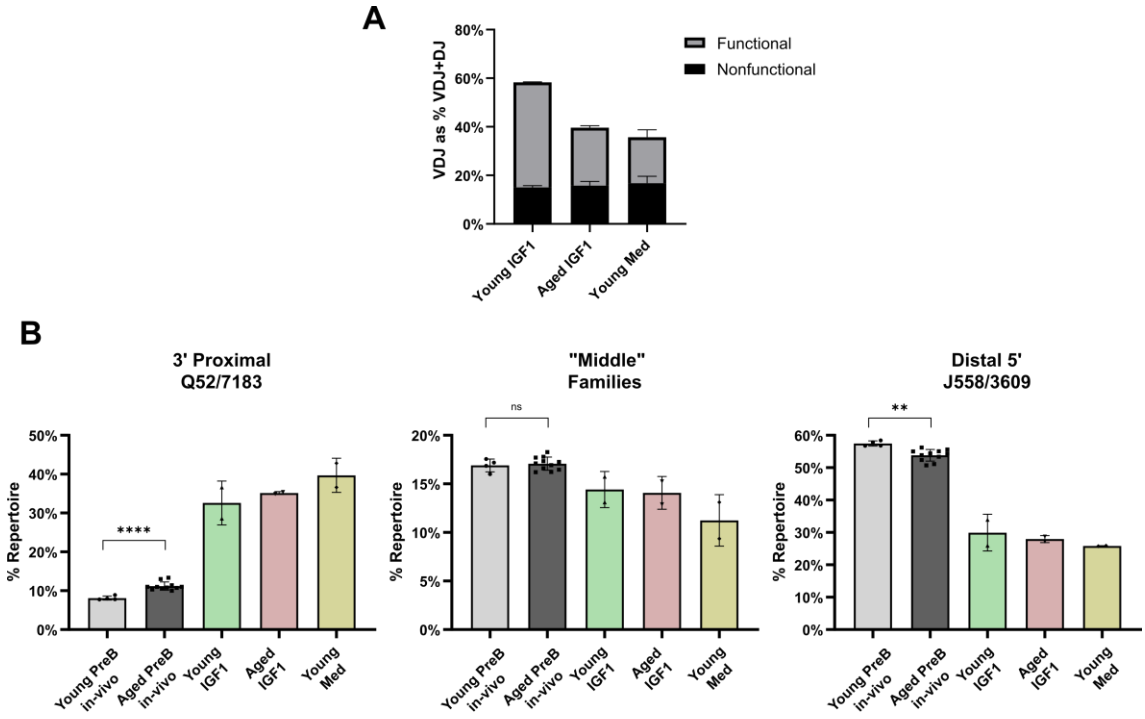

Figure 4-13: VDJ_H recombination dynamics of young and aged $B220^+$ cells at day 18. (A) VDJ_H recombination status of the Ig_H locus by VDJseq (% VDJ reads from all recombination events in $B220^+$ cells) Proportions of functional VDJ recombination events are reduced in aged cells exposed to IGF1, and are comparable to young cells exposed to the Medium-only condition. (B) V-gene usage across the Ig_H locus, grouped geographically into 3' proximal, middle, and distal 5' V-genes. In-vitro derived $B220^+$ cells at day

18 have greater proportions of 3' proximal V-genes, and fewer middle and distal V-genes represented in their repertoire compared to in-vivo derived Late Pre-B cells (from Chapter 3). Young cells exposed to Med conditions have greater proportions of 3' proximal V-genes used and less middle and distal 5' V-genes compared to cells exposed to IGF1. Aged cells exposed to IGF1 potentially have a greater proportion of 3' proximal V-genes used and less distal 5' V-genes, as seen also with in-vivo Late Pre-B cells. (Young IGF1 n=2, Young Med =2, Aged IGF1 n=2. Young in-vivo Late Pre-B cells n=4, Aged in-vivo Late Pre-B n=11; pval <0.05 unpaired t-test).

4.5 Chimeric cultures reveal intrinsic aged B cell defects

In an isolated in-vitro environment, aged progenitor B cells exhibit an impaired ability to differentiate when exposed to the same conditions as young B cells. Whilst these results suggest a defect intrinsic to the aged B cells, it is possible that the stromal cells present in the culture (derived from the bone marrow of each mouse) may be providing insufficient support, and that this may contribute to observed aged phenotype. To address this issue, I set out to determine the impact of culturing young and aged bone marrow cells together on the terminal fate of their B cells.

To this end, mixed cultures were set up, such that lineage-depleted bone marrow progenitor cells of young (~3 months) mice on the CD45.1 background were mixed with the same starting cells of aged (~24 months) mice on the CD45.2 background at a 1:1 mixture prior to culture initiation. As a result, an even proportion of young and aged bone marrow progenitors competitively progress through a culture consisting of the same chimeric environment of endogenous stromal cells, and can be distinguished based on their mutually-exclusive expression of the different isoforms to the pan-leukocyte marker CD45 (Figure 4-14).

For the first 8 days of culture bone marrow progenitor cells differentiate into $B220^+$ B cells in the presence of IL7 (and FLT3L), and from a starting split of 50:50 young and aged $CD45^+$ cells at day 0 (CD45.1:CD45.2), by day 8 this ratio skews to a ~75:25 split in favour of young cells (Figure 4-15). Reduced representation of aged $CD45.2^+$ cells in the early stages of the mixed culture is therefore reflective of the slower dynamics in the differentiation and proliferation of these aged $B220^+$ cells, as shown in Figure 4-10. This

CD45.1:CD45.2 ratio remains relatively unchanged as the $B220^+$ cells undergo a proliferative burst phase to confluence during days 8-15. However, as cells go through the selection stage to day 18, this ratio once again skews in favour of young to a final ~90:10 split of young versus aged cells. What these dynamics demonstrate therefore is a reduced capacity for aged progenitor B cells to differentiate in-vitro, even in the presence of young stromal cells. On the contrary, it would seem that the presence of young B cells is competitively inhibiting the aged cells from sustaining their levels of $B220^+$ cells by day 18. This is evident in the ~10-fold difference in number of young $B220^+$ cells versus aged in the mixed culture at day 18 (mean $3.16x10^6$ and $3.26x10^5$ respectively) compared to the ~2-fold difference shown in Figure 4-10 (Figure 4-15). Therefore, over the course of the mixed culture, young $B220^+$ cells almost completely out-compete aged $B220^+$ cells.

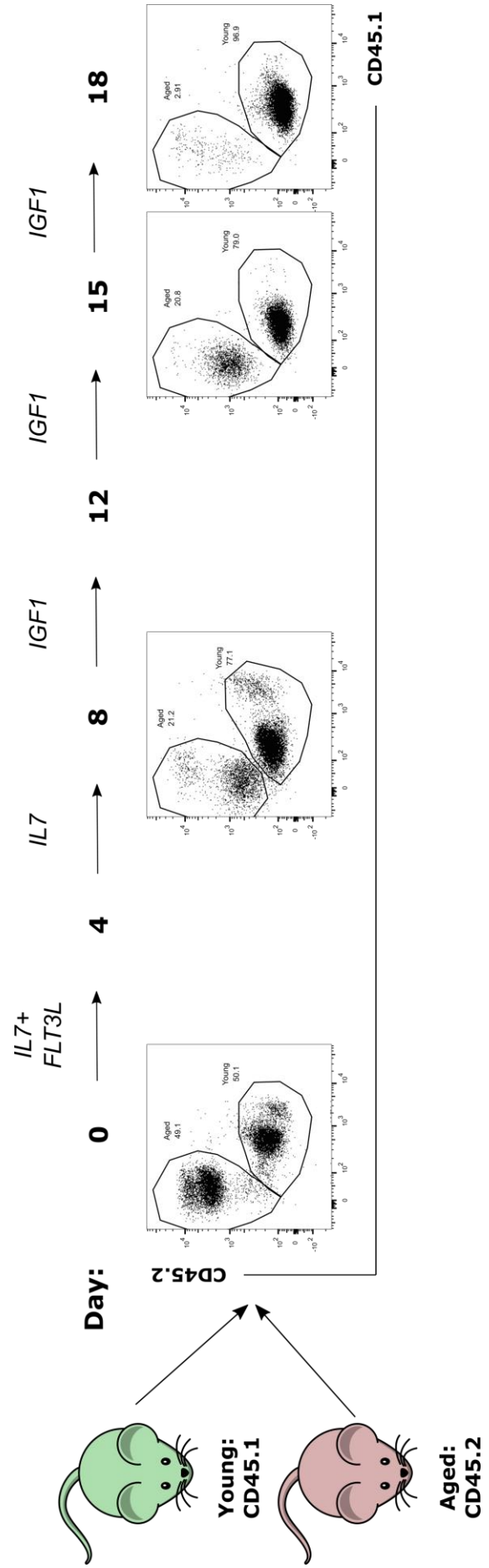
Young:
CD45.1
Aged:
CD45.2
Day:
0
4
8
12
15
18
IL7+
FLT3L
IL7
IGF1
IGF1
IGF1
CD45.2
CD45.1
Aged
49.1
Young
50.1
Aged
21.2
Young
77.1
Aged
20.8
Young
79.0
Aged
2.91
Young
96.9

Figure 4-14: In-vitro mixed young and aged chimeric culture system schematic. Lineage-depleted bone marrow from young (CD45.1; 3 months) and aged (CD45.2; ~24 months) mice that do not contain B cells (B220/CD19) are 1:1 mixed at day 0 and the culture initiated. Ratio of young (CD45.1) and aged (CD45.2) cells are measured at day 8, 15 and 18 timepoints. All cells were gated for live singlet lymphocytes prior to this gating strategy.

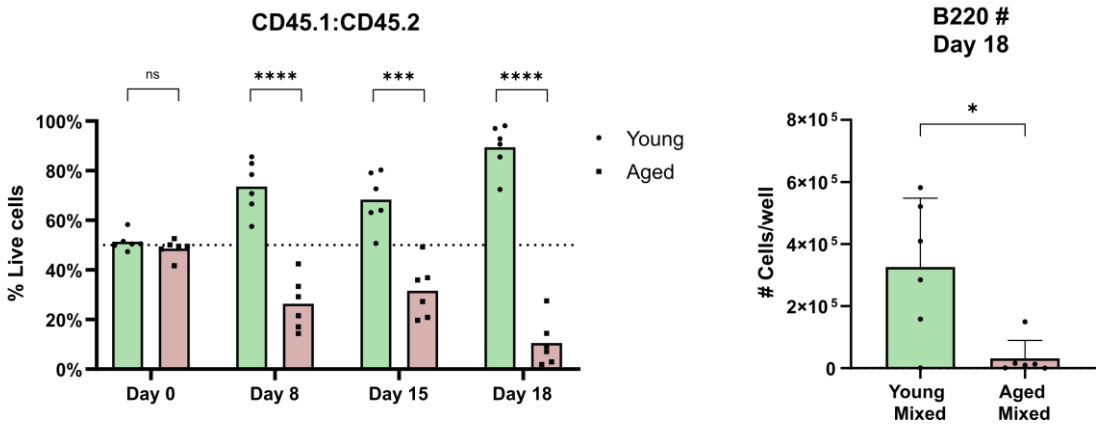

Figure 4-15: Young B cells out-compete aged B cells in a mixed chimeric culture. At day 0, there is a starting 50:50 ratio of CD45.1:CD45.2 (Young:Aged) cells, but at days 8, 15 and 18 timepoints there are greater proportions of young (CD45.1) cells (left; Young n=6, Aged n=6; padj <0.05, multiple t-test with FDR correction). At day 18, there are ~10-fold more young B220⁺ cells than aged B220⁺ cells (right; Young n=6, Aged n=6; pval <0.05, unpaired t-test).

With the remaining B220⁺ cells at day 18, cytoplasmic Mu and surface IgM expression was measured to see if there were any further positive or negative influences on B cell differentiation in this chimeric environment. Pairwise comparisons of young B220⁺ cells either differentiated on their own or with aged cells showed that there was no difference in the proportions of cytoplasmic Mu or surface IgM cells at day 18 (Figure 4-16). On the other hand, the remaining aged B220⁺ cells that survived in a mixed culture show a statistically significant increase in the proportion of IgM⁺ expression at day 18 compared to when they were cultured without the young cells. This shows therefore that young progenitor B cell development is unimpeded by the presence of aged cells, whereas the aged progenitor B cells being competitively out-competed by the young B cells are perhaps being exposed to a selective pressure that favours the survival of successfully differentiated IgM⁺ cells. Together, these results suggest that age-

associated defects in B cell development are being driven by mechanisms intrinsic to B cells and their progenitors.

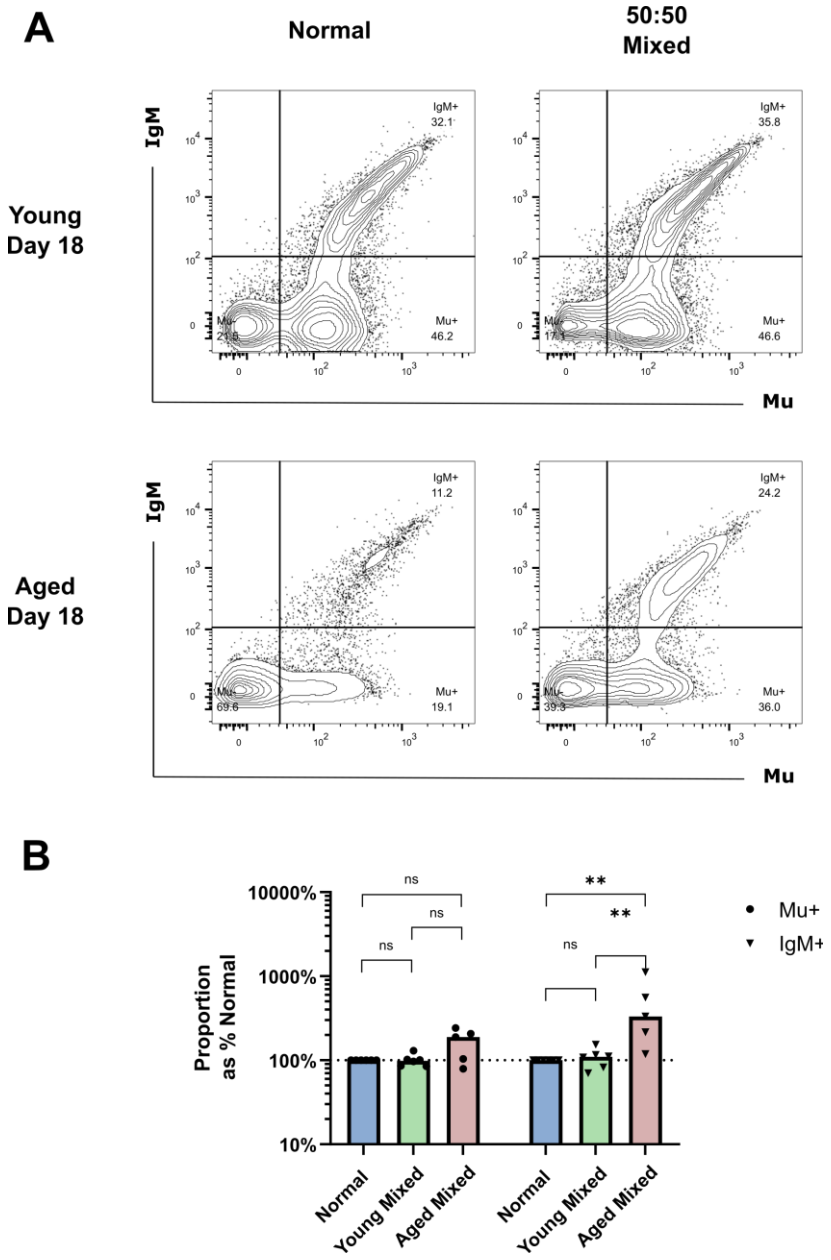

Figure 4-16: Proportions of cytoplasmic Mu and surface IgM-expressing cells from a mixed chimeric culture. (A) Representative FACS plots for the expression of cytoplasmic Mu or surface IgM on B220⁺ cells at day 18 from young (top panel) and aged (bottom panel) mice either cultured separately (Normal, left column) or together (50:50 Mixed, right column). All cells were gated for live singlet lymphocytes prior to this gating strategy. (B) Pairwise comparisons of the proportions of B220⁺ cells at day 18 expressing either cytoplasmic Mu or surface IgM, relative to its levels when cultured separately (Normal). There is a relative increase in the proportions of aged B220⁺ cells that express surface IgM (Young n=6, Aged n=6, padj <0.05, 2-way ANOVA).

4.6 Effects of inhibiting JMJD3/Ezh2 on young and aged B cell development in-vitro

One such intrinsic mechanism that could be contributing to these observed aged defects is epigenetic suppression of the IGF1R signalling component *Irs1* by H3K27me3. In Chapter 3, it was found that the downregulation of *Irs1* transcripts across the Pro-B and Pre-B cell stages in ageing coincided with a reduced expression of the H3K27 demethylase JMJD3 (*Kdm6b*), while levels of the H3K27 methyltransferase Ezh2 remained unaffected. Disproportionate expression of these 2 opposing enzymes in this way could shift reaction dynamics in favour of more H3K27 methylation by Ezh2, resulting in aged cells possessing more of the suppressive H3K27me3 marker. The findings from *Koohy et al* that there is enrichment of H3K27me3 over the *Irs1* promoter of aged Pre-B cells may connect this suppressive epigenetic mechanism to the reduced ability for aged cells to differentiate into IgM^+ B cells in-vitro.

With an in-vitro system that demonstrates a defect in aged progenitor B cell development, it is therefore possible to measure the impact of these epigenetic regulators on IGF1-driven differentiation using small molecule inhibitors to JMJD3 and Ezh2. It is hypothesised that JMJD3 inhibition would block progenitor B cell development (thus mimicking the aged phenotype) whereas Ezh2 inhibition would enable it (thus restore a younger phenotype). To test this, young (3 months) and aged (~24 months) bone marrow progenitors were first differentiated into $B220^+$ B cells with IL7 (and FLT3L) before being treated with small molecule inhibitors to JMJD3 or Ezh2 for the duration of the culture – in line with their exposure to IGF1 (Figure 4-17) – with the final readout being changes in the number and proportion of IgM^+ B cells.

GSK have developed small molecule inhibitors to JMJD3 (GSK-J4, herein named "JMJD3i") and Ezh2 (GSK-503, herein named "Ezh2i"). JMJD3 enzymatic activity is dependent on Fe^{2+} and α-ketoglutarate, so the antagonistic binding of JMJD3i to the α-ketoglutarate binding site on JMJD3 inhibits its activity[349]. Ezh2 is the enzymatic subunit of the PRC2 complex, and Ezh2i antagonistic binding of its catalytic SET domain results

in the inhibition of this catalytic activity[350]. JMJD3i and Ezh2i were thus used in the subsequent experiments.

Upon first introduction of the inhibitors into the culture (at day 8), cells were as usual replenished with fresh medium, this time however containing twice the final concentration of both exogenous IGF1 and the inhibitor in a 1:1 dilution to achieve the 1x final concentration desired. Since the inhibitors used were dissolved in 100% DMSO, another consideration when treating the cells was to ensure inhibitors were introduced into culture at a final DMSO concentration of 0.1% to prevent cell toxicity whilst also retaining the inhibitor in solution. At the subsequent media replenishment timepoints of day 12 and day 15, IGF1 was again added to cells at a 1:1 dilution along with the inhibitor, however at these stages the inhibitors were added already at their 1x final concentration, in 0.1% DMSO. This change was to prevent concentration build-up of both inhibitor and DMSO concentrations that could have led to toxic effects to the cells. Alongside treatment with inhibitors, cells were also treated with DMSO-only to act as a vehicle control for pairwise comparisons.

Prior to measuring biological differences, inhibitor concentrations for both JMJD3i and Ezh2i at the 3 replenishment stages – day 8, 12 and 15 – were determined and validated. "Expected vs actual" concentration measurements of JMJD3i and Ezh2i in an 8-step, 2-fold serial dilution based around their pIC50 values gave confirmation that the expected concentrations of the inhibitors for which the cells were to be exposed to from day 8 were in line with the actual readings (Figure 4-17). Subsequent readings of inhibitor concentrations taken from the culture medium at day 12 and 15 reveal that the Ezh2i maintained a similar starting concentration throughout the culture (with some variability), whereas the concentration of JMJD3i in culture halves by day 15 (Figure 4-17). This reduction in the bioavailability of JMJD3i through the culture may represent a shorter half-life of the compound compared to Ezh2i, and is a caveat to consider when interpreting the biological results.

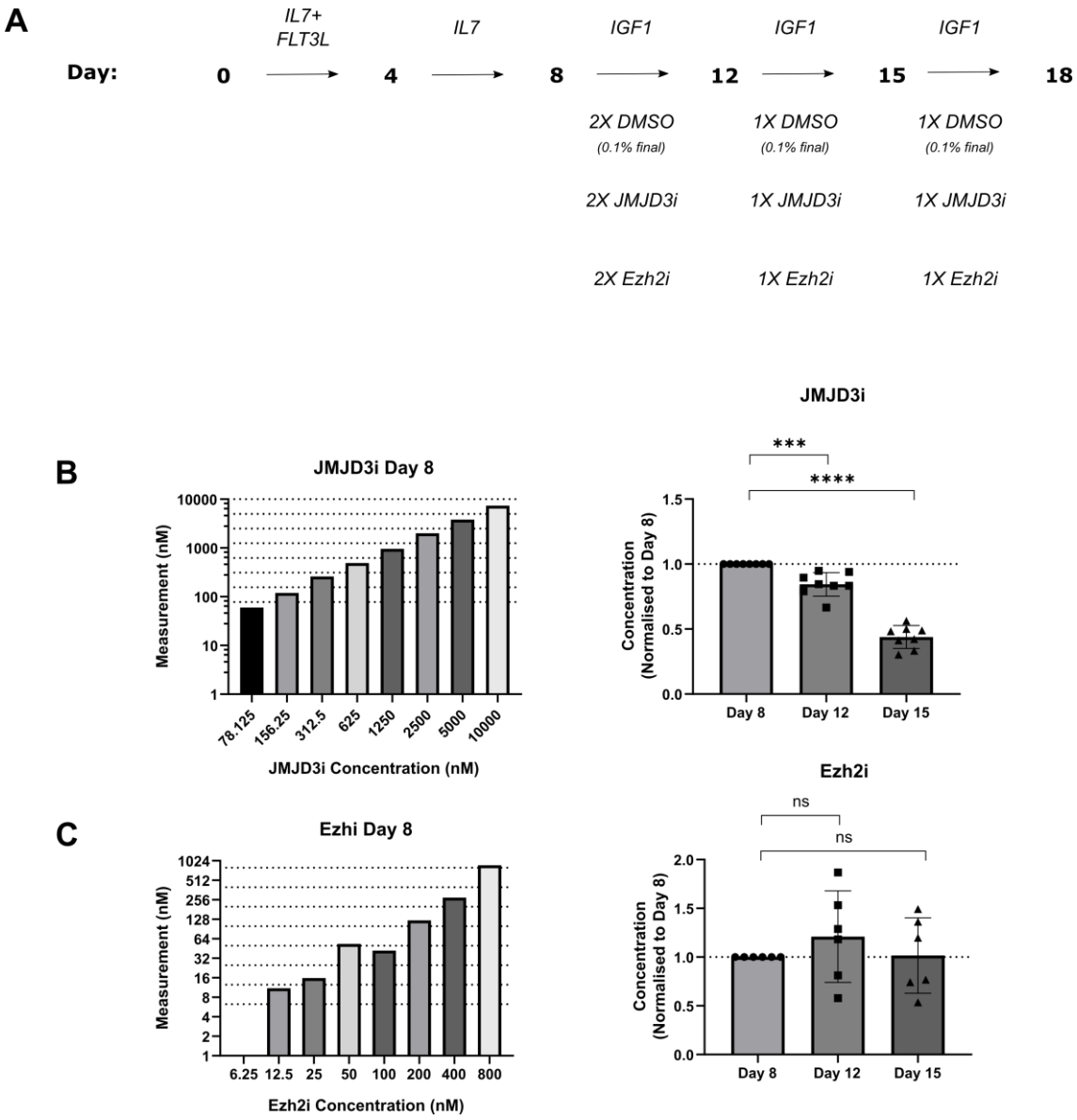

Figure 4-17: Concentration stability of JMJD3i and Ezh2i through in-vitro culture system. (A) Lineage-depleted bone marrow cells that do not contain B cells (B220/CD19) were first differentiated into B cells with IL7 (and FLT3L) for days 0-8, then on exposure to IGF1, cells were also treated with JMJD3i or Ezh2i or DMSO-only control at final DMSO concentration of 0.1%. At day 12, when the inhibitors were first introduced, cells were replenished with medium containing 2x final concentration for a 1x final concentration on cells (1:1 dilution). For subsequent day 15 and 18 timepoints, replenishing media contained inhibitors at 1x final concentration to prevent toxic accumulation of inhibitor and/or DMSO. (B) Measurements of expected (dashed line) vs actual (barplot) 2-fold serial dilutions of both JMJD3i and Ezh2i at day 8. (C) Fold change in concentration of both JMJD3i and Ezh2i in culture at day 8, 12, and 15, relative to starting concentration (day 8). (padj <0.05, one-way ANOVA).

To determine which concentrations of JMJD3i and Ezh2i to focus on biologically, young and aged cells (cultured separately) were again treated with a range of concentrations

around the pIC50 values for each inhibitor, and the % change in the proportion of B220$^+$ cells expressing surface IgM$^+$ at day 18 was pairwise compared to a DMSO control (Figure 4-18). For JMJD3i, this lead to a reduction in IgM$^+$ cells at 2.5µM and 5µM. For Ezh2i, the change in IgM$^+$ was not as clear, but at 18.5nM and 55.6nM there appeared to be an increase in aged B cells expressing IgM$^+$. Therefore, these concentrations were taken into the final experiment.

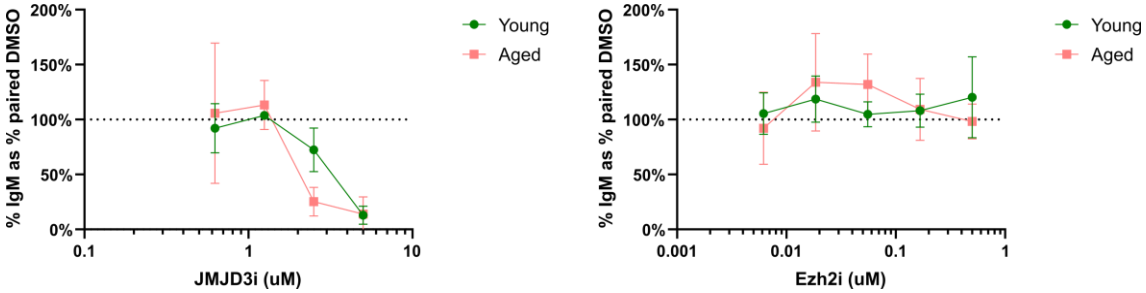

Figure 4-18: Determining concentrations of JMJD3i and Ezh2i for a change in B cell output. Proportion of B220$^+$ cells expressing IgM$^+$ at day 18 when treated with JMJD3i (left) or Ezh2i (right), shown as a % of their paired DMSO control. (Young n=3, Aged n=3).

For the final experiment, cells from both young and aged mice were treated with either DMSO-only, JMJD3i (2.5uM or 5uM), or Ezh2i (18.5nM or 55.6nM), and at day 18 their B220$^+$ cells were compared for expression of cytoplasmic Mu and surface IgM. Cells treated with inhibitors were then pairwise compared to cells from the same mouse that were treated with DMSO-only as an internal control.

Inhibition of JMJD3 resulted in a dose-dependent reduction in the proportion of IgM$^+$ cells in both young and aged (Figure 4-19). Interestingly, reduction in IgM$^+$ cells by JMJD3i lead to an increase in the proportion of cytoplasmic Mu$^+$ B cells, whilst the proportions of cytoplasmic Mu$^-$ cells remained unaffected. This suggests that JMJD3i specifically inhibits B cell development from cytoplasmic Mu$^+$ to surface IgM$^+$ B cell stages in-vitro. Most striking about these results is the age-dependant sensitivity to JMJD3 inhibition. Aged cells succumb to the reduction in IgM$^+$ expression with half the amount of inhibitor (2.5uM vs 5uM). In fact, aged cells exposed to the higher concentration of 5uM JMJD3i even began to show toxic effects (aged cells from 5/7 mice died). Reduced proportions of IgM$^+$ cells in the presence of JMJD3i also translates to reduction in the number of IgM$^+$ cells produced (Figure 4-19). This increased sensitivity

to JMJD3 inhibition in aged cells perhaps reflects the differences in JMJD3 protein availability within young and aged cells that were inferred from the transcriptional data in Chapter 3 (reduced expression of JMJD3 in aged Pre-B cells) and would fit a hypothesis that, as a result of this skew in JMJD3 expression, aged B cells are more predisposed to H3K27 methylation by Ezh2. Validations at the protein level for JMJD3 and Ezh2 will need to be carried out to confirm this suggestion.

In terms of changes in the proportion of $B220^+$ cells expressing either cytoplasmic Mu or surface IgM when treated with Ezh2i, there was no difference to either young or aged cells compared to their DMSO control (Figure 4-20). For young cells, this also resulted in no change in the number of IgM^+ cells produced. This result was contrary to that expected from the hypothesis, as it was expected that an opposing phenotype to JMJD3 inhibition of an increase in the number and proportion of IgM^+ cells would be observed in cells treated with Ezh2i. For aged cells on the other hand, there was a potential overall increase in IgM^+ cell production upon Ezh2 inhibition that would fit this ageing hypothesis, although this did not reach statistical significance due to variation between individuals.

Nevertheless, these finding provide strong evidence that inhibiting the enzymatic activity of JMJD3 and Ezh2 during in-vitro differentiation of progenitor B cells has functional consequences to their ability to differentiate. The directionality of these functional consequences also fits the proposed model of ageing regarding the suppression of IGF1R signalling by H3K27me3. However the use of pan-inhibitors to JMJD3 and Ezh2 may be affecting other genes targeted for H3K27me3. Thus, a direct link to H3K27me3 enrichment over the *Irs1* promoter, resulting in reduced protein expression that in turn causes impaired differentiation in-vitro has not fully been established. Such pan-inhibition might explain the modest phenotype in Ezh2 inhibition if, for example, global losses of H3K27me3 are cancelling out the benefits of localised losses of H3K27me3. But this is also a reason why further experiments will need to be carried out, in order to characterise the mechanism behind this phenotype.

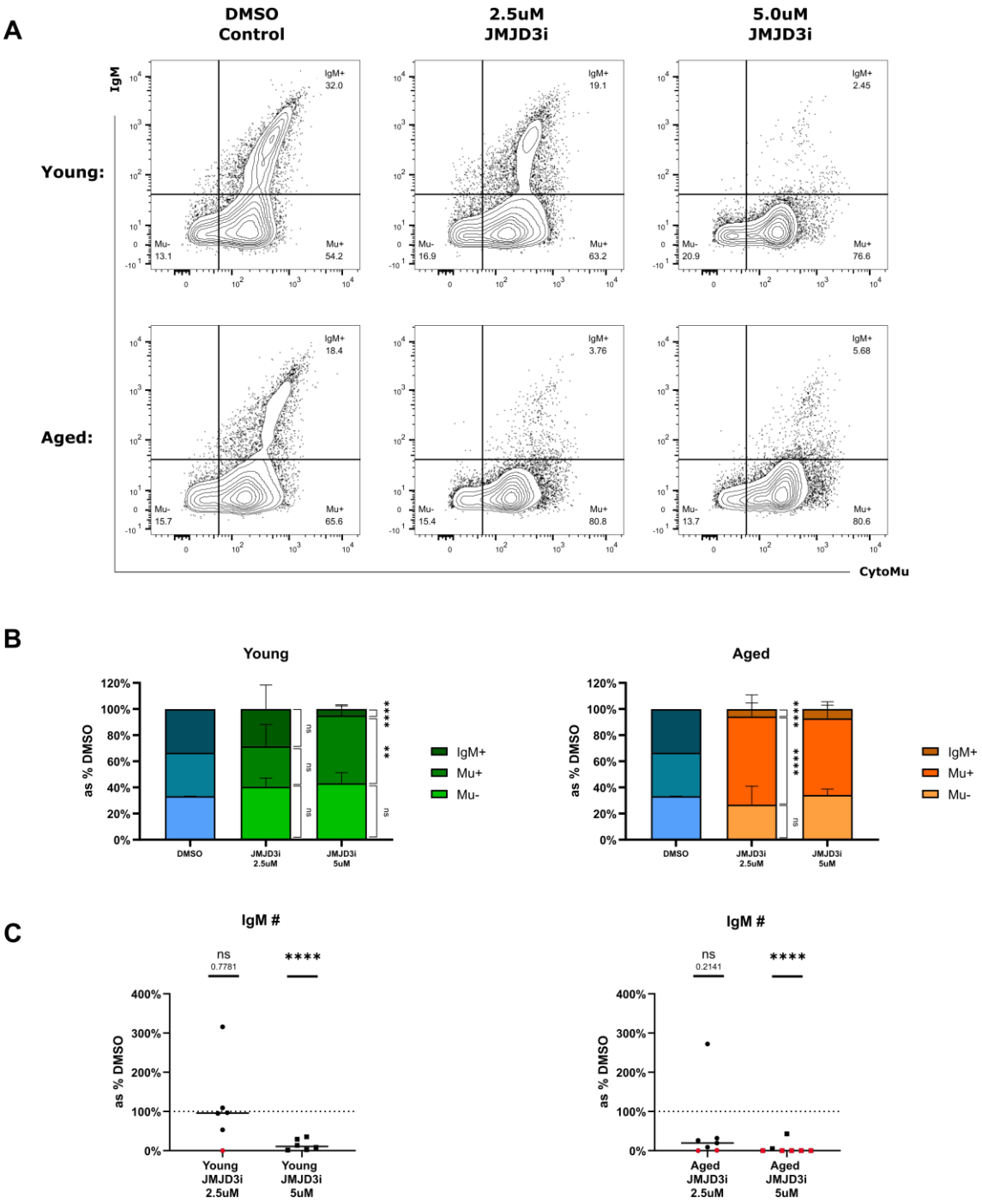

Figure 4-19: Effects of JMJD3 inhibition on cytoplasmic Mu and surface IgM expression at day 18. (A) Representative FACS plots for the expression of cytoplasmic Mu and surface IgM on B220⁺ cells at day 18 from young (top panel) and aged (bottom panel) mice either cultured in DMSO-only (left), 2.5uM JMJD3i (middle), or 5uM JMJD3i (right). All cells were gated for live singlet lymphocytes prior to this gating strategy. (B) Pairwise comparisons looking at changes in the proportions of B220⁺ cells that either do not express cytoplasmic Mu (Mu-), do express cytoplasmic Mu (Mu+), or express IgM (IgM+), relative to their paired DMSO-only control in young (left) and aged (right) mice. (Young n=6, Aged n=7, except for in JMJD3i 5uM condition, where cells from only 2/7 mice survived; padj <0.05, 2-way ANOVA). (C) Pairwise comparisons looking changes in the number of B220⁺IgM⁺ cells produced, relative to their paired DMSO-

only control in young (left) and aged (right) mice. Median average shown as black line. Cells that died are shown as red point. (Young n=6, Aged n=7; pval <0.05, unpaired t-test).

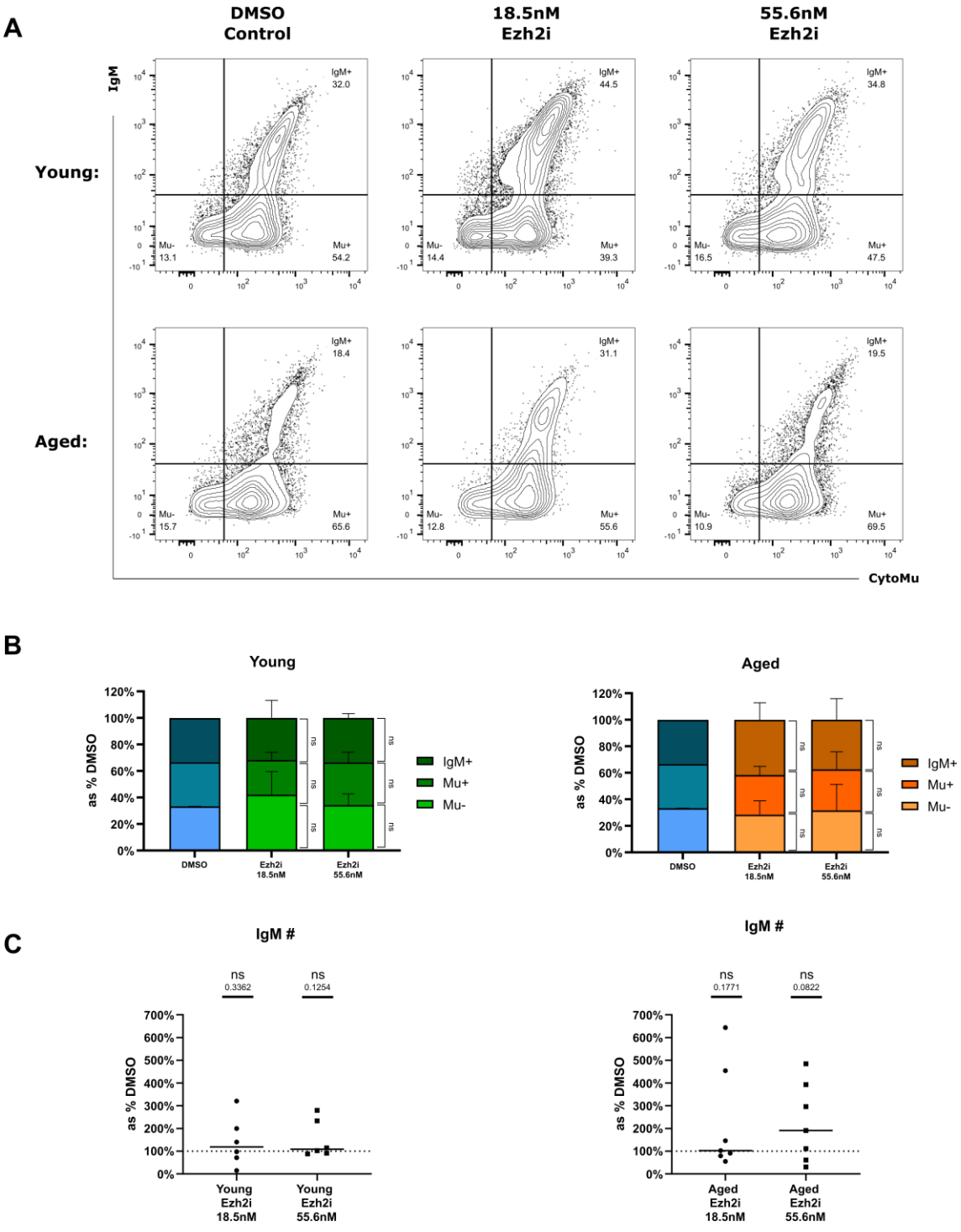

Figure 4-20: Effects of Ezh2 inhibition on cytoplasmic Mu and surface IgM expression at day 18. (A) Representative FACS plots for the expression of cytoplasmic Mu and surface IgM on B220⁺ cells at day 18 from young (top panel) and aged (bottom panel) mice either cultured in DMSO-only (left), 18.5nM Ezh2i (middle), or 55.6nM Ezh2i (right). All cells were gated for live singlet lymphocytes prior to this gating strategy. (B) Pairwise comparisons looking at changes in the proportions of B220⁺ cells that either do not

express cytoplasmic Mu (Mu-), do express cytoplasmic Mu (Mu+), or express IgM (IgM+), relative to their paired DMSO-only control in young (left) and aged (right) mice. (Young n=6, Aged n=7; padj <0.05, 2-way ANOVA). (C) Pairwise comparisons looking changes in the number of $B220^{+}IgM^{+}$ cells produced, relative to their paired DMSO-only control in young (left) and aged (right) mice. Median average shown as black line (Young n=6, Aged n=7; pval <0.05, unpaired t-test).

4.7 Discussion

In this chapter, progress has been made in assessing the validity of some of the findings from Chapter 3. A large focus of this work has been on the active suppression of IGF1R signalling in aged early B cell development, since it has been strongly associated with most aspects of the aged phenotype, either directly or indirectly.

One such association is in the regulation of cell cycle. Here, I confirm in-vivo that there is a modest reduction in aged cells actively engaging in S-phase across the proliferative Pro-B and Pre-B cell stages. In Chapter 3, I showed reductions in the number of Pro-B and Pre-B cells in aged mice, and comprehensive transcriptomic analysis revealed an enrichment in transcripts differentially expressed in aged Pro-B and Pre-B cells which suggested that cell cycle pathways were disrupted with age. Thus, these additional findings that less aged Pro-B and Pre-B cells are entering S-phase is consistent with this work.

The additional discovery that there was an increased proportion of aged immature B cells engaged in S-phase poses interesting questions as to what may be driving this increased proliferation in this cell stage. To explore this avenue further, it would be possible to retrospectively generate complementary RNAseq (and VDJseq) libraries to accompany those for the Pro-B and Late-Pre-B cells presented in Chapter 3 (Young n=4, Aged n=12), since the immature B cells were also extracted from these same mice. The same transcriptomic analysis can then be applied to these libraries, and perhaps reveal enriched upregulation of cell cycle pathways.

The observations from Chapter 3 that aged Late Pre-B cells possess more DNA per cell did not, in these experiments, translate to an increase in the proportion of these cells occupying the G2M-phase of cell cycle. These findings raise more unanswered questions

of why the measurement of absolute DNA extracted from these aged Late Pre-B cells does not match up to the measurement of DNA in-situ. One way to resolve this confliction would be to once again perform an in-situ DNA stain (like 7AAD), as well as quantify the total DNA extracted per cell, but this time taking measurements from Pre-B cells of the same aged mice. If the discrepancy persists, alternative methods for measuring cell cycle and DNA content in-situ should be explored. For example, Hoechst staining of aged Pre-B cell DNA in-situ, as it does not require cells to be fixated (unlike 7AAD), and also allows live cell imaging to be performed to explore possible aged differences in the stages of mitosis.

Also in this chapter, I introduce a novel culture system for differentiating non-B cell bone marrow progenitors into B cells that undergo V(D)J recombination in-vitro. Through this system, cytoplasmic Mu protein expression was seen at day 8 following continuous exposure to IL7, and transition to IgM^+ expression occurred when cells were exposed to IGF1. It is interesting to note that the proportions of $B220^+$ cells expressing cytoplasmic Mu at day 8, which have therefore undergone V-DJ_H recombination, reflect the statistical model of 33% probability that a V(D)J recombination event is productive (31.9% actual)[89,351]. These successfully VDJ_H recombined cells could theoretically pair their heavy chain protein Mu with a surrogate light chain to form the preBCR. Cell signalling via the preBCR is initially associated with a proliferative burst, but it is also known to downregulate IL7R signalling[352,353], which could explain the striking relative expansion of cytoplasmic Mu^- cells between days 8-12. Such differences in proliferation between cytoplasmic Mu^- and cytoplasmic Mu^+ cells at this stage could partly explain the observed proportional reductions in cytoplasmic Mu^+ B cells between days 8-12. One way to better understand these early culture dynamics could be to carry out an in-vitro BrdU experiment on cells cultured between days 8-12, and compare the cell cycle profiles of cells that are cytoplasmic Mu^+ versus those that are Mu^-. It would be anticipated that the cytoplasmic Mu^- cells have proportionally more cells in S-phase than those that are Mu^+.

The latter stages of this in-vitro system have been designed to explore links to an impaired IGF1R signalling response in aged B cells by differentiating these cells in the presence of IGF1. Comparisons with other conventional methods (TSLP and Medium-

only) has demonstrated both the importance of IGF1 in normal Pro-B and Pre-B cell development, and desensitisation to its influence in ageing.

Additionally, this culture system shows that not only is this age-associated defect in B cell development regulated intrinsically, but that these B cell developmental defects seem to be predetermined in their haematopoietic progenitors before they have even become B cells in-vitro. These findings pose interesting insights into the overall ageing mechanism in effect in the bone marrow niche. Taken together with the findings from Chapter 3, it could be suggested that the proposed chronic overstimulation of the Akt signalling pathway in ageing from an inflammatory niche may even induce these intrinsic suppressive mechanisms in non-committed haematopoietic progenitors. To this end, future work could be to explore earlier cell populations such as aged CLP's for Akt phosphorylation, and differential gene expression of *Irs1*.

At the other end of the developmental spectrum, it was shown that there is a reduction in the proportion of aged cells that can differentiate in-vitro into mature B cells. It is attractive to suggest that this later stage aged defect is also the result of IGF1 desensitisation. However, the mature B cell population was not looked at in cells cultured using the other 2 culture methods explored (TSLP and Medium-only) and so a role for IGF1 in IgD expression cannot be definitively concluded. Therefore, repeat experiments could be done here to compare the proportions of this mature B cell population in the other conditions.

While this work shows a causal link between aged progenitor B cell development and downregulation of IGF1R signalling, culturing bone marrow cells from conditional B-lineage *Irs1* or *Igf1r* knockout mice through this system would determine whether loss of IGF1R signalling components is sufficient to recapitulate the aged phenotype in-vitro. Also, while it is known that Irs1 and IGF1R are downregulated at both the transcript and protein level in aged Pre-B cells in-vivo, expression levels in-vitro have not been shown. Therefore to support this, transcript and protein expression levels of Irs1 and IGF1R in wildtype young and aged B cells in-vitro could be measured to see if they correspond with the observed in-vivo reductions and thus, could still be contributing to this aged phenotype in-vitro.

Interrogation of the Ig_H locus as cells undergo V-DJ_H recombination in-vitro showed that whilst B cells were able to successfully complete this process and progress, the frequency of individual V-gene usage was different to B cells that differentiated in-vivo. As a result, B cells derived in-vitro through this culture system possess a less diverse antibody repertoire. It is therefore clear that these in-vitro systems are missing some factors or cells from the bone marrow niche that would otherwise support optimal V(D)J recombination in-vivo – for example the presence of CXCL12 (although its cognate receptor CXCR4 has only been linked to Ig_κ recombination[77]) . Despite this, preliminary data suggests that exposure to IGF1 in-vitro compared to no additional growth factors gave a somewhat more diverse repertoire. Additionally, these VDJseq libraries were generated from an overall $B220^+$ cell population that consists of a heterogeneous pool of cells that have either undergone D-J_H (cytoplasmic Mu^-), V-DJ_H (cytoplasmic Mu^+), or V-J_κ (IgM^+)recombination, and so represent cells at different in-vitro developmental stages. It would be interesting to see if analysis of only those cells that are IgM^+ – and so have passed all early developmental checkpoints – gives a more/less diverse antibody repertoire with regards to V-gene usage at the Ig_H locus.

The culture system created in this chapter was utilised to interrogate additional characteristics of ageing biology. In-vitro differentiation of young and aged cells in a chimeric culture helped shed light on the intrinsic defects of aged B cell development. However, it should be noted that while the starting proportions of $CD45^+$ were even in number, the composition of cells that make up this heterogeneous pool is likely to be different between the young and aged mice. It is known that ageing is associated with an increase in myeloid precursors at the expense of lymphoid precursors[268,269], and this could impact on the availability of cells that are able to differentiate into B cells, putting the aged mice at a disadvantage in the early stages of the culture. Despite this potential disadvantage, aged B cells managed to establish themselves in the mixed culture, but then still show further B cell loss in the latter stages of the culture, which is likely to be as a result of intrinsic aged B cell defects.

I ended by exploring the functional role of H3K27me3 on the development of B cells in-vitro. Inhibition of the H3K27 demethylase JMJD3 mimicked the aged phenotype by blocking B cell development, with aged cells demonstrating an increased susceptibility to this inhibition. Inhibition of the H3K27 methyltransferase Ezh2 did not fully

reciprocate the effects of JMJD3 inhibition, but there were some age-specific increases in IgM^+ cell production that could be interpreted as consistent with the proposed model that aged B cell development is impaired by lack of *Irs1*, whose suppressed expression is in part regulated by H3K27me3. However the use of these pan-inhibitors may be affecting other genes targeted for H3K27me3. For example, the Ig_K locus is suppressed by H3K27me3 induced by IL7R signalling[113]. Additionally, these inhibitors will be acting on all cells in the culture, which includes the supportive stromal cell layer. Together, these limitations mean that the results cannot be definitively attributed to H3K27me3 regulation over the *Irs1* promoter. To progress this work, next steps could be to measure the transcript levels of *Irs1* when JMJD3/Ezh2 are inhibited, alongside ChIP-qPCR of H3K27me3 over the *Irs1* promoter in these cells to see if the presence/absence of this histone marker corresponds to differential *Irs1* expression.

What these experiments show more generally is the capacity for this culture system to be used as a platform for testing other therapeutic interventions and hypotheses surrounding B cell development, opening the door for future discoveries. For example, unexpectedly this system was able to generate mature B cells expressing Igκ and IgD which to date have been difficult to recapitulate in bone marrow B cell cultures. This work sets the stage for further in-vitro studies to characterise these cells and to explore further the life cycle of B cells. In the final results chapter, I will explore to what extent these insights from murine biology are applicable to humans, both in normal B cell development and in ageing.

5 Alterations in Ageing Human B cell Progenitors

5.1 Introduction

Mice and humans share very striking DNA sequence homology. At least 80% of all mouse genes have a human ortholog, while the remaining noncoding regions share about 50% homology[354]. This close genetic relationship is also conserved at the cellular level, as mice and humans possess comparable cell lineages, but with some subtle distinctions. In the context of early B cell development, human $Lin^{-}CD34^{+}$ HSCs in the bone marrow differentiate into $CD34^{+}CD38^{+}$ CLPs that in turn commit to the B-lineage as $CD19^{+}$ Pro-B cells, undergoing systematic cell proliferation and V(D)J recombination of both their heavy and light chain gene loci to produce and present a functioning BCR as an immature B cell (Figure 5-1)[355,356,357,358].

While the shared objective of early B cell development for both mice and humans is V(D)J recombination, there are some differences of note. At the level of the Ig_H locus for example, humans possess 56 V, 23 D, and 6 J gene segments, compared to the 195 V (110 functional, 85 pseudogenes), 10 D, and 4 J gene segments of C57BL/6 mice[359,313]. There are also differences in the biomarkers that define the homologous progenitor B cell subtypes. For example, human progenitor B cells do not possess the B cell specific B220 isoform of the pan-leukocyte CD45 marker that is ubiquitous to the mouse B cell lineage[360]. Conversely, mouse progenitor B cells do not express the CD10 marker commonly found on human progenitor B cells[361]. Whether these distinguishable features between mice and humans represents any form of divergence in the way early B cells differentiate remains a field of active research.

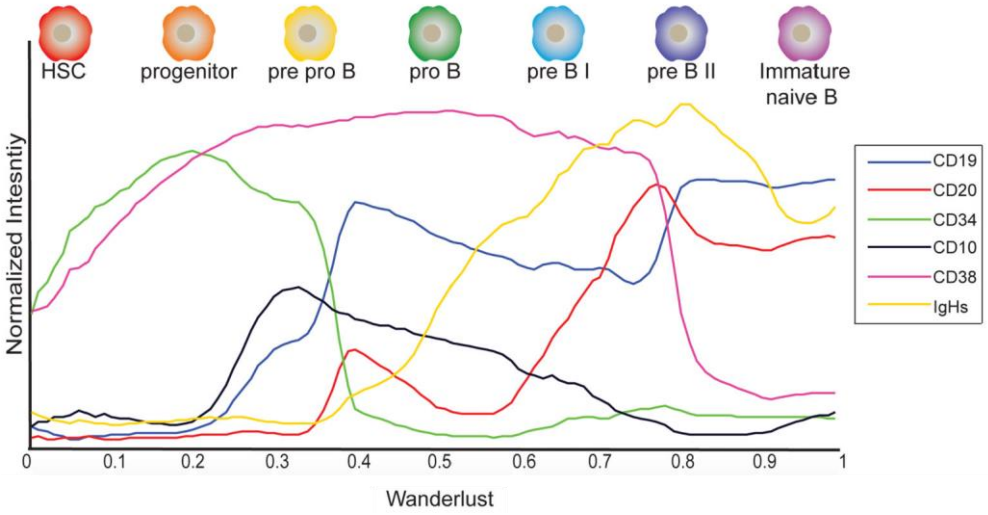

Figure 5-1: Biomarker expression during early B cell development in humans. CD34⁺ HSCs differentiate in the bone marrow into CD19⁺ progenitor B cells that differentially express markers such as CD10, CD20, and CD38 as they undergo V(D)J recombination to express heavy chain (IgH) and light chain protein as BCR on the surface of immature B cells. (Taken from Bendall et al[355]).

Overlapping dependencies of early B cell development on certain growth factors are also observed between mice and humans. In mice, IL7 plays a vital role in both differentiation and proliferation of adult progenitor B cells, though in foetal liver (FL) derived B cell development it is only required for proliferation[102,362]. For humans, much of the work on progenitor B cell development has been on foetal-derived cord blood (CB) samples and these studies have found IL7 to only provide a proliferative benefit[363]. However, a study on adult human bone marrow cells concluded that, as in mice, IL7 is required for both differentiation and proliferation[364], though consensus opinion on the matter remains inconclusive. Similarly, FLT3L, but not SCF, has been shown to support B-lineage commitment in humans as it does in mice, though again this work has been done on CB samples[365].

The role of IGF1 in normal human progenitor B cell development on the other hand has not yet been fully elucidated. One study has demonstrated a dependency on IGF1 for the commitment of bone marrow-derived CD34⁺ HSCs into CD19⁺ B cell progenitors[366], but whether or not it also drives further differentiation of Pro-B and Pre-B cells, as it does in mice, has yet to be shown. It is therefore the aim of this chapter to explore further the role of IGF1 in human progenitor B cell development, and to what extent it plays a part in the aged phenotype.

Research on the effects of ageing on human B cell development is very limited, controversial and, in many cases, conflicts that of the mouse aged phenotype. For example, it is known that the number and proportions of murine progenitor B cells declines with age, as shown in the literature and in Chapter 3. In humans, one study claims that, unlike mice, there is no change in the generation of B cells ($CD19^+$) in the bone marrow that are either IgM^- or IgM^+ throughout life (ages 10-80)[367]. Another study furthers this claim by stating that the Pro-B, Pre-B, and Immature B cell populations analysed in their study "…represented relatively constant percentages of the $CD19^+$ lymphocytes over a 24- to 88- year age range"[368]. However, both studies present their B cell progenitor proportions as a percentage of either all lymphoid cells[367] or all $CD19^+$ cells[368] of the bone marrow, as opposed to a percentage of the progenitor B cell niche exclusively. In doing so they do not capture potential age-related changes in the proportional representation of the cells confined to the progenitor B cell niche. Furthermore, the authors of the latter study report considerable sample-to-sample variability which, combined with their analytical approach, could be concealing aged differences in their work[367]. In fact, it could be argued that their findings do indeed show an aged reduction in the proportions and functionality of Pre-B cells – a phenotype that is also characteristic of murine Pre-B cell ageing. Indeed, a more comprehensive study of over 600 bone marrow samples demonstrated an aged reduction in the proportions of human B cell progenitors[369].

Irrespective of proportional differences in the bone marrow, it appears that a reduction in total peripheral B cell numbers and proportions is found in ageing humans (though, more specific aged differences in naïve and memory B cell subsets is very conflicting)[259,260]. However, this is not the case in C57BL/6 mice which, despite the defects in progenitor B cell development, appear to have maintained peripheral splenic B cell numbers as they age[370]. In any case, there are still some important similarities between the aged phenotypes of mice and humans, such as the emergence of age-associated B cells (ABCs)[254,371], alterations in antibody repertoire diversity and increase in autoreactive clones[255,358,372], and reduced B cell activation[373].

Given the precious nature of human samples, much of the work exploring early B cell development has been achieved through in-vitro cultures. Predominantly, these cultures consist of a starting cell population of frozen human $CD34^+$ small HSCs, derived

from either CB or bone marrow, on a stromal cell line feeder layer. The stromal cell lines are typically of murine origin – the most frequently used being MS5 and S17. These stromal cells are first grown to confluence and then cell cycle arrested, either by irradiation or mitomycin C treatment, prior to adding the human HSCs. Through these hybrid culture systems, the importance of FLT3L, IL7, and IGF1 to the commitment of human haematopoietic progenitors to the B lineage have been demonstrated[364,365,366]. So too have murine MS5 stromal cells been shown to produce more B cells from a starting population of $CD34^+$ HSCs than S17 cells, or without a stromal cell layer entirely[278].

The ambiguities of the literature on aged progenitor B cell development leave its characteristics unclear. It would be interesting therefore to determine to what extent the findings from Chapters 3 and 4 on aged progenitor B cell development in mice can be applied to that of the human biology.

5.2 In-vitro differentiation of human HSCs to the B-lineage

The confinement of human studies to in-vitro systems presents an opportunity to explore whether culture conditions in Chapter 4 used to differentiate murine haematopoietic progenitors in the presence of IGF1 to produced IgM^+ B cells will have the same outcome with human bone marrow cells. When it comes to human culture conditions however, the methodology in the literature differs to that of my murine system from Chapter 4 in many ways, owing perhaps to the limited availability of cell sample. This published expertise was nonetheless used as a framework to design a culture system to differentiate progenitor B cells in the presence of IGF1 (an adaptation to the culture system presented by *Lee et al*[278]). To this end, there are some notable differences between the conditions used in Chapter 4 and those used in this human work.

Firstly, the starting haematopoietic cell population of the human culture is an enriched population of 3,000 $CD34^+$ small HSCs from the bone marrow of healthy donors (sorted by FACS) per well of a 96-well plate, as opposed to a lineage-depleted heterogeneous

population of bone marrow cells (depleted by MACS) in a 24-well plate in the mouse system. Thus, a confluent monolayer of 30,000 mitomycin C treated murine MS5 stromal cells was included per well to support human HSC differentiation into B cells. This was not needed in the murine system due to the presence of endogenous stromal cells and more committed haematopoietic precursors. Both the primary human $CD34^+$ HSCs and murine MS5 cell line were also reconstituted from a cryogenically frozen state, whereas the murine cells were extracted fresh from the organism. These human haematopoietic-derived cells also never reach confluence in their wells through the culture (data not shown), unlike the murine system which does so by day 12.

The human system does however resemble the murine system is in its use of exogenously added (recombinant human) growth factors. An initiated culture of human $CD34^+$ HSCs on a monolayer of MS5 cells was exposed to IL7 and FLT3L for 4 days, then IL7 alone for 4 days, followed by IGF1 for the remainder of the 18-day culture. To increase the chances of creating and enriching for IgM^+ B cells ($CD19^+$), BAFF was also included with IGF1 from day 12 to 18, despite it not showing added benefits in mouse (Figure 5-2, and Figure 4-5) because it shows similar pro-survival capabilities in human B cells[374]. In parallel to this, cells were also exposed to just IL7 for the duration of the 18 day culture to act as a comparator. At days 8, 12, 15, and 18, non-adherent cells were analysed by flow cytometry to measure $CD19^+$ cells, and their expression of cytoplasmic Mu and surface IgM (Figure 5-2).

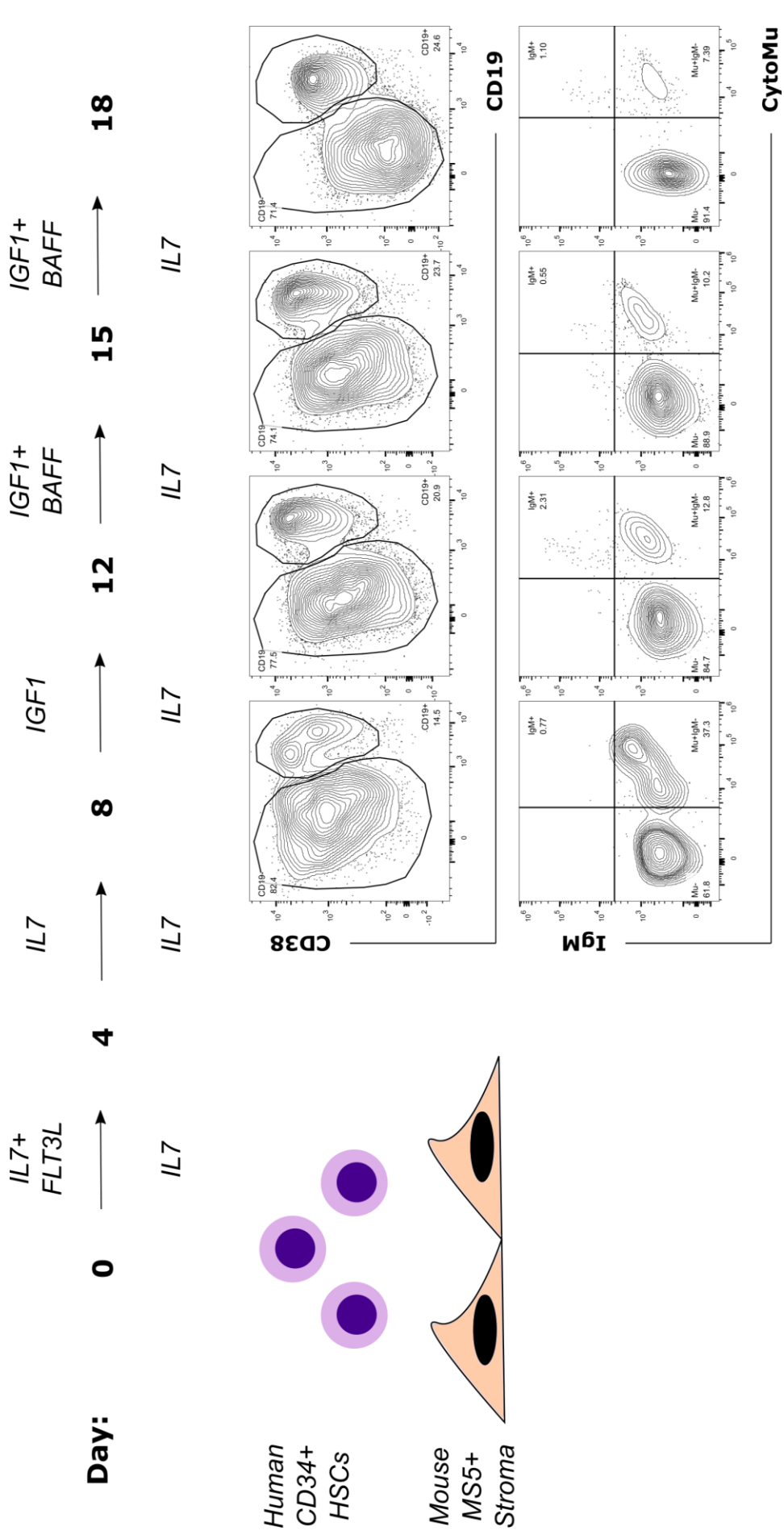
Day:
0
4
8
12
15
18
IL7+ FLT3L
IL7
IGF1
IL7
IGF1+ BAFF
IL7
IGF1+ BAFF
IL7
Human CD34+ HSCs
Mouse MS5+ Stroma
CD38
IgM
CD19
CytoMu

Figure 5-2: In-vitro human culture system schematic. 30,000 mitomycin C-treated murine MS5 cells were cultured overnight in a 96-well plate. The following day, 3,000 human CD34$^+$ bone marrow cells from healthy donors were added to the adherent MS5 monolayer, signalling day 0 of the 18-day culture system. Over the course of the culture, cells were exposed either to IL7 throughout ("IL7"), or a combination of IL7, FLT3L, IGF1, and BAFF ("IGF1"). At days 8, 12, 15, and 18, human cell differentiation into CD19$^+$ B cells, and their expression of cytoplasmic Mu and surface IgM, were determined by flow cytometry. FACS plots represent cells from a young healthy donor at these time points through the "IGF1" condition, and were gated for live singlet lymphocytes prior to this gating strategy.

CD34$^+$ HSCs from 3 young (ages 18, 19, and 21; 2 males, 1 female) human donors were passed through the 2 culture conditions, hereafter referred to as "IL7" and "IGF1". Both conditions were able to successfully produce CD19$^+$ cells, with some notable differences in their trajectories. In the presence of IL7, there appears to be a greater proportion of CD19$^+$ cells from the total lymphocytes produced compared to when IGF1 is introduced from day 12 onwards (Figure 5-3). By day 18, an average of 47.2% (±9.84) of the human lymphocytes exposed to IL7-only in-vitro were CD19$^+$, compared to 25.7% (±14.4) in the IGF1 condition (Figure 5-3A). However, this difference does not reach statistical significance, perhaps due to the small sample size (n=3) and sample-to-sample variability. This also coincides with an overall greater number of CD19$^+$ cells produced (again, not statistically significant), as the numbers of CD19$^+$ cells in culture decline from $1.02x10^4$ ($\pm0.28x10^4$) CD19$^+$ cells at day 15 to $0.65x10^4$ ($\pm0.30x10^4$) cells at day 18 in the presence of IGF1, whilst increase from $1.28x10^4$ ($\pm0.69x10^4$) to $1.87x10^4$ ($\pm1.19x10^4$) over the same timeframe when exposed to IL7 (Figure 5-3B). These differences highlight the proliferative effects of IL7 on human B cells and, given that cells exposed to IL7 at day 18 have still not reached confluence, one would assume that this upward trajectory of CD19$^+$ cells would continue.

The decline in B cell numbers in the presence of IGF1 would suggest a similar dynamic of differentiation as seen in the murine system, where a decline in B cells corresponded to the production of IgM$^+$ cells (Chapter 4, Figure 4-4). The comparative proportions of cytoplasmic Mu$^+$ B cells at day 8 between the human and mouse systems also pointed to a similar culture dynamic (average 31.9% in mice, average 43.4% in humans; Figure 5-3C). However, in the presence of IGF1 there was no increased expression of either cytoplasmic Mu or surface IgM from the human CD19$^+$ cells (Figure 5-3C and D).

The results of these cultures would indicate that although CD19$^+$ cells can be produced from human CD34$^+$ HSCs exposed to IL7 on an MS5 stromal layer, they are unable to further proliferate, or differentiate into IgM$^+$ cells, when exposed to IGF1 (and BAFF). This may suggest that IGF1 does not play the same role in differentiating Pro-B cells into Pre-B cells as it does in mice. However, it is equally feasible that the differences in culture conditions between the human and mouse systems could be contributing to the differences in culture dynamics. For example, MS5 cells may be providing unwanted inhibitory signals to B cells, or the initial CD34$^+$ HSCs lacked a committed state that would permit certain cell fate decisions, both of which potentially preventing progression to IgM$^+$ stage. The culture limitations may therefore be masking a role for IGF1R signalling in normal human progenitor B cell development.

In any case, this human system provides an opportunity to compare age-associated differences in a HSCs ability to differentiate into CD19$^+$ B cells and proliferate in response to IL7 in-vitro. It also allows for enough B cells to be propagated in-vitro for transcriptomic differences between young and aged samples to be explored.

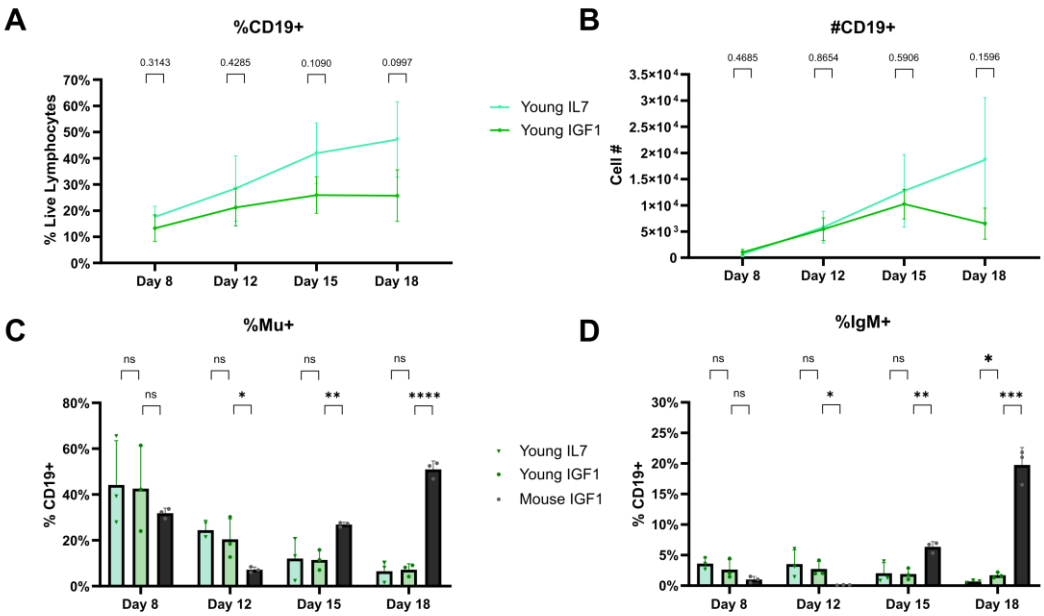

Figure 5-3: Summary of the in-vitro growth dynamics for human cells from young individuals (n=3, age 18-24). (A) From a starting population of CD34$^+$ HSCs, CD19$^+$ B cells are present in culture as early as day 8. (B) Cells exposed to IL7-only throughout the culture appear to produce more CD19$^+$ cells compared to when IGF1 is introduced. (C) Cytoplasmic Mu is expressed as early as day 8, but is proportionally lost as the culture progresses without the subsequent enrichment as was found in the mouse system from days 15-

18. (D) There was also no increase in IgM$^+$ cells as was seen in the mouse system from days 15-18. (pval <0.05, multiple t-test).

5.3 Impairments in human B cell development with age

Samples from three older donors were used in these studies. The CD34$^+$ HSC donors were age 55, 57, and 62 (n=3; 1 male, 2 females). As with the young donors, these aged samples were cultured in both the IL7 and IGF1 conditions, and compared for age-associated differences in their B cell production (Figure 5-4).

An aged reduction in the proportion of CD19$^+$ cells from days 8-18 of the culture, and in both conditions (IL7 and IGF1) was observed in the aged cultures (Figure 5-5). This corresponded to fewer CD19$^+$ B cells in-vitro that, in the IL7 condition, resulted in approximately 5-fold fewer aged CD19$^+$ cells than young CD19$^+$ cells by day 18 ($1.87x10^4$ $\pm1.19x10^4$ young CD19$^+$ cells versus $0.33x10^4$ $\pm0.15x10^4$ aged CD19$^+$ cells). Again however, due to the low sample size and sample-to-sample variability, the statistical power is limiting. Nevertheless, what these findings seem to suggest is either a reduced ability for older HSCs to differentiate into CD19$^+$ B cells, or a reduced proliferative capacity of the aged B cells in response to IL7, or indeed both. Overall, there is an age-associated reduction in B cell numbers through this in-vitro system.

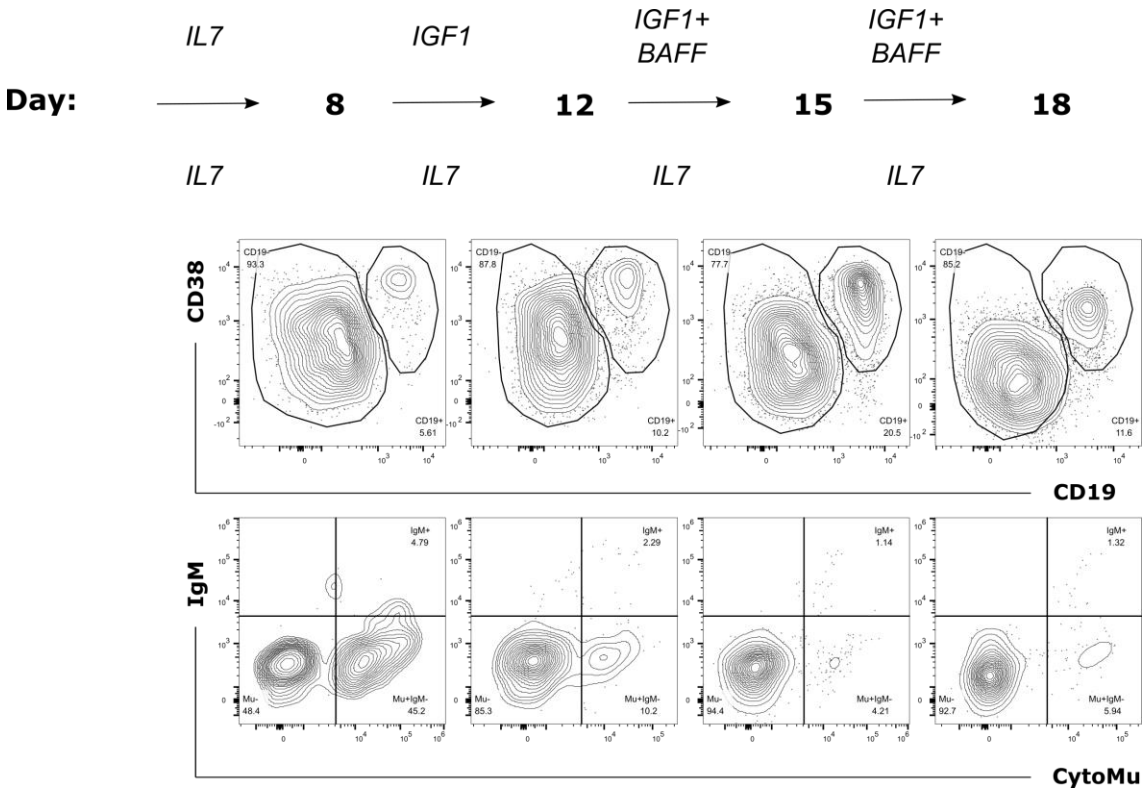

Figure 5-4: In-vitro human culture system schematic from older donors. CD34⁺ bone marrow cells from older healthy human donors (n=3, ages 55, 57, 62) were exposed to the same culture conditions as the young healthy human donors (n=3, ages 18, 19, 24) as described in Figure 5-2. FACS plots represent cells from an older, healthy donor at these time points through the "IGF1" condition, and were gated for live singlet lymphocytes prior to this gating strategy.

Despite there being no notable induction of cytoplasmic Mu⁺ or surface IgM⁺ B cells in response to IGF1 through this human system (Figure 5-5), comparisons were still made between the young and aged cells. As with mice, the proportion of cytoplasmic Mu⁺ cells at day 8 were comparable between the Young and Aged groups. However, unlike mice, there were no age-associated differences in the proportions of Mu⁺ or IgM⁺ cells in the CD19⁺ population at days 15-18 (Figure 5-6).

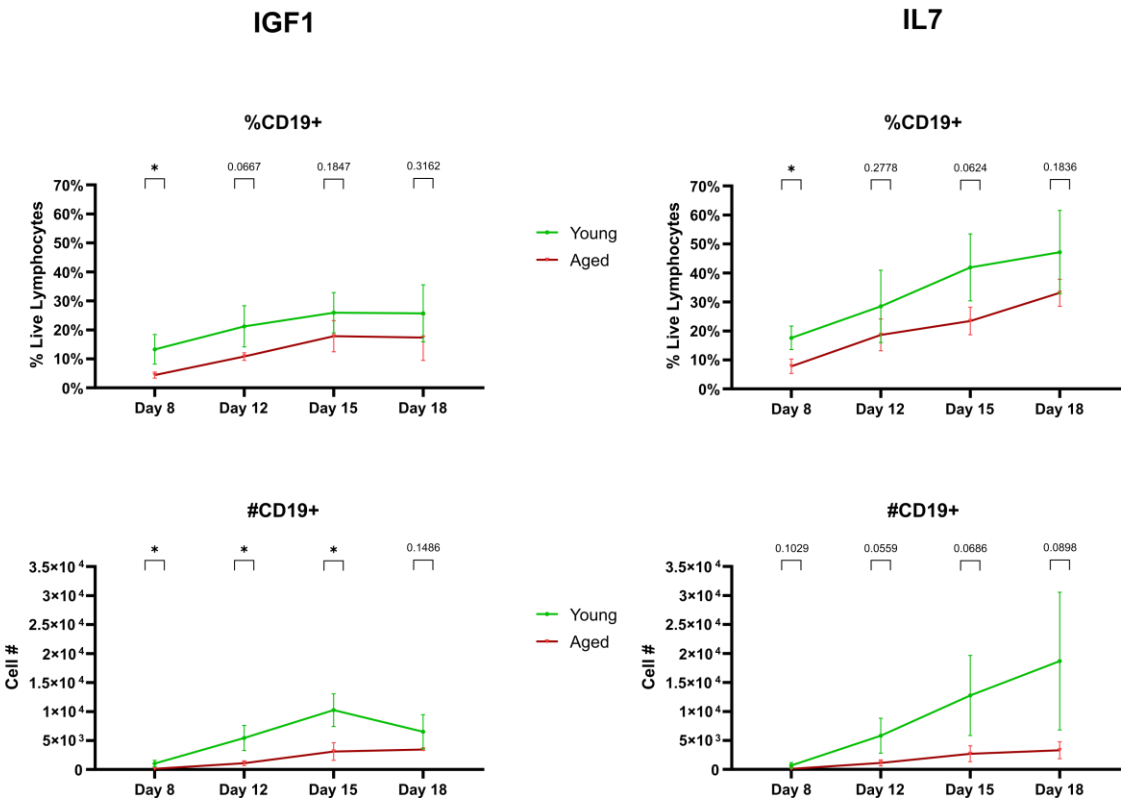

Figure 5-5: Comparative summary of the in-vitro growth dynamics for human cells from young (n=3, aged 18-24) and aged (n=3, aged 55-62) individuals. Human CD34⁺ HSCs were exposed to the two culture conditions described in Figure 5-2: "IGF1" and "IL7". In both conditions, aged individuals on average show reduced numbers and proportion of CD19⁺ cells in-vitro. (pval <0.05, multiple t-test).

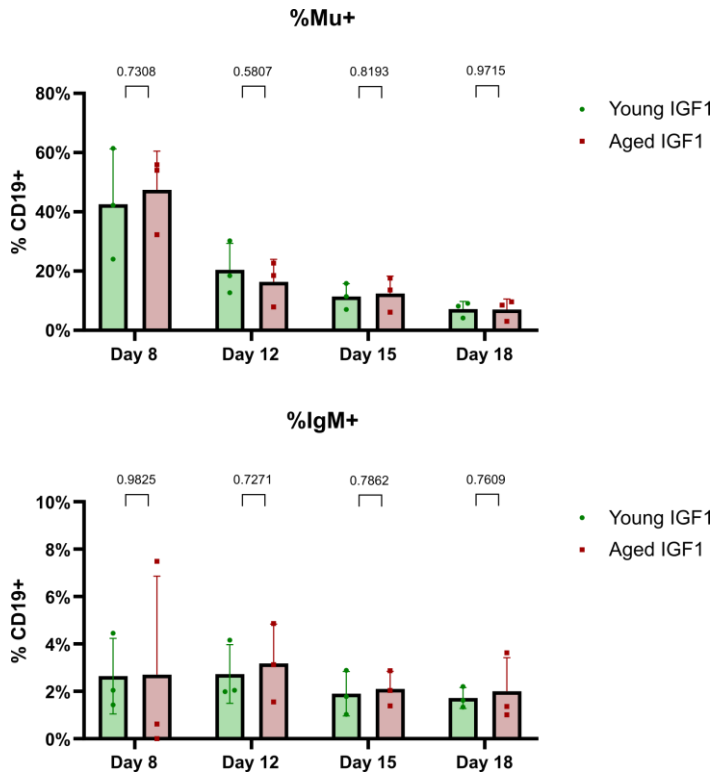

Figure 5-6: Comparative summary of the in-vitro expression of Cytoplasmic Mu and Surface IgM. There were no age-associated differences in the proportions of Mu^+ or IgM^+ cells in the $CD19^+$ population at days 8-18 (pval <0.05, multiple t-test).

As mentioned, the inability of young human $CD19^+$ cells to differentiate beyond a Pro-B cell-like stage (expressing either cytoplasmic Mu or surface IgM) through this in-vitro system in response to IGF1 may not reflect the in-vivo dynamics of human Pro-B to Pre-B cell differentiation in response to IGF1, but rather it is a limitation of the system itself. With this in mind, the aged downregulation of IGF1R signalling found in mice may still be found in humans, but is not captured through an observed functional defect in this in-vitro setting.

To explore further aged differences in developing human progenitor B cells exposed to IGF1, differential gene expression of human $CD19^+$ B cells derived through this in-vitro system were analysed.

5.4 Aged transcriptional differences in human B cells exposed to IGF1

By day 12 of the culture, human $CD34^+$ HSCs have differentiated into $CD19^+$ B cells, and have been exposed to IGF1 for 4 days. It is at this timepoint therefore that live singlet $CD19^+$ cells were extracted from the young (n=3) and aged (n=3) cultures by FACS to analyse their differential gene expression. Pooling wells gave enough cells to analyse (~$1.5x10^5$-$4.5x10^5$ for young, ~$4.5x10^4$-$1.2x10^5$ for aged) by RNAseq. With these cells, differential expression analysis by DESeq2 was performed between the young and aged groups, with sex variations between individuals accounted for in the analysis (see Materials & Methods). This gave a total of 665 differentially expressed (DE) genes between the young and aged $CD19^+$ cells (431 up, 234 down).

Interestingly, the most statistically significant and differentially expressed genes between these young and aged $CD19^+$ cells are associated with antigen presentation (Figure 5-7). *HLA-DQA1*, *HLA-DQB1*, and *HLA-DPB1* are Major Histocompatibility Complex Class II (MHC-II) proteins that are upregulated in the aged cells, whereas *KLRK1* and *KLRC4-KLRK1* are Killer Cell Lectin-Like Receptors that play a role in MHC-I antigen presentation, and which are downregulated in the aged $CD19^+$ cells. It would seem therefore that the aged $CD19^+$ cells are engaging in antigen presentation in these cultures, although this would need to be validated at the protein level.

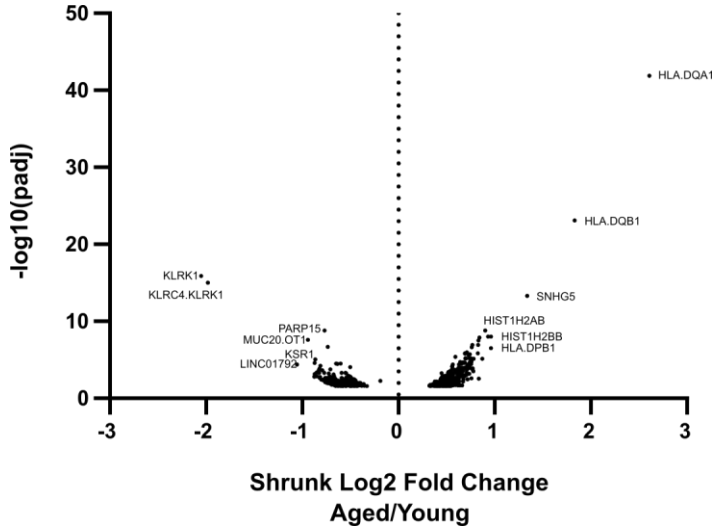

Figure 5-7: Volcano plot for the 665 DE genes between Young and Aged CD19⁺ cells at day 12. RNAseq libraries were generated from live CD19⁺ cells from Young (n=3) and Aged (n=3) individuals that were extracted from culture at day 12. DESeq2 analysis revealed the most statistically significant (-log10(padj)) and differentially expressed (Shrunk Log2 Fold Change) of the 665 DE genes to be HLA genes (upregulated).

To explore more comprehensively which pathways were being differentially utilised between these young and aged CD19⁺ cells, Gene Set Enrichment Analysis (GSEA) was performed using the 665 DE genes for GO symbol enrichment. Of the 535 GO symbols enriched, only 5 were statistically significant (p-value <0.05), all of which were upregulated in the aged group (Figure 5-8). Two of the five GO symbols statistically enriched in ageing were associated with antigen presentation (*Antigen Processing and Presentation* and *Antigen Processing and Presentation of Peptide Antigen*), and genes included in the enrichment were the upregulated *HLA* genes *HLA-DQA1*, *HLA-DQB1*, and *HLA-DPB1*. Another two of the five GO symbols enriched were associated with cell cycle regulation (*Regulation of Cell Cycle Phase Transition* and *Negative Regulation of Cell Cycle Phase Transition*). Increased negative regulation of cell cycle in these aged CD19⁺ B cells would support defective culture dynamics seen in Figure 5-5, since the cells would be less proliferative and so produce fewer CD19⁺ B cells. However, since 25% (6 out of 24) of the genes enriched for in the GO symbol *Negative Regulation of Cell Cycle Phase Transition* are also enriched for in *Antigen Processing and Presentation*, it is possible that any cell cycle suppression through this pathway is a consequence of the same antigen presentation mechanism.

A

	SIZE	NES	NOM p-val	FDR q-val
GO INTRINSIC COMPONENT OF PLASMA MEMBRANE	16	1.29473	<0.0001	1
GO NEGATIVE REGULATION OF CELL CYCLE PHASE TRANSITION	24	1.248798	<0.0001	1
GO REGULATION OF CELL CYCLE PHASE TRANSITION	34	1.223116	<0.0001	1
GO ANTIGEN PROCESSING AND PRESENTATION OF PEPTIDE ANTIGEN	17	1.210215	<0.0001	1
GO ANTIGEN PROCESSING AND PRESENTATION	17	1.210215	<0.0001	1

B

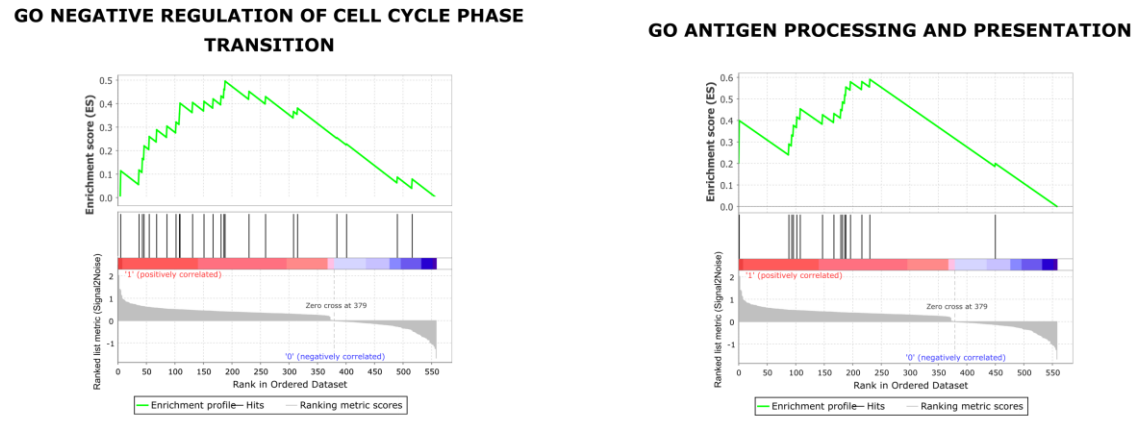

C

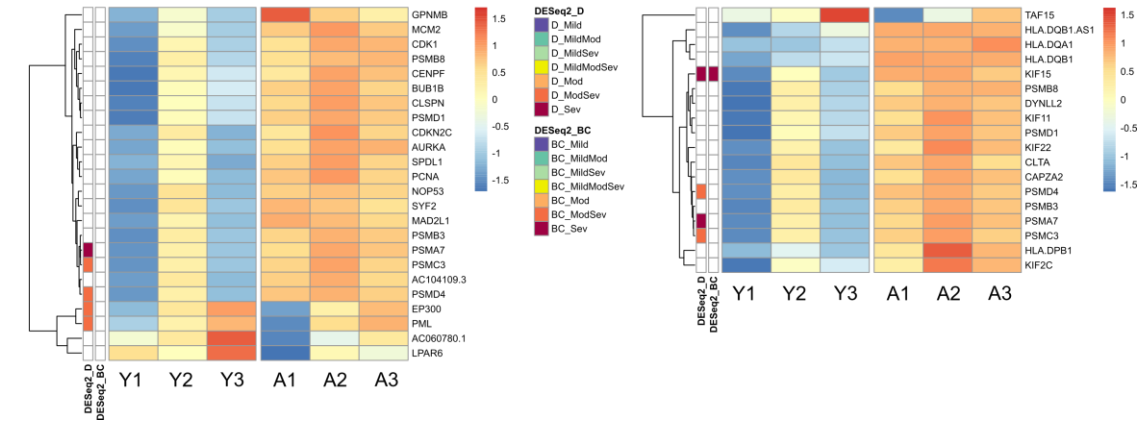

Figure 5-8: Gene Set Enrichment Analysis (GSEA) of the 665 DE genes between Young and Aged. (A) Only 5 GO symbols were enriched to statistical significance between Young (n=3) and Aged (n=3) (pval <0.05). High FDR values are likely due to low sample sizes. All 5 GO symbols were upregulated in the Aged group. 2/5 were linked to cell cycle, another 2/5 were linked to antigen presentation. (B) Enrichment plots for "Negative Regulation of Cell Cycle" and "Antigen Processing and Presentation". Shows the running Enrichment Score (ES) for the GO symbol along the 665 DE genes, ranked based on their signal-to-noise ratio. (C) Heatmap showing z-score for each gene in the GO symbols "Negative Regulation of Cell Cycle" (left) and "Antigen Processing and Presentation" (right) for young ("Y") and aged ("A") samples. Each gene is annotated to show which aged murine Pro-B (BC) or Pre-B (D) subgroups also have this gene differentially expressed versus Young by DESeq2 (as determined in Chapter 3).

To determine whether the age-associated upregulation in *HLA* genes in CD19^{+} B cells was unique to this human in-vitro system, comparisons were made between mouse progenitor B cells either derived in-vivo (Late Pre-B cells from Chapter 3; Young n=4,

Aged n=12) or in-vitro (B220$^+$ cells at day 12 of the murine in-vitro system described in Chapter 4; Young n=1, Aged n=2). Of the differentially expressed *HLA* genes in humans, only *HLA-DQB1* has a mouse ortholog: *H2-Ab1*. Comparative gene expression of *HLA-DQB1*/*H2-Ab1* in the young and aged human/mouse cells confirmed that the aged upregulation of this gene is found only in the human B cells cultured through this system (Figure 5-9). Whether this differential gene expression is indicative of a human-specific defect in aged progenitor B cells, or represents a cross-species aged defect captured only in the human in-vitro system due to its different technical elements (such as the murine stromal cell line), remains a topic of discussion and future work.

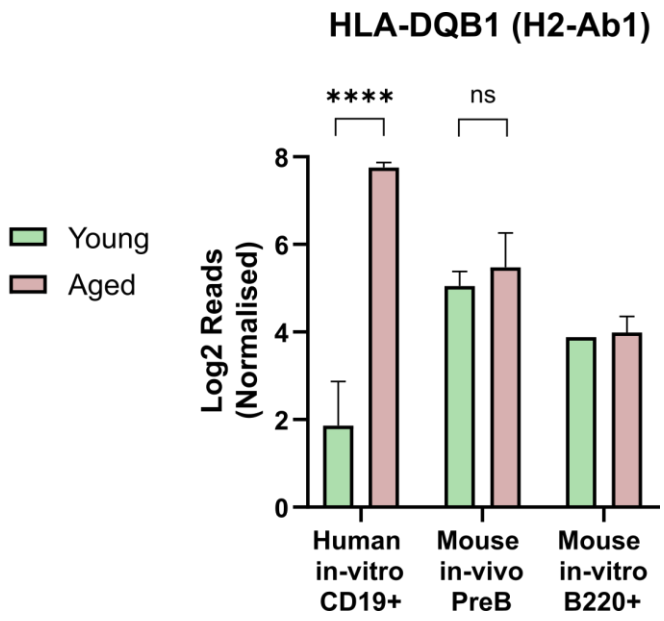

Figure 5-9: Expression of HLA-DQB1 (H2-Ab1) in Young and Aged Humans and Mice. Of the upregulated HLA genes in the aged human CD19$^+$ cells, only HLA-DQB1 has a mouse ortholog gene: H2-Ab1. Gene expression of H2-Ab1 in in-vivo derived mouse Late Pre-B cells (Young n=4, Aged n=12; from Chapter 3) and in-vitro derived mouse B220$^+$ cells cultured to day 12 (Young n=1, Aged n=2; as described in Chapter 4) is comparable between young (3 months) and aged (~24 months) individuals. (Log2 reads per million reads. Statistics by DESeq2 padj <0.05).

5.5 Differential gene expression in aged human and mouse progenitor B cells

Despite subtle differences in experimental design and the cell types captured, identifying genes that were differentially expressed in both mouse and human aged progenitor B cells (in-vitro and in-vivo) could provide some interesting insights into shared aged defects in B cell development. To achieve this, mouse orthologs to the 665 DE genes of the human in-vitro derived young and aged $CD19^+$ B cells were determined in order to make comparisons in cross-species DE gene expression. 516 of the 665 (77.6%) DE genes contain a mouse ortholog.

In Chapter 3, differential gene expression in murine Pro-B cells revealed 916 DE genes between young and aged individuals, while Late Pre-B cells there were 1164 DE genes (Young n=4, Aged n=12). More comprehensive interrogation of the aged Pre-B cells by subgrouping into Mild (n=4), Moderate (n=4), and Severe (n=4), and independently comparing against the young Pre-B cells gave differential gene list sizes of 148, 2561, and 3596 respectively. Combined, this gave a total of 4171 unique DE genes across the Mild, Moderate, and Severe aged Pre-B cells.

Comparisons were therefore made between the 516 DE genes of the human in-vitro derived $CD19^+$ B cells and the murine in-vivo derived Pro-B and Pre-B cells (Figure 5-10). 39 DE genes (7.6%) were shared with Pro-B cells and 61 (11.8%) with Pre-B cells of the aged mice. When considering all of the DE genes across the Mild, Moderate, and Severe subgroups, aged human $CD19^+$ cells share 225 DE genes (43.6%) with aged murine Pre-B cells (68% of which are DE in both Moderate and Severe aged murine Pre-B cells; not shown). Therefore, comparisons herein were made with the latter murine Pre-B cells.

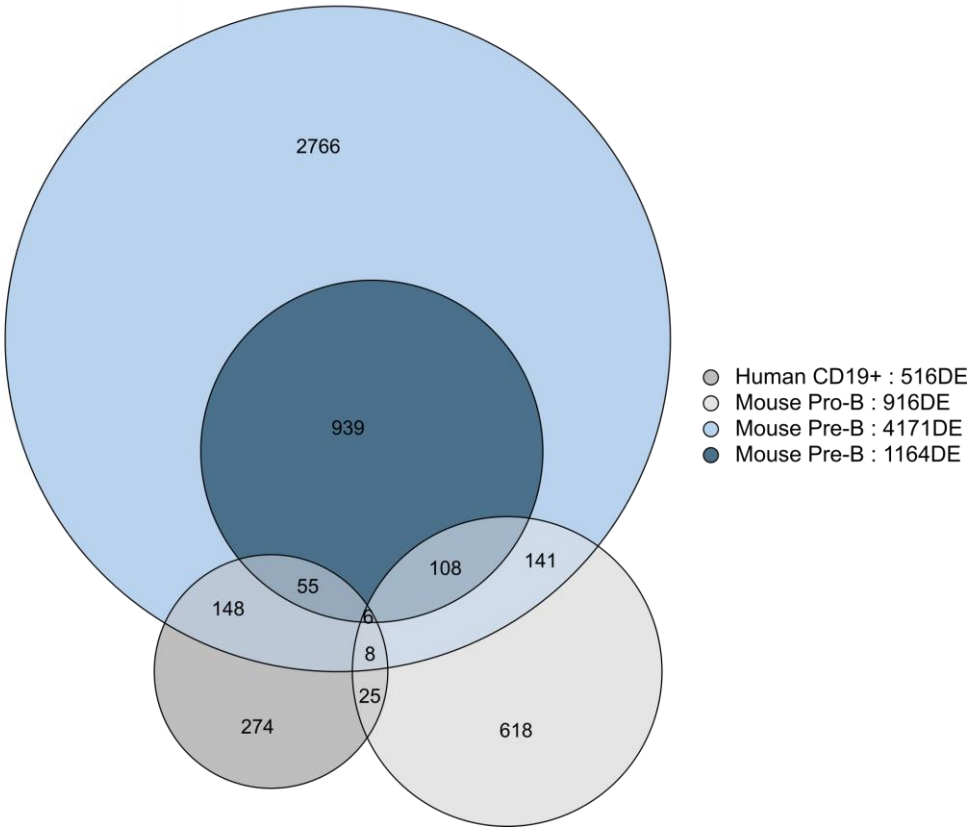

Figure 5-10: Overlaps in orthologous DE genes between Young and Aged in-vitro derived Human CD19⁺ cells and in-vivo derived Murine Pro-B and Pre-B cells. 516 of the 665 DE genes between Young (n=3) and Aged (n=3) human CD19⁺ cells derived in-vitro have an orthologous mouse gene. The shared presence of aged DE genes between these human CD19⁺ cells and Pro-B (916 DE genes – from Chapter 3) and Pre-B (1164 DE and 4171DE – from Chapter 3) cells was determined and visualised as a Venn diagram.

With the 61 DE genes shared between the human CD19⁺ cells and the murine Pre-B cells (using the 1164 DE gene list), there was a positive correlation in the directionality and intensity of the differential gene expression between young and aged (R^2=0.6681, Figure 5-11). Only 5 of the DE genes showed an inverse relationship in its differential expression: *ARID5B, BARD1, CENPF, KIFC1*, and *LMNB1*. These genes appear to be upregulated in aged human CD19⁺ cells but downregulated in aged murine Pre-B cells and, given that they do not follow the same differential expression trend, were not considered in downstream analysis. A possible explanation for this discrepancy could be a result of human cells being in-vitro derived and the mouse cells in-vivo derived.

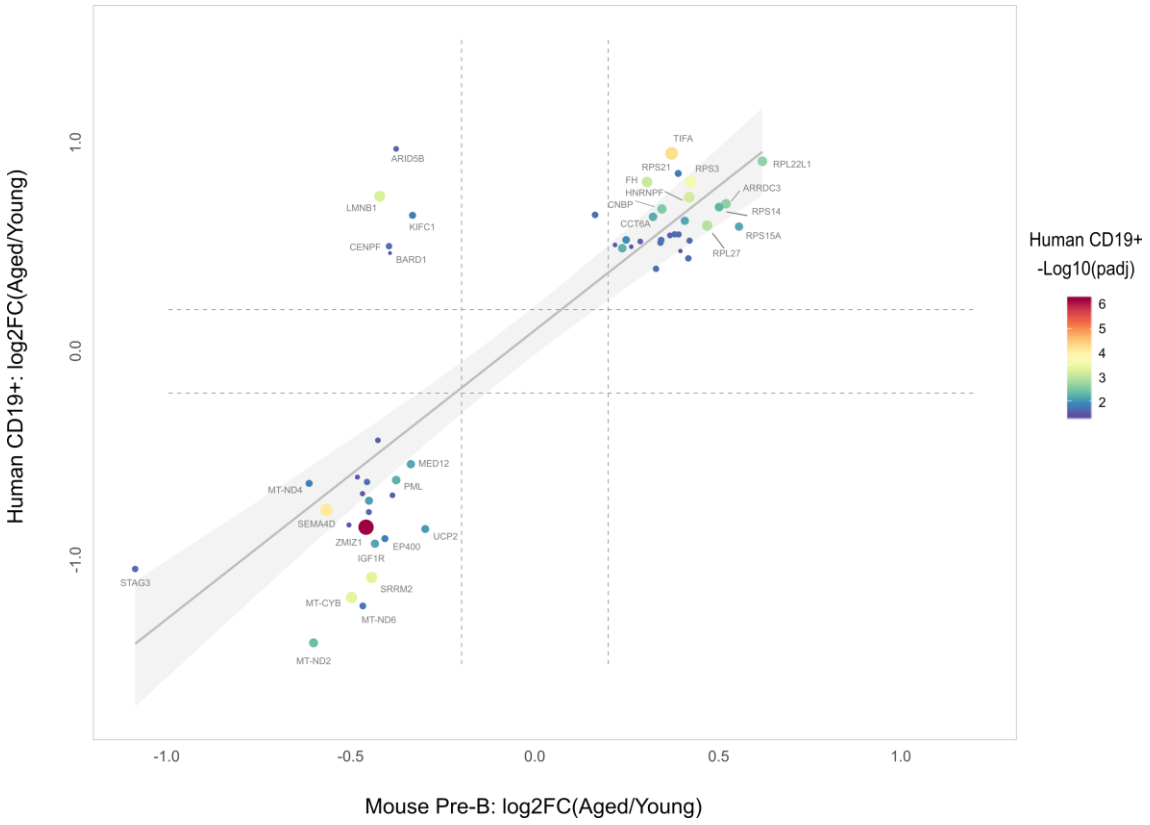

Figure 5-11: Log2 fold expression change in genes between Aged and Young in-vitro derived Human CD19⁺ cells and Murine in-vivo derived Pre-B cells. 61 genes were differentially expressed in both mouse Pre-B (1164 DE genes, x-axis) and human CD19⁺ cells (665 DE genes, 516 orthologous DE genes, y-axis) derived in-vitro (R^2=0.6681). Values below 0 are downregulated in ageing and values above 0 are upregulated in ageing. The size and colour of each gene represents the -Log10(padj) value for Human CD19⁺ cells (Aged/Young).

For the DE genes that correlate across human CD19⁺ cells and mouse Pre-B cells, there were some interesting genes, most notably in the genes that were downregulated. Mitochondrial genes involved in the electron transport chain complex were once again shown to be downregulated, this time in aged human CD19⁺ cells. These include *MT-ND2, MT-ND4, MT-ND6,* and *MT-CYB* of the electron transport chain complex. These genes were downregulated in the aged murine Pro-B and Pre-B cells in Chapter 3 (through both bulk RNAseq and single-cell RNAseq methods), and murine B220⁺ B cells derived in-vitro also appear to show reductions (Figure 5-12). This would suggest that aged progenitor B cells of both mice and humans will have a reduced metabolic output compared to their younger counterparts, and could be contributing to the impaired B cell development observed with age.

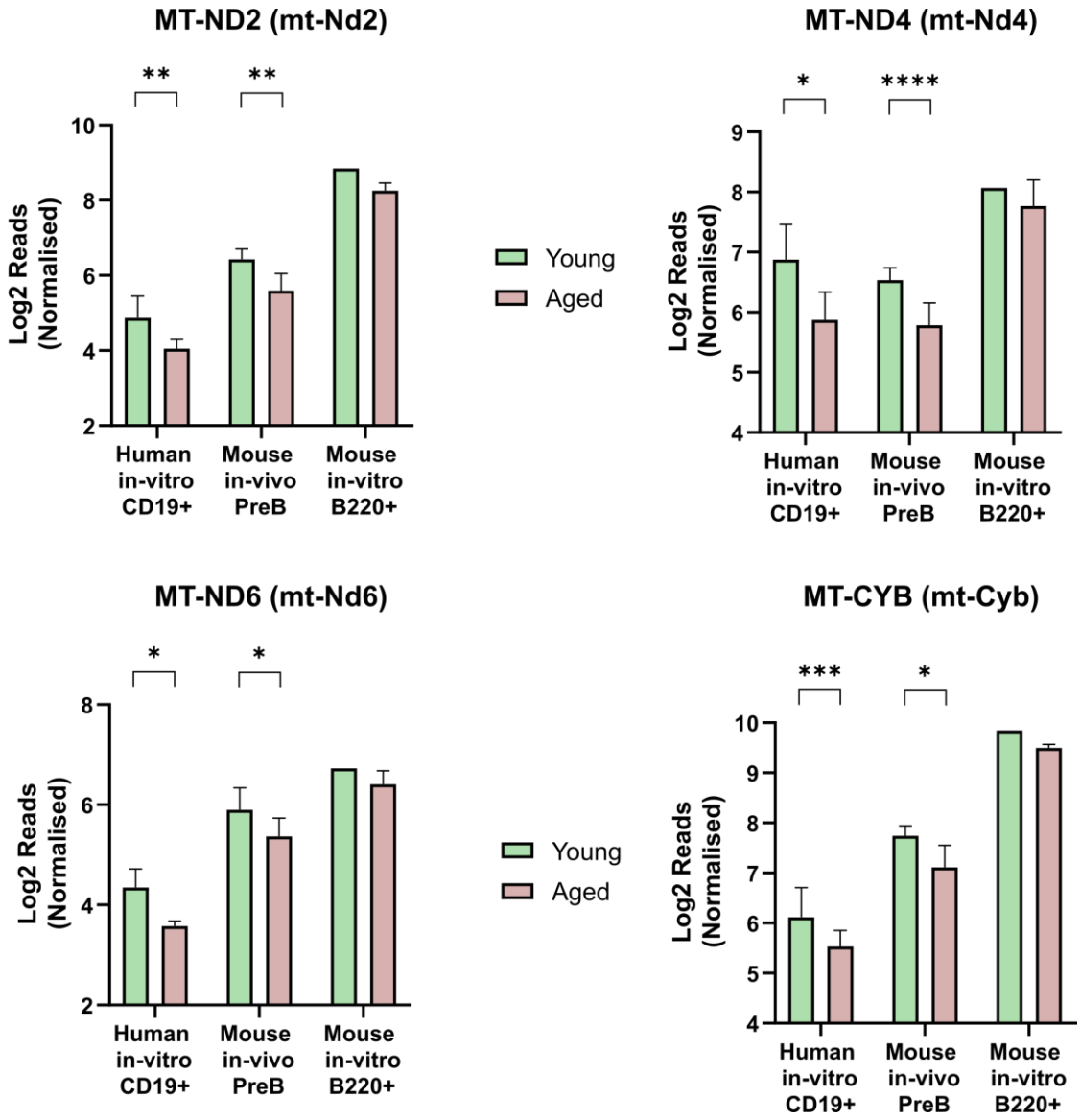

Figure 5-12: Reduced expression of mt-genes in Young and Aged Humans and Mice. Genes coding for components of the electron transport chain – e.g. MT-ND2, MT-ND4, MT-ND6, MT-CYB – have reduced expression in the aged cells of human in-vitro derived CD19⁺ cells (Young n=3, Aged n=3), murine in-vivo derived Pro-B (not shown, Young n=4, Aged n=12; from Chapter 3), murine in-vivo derived Pre-B (Young n=4, Aged n=12; from Chapter 3), and murine in-vitro derived B220⁺ cultured to day 12 (Young n=1, Aged n=2; as described in Chapter 4). (Log2 reads per million reads. Statistics by DESeq2 padj <0.05).

Other shared DE genes include *STAG3* (downregulated) and *ARRDC3* (upregulated). *STAG3* (Stromal Antigen 3) is a cohesin subunit that has been shown to be required for sister chromatid cohesion specifically during meiosis[375]. Despite not undergoing meiosis, *STAG3/Stag3* is strongly downregulated in all aged murine Pro-B and Pre-B cells (Mild,

Moderate, and Severe subgroups), as well as murine B220^{+} B cells derived in-vitro and now human CD19^{+} B cells derived in-vitro (Figure 5-13). This strong association of *STAG3* downregulation with ageing progenitor B cells would suggest that it plays a role in the aged phenotype. Since its characterised role in meiosis does not occur in B cell development, this is likely to be through an uncharacterised mechanism – and thus poses an exciting target for future research. Validations of (differential) expression at the protein level should be explored as a next step.

ARRDC3 (Arrestin domain-containing protein 3) on the other hand is an adaptor to G protein-coupled receptors and target them for degradation, and has been linked to metabolism in other cell types[376,377]. *ARRDC3* is also upregulated in all aged murine Pro-B and Pre-B cells (Mild, Moderate, and Severe subgroups), as well as these human CD19^{+} B cells derived in-vitro. However, preliminary data with B220^{+} B cells derived in-vitro suggests there is not as strong an association with the aged phenotype as *STAG3* (Figure 5-13). As with *STAG3*, a role for *ARRDC3* in progenitor B cells has not been characterised, and so may be a candidate for future research, from an ageing context.

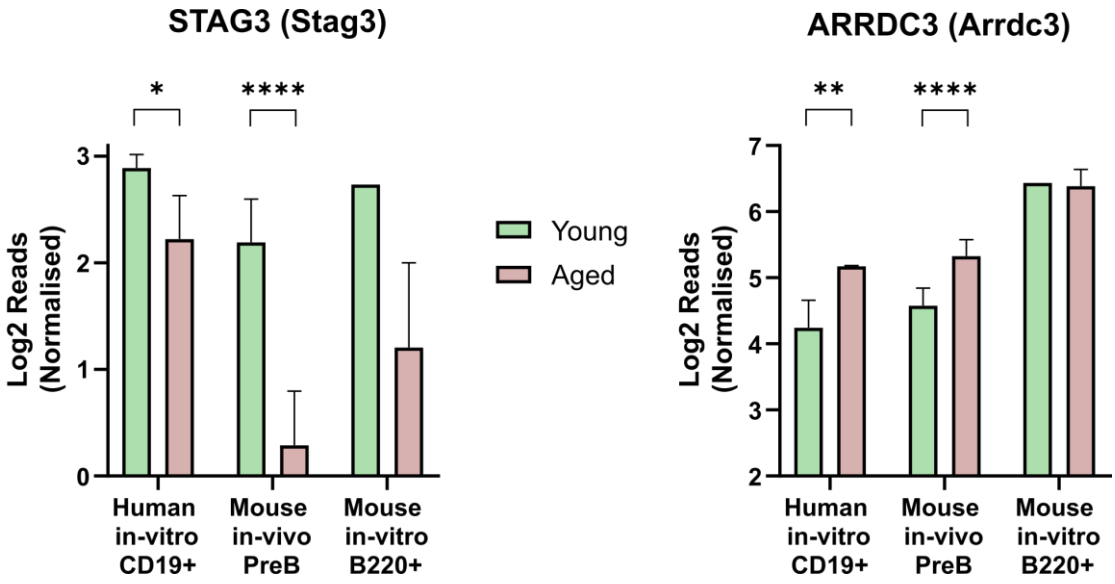

Figure 5-13: Differential expression of STAG3 and ARRDC3 in Young and Aged Humans and Mice. STAG3 (down) and ARRDC3 (up) are differentially expressed in the aged cells of human in-vitro derived CD19^{+} cells (Young n=3, Aged n=3), murine in-vivo derived Pro-B (not shown, Young n=4, Aged n=12; from Chapter 3), and murine in-vivo derived Pre-B (Young n=4, Aged n=12; from Chapter 3). Murine in-vitro derived B220^{+}

cultured to day 12 (Young n=1, Aged n=2; as described in Chapter 4) show the same reduction in Stag3 expression, but not Arrdc3. (Log2 reads per million reads. Statistics by DESeq2 padj <0.05).

Of particular note was the downregulation of *IGF1R* in these aged human B cells (Figure 5-11 and Figure 5-14), providing first insight into a potential shared mechanism of IGF1R signal suppression in both human and mouse progenitor B cells, which could in turn be impairing B cell development. Deeper comparisons between these human $CD19^+$ B cells and murine Pre-B cells were made by comparing the 516 DE gene orthologs with the unique combination of 4171 DE genes across the Mild, Moderate, and Severe aged Pre-B cells. Of the 225 DE genes shared between these gene lists, 65 have a padj value of <0.01 (Figure 5-14). Through this analysis, *IGF1R* once again appeared as differentially downregulated in aged human $CD19^+$ B cells and murine Pre-B cells (Moderate and Severe aged Pre-B cells).

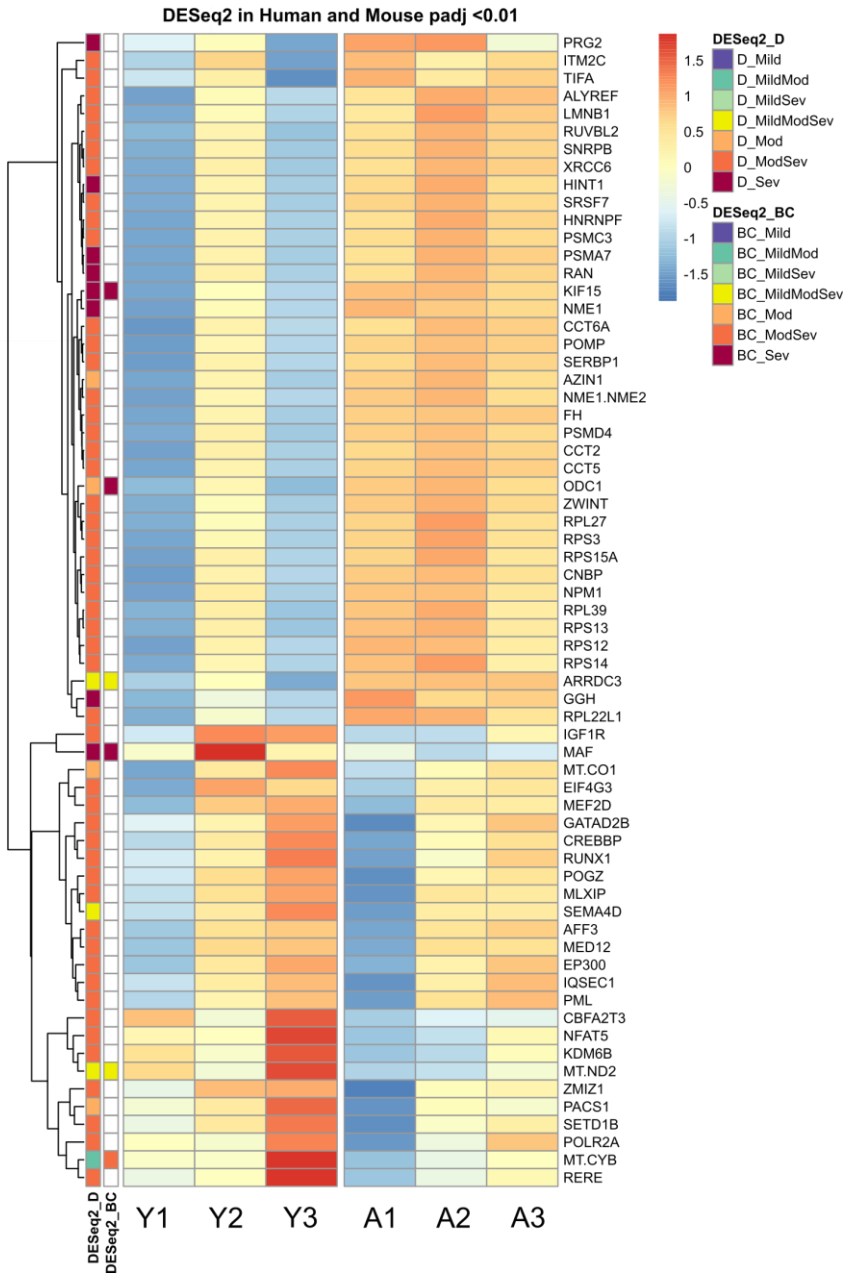

Figure 5-14: The most statistically significant orthologous aged DE genes between in-vitro derived Human CD19⁺ cells and in-vivo derived Mild/Moderate/Severe aged Pre-B cells. Z-score expression values in Young (n=3) and Aged (n=3) human in-vitro derived CD19⁺ cells for 65 (padj <0.01) of the 225 (padj <0.05) DE genes shared with mouse Mild/Moderate/Severe aged Pre-B cells. Each gene is annotated to show which aged murine Pro-B (BC) or Pre-B (D) subgroups also have this gene differentially expressed versus Young by DESeq2 (as determined in Chapter 3).

It was postulated in Chapters 3 and 4 that downregulation of the H3K27 demethylase *Kdm6b* in aged murine Pre-B cells, without reciprocal fold-decrease in the H3K27 methyltransferase *Ezh2*, may contribute to impaired IGF1R signalling through *Irs1*

suppression by H3K27me3. For instance, aged murine Pre-B cells of the Severe subgroup were shown by DESeq2 in Chapter 3 to have a less than 1.2-fold reduction in *Ezh2* expression, compared to over 2.6-fold reduced expression in *Kdm6b*. This hypothesis could translate across the species, since aged human $CD19^+$ cells also presented with downregulation of *KDM6B*, which was a near 2-fold reduction compared to young B cells (Figure 5-14 and Figure 5-15). *EZH2* expression on the other hand appears to increase (albeit not to a statistical significance by DESeq2). Aged $B220^+$ murine B cells derived in-vitro also seem to follow the same trend as the human $CD19^+$ B cells in their differential expression of *Kdm6b* and *Ezh2*.

However, despite reduced expression of *IGF1R*, aged human $CD19^+$ cells show no differential expression in *IRS1*. Interestingly, murine in-vitro derived $B220^+$ cells show the inverse trend of an aged reduction in *Irs1* expression, but not in *Igf1r*. Together, what this could indicate is in-vitro derived human B cells are at a stage in development in which *IRS1* expression has not yet been upregulated compared to murine B cells. Alternatively, it could be that downregulation of the IGF1R signal in mice is predominantly driven by downregulation of Irs1, whereas in humans it is through downregulation of IGF1R itself.

Comparisons made between the DE genes of aged human in-vitro derived $CD19^+$ cells and aged murine in-vivo derived Pre-B cells have revealed some exciting similarities, from suppression of cell cycle to reduced mitochondrial output. This preliminary data also implicates IGF1R signalling defects in ageing human B cells which, taken together with the mouse findings of Chapters 3 and 4, suggest that IGF1R could have a direct impact on progenitor B cell development.

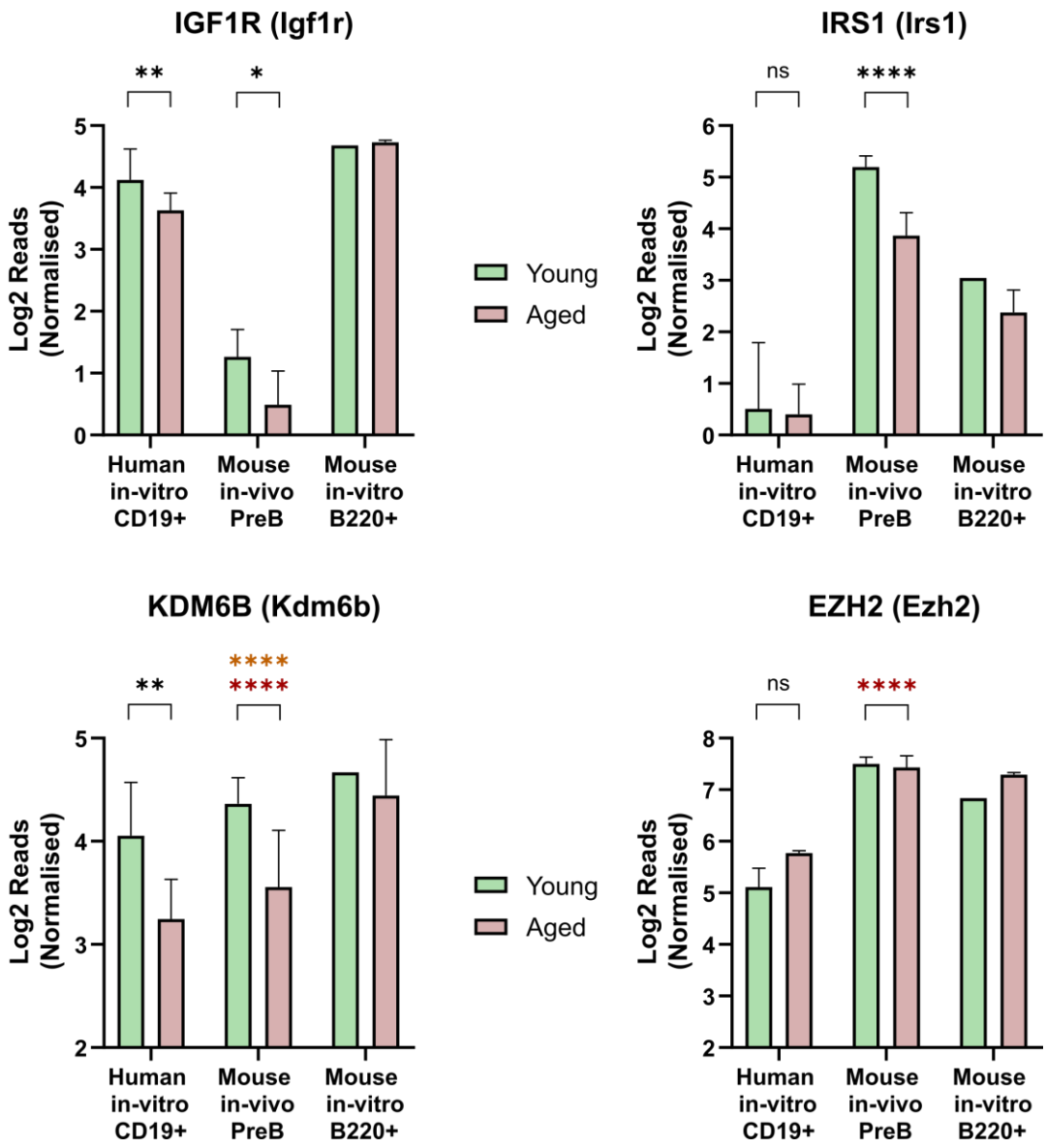

Figure 5-15: Differential expression of IGF1R/IRS1 and KDM6B/EZH2 in Young and Aged Humans and Mice. Showing normalised gene expression values for Human in-vitro derived CD19⁺ cells (Young n=3, Aged n=3), Murine in-vivo derived Pre-B cells (Young n=4, Aged n=12), and Murine in-vitro derived B220⁺ cells cultured to day 12 (Young n=1, Aged n=2; as described in Chapter 4). Asterisks (DESeq2) for in-vivo derived Pre-B cells: black= Young (n=4) vs Aged (n=12); orange= Young (n=4) vs Moderate Aged (n=4); red= Young (n=4) vs Severe Aged (n=4). (Log2 reads per million reads. Statistics by DESeq2 padj <0.05).

5.6 Discussion

This translational chapter of murine insights to the biology of ageing human B cell development has raised several points of discussion. It is first worth mentioning that the

age of the older human donors (ages 55, 57, and 62) used in these experiments were fairly young compared to the equivalent ages of the mice used in Chapters 3 and 4 (24+ months). According to *The Mouse in Biomedical Research*, 56-69 years in humans is equivalent to 18-24 months in mice[378]. Nonetheless, through in-vitro differentiation, it has been possible to demonstrate a reduced capacity of aged HSCs to differentiate down the B-lineage and proliferate in response to IL7. However, due to sample-to-sample variability and low sample size, the statistical power of these observations was, in places, lacking. More biological repeats of these cultures should resolve the significance of these findings. To also better elucidate if these aged $CD19^+$ cells are less proliferative in response to IL7, BrdU cell cycle analysis – similar to that done in Chapter 4 – could be performed in-vitro.

The production of IgM^+ cells in this human culture system is comparable to that of other cultures using human BM-derived $CD34^+$ HSCs[379]. Unfortunately, it was not possible to capture greater differentiation of human $CD19^+$ B cells to an IgM^+ stage in the presence of IGF1. While this may suggest that this growth factor does not possess the same ability to drive Pro-B to Pre-B cell differentiation in humans as has been shown to in mice, this conclusion cannot yet be drawn from these experiments. To do so, one could re-design the human in-vitro system so that it better resembles the murine culture conditions found in Chapter 4. For instance, to culture lineage-depleted human bone marrow cells – and thus of both haematopoietic and stromal origin – rather than $CD34^+$ HSCs, without the inclusion of the murine MS5 feeder cell line.

Absence of a stromal cell line may also ameliorate the surprising finding that aged $CD19^+$ B cells specifically upregulate HLA genes and antigen presentation pathways. If this is the case, it is possible that human $CD19^+$ B cells in the presence of a murine stromal cell line are causing a form of antigenic recognition that is affecting aged cells more than young, since this same upregulation of orthologous HLA genes was not detected in mice (in-vivo and in-vitro). Mixed allelic cultures are commonly used to test graft-versus-host reactions between individuals of different genetic background, and could provide an explanation for these experimental observations[380]. However, graft-versus-host disease (GVHD) is generally considered to be a T cell driven pathology[381]. Although, studies have shown a correlation in progenitor B cell numbers and severity of acute GVHD[382], and people over the age of 50 years have an increased incidence of GVHD[383], so it is possible

that what these experiments are capturing is an age-associated susceptibility of human progenitor B cells to present antigen from the murine cell line. This in itself is a fascinating speculation that would be worth exploring further. One way to do so would be to set up mixed murine cultures – similar to that done in Chapter 4 – of aged mice on different genetic backgrounds (such as C57BL/6 and BALB/c) and see if they too show an aged increased expression of MHC class II genes. Such experiments could provide interesting scope to look at aged progenitor B cells in the bone marrow as antigen presenters in bone marrow transplants.

Irrespective of the technical limitations with the human in-vitro system, there remains a very striking correlation between human and mouse progenitor B cells in the differential expression of some genes. All of the gene expression analyses throughout this thesis have revealed mitochondrial genes to be expressed at lower levels with age, regardless of progenitor B cell subset or species. Reduced expression of mt-genes coding for components of the respiratory transport chain – as is the case in both humans and mice – would suggest that these cells have a reduced mitochondrial output and thus, are less metabolically active. Such a molecular observation would be consistent with observations at the organism level, in that ageing is associated with a slowing down of metabolism[384]. Mitochondria have long been associated with ageing for many reasons, such as their production of reactive oxygen species (ROS)[225], but also because of increase mitochondrial DNA (mt-DNA) level in blood circulation with age[228]. mt-DNA is a Danger Associated Molecular Pattern (DAMP) that can activate inflammation via the IL1B pathway[385,226] – a pathway which is central to ageing biology, and which also appears to be upregulated at the transcript level in aged murine progenitor B cells (as shown in Chapter 3). It is thought that mitochondrial exhaustion with age leads to organelle degradation, which would facilitate the decline in a cell's metabolism. It is possible that the perceived downregulation of mt-genes in the aged cells is instead the result of there being less mitochondrial organelles compared to in young cells. To determine if this is the case in aged human progenitor B cells, respiratory output can be measured by Seahorse, and mitochondrial mass can be measured by Mitotracker, on ex-vivo or in-vitro derived B cells.

Proposed aged reductions in mitochondrial mass in these human progenitor B cells may also be driven by its downregulation in IGF1R, since suppression of mTOR signalling

would also reduce biogenesis. In mice, suppression of IGF1R signalling components has been strongly linked to impaired progenitor B cell development and function (Chapters 3 and 4) and so these murine parallels would suggest a similar defect in human progenitor B cells. IGF1 has been shown to support differentiation of human HSCs into $CD19^+$ B cells[149], but has not yet been shown to drive Pro-B to Pre-B cell differentiation as demonstrated in mice – something this chapter also failed to show. This does not necessarily mean however that in-vitro derived $CD19^+$ B cells are not responding to the exogenous IGF1. In this scenario, it could be that aged $CD19^+$ B cells are less responsive to IGF1, due to their reduced expression of IGF1R, and this could be captured transcriptionally by generating complimentary RNAseq libraries of young and aged $CD19^+$ B cells that were exposed to either the "IL7" condition or the "IGF1" condition to see what transcriptional networks, if any, are activated specifically by IGF1 exposure.

In Drosophila, It has been postulated that ageing is associated with an "epigenetic drift" in H3K27me3 accumulation that has negative implications for normal cell metabolism[386,220]. Aged murine progenitor B cells have more specifically shown H3K27me3 to be over the *Irs1* promotor to suppress its transcription and downstream protein expression[275] and with it the IGF1R signal, which could in turn be impairing metabolism and cell differentiation. Here, this mechanism of epigenetic suppression in mice has been supported by the reduced expression of the H3K27 demethylase *Kdm6b* in aged Pre-B cells (Chapter 3) Furthermore, inhibiting its protein (JMJD3) leads to the inhibition of IgM^+ expressing $B220^+$ B cells in-vitro (Chapter 4). The relative reductions in *KDM6B* expression in aged human $CD19^+$ B cells would suggest an age-related accumulation of H3K27me3, although where this suppressive histone mark is deposited may be different between humans and mice, since there is no aged reduction in *IRS1* gene expression in human B cells. For example, H3K27me3 deposits could be found over *IGF1R* instead. In support of this, loss of the H3K27 demethylase UTX1 in *C.elegans* increases H3K27me3 on the Igf1r/daf-2 gene[221], which could also be the case for humans with reduced JMJD3 expression. To explore this suggestion, ChIPseq for H3K27me3 on human young and aged $CD19^+$ B cells derived in-vitro could be performed in parallel with this RNAseq analysis to identify aged regions of H3K27me3 accumulation and subsequent gene downregulation.

Due to the limited availability of human bone marrow samples, this work – along with the majority of the literature on human progenitor B cell development – has been performed in-vitro. The limitations of these in-vitro experiments, and the comparisons made with in-vivo derived murine progenitor B cells, have been addressed throughout the chapter. It would be ideal to instead analyse bone marrow progenitor B cells from young and aged human donors' ex-vivo in order to get a true comparison of aged differences between humans and mouse. Several studies have explored human ageing bone marrow B cells ex-vivo[358,367,368,369], but some have reported sample-to-sample variability, and none have explored the transcriptome. Comparative RNAseq analysis should therefore be performed on in-vivo derived Pro-B cell ($CD19^{+}CD20^{-}IgM^{-}$) and Pre-B cell ($CD19^{+}CD20^{+}IgM^{-}$) populations from young and aged human individuals. In doing so, it may even be possible to apply a similar analytical approach to that performed in Chapter 3, doing so could deconvolute this sample variability based on transcriptome variability.

Through this chapter, it has been possible to provide early insights into the ageing biology of human progenitor B cells. Direct comparison with more the comprehensive mouse studies allow for the role and suppression of IGF1R signalling in aged progenitor B cell to be translated into a clinical setting, and will be discussed further in the final chapter.

6 FINAL DISCUSSION

This thesis set out to deconvolute the heterogeneity of ageing in progenitor B cells at the transcriptomic level to explore IGF1R signalling as a pathway targeted for downregulation. IGF1R signalling has been shown to play a role in Pro-B and Pre-B cell development in mice[84,67,133,134] and for B-lineage commitment of CLPs in humans[366]. As such, age-associated downregulation of this pathway was hypothesised to contribute to observed defects in biological output – such as reduced progenitor B cell numbers and immunoglobulin repertoire diversity. In this thesis, connections have been made between both the transcriptomic variability and IGF1 response of these aged murine progenitor B cells to their defective biological output. Further in-vitro experiments with human cells have subsequently provided preliminary evidence, at the transcriptomic level, to suggest a similar mechanism to mice by which IGF1R signalling is downregulated in aged bone marrow-derived B cells.

6.1 Heterogeneity and the hallmarks of ageing progenitor B cells

Heterogeneous transcriptomic dysregulation is associated with ageing[387] and was explored here in the context of murine progenitor B cells. While, at the achieved resolutions, there was no indication of aged transcriptional heterogeneity at the single-cell level, heterogeneity was evident at the cell population level, and this was explored to a greater sequencing depth in Pro-B and Pre-B cell populations. Deconvolution of this aged heterogeneity was accomplished using a novel approach: by kmeans clustering of individual young and aged mice based on the transcriptomic variability of their Pre-B cell populations into “Mild” “Moderate” and “Severe” aged subgroups. Comprehensive analysis of Pro-B and Pre-B cell populations from the same mice allowed pairwise comparisons to be made across this developmental stage, revealing subgroup-dependent differences in aged deficiencies. Such heterogeneous aged deficiencies

include reductions in progenitor B cell numbers (Moderate and Severe, but not Mild aged subgroups), reduced Pre-B cell VDJ_H:DJ_H recombination (Mild, Moderate, and Severe, but at varying levels), and differential V_H gene usage (Mild, Moderate, and Severe, 3'-proximal>5'-distal V-genes). This analytical approach has also allowed specific ageing hallmarks to be clarified amongst the ageing heterogeneity. As a result, some of the well-established hallmarks of cellular ageing[212] were implicated through the transcriptomic dysregulation of these aged Pro-B and Pre-B cells.

6.1.1 Cell exhaustion

Ageing is associated with stem (progenitor) cell exhaustion, characterised by a reduction in cell cycle and a decline the regenerative potential of tissues[212]. In haematopoiesis, this leads to immunosenescence, and can be caused by known age-associated mechanisms such as DNA damage and mitochondrial dysfunction[212,388].

Downregulation of cell cycle pathways in aged Pro-B and Pre-B cells, combined with upregulation of inflammatory pathways, could be indicative of progenitor B cell exhaustion. In-vivo BrdU experiments showing S-phase reductions in Pro-B and Pre-B cells support this theory, but do not take into consideration potential aged deficiencies in the extracellular bone marrow environment, such as in the supportive stromal niches. However, in-vitro chimeric cultures of young and aged mice found that young B cells propagate better than aged B cells when on the same mixed stromal background and exposed to the same exogenous growth factors, which is consistent with an exhausted phenotype intrinsic to these aged B cells. To confirm aged progenitor B cell exhaustion, in-vivo mixed bone marrow chimeras or adoptive transfer experiments should be considered in order to phenotype aged progenitor B cells derived within the bone marrow of young mice, and vice versa. This has been attempted before by *Labrie et al*[389], where they performed adoptive transfer of T cell and surface-Ig^+ cell-depleted bone marrow from young or aged mice into irradiated young recipients, and measured Pre-B:Pro-B cell ratios. They report that, prior to adoptive transfer, young mice have a greater Pre-B:Pro-B cell ratio than aged mice, and conclude that there is no intrinsic defect in aged progenitor B cell development, largely based on the finding that this Pre-

B:Pro-B cell ratio is comparable between young and aged cells upon adoptive transfer. However, this equivalence in Pre-B:Pro-B cell ratio is largely the result of a young reduction rather than an aged increase, and without the relevant control conditions (such as aged donor into aged recipient), this result remains ambiguous. Given the findings from this thesis, there is rationale to approach this subject again.

6.1.2 Mitochondrial dysfunction

Mitochondrial dysregulation may also be present in aged Pro-B and Pre-B cells, since numerous mitochondrial genes were downregulated, irrespective of the ageing heterogeneity. In particular, *mt-Nd2* and *mt-Nd4* – components of the respiratory transport chain – were downregulated in all aged Pro-B and Pre-B cells (Mild, Moderate, and Severe aged subgroups), and so would suggest a reduced mitochondrial, and thus respiratory, output with age. Confirmation of this mitochondrial dysregulation in aged Pro-B and Pre-B cells should be further validated by measuring levels of reactive oxygen species (ROS) (by MitoSOX), mitochondrial mass (by MitoTracker), and oxidative phosphorylation and glycolysis potential (by Seahorse).

6.1.3 Downregulation of IGF1R signalling

It was hypothesised in this thesis that the downregulation of IGF1R signalling would be a hallmark of ageing progenitor B cells, irrespective of heterogeneity. Although the number of transcriptionally dysregulated IGF1R signalling components differed depending on cell type and aged subgroup, downregulation of IGF1R signalling was found in all aged mice. For instance, *Irs1* expression was downregulated in all aged Pro-B and Pre-B cell populations (Mild, Moderate, and Severe aged subgroups), whilst *Socs2* and *Igfbp4* were upregulated in all aged Pre-B cell populations (Mild, Moderate, and Severe) but not aged Pro-B cells, and *Igf1r* and *Grb2* were downregulated in two subsets of the aged Pre-B cell populations (Moderate and Severe). Therefore, a multi-layered downregulation of IGF1R signalling across the Pro-B to Pre-B cell transition is in effect in

ageing mice, irrespective of heterogeneity. In support of these findings, Irs1 and IGF1R have already been shown to have reduced protein expression levels in aged Pro-B and Pre-B cells[275], but further comparative protein expression should be carried out for the other transcriptionally dysregulated IGF1R signalling components described. To explore to what extent this downregulated IGF1R signalling contributes to other aged phenotypes reported – such as reductions in progenitor B cell numbers and/or deficient VDJ_H recombination – B-lineage conditional IGF1R/Irs1 knockout mice should be generated and phenotyped by flow cytometry and VDJseq.

Since IGF1R signalling has been shown to play a role in early B cell development, a novel in-vitro culture system was developed which differentiates lineage-depleted bone marrow cells into B cells in the presence of IGF1. Through this system, it has been possible to determine that, compared to young mice, aged progenitor B cells have a reduced ability to differentiate into IgM-expressing B cells. Thus, age-associated downregulation of IGF1R signalling appears to be contributing to the deficiency in aged progenitor B cell development. Confirmation of this finding can be achieved by culturing the previously-proposed B-lineage conditional IGF1R/Irs1 knockout mice in this system. If the hypothesis is correct, it would be anticipated that a similar reduction in IgM-expressing B cells to aged mice would be found.

6.1.4 Epigenetic alterations

Epigenetic alterations are another ageing hallmark that has been shown by *Koohy et al* in aged Pre-B cells[275]. Strikingly, many of their age-associated epigenetic alterations can be linked to the regulation of IGF1R signalling. For example, they showed an increase in the expression of miRNA's in aged Pre-B cells that target *Irs1* (*miR-221*, *miR-222*) and *Igf1r* (*Let-7f-2*) transcripts for degradation, as well as an enrichment of the suppressive histone mark H3K27me3 over the *Irs1* promoter. Both of these epigenetic mechanisms could be contributing to the observed downregulation in *Irs1* (and *Igf1r*) transcripts found by *Koohy et al,* and in this thesis. Furthermore, the combined deconvolution of aged transcriptomic heterogeneity and pairwise Pro-B and Pre-B cell comparisons performed in this thesis has revealed a skew in the expression of the H3K27 demethylase

JMJD3 (*Kdm6b*) and methyltransferase Ezh2 (*Ezh2*) in a subset of aged Pre-B cells (Moderate and Severe). Greater reductions in *Kdm6b* expression favours H3K27 methylation, and suggests and mechanism for the enrichment of H3K27me3 over genes, such as *Irs1*, in aged Pre-B cells.

Continuing with this hypothesis, the effects of blocking JMJD3 and Ezh2 in-vitro with small molecule inhibitors on the developmental outcome of young and aged progenitor B cells in the presence of IGF1 was explored. Theoretically, inhibiting JMJD3 would favour genome-wide H3K27 methylation, whilst Ezh2 inhibition would favour H3K27 demethylation. H3K27me3 over the Ig_K locus is known to suppress its recombination in normal B cell development[113] and H3K27me3 over the *Irs1* gene has been reported in aged progenitor B cells[275]. Moreover, aged B cells show greater susceptibility to JMJD3 inhibition in their ability to produce IgM-expressing cells, whilst also showing a trend towards increased IgM-expressing cells upon Ezh2 inhibition – consistent with the observed skew in JMJD3:Ezh2 expression found in aged Pre-B cells in-vivo.

These preliminary experiments, through a newly-developed in-vitro system, were an exploration into the mechanisms and dynamics of JMJD3 and Ezh2 function during young and aged B cell development. However, the global effects these inhibitors have on H3K27me3 levels means that no definitive conclusions can be drawn regarding the role of H3K27me3 in the downregulation of *Irs1* (and therefore IGF1R signalling) that could be driving the aged defect in B cell development. Instead, I provide a framework for future interrogative research that could explore the role of epigenetic alterations on B cell developmental defects. For instance, ChIPseq and RNAseq could be performed in parallel on young and aged B cells treated with the JMJD3/Ezh2 inhibitors to combine genome-wide H3K27me3 and transcriptomic changes, and provide a better understanding of which genes are epigenetically regulated during B cell development. More precisely, induction/removal of H3K27me3 at certain positions of the genome – such as at the *Irs1* promotor – could perhaps be achieved using novel CRISPR-based dCas9 epigenome editing techniques[390], although I anticipate this to be challenging with primary young and aged bone marrow cells. Moreover, anti-microRNA oligonucleotides (AMOs) such as locked nucleic acids (LNAs) could also be used in this in-vitro system to explore the role of miRNA's upregulated in aged progenitor B cells – such as *miR-221*, *miR-222* and *Let-7f-2*[391].

6.1.5 Inflammageing

The chronic and systemic inflammation associated with ageing – known as "inflammageing"[262] – appears to be another ageing hallmark influencing progenitor B cell development, as has been reported previously in the literature[345,392] and now in this thesis from the abundant transcriptional upregulation of several inflammatory pathways. Inflammageing is particularly associated with activation of the innate immune NLRP3 (NOD-, LRR- and pyrin domain-containing protein 3) inflammasome pathway which, amongst other functions, upregulates IL1B expression/activation in response to metabolic stress signals (such as ROS and mt-DNA), and is also primed by inflammatory mediators (such as TNFα)[393]. Though an innate immune pathway, mature B cells can activate the NLRP3 inflammasome[394], and transcriptional upregulation of Cathepsin S (*Ctss*), Caspase 1 (*Casp1*), and IL1B itself (*Il1b*) in a subset of aged Pre-B cells (Moderate and Severe aged subgroups) could represent an activated NLRP3 inflammasome.

It is likely that the inflammatory response detected in these aged Pre-B cells is derived from a combination of extracellular and intracellular signals. But, in line with the inflammaging literature, I propose one of the inflammatory responses to be the activation of the NLRP3 inflammasome in these aged Pre-B cells, brought about by intrinsic metabolic stress and an extrinsic inflammatory environment. Future experiments in this area therefore could include the detection of possible inflammatory mediators (such as TNFα and IL1B – by ELISA) and DAMPs (such as mt-DNA – by qPCR[228]) in the extracellular bone marrow of aged mice, as well as the measurement of cleaved Caspase 1 and/or IL1B protein (indicative of activated NLRP3 inflammasome – by western blot) in aged Pre-B cells.

6.1.6 Proposed model for the multi-layered downregulation of IGF1R signalling

Central to the aged deficiencies in progenitor B cell development is a robust multi-layered downregulation of IGF1R signalling in aged Pre-B cells (and to a lesser extent Pro-B cells), at the stage at which it is required for differentiation (Figure 6-1). At the transcript-level, there is downregulation of *Igf1r*, as well as its adaptor proteins *Irs1* and *Grb2* (reduced protein levels also confirmed for IGF1R and Irs1). This could be regulated by epigenetic alterations at the chromatin- (e.g. H3K27me3 over the *Irs1* promoter) and post-transcriptional level (e.g. *miR-221*, *miR-222* and *Let-7f-2* for *Irs1* and *Igf1r*). Additionally, upregulated expression of the IGF1-binding protein IGFBP4 in aged Pre-B cells may inhibit IGF1 binding to its cognate IGF1R[395,305], whilst upregulation of the negative regulator Socs2 may lead to inhibition of IGF1R at its intracellular binding domains[302,303], thus resulting in suppressions at the protein-level. Moreover, cross-talk between other key receptor signalling pathways IL7R and preBCR across the Pro-B and Pre-B cell stages could mean that suppressive elements in aged progenitor B cells permeate into these other pathways. For example, Socs2 also suppresses STAT5 signalling downstream of IL7R[159], whilst reduced Grb2 would downregulate preBCR signalling via RAS/ERK[124].

It is tempting to suggest a contributory role for inflammageing in the deficiencies associated with ageing progenitor B cell development, perhaps even in the downregulation of IGF1R signalling itself. Several inflammatory pathways, including IL1B, utilise AKT signalling to determine their effector responses[396], and this thesis demonstrated a transcriptional upregulation in the AKT signalling pathway. Overstimulation of AKT signalling can result in a direct negative feedback inactivation (and subsequent degradation) of Irs1 protein via mTORC1 and the S6K kinase[330,331]. AKT activation is marked by phosphorylation at Thr308 and Ser473 of Akt1, and Irs1 inactivation by the phosphorylation of Ser636/639 (by mTORC1) and Ser270/307/636/1001 (by S6K)[397]. Therefore, to test this theory, levels of AKT and Irs1 phosphorylation at these specific sites should be measured in aged Pre-B cells.

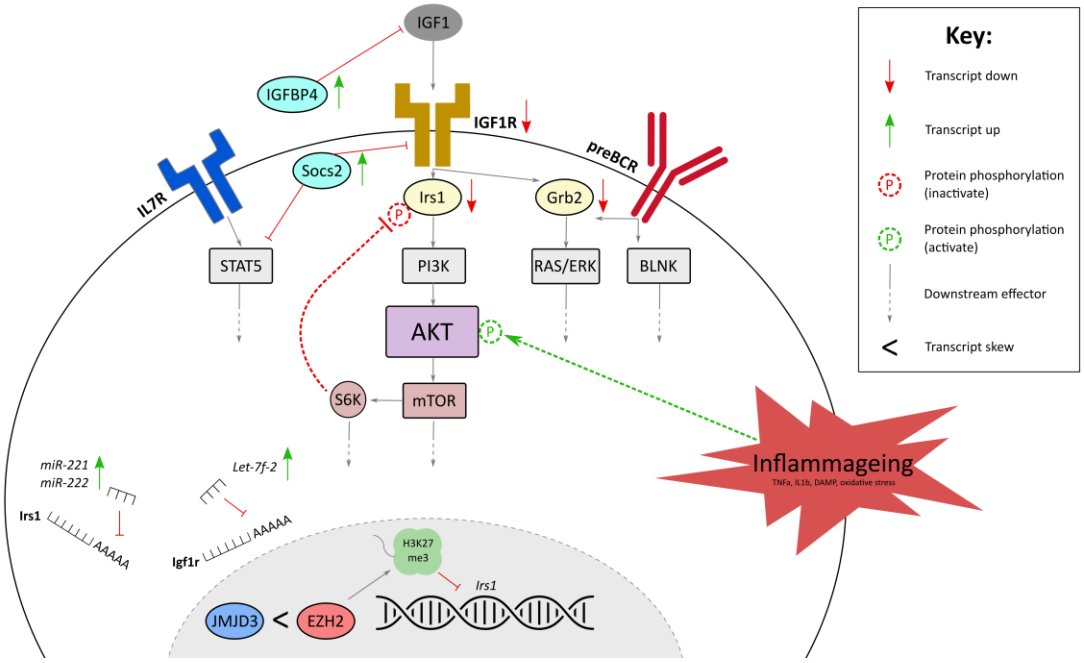

Figure 6-1: Multi-layered suppression of IGF1R signalling in aged Pre-B cells. ***Chromatin:*** *Koohy et al show enriched H3K27me3 at Irs1 gene*[275]*. This thesis also shows transcript skew in JMJD3<EZH2 expression in favour of H3K27 methyltransferase (Figure 3-12).* ***miRNA:*** *Koohy et al show upregulation of miRNAs which target Irs1 (miR-221, miR-222) and Igf1r (Let-7f-2) transcripts for degradation (Figure 3-6).* ***Gene expression:*** *Reduced transcript levels for Igf1r, Irs1, and Grb2 (Figure 3-5 and Figure 3-6).* ***Protein inhibition:*** *Increased transcript levels for IGFBP4 (sequester IGF1) and Socs2 (suppress IGF1R and IL7R) (Figure 3-5).* ***AKT overstimulation?:*** *GSEA show upregulated transcripts for AKT signalling (Figure 3-6), perhaps through inflammageing (Figure 3-10), that could result in negative feedback inacativation of Irs1 protein by mTOR/S6K.*

6.2 Human translation

Human experiments from this thesis have thus revealed strikingly similar ageing hallmark signatures in their progenitor B cells to those found in mice. For instance, aged human progenitor B cells showed reduced ability to propagate in-vitro, whilst at the transcript level also had reduced expression of mitochondrial genes (including *MT-ND2* and *MT-ND4*), *IGF1R*, and *KDM6B* (JMJD3). Progressing this human work in parallel to advancing our murine understandings of ageing progenitor B cell development could therefore be of clinical importance. Initial focus should be on improving the literature's phenotyping of young and aged bone marrow B cell population's in-vivo – either by flow

cytometry or single-cell transcriptomics – to better resolve any aged differences. Following this, more detailed transcriptomic and protein analysis should be carried out on young and aged progenitor B cells in continuation of the progress made in this thesis. A limitation to human studies however is the availability of samples, so a compromise could be to expand human B cells in-vitro with IL7 to acquire sufficient sample to achieve this work.

Human B cell repertoires were not explored in this thesis, but others have shown mild alterations to the frequency of V_H gene family usage in aged circulating mature naïve and transitional B cells, and increases in CDR3 length with age[255,358]. Through this thesis, aged murine Pre-B cells show a reduction in VDJ_H:DJ_H read ratio, and a geographical skew in V-gene usage across the Ig_H locus, with a greater representation of 3' V-genes and a reduction in 5' V-genes. It would therefore be interesting to speculate whether human Pre-B cells show a similar phenotype, and thus could be an area of future research.

6.3 Concluding remarks

Aged murine progenitor B cells present with intrinsic cellular deficiencies that are indicative of ageing biology. These ageing effects have detrimental consequences to early B cell development that result in sub-optimal cellular output and reduced immunoglobulin diversity. If translatable to humans, these murine insights could provide a clinical angle for treating and protecting our elderly population: by managing potential causes (inflammageing) and side-effects (downregulated IGF1R signalling) of ageing inflicted upon progenitor B cells.

Age-related immune dysfunction leaves the elderly members of society susceptible to disease and infections. It also results in a marked reduction in vaccine efficacy, with only 17-53% of patients over the age of 60 mounting immune protection to influenza after vaccination[249], further exacerbating their vulnerable status. The work presented in this thesis could therefore provide viable treatment options for elderly patients, particularly in the context of vaccine therapy. Temporary restoration of the IGF1R signalling lost in these elderly patients during a vaccine treatment could recover some of their B cell

development/function, which could in turn lead to improved vaccine efficacy. Therefore, therapeutic intervention with IGF1 analogues (such as Mecasermin) may compensate for the known reductions in endogenous circulating IGF1[232,233]. Alternatively inhibiting IGFBP4, either antagonistically with small molecules or by proteolysis with its protease Pappalysin-1, could reconstitute the endogenous levels of IGF1.

Human lifespan is increasing[398], so it is of public health importance that healthspan reciprocates. As the world currently battles the COVID-19 pandemic, a disease which disproportionately affects the elderly (according to data taken from the Office of National Statistics in June 2020, 90% of deaths in the UK have been people aged 65 or over), solutions to the ageing health problem have never been more relevant. With this in mind, our global efforts to develop a vaccine against COVID-19 will need to find ways of improving its efficacy in the elderly – and targeting IGF1R signalling could be an option.

7 REFERENCES

1. Germain RN. T-cell development and the CD4–CD8 lineage decision. *Nat Rev Immunol Publ online 01 May 2002; | doi101038/nri798*. 2002;2(5):309. doi:10.1038/nri798

2. Charles A Janeway J, Travers P, Walport M, Shlomchik MJ. Macrophage activation by armed CD4 TH1 cells. *Immunobiol Immune Syst Heal Dis 5th Ed*. 2001. https://www.ncbi.nlm.nih.gov/books/NBK27153/. Accessed June 21, 2017.

3. Charles A Janeway J, Travers P, Walport M, Shlomchik MJ. Immunobiology: The Immune System in Health and Disease. 5th edition. In: Vol 81. 5th ed. Garland Science; 2015:1-17. https://www.ncbi.nlm.nih.gov/books/NBK27142/. Accessed June 29, 2020.

4. Shevyrev D, Tereshchenko V. Treg Heterogeneity, Function, and Homeostasis. *Front Immunol*. 2020;10:3100. doi:10.3389/fimmu.2019.03100

5. van der Leun AM, Thommen DS, Schumacher TN. CD8+ T cell states in human cancer: insights from single-cell analysis. *Nat Rev Cancer*. 2020;20(4):218-232. doi:10.1038/s41568-019-0235-4

6. Schmidt ME, Varga SM. The CD8 T cell response to respiratory virus infections. *Front Immunol*. 2018;9(APR):678. doi:10.3389/fimmu.2018.00678

7. Carsetti R. The development of B cells in the bone marrow is controlled by the balance between cell-autonomous mechanisms and signals from the microenvironment. *J Exp Med*. 2000;191(1):5-8. http://www.ncbi.nlm.nih.gov/pubmed/10620600. Accessed June 21, 2017.

8. Osmond DG, Rolink A, Melchers F. Murine B lymphopoiesis: Towards a unified model. *Immunol Today*. 1998;19(2):65-68. doi:10.1016/S0167-5699(97)01203-6

9. Rolink AG, Andersson J, Melchers F. Molecular mechanisms guiding late stages of B-cell development. *Immunol Rev*. 2004;197(1):41-50. doi:10.1111/j.0105-2896.2004.0101.x

10. Charles A Janeway J, Travers P, Walport M, Shlomchik MJ. *B - Cell Activation by Armed Helper T Cells*. Vol 81. Garland Science; 2015. https://www.ncbi.nlm.nih.gov/books/NBK27142/. Accessed June 29, 2020.

11. Coutinho A, Möller G. Thymus-Independent B-Cell Induction and Paralysis. *Adv Immunol*. 1975;21(C):113-236. doi:10.1016/S0065-2776(08)60220-5

12. Bottomly K, Tite JP, Jones B, et al. Control of B Cell Activation by Helper T Cells. In: *The Molecular Basis of B-Cell Differentiation and Function*. Vol 81. Garland Science; 1986:83-94. doi:10.1007/978-1-4684-7035-2_13

13. Miyazaki K, Miyazaki M, Murre C. The establishment of B versus T cell identity. *Trends Immunol*. 2014;35(5):205-210. http://www.cell.com/article/S1471490614000374/fulltext. Accessed September 18, 2014.

14. Schroeder HW, Cavacini L, Cavacini L. Structure and function of immunoglobulins. *J Allergy Clin Immunol*. 2010;125(2 Suppl 2):S41-52. doi:10.1016/j.jaci.2009.09.046

15. Tiselius A, Kabat EA. AN ELECTROPHORETIC STUDY OF IMMUNE SERA AND PURIFIED ANTIBODY PREPARATIONS. *J Exp Med*. 1939;69(1):119-131. http://www.ncbi.nlm.nih.gov/pubmed/19870831. Accessed June 21, 2017.

16. Kirkham PM, Schroeder HW. Antibody structure and the evolution of immunoglobulin V gene segments. *Semin Immunol*. 1994;6(6):347-360. doi:10.1006/smim.1994.1045

17. Georgiou G, Ippolito GC, Beausang J, Busse CE, Wardemann H, Quake SR. The promise and challenge of high-throughput sequencing of the antibody repertoire. *Nat Biotechnol*. 2014;32(2):158-168. doi:10.1038/nbt.2782

18. Kerr WG, Hendershot LM, Burrows PD. Regulation of IgM and IgD expression in human B-lineage cells. *J Immunol*. 1991;146(10):3314-3321.

19. Chen K, Cerutti A. The function and regulation of immunoglobulin D. *Curr Opin Immunol*. 2011;23(3):345-352. doi:10.1016/j.coi.2011.01.006

20. Li YS, Wasserman R, Hayakawa K, Hardy RR. Identification of the earliest B lineage stage in mouse bone marrow. *Immunity*. 1996;5(6):527-535. doi:10.1016/S1074-

7613(00)80268-X

21. Rolink A, Ten Boekel E, Melchers F, Fearon DT, Krop I, Andersson J. A subpopulation of B220+ cells in murine bone marrow does not express CD19 and contains natural killer cell progenitors. *J Exp Med*. 1996;183(1):187-194. doi:10.1084/jem.183.1.187

22. Hardy RR, Kincade PW, Dorshkind K. The Protean Nature of Cells in the B Lymphocyte Lineage. *Immunity*. 2007;26(6):703-714. doi:10.1016/j.immuni.2007.05.013

23. Allman D, Lindsley RC, DeMuth W, Rudd K, Shinton SA, Hardy RR. Resolution of Three Nonproliferative Immature Splenic B Cell Subsets Reveals Multiple Selection Points During Peripheral B Cell Maturation. *J Immunol*. 2001;167(12):6834-6840. doi:10.4049/jimmunol.167.12.6834

24. Loder F, Mutschler B, Ray RJ, et al. B cell development in the spleen takes place in discrete steps and is determined by the quality of B cell receptor-derived signals. *J Exp Med*. 1999;190(1):75-89. doi:10.1084/jem.190.1.75

25. Shlomchik MJ, Weisel F. Germinal center selection and the development of memory B and plasma cells. *Immunol Rev*. 2012;247(1):52-63. doi:10.1111/j.1600-065X.2012.01124.x

26. Martin F, Kearney JF. Marginal-zone B cells. *Nat Rev Immunol*. 2002;2(5):323-335. doi:10.1038/nri799

27. Hayakawa K, Hardy RR, Herzenberg LA, Herzenberg LA. Progenitors for Ly-1 b cells are distinct from progenitors for other b cells. *J Exp Med*. 1985;161(6):1554-1568. doi:10.1084/jem.161.6.1554

28. Baumgarth N. The double life of a B-1 cell: Self-reactivity selects for protective effector functions. *Nat Rev Immunol*. 2011;11(1):34-46. doi:10.1038/nri2901

29. Johnston CM, Wood AL, Bolland DJ, Corcoran AE. Complete Sequence Assembly and Characterization of the C57BL/6 Mouse Ig Heavy Chain V Region. *J Immunol Ref*. 2016;176:4221-4234. doi:10.4049/jimmunol.176.7.4221

30. Johnston CM, Wood AL, Bolland DJ, Corcoran AE. Complete Sequence Assembly and Characterization of the C57BL/6 Mouse Ig Heavy Chain V Region. *J Immunol*

Ref. 2016;176:4221-4234. doi:10.4049/jimmunol.176.7.4221

31. Kirkham PM, Mortari F, Newton JA, Schroeder HW. Immunoglobulin VH clan and family identity predicts variable domain structure and may influence antigen binding. *EMBO J*. 1992;11(2):603-609. http://www.ncbi.nlm.nih.gov/pubmed/1537339. Accessed July 12, 2017.

32. Woloschak GE, Krco CJ. Regulation of kappa/lambda immunoglobulin light chain expression in normal murine lymphocytes. *Mol Immunol*. 1987;24(7):751-757. http://www.ncbi.nlm.nih.gov/pubmed/3116408. Accessed June 21, 2017.

33. Blomberg B, Traunecker A, Eisent H, Tonegawa S. Organization of four mouse A light chain immunoglobulin genes. *Genetics*. 1981;78(6):3765-3769. http://www.pnas.org/content/78/6/3765.full.pdf. Accessed June 21, 2017.

34. Ye J. The immunoglobulin IGHD gene locus in C57BL/6 mice. *Immunogenetics*. 2004;56(6):399-404. doi:10.1007/s00251-004-0712-z

35. Eastman QM, Leu TMJ, Schatz DG. Initiation of V(D)J recombination in vitro obeying the 12/23 rule. *Nature*. 1996;380(6569):85-88. doi:10.1038/380085a0

36. Rose DR. The generation of antibody diversity. *Am J Hematol*. 1982;13(1):91-99. doi:10.1002/ajh.2830130111

37. Manis JP, Tian M, Alt FW. Mechanism and control of class-switch recombination. *Trends Immunol*. 2002;23(1):31-39. doi:10.1016/S1471-4906(01)02111-1

38. Koipally J, Renold A, Kim J, Georgopoulos K. Repression by Ikaros and Aiolos is mediated through histone deacetylase complexes. *EMBO J*. 1999;18(11):3090-3100. doi:10.1093/emboj/18.11.3090

39. Yoshida T, Yao-Ming Ng S, Zuniga-Pflucker JC, Georgopoulos K. Early hematopoietic lineage restrictions directed by Ikaros. *Nat Immunol*. 2006;7(4):382-391. doi:10.1038/ni1314

40. Sellars M. Ikaros in B cell development and function. *World J Biol Chem*. 2011;2(6):132. doi:10.4331/wjbc.v2.i6.132

41. Reynaud D, Demarco IA, Reddy KL, et al. Regulation of B cell fate commitment and immunoglobulin heavy-chain gene rearrangements by Ikaros. *Nat Immunol*.

2008;9(8):927-936. doi:10.1038/ni.1626

42. Brown KE, Guest SS, Smale ST, Hahm K, Merkenschlager M, Fisher AG. Association of transcriptionally silent genes with Ikaros complexes at centromeric heterochromatin. *Cell*. 1997;91(6):845-854. doi:10.1016/S0092-8674(00)80472-9

43. Ma S, Pathak S, Trinh L, Lu R. Interferon regulatory factors 4 and 8 induce the expression of Ikaros and Aiolos to down-regulate pre-B-cell receptor and promote cell-cycle withdrawal in pre-B-cell development. *Blood*. 2008;111(3):1396-1403. doi:10.1182/blood-2007-08-110106

44. DeKoter RP, Singh H. Regulation of B lymphocyte and macrophage development by graded expression of PU.1. *Science (80-)*. 2000;288(5470):1439-1442. doi:10.1126/science.288.5470.1439

45. DeKoter RP, Schweitzer BL, Kamath MB, et al. Regulation of the interleukin-7 receptor α promoter by the Ets transcription factors PU.1 and GA-binding protein in developing B cells. *J Biol Chem*. 2007;282(19):14194-14204. doi:10.1074/jbc.M700377200

46. Lu D, Nakagawa R, Lazzaro S, et al. The miR-155-PU.1 axis acts on Pax5 to enable efficient terminal B cell differentiation. *J Exp Med*. 2014;211(11):2183-2198. doi:10.1084/jem.20140338

47. Eisenbeis CF, Singh H, Storb U. PU.1 is a component of a multiprotein complex which binds an essential site in the murine immunoglobulin lambda 2-4 enhancer. *Mol Cell Biol*. 1993;13(10):6452-6461. doi:10.1128/MCB.13.10.6452.Updated

48. Batista CR, Li SKH, Xu LS, Solomon LA, DeKoter RP. PU.1 Regulates Ig Light Chain Transcription and Rearrangement in Pre-B Cells during B Cell Development. *J Immunol*. 2017;198(4):1565-1574. doi:10.4049/jimmunol.1601709

49. Murre C, McCaw PS, Baltimore D. A new DNA binding and dimerization motif in immunoglobulin enhancer binding, daughterless, MyoD, and myc proteins. *Cell*. 1989;56(5):777-783. doi:10.1016/0092-8674(89)90682-X

50. Bain G, Maandag ECR, Izon DJ, et al. E2A proteins are required for proper B cell development and initiation of immunoglobulin gene rearrangements. *Cell*. 1994;79(5):885-892. doi:10.1016/0092-8674(94)90077-9

51. Greenbaum S, Lazorchak AS, Zhuang Y. Differential functions for the transcription factor E2A in positive and negative gene regulation in pre-B lymphocytes. *J Biol Chem*. 2004;279(43):45028-45035. doi:10.1074/jbc.M400061200

52. Ungerbäck J, Åhsberg J, Strid T, Somasundaram R, Sigvardsson M. Combined heterozygous loss of Ebf1 and Pax5 allows for T-lineage conversion of B cell progenitors. *J Exp Med*. 2015;212(7):1109-1123. doi:10.1084/jem.20132100

53. Jiang XX, Nguyen Q, Chou YC, et al. Control of B Cell Development by the Histone H2A Deubiquitinase MYSM1. *Immunity*. 2011;35(6):883-896. doi:10.1016/j.immuni.2011.11.010

54. Roessler S, Györy I, Imhof S, et al. Distinct Promoters Mediate the Regulation of Ebf1 Gene Expression by Interleukin-7 and Pax5. *Mol Cell Biol*. 2007;27(2):579-594. doi:10.1128/mcb.01192-06

55. Nutt SL, Heavey B, Rolink AG, Busslinger M. Commitment to the B-lymphoid lineage depends on the transcription factor Pax5. *J Immunol*. 2015;195(3):766-772. doi:10.1038/44076

56. Lin H, Grosschedl R. Failure of B–cell differentiation in mice lacking the transcription factor EBF. *Nature*. 1995;376(6537):263-267. doi:10.1038/376263a0

57. Rolink AG, Nutt SL, Melchers F, Busslinger M. Long-term in vivo reconstitution of T-cell development by Pax5-deficient B-cell progenitors. *Nature*. 1999;401(6753):603-606. doi:10.1038/44164

58. Zandi S, Mansson R, Tsapogas P, Zetterblad J, Bryder D, Sigvardsson M. EBF1 Is Essential for B-Lineage Priming and Establishment of a Transcription Factor Network in Common Lymphoid Progenitors. *J Immunol*. 2008;181(5):3364-3372. doi:10.4049/jimmunol.181.5.3364

59. Nutt SL, Heavey B, Rolink AG, Busslinger M. Commitment to the B-lymphoid lineage depends on the transcription factor Pax5. *J Immunol*. 2015;195(3):766-772. doi:10.1038/44076

60. Souabni A, Cobaleda C, Schebesta M, Busslinger M. Pax5 promotes B lymphopoiesis and blocks T cell development by repressing Notch1. *Immunity*.

2002;17(6):781-793. doi:10.1016/S1074-7613(02)00472-7

61. Ebert A, McManus S, Tagoh H, et al. The Distal VH Gene Cluster of the Igh Locus Contains Distinct Regulatory Elements with Pax5 Transcription Factor-Dependent Activity in Pro-B Cells. *Immunity*. 2011;34(2):175-187. doi:10.1016/j.immuni.2011.02.005

62. Sun B, Mallampati S, Gong Y, Wang D, Lefebvre V, Sun X. Sox4 Is Required for the Survival of Pro-B Cells. *J Immunol*. 2013;190(5):2080-2089. doi:10.4049/jimmunol.1202736

63. Reya T, O'Riordan M, Okamura R, et al. Wnt signaling regulates B lymphocyte proliferation through a LEF-1 dependent mechanism. *Immunity*. 2000;13(1):15-24. doi:10.1016/S1074-7613(00)00004-2

64. Aurrand-Lions M, Mancini SJC. Murine bone marrow niches from hematopoietic stem cells to B cells. *Int J Mol Sci*. 2018;19(8). doi:10.3390/ijms19082353

65. Itkin T, Gur-Cohen S, Spencer JA, et al. Distinct bone marrow blood vessels differentially regulate haematopoiesis. *Nature*. 2016;532(7599):323-328. doi:10.1038/nature17624

66. Kusumbe AP, Ramasamy SK, Adams RH. Coupling of angiogenesis and osteogenesis by a specific vessel subtype in bone. *Nature*. 2014;507(7492):323-328. doi:10.1038/nature13145

67. Yu VWC, Lymperi S, Oki T, et al. Distinctive Mesenchymal-Parenchymal Cell Pairings Govern B Cell Differentiation in the Bone Marrow. *Stem Cell Reports*. 2016;7(2):220-235. doi:10.1016/j.stemcr.2016.06.009

68. Kunisaki Y, Bruns I, Scheiermann C, et al. Arteriolar niches maintain haematopoietic stem cell quiescence. *Nature*. 2013;502(7473):637-643. doi:10.1038/nature12612

69. Egawa T, Kawabata K, Kawamoto H, et al. The earliest stages of B cell development require a chemokine stromal cell-derived factor/pre-B cell growth-stimulating factor. *Immunity*. 2001;15(2):323-334. doi:10.1016/S1074-7613(01)00185-6

70. Peschon JJ, Morrissey PJ, Grabstein KH, et al. Early Lymphocyte Expansion Is

Severely Impaired in Interleukin 7 Receptor-deficient Mice. *J Exp Med*. 1994;180(5):1955-1960. doi:10.1084/jem.180.5.1955

71. Dias S, Silva H, Cumano A, Vieira P. Interleukin-7 is necessary to maintain the B cell potential in common lymphoid progenitors. *J Exp Med*. 2005;201(6):971-979. doi:10.1084/jem.20042393

72. Sitnicka E, Brakebusch C, Martensson IL, et al. Complementary Signaling through flt3 and Interleukin-7 Receptor α Is Indispensable for Fetal and Adult B Cell Genesis. *J Exp Med*. 2003;198(10):1495-1506. doi:10.1084/jem.20031152

73. Kong YY, Yoshida H, Sarosi I, et al. OPGL is a key regulator of osteoclastogenesis, lymphocyte development and lymph-node organogenesis. *Nature*. 1999;397(6717):315-323. doi:10.1038/16852

74. Yu VWC, Lymperi S, Oki T, et al. Distinctive Mesenchymal-Parenchymal Cell Pairings Govern B Cell Differentiation in the Bone Marrow. *Stem Cell Reports*. 2016;7(2):220-235. doi:10.1016/j.stemcr.2016.06.009

75. Waskow C, Paul S, Haller C, Gassmann M, Rodewald HR. Viable c-KitW/W mutants reveal pivotal role for c-Kit in the maintenance of lymphopoiesis. *Immunity*. 2002;17(3):277-288. doi:10.1016/S1074-7613(02)00386-2

76. Perlot T, Penninger JM. Development and Function of Murine B Cells Lacking RANK. *J Immunol*. 2012;188(3):1201-1205. doi:10.4049/jimmunol.1102063

77. Mandal M, Okoreeh MK, Kennedy DE, et al. CXCR4 signaling directs Igk recombination and the molecular mechanisms of late B lymphopoiesis. *Nat Immunol*. 2019;20(10):1393-1403. doi:10.1038/s41590-019-0468-0

78. Johnson K, Hashimshony T, Sawai CM, et al. Regulation of Immunoglobulin Light-Chain Recombination by the Transcription Factor IRF-4 and the Attenuation of Interleukin-7 Signaling. *Immunity*. 2008;28(3):335-345. doi:10.1016/j.immuni.2007.12.019

79. Tokoyoda K, Egawa T, Sugiyama T, Choi B Il, Nagasawa T. Cellular niches controlling B lymphocyte behavior within bone marrow during development. *Immunity*. 2004;20(6):707-718. doi:10.1016/j.immuni.2004.05.001

80. Fistonich C, Zehentmeier S, Bednarski JJ, et al. Cell circuits between B cell

progenitors and IL-7+ mesenchymal progenitor cells control B cell development. *J Exp Med*. 2018;215(10):2586-2599. doi:10.1084/jem.20180778

81. Zehentmeier S, Pereira JP. Cell circuits and niches controlling B cell development. *Immunol Rev*. 2019;289(1):142-157. doi:10.1111/imr.12749

82. Taichman RS, Emerson SG. Human osteoblasts support hematopoiesis through the production of granulocyte colony-stimulating factor. *J Exp Med*. 1994;179(5):1677-1682. doi:10.1084/jem.179.5.1677

83. Youssef A, Aboalola D, Han VKM. The roles of insulin-like growth factors in mesenchymal stem cell niche. *Stem Cells Int*. 2017;2017:9453108. doi:10.1155/2017/9453108

84. Landreth K, Narayanan R, Dorshkind K. Insulin-like growth factor-I regulates pro-B cell differentiation. *Blood*. 1992;80(5). http://www.bloodjournal.org/content/80/5/1207.long?sso-checked=true. Accessed July 13, 2017.

85. Nagasawa T. Microenvironmental niches in the bone marrow required for B-cell development. *Nat Rev Immunol*. 2006;6(2):107-116. doi:10.1038/nri1780

86. Hewitt SL, Yin B, Ji Y, et al. RAG-1 and ATM coordinate monoallelic recombination and nuclear positioning of immunoglobulin loci. *Nat Immunol*. 2009;10(6):655-664. doi:10.1038/ni.1735

87. Hewitt SL, Farmer D, Marszalek K, et al. Association between the Igk and Igh immunoglobulin loci mediated by the 3' Igk enhancer induces "decontraction" of the Igh locus in pre-B cells. *Nat Immunol*. 2008;9(4):396-404. doi:10.1038/ni1567

88. Mostoslavsky R, Singh N, Tenzen T, et al. Asynchronous replication and allelic exclusion in the immune system. *Nature*. 2001;414(6860):221-225. doi:10.1038/35102606

89. Alt FW, Yancopoulos GD, Blackwell TK, et al. Ordered rearrangement of immunoglobulin heavy chain variable region segments. *EMBO J*. 1984;3(6):1209-1219. doi:10.1002/j.1460-2075.1984.tb01955.x

90. Mårtensson I-L, Almqvist N, Grimsholm O, Bernardi AI. The pre-B cell receptor checkpoint. *FEBS Lett*. 2010;584(12):2572-2579.

doi:10.1016/j.febslet.2010.04.057

91. Nemazee D. Receptor editing in lymphocyte development and central tolerance. *Nat Rev Immunol*. 2006;6(10):728-740. doi:10.1038/nri1939

92. Melchers F. The pre-B-cell receptor: selector of fitting immunoglobulin heavy chains for the B-cell repertoire. *Nat Rev Immunol*. 2005;5(7):578-584. doi:10.1038/nri1649

93. Rolink AG, Andersson J, Melchers F. Molecular mechanisms guiding late stages of B-cell development. *Immunol Rev*. 2004;197(1):41-50. doi:10.1111/j.0105-2896.2004.0101.x

94. Allman D, Lindsley RC, DeMuth W, Rudd K, Shinton SA, Hardy RR. Resolution of Three Nonproliferative Immature Splenic B Cell Subsets Reveals Multiple Selection Points During Peripheral B Cell Maturation. *J Immunol*. 2001;167(12):6834-6840. doi:10.4049/jimmunol.167.12.6834

95. Pelanda R, Torres RM. Central B-cell tolerance: where selection begins. *Cold Spring Harb Perspect Biol*. 2012;4(4):a007146-a007146. doi:10.1101/cshperspect.a007146

96. McElroy CA, Holland PJ, Zhao P, et al. Structural reorganization of the interleukin-7 signaling complex. *Proc Natl Acad Sci U S A*. 2012;109(7):2503-2508. doi:10.1073/pnas.1116582109

97. Noguchi M, Nakamura Y, Russell SM, et al. Interleukin-2 receptor γ chain: A functional component of the interleukin-7 receptor. *Science (80-)*. 1993;262(5141):1877-1880. doi:10.1126/science.8266077

98. O'Shea JJ, Plenge R. JAK and STAT Signaling Molecules in Immunoregulation and Immune-Mediated Disease. *Immunity*. 2012;36(4):542-550. doi:10.1016/j.immuni.2012.03.014

99. Corfe SA, Paige CJ. The many roles of IL-7 in B cell development; Mediator of survival, proliferation and differentiation. *Semin Immunol*. 2012;24(3):198-208. doi:10.1016/j.smim.2012.02.001

100. Corcoran AE, Smart FM, Cowling RJ, Crompton T, Owen MJ, Venkitaraman AR. The interleukin-7 receptor alpha chain transmits distinct signals for proliferation and

differentiation during B lymphopoiesis. *EMBO J*. 1996;15(8):1924-1932. http://www.ncbi.nlm.nih.gov/pubmed/8617239. Accessed June 30, 2020.

101. Yu M, Chen Y, Zeng H, et al. PLCγ-dependent mTOR signalling controls IL-7-mediated early B cell development. *Nat Commun*. 2017;8(1):1-18. doi:10.1038/s41467-017-01388-5

102. Corcoran AE, Riddell A, Krooshoop D, Venkitaraman AR. Impaired immunoglobulin gene rearrangement in mice lacking the IL-7 receptor. *Nature*. 1998;391(6670):904-907. doi:10.1038/36122

103. Kikuchi K, Lai AY, Hsu CL, Kondo M. IL-7 receptor signaling is necessary for stage transition in adult B cell development through up-regulation of EBF. *J Exp Med*. 2005;201(8):1197-1203. doi:10.1084/jem.20050158

104. Yao Z, Cui Y, Watford WT, et al. Stat5a/b are essential for normal lymphoid development and differentiation. *Proc Natl Acad Sci U S A*. 2006;103(4):1000-1005. doi:10.1073/pnas.0507350103

105. Dai X, Chen Y, Di L, et al. Stat5 Is Essential for Early B Cell Development but Not for B Cell Maturation and Function. *J Immunol*. 2007;179(2):1068-1079. doi:10.4049/jimmunol.179.2.1068

106. Ramadani F, Bolland DJ, Garcon F, et al. The PI3K isoforms p110α and p110δ are essential for pre-B cell receptor signaling and B cell development. *Sci Signal*. 2010;3(134):ra60. doi:10.1126/scisignal.2001104

107. Cooper AB, Sawai CM, Sicinska E, et al. A unique function for cyclin D3 in early B cell development. *Nat Immunol*. 2006;7(5):489-497. doi:10.1038/ni1324

108. Essafi A, Fernández De Mattos S, Hassen YAM, et al. Direct transcriptional regulation of Bim by FoxO3a mediates STI571-induced apoptosis in Bcr-Abl-expressing cells. *Oncogene*. 2005;24(14):2317-2329. doi:10.1038/sj.onc.1208421

109. Malin S, McManus S, Cobaleda C, et al. Role of STAT5 in controlling cell survival and immunoglobulin gene recombination during pro-B cell development. *Nat Immunol*. 2010;11(2):171-179. doi:10.1038/ni.1827

110. Jiang Q, Li WQ, Hofmeister RR, et al. Distinct Regions of the Interleukin-7 Receptor Regulate Different Bcl2 Family Members. *Mol Cell Biol*. 2004;24(14):6501-6513.

doi:10.1128/mcb.24.14.6501-6513.2004

111. Wofford JA, Wieman HL, Jacobs SR, Zhao Y, Rathmell JC. IL-7 promotes Glut1 trafficking and glucose uptake via STAT5-mediated activation of Akt to support T-cell survival. *Blood*. 2008;111(4):2101-2111. doi:10.1182/blood-2007-06-096297

112. Zeng H, Yu M, Tan H, et al. Discrete roles and bifurcation of PTEN signaling and mTORC1-mediated anabolic metabolism underlie IL-7-driven B lymphopoiesis. *Sci Adv*. 2018;4(1). doi:10.1126/sciadv.aar5701

113. Mandal M, Powers SE, Maienschein-Cline M, et al. Epigenetic repression of the Igk locus by STAT5-mediated recruitment of the histone methyltransferase Ezh2. *Nat Immunol*. 2011;12(12):1212-1220. doi:10.1038/ni.2136

114. Clark MR, Mandal M, Ochiai K, Singh H. Orchestrating B cell lymphopoiesis through interplay of IL-7 receptor and pre-B cell receptor signalling. *Nat Rev Immunol*. 2014;14(2):69-80. doi:10.1038/nri3570

115. Karasuyama H, Kudo A, Melchers F. The proteins encoded by the VpreB and λ5 Pre-B cell-specific genes can associate with each other and with μ heavy chain. *J Exp Med*. 1990;172(3):969-972. doi:10.1084/jem.172.3.969

116. Pelanda R, Braun U, Hobeika E, Nussenzweig MC, Reth M. B Cell Progenitors Are Arrested in Maturation but Have Intact VDJ Recombination in the Absence of Ig-α and Ig-β. *J Immunol*. 2002;169(2):865-872. doi:10.4049/jimmunol.169.2.865

117. Shinkai Y, Rathbun 0Gary, Lam KP, et al. RAG-2-deficient mice lack mature lymphocytes owing to inability to initiate V(D)J rearrangement. *Cell*. 1992;68(5):855-867. doi:10.1016/0092-8674(92)90029-C

118. Spanopoulou E, Roman CAJ, Corcoran LM, et al. Functional immunoglobulin transgenes guide ordered B-cell differentiation in Rag-1-deficient mice. *Genes Dev*. 1994;8(9):1030-1042. doi:10.1101/gad.8.9.1030

119. Rolink A, Grawunder U, Winkler TH, Karasuyama H, Melchers F. IL-2 receptor α chain (CD25JAC) expression defines a crucial stage in pre-B cell development. *Int Immunol*. 1994;6(8):1257-1264. doi:10.1093/intimm/6.8.1257

120. Shimizu T, Mundt C, Licence S, Melchers F, Mårtensson I-L. VpreB1/VpreB2/λ5 Triple-Deficient Mice Show Impaired B Cell Development but Functional Allelic

Exclusion of the IgH Locus. *J Immunol*. 2002;168(12):6286-6293. doi:10.4049/jimmunol.168.12.6286

121. Keenan RA, De Riva A, Corleis B, et al. Censoring of autoreactive B cell development by the pre-B cell receptor. *Science (80-)*. 2008;321(5889):696-699. doi:10.1126/science.1157533

122. Erlandsson L, Licence S, Gaspal F, Lane P, Corcoran AE, Mårtensson IL. Both the pre-BCR and the IL-7Rα are essential for expansion at the pre-BII cell stage in vivo. *Eur J Immunol*. 2005;35(6):1969-1976. doi:10.1002/eji.200425821

123. Ochiai K, Maienschein-Cline M, Mandal M, et al. A self-reinforcing regulatory network triggered by limiting IL-7 activates pre-BCR signaling and differentiation. *Nat Immunol*. 2012;13(3):300-307. doi:10.1038/ni.2210

124. Mandal M, Powers SE, Ochiai K, et al. Ras orchestrates exit from the cell cycle and light-chain recombination during early B cell development. *Nat Immunol*. 2009;10(10):1110-1117. doi:10.1038/ni.1785

125. Ma S, Pathak S, Trinh L, Lu R. Interferon regulatory factors 4 and 8 induce the expression of Ikaros and Aiolos to down-regulate pre-B-cell receptor and promote cell-cycle withdrawal in pre-B-cell development. *Blood*. 2008;111(3):1396-1403. doi:10.1182/blood-2007-08-110106

126. Ma S, Pathak S, Mandal M, Trinh L, Clark MR, Lu R. Ikaros and Aiolos Inhibit Pre-B-Cell Proliferation by Directly Suppressing c-Myc Expression. *Mol Cell Biol*. 2010;30(17):4149-4158. doi:10.1128/mcb.00224-10

127. Lu R, Medina KL, Lancki DW, Singh H. IRF-4,8 orchestrate the pre-B-to-B transition in lymphocyte development. *Genes Dev*. 2003;17(14):1703-1708. doi:10.1101/gad.1104803

128. Lazorchak AS, Schlissel MS, Zhuang Y. E2A and IRF-4/Pip Promote Chromatin Modification and Transcription of the Immunoglobulin κ Locus in Pre-B Cells. *Mol Cell Biol*. 2006;26(3):810-821. doi:10.1128/mcb.26.3.810-821.2006

129. Turner M, Mee PJ, Costello PS, et al. Perinatal lethality and blocked B-cell development in mice lacking the tyrosine kinase Syk. *Nature*. 1995;378(6554):298-302. doi:10.1038/378298a0

130. Jumaa H, Wollscheid B, Mitterer M, Wienands J, Reth M, Nielsen PJ. Abnormal development and function of B lymphocytes in mice deficient for the signaling adaptor protein SLP-65. *Immunity*. 1999;11(5):547-554. doi:10.1016/S1074-7613(00)80130-2

131. Qing M, Jones D, Springer TA. The chemokine receptor CXCR4 is required for the retention of B lineage and granulocytic precursors within the bone marrow microenvironment. *Immunity*. 1999;10(4):463-471. doi:10.1016/S1074-7613(00)80046-1

132. Mandal M, Maienschein-Cline M, Maffucci P, et al. BRWD1 orchestrates epigenetic landscape of late B lymphopoiesis. *Nat Commun*. 2018;9(1):1-15. doi:10.1038/s41467-018-06165-6

133. Stephan RP, Lill-Elghanian D a, Witte PL. Development of B cells in aged mice: decline in the ability of pro-B cells to respond to IL-7 but not to other growth factors. *J Immunol*. 1997;158(4):1598-1609. http://www.ncbi.nlm.nih.gov/pubmed/9029095.

134. Gibson LF, Piktel D, Landreth KS. Insulin-like growth factor-1 potentiates expansion of interleukin-7-dependent pro-B cells. *Blood*. 1993;82(10):3005-3011.

135. LeRoith D, Werner H, Beitner-Johnson D, Roberts Jr. CT. Molecular and Cellular Aspects of the Insulin-Like Growth Factor I Receptor. *Endocr Rev*. 1995;16(2):143-163. doi:10.1210/edrv-16-2-143

136. Czech MP. Signal transmission by the insulin-like growth factors. *Cell*. 1989;59(2):235-238. doi:10.1016/0092-8674(89)90281-x

137. Thiebaud D, Jacot E, DeFronzo RA, Maeder E, Jequier E, Felber JP. The effect of graded doses of insulin on total glucose uptake, glucose oxidation, and glucose storage in man. *Diabetes*. 1982;31(11):957-963. doi:10.2337/diacare.31.11.957

138. Kubota T, Kubota N, Kumagai H, et al. Impaired insulin signaling in endothelial cells reduces insulin-induced glucose uptake by skeletal muscle. *Cell Metab*. 2011;13(3):294-307. doi:10.1016/j.cmet.2011.01.018

139. Benito M, Valverde AM, Lorenzo M. IGF-I: A Mitogen also involved in

differentiation processes in mammalian cells. *Int J Biochem Cell Biol*. 1996;28(5):499-510. doi:10.1016/1357-2725(95)00168-9

140. Alessi DR, Andjelkovic M, Caudwell B, et al. Mechanism of activation of protein kinase B by insulin and IGF-1. *EMBO J*. 1996;15(23):6541-6551. doi:10.1002/j.1460-2075.1996.tb01045.x

141. Hunter SJ, Garvey WT. Insulin action and insulin resistance: diseases involving defects in insulin receptors, signal transduction, and the glucose transport effector system. *Am J Med*. 1998;105(4):331-345. doi:10.1016/s0002-9343(98)00300-3

142. Aguirre GA, De Ita JR, de la Garza RG, Castilla-Cortazar I. Insulin-like growth factor-1 deficiency and metabolic syndrome. *J Transl Med*. 2016;14:3. doi:10.1186/s12967-015-0762-z

143. Hannon K, Gronowski A, Trenkle A. Relationship of Liver and Skeletal Muscle IGF-1 mRNA to Plasma GH Profile, Production of IGF-1 by Liver, Plasma IGF-1 Concentrations, and Growth Rates of Cattle. *Proc Soc Exp Biol Med*. 1991;196(2):155-163. doi:10.3181/00379727-196-43172

144. Álvarez-Nava F, Lanes R. GH/IGF-1 signaling and current knowledge of epigenetics; A review and considerations on possible therapeutic options. *Int J Mol Sci*. 2017;18(10). doi:10.3390/ijms18101624

145. Yakar S, Liu JL, Stannard B, et al. Normal growth and development in the absence of hepatic insulin-like growth factor I. *Proc Natl Acad Sci U S A*. 1999;96(13):7324-7329. doi:10.1073/pnas.96.13.7324

146. Wang E, Wang J, Chin E, Zhou J, Bondy CA. Cellular patterns of insulin-like growth factor system gene expression in murine chondrogenesis and osteogenesis. *Endocrinology*. 1995;136(6):2741-2751. doi:10.1210/endo.136.6.7750499

147. Wang Y, Bikle DD, Chang W. Autocrine and Paracrine Actions of IGF-I Signaling in Skeletal Development. *Bone Res*. 2013;1(3):249-259. doi:10.4248/BR201303003

148. Duan C, Xu Q. Roles of insulin-like growth factor (IGF) binding proteins in regulating IGF actions. *Gen Comp Endocrinol*. 2005;142(1-2):44—52. doi:10.1016/j.ygcen.2004.12.022

149. Taguchi T, Takenouchi H, Matsui J, et al. Involvement of insulin-like growth factor-I and insulin-like growth factor binding proteins in pro-B-cell development. *Exp Hematol*. 2006;34(4):508-518. doi:10.1016/j.exphem.2006.01.009

150. Cai W, Sakaguchi M, Kleinridders A, et al. Domain-dependent effects of insulin and IGF-1 receptors on signalling and gene expression. *Nat Commun*. 2017;8(1):1-14. doi:10.1038/ncomms14892

151. Riedemann J, Macaulay VM. IGF1R signalling and its inhibition. In: *Endocrine-Related Cancer*. Vol 13. BioScientifica; 2006:S33-S43. doi:10.1677/erc.1.01280

152. Mao Z, Zhang W. Role of mTOR in Glucose and Lipid Metabolism. *Int J Mol Sci*. 2018;19(7). doi:10.3390/ijms19072043

153. Ahamed K, Epaud R, Holzenberger M, et al. Deficiency in type I insulin-like growth factor receptor in mice protects against oxygen-induced lung injury. *Respir Res*. 2005;6(1):31. doi:10.1186/1465-9921-6-31

154. Epaud R, Aubey F, Xu J, et al. Knockout of insulin-like growth factor-1 receptor impairs distal lung morphogenesis. *PLoS One*. 2012;7(11). doi:10.1371/journal.pone.0048071

155. Baudler S, Baumgartl J, Hampel B, et al. Insulin-Like Growth Factor-1 Controls Type 2 T Cell-Independent B Cell Response. *J Immunol*. 2005;174(9):5516-5525. doi:10.4049/jimmunol.174.9.5516

156. Iwata TN, Ramírez JA, Tsang M, et al. Conditional Disruption of Raptor Reveals an Essential Role for mTORC1 in B Cell Development, Survival, and Metabolism. *J Immunol*. 2016;197(6):2250-2260. doi:10.4049/jimmunol.1600492

157. Martin SK, Fitter S, El Khawanky N, et al. mTORC1 plays an important role in osteoblastic regulation of B-lymphopoiesis. *Sci Rep*. 2018;8(1). doi:10.1038/s41598-018-32858-5

158. Dey BR, Spence SL, Nissley P, Furlanetto RW. Interaction of human suppressor of cytokine signaling (SOCS)-2 with the insulin-like growth factor-I receptor. *J Biol Chem*. 1998;273(37):24095-24101. doi:10.1074/jbc.273.37.24095

159. Kazi JU, Rönnstrand L. Suppressor of cytokine signaling 2 (SOCS2) associates with FLT3 and negatively regulates downstream signaling. *Mol Oncol*. 2013;7(3):693-

703. doi:10.1016/j.molonc.2013.02.020

160. Huffman J, Hoffmann C, Taylor GT. Integrating insulin-like growth factor 1 and sex hormones into neuroprotection: Implications for diabetes. *World J Diabetes*. 2017;8(2):45. doi:10.4239/wjd.v8.i2.45

161. Tao Y, Pinzi V, Bourhis J, Deutsch E. Mechanisms of Disease: Signaling of the insulin-like growth factor 1 receptor pathway - Therapeutic perspectives in cancer. *Nat Clin Pract Oncol*. 2007;4(10):591-602. doi:10.1038/ncponc0934

162. Mercer EM, Lin YC, Benner C, et al. Multilineage Priming of Enhancer Repertoires Precedes Commitment to the B and Myeloid Cell Lineages in Hematopoietic Progenitors. *Immunity*. 2011;35(3):413-425. doi:10.1016/j.immuni.2011.06.013

163. Lin YC, Jhunjhunwala S, Benner C, et al. A global network of transcription factors, involving E2A, EBF1 and Foxo1, that orchestrates B cell fate. *Nat Immunol*. 2010;11(7):635-643. doi:10.1038/ni.1891

164. Shilatifard A. The COMPASS Family of Histone H3K4 Methylases: Mechanisms of Regulation in Development and Disease Pathogenesis. *Annu Rev Biochem*. 2012;81(1):65-95. doi:10.1146/annurev-biochem-051710-134100

165. Shi Y, Lan F, Matson C, et al. Histone demethylation mediated by the nuclear amine oxidase homolog LSD1. *Cell*. 2004;119(7):941-953. doi:10.1016/j.cell.2004.12.012

166. Højfeldt JW, Agger K, Helin K. Histone lysine demethylases as targets for anticancer therapy. *Nat Rev Drug Discov*. 2013;12(12):917-930. doi:10.1038/nrd4154

167. Agger K, Cloos PAC, Christensen J, et al. UTX and JMJD3 are histone H3K27 demethylases involved in HOX gene regulation and development. *Nature*. 2007;449(7163):731-734. doi:10.1038/nature06145

168. Young MD, Willson TA, Wakefield MJ, et al. ChIP-seq analysis reveals distinct H3K27me3 profiles that correlate with transcriptional activity. *Nucleic Acids Res*. 2011;39(17):7415-7427. doi:10.1093/nar/gkr416

169. Wiles ET, Selker EU. H3K27 methylation: a promiscuous repressive chromatin mark. *Curr Opin Genet Dev*. 2017;43:31-37. doi:10.1016/j.gde.2016.11.001

170. Margueron R, Reinberg D. The Polycomb complex PRC2 and its mark in life. *Nature*. 2011;469(7330):343-349. doi:10.1038/nature09784

171. Kuchen S, Resch W, Yamane A, et al. Regulation of microRNA expression and abundance during lymphopoiesis. *Immunity*. 2010;32(6):828-839. doi:10.1016/j.immuni.2010.05.009

172. Didiano D, Hobert O. Molecular architecture of a miRNA-regulated 3' UTR. *RNA*. 2008;14(7):1297-1317. doi:10.1261/rna.1082708

173. O'Brien J, Hayder H, Zayed Y, Peng C. Overview of MicroRNA Biogenesis, Mechanisms of Actions, and Circulation. *Front Endocrinol (Lausanne)*. 2018;9:402. doi:10.3389/fendo.2018.00402

174. Chen CZ, Li L, Lodish HF, Bartel DP. MicroRNAs Modulate Hematopoietic Lineage Differentiation. *Science (80-)*. 2004;303(5654):83-86. doi:10.1126/science.1091903

175. Koralov SB, Muljo SA, Galler GR, et al. Dicer ablation affects antibody diversity and cell survival in the B lymphocyte lineage. *Cell*. 2008;132(5):860-874. doi:10.1016/j.cell.2008.02.020

176. Rao DS, O'Connell RM, Chaudhuri AA, Garcia-Flores Y, Geiger TL, Baltimore D. MicroRNA-34a perturbs B lymphocyte development by repressing the forkhead box transcription factor Foxp1. *Immunity*. 2010;33(1):48-59. doi:10.1016/j.immuni.2010.06.013

177. Ventura A, Young AG, Winslow MM, et al. Targeted deletion reveals essential and overlapping functions of the miR-17 through 92 family of miRNA clusters. *Cell*. 2008;132(5):875-886. doi:10.1016/j.cell.2008.02.019

178. Smith ZD, Meissner A. DNA methylation: roles in mammalian development. *Nat Rev Genet*. 2013;14(3):204-220. doi:10.1038/nrg3354

179. Probst A V, Dunleavy E, Almouzni G. Epigenetic inheritance during the cell cycle. *Nat Rev Mol Cell Biol*. 2009;10(3):192-206. doi:10.1038/nrm2640

180. He Y-F, Li B-Z, Li Z, et al. Tet-mediated formation of 5-carboxylcytosine and its excision by TDG in mammalian DNA. *Science*. 2011;333(6047):1303-1307. doi:10.1126/science.1210944

181. Gao H, Lukin K, Ramírez J, Fields S, Lopez D, Hagman J. Opposing effects of SWI/SNF and Mi-2/NuRD chromatin remodeling complexes on epigenetic reprogramming by EBF and Pax5. *Proc Natl Acad Sci U S A*. 2009;106(27):11258-11263. doi:10.1073/pnas.0809485106

182. Maier H, Ostraat R, Gao H, et al. Early B cell factor cooperates with Runx1 and mediates epigenetic changes associated with mb-1 transcription. *Nat Immunol*. 2004;5(10):1069-1077. doi:10.1038/ni1119

183. Banerji J, Olson L, Schaffner W. A lymphocyte-specific cellular enhancer is located downstream of the joining region in immunoglobulin heavy chain genes. *Cell*. 1983;33(3):729-740. doi:10.1016/0092-8674(83)90015-6

184. Bowen AJ, Corcoran AE. How chromatin remodelling allows shuffling of immunoglobulin heavy chain genes. *Mol Biosyst*. 2008;4(8):790-798. doi:10.1039/b719771n

185. Yang Q, Riblet R, Schildkraut CL. Sites that direct nuclear compartmentalization are near the 5' end of the mouse immunoglobulin heavy-chain locus. *Mol Cell Biol*. 2005;25(14):6021-6030. doi:10.1128/MCB.25.14.6021-6030.2005

186. Marquet M, Garot A, Bender S, et al. The Eμ Enhancer Region Influences H Chain Expression and B Cell Fate without Impacting IgVH Repertoire and Immune Response In Vivo. *J Immunol*. 2014;193(3):1171-1183. doi:10.4049/jimmunol.1302868

187. Afshar R, Pierce S, Bolland DJ, Corcoran A, Oltz EM. Regulation of IgH gene assembly: role of the intronic enhancer and 5'DQ52 region in targeting DHJH recombination. *J Immunol*. 2006;176(4):2439-2447. doi:10.4049/jimmunol.176.4.2439

188. Hiramatsu R, Akagi K, Matsuoka M, et al. The 3' Enhancer Region Determines the B/T Specificity and Pro-B/Pre-B Specificity of Immunoglobulin K-J, Joining. *Cell*. 1995;83:1113-1123. http://ac.els-cdn.com/0092867495901388/1-s2.0-0092867495901388-main.pdf?_tid=e0991e64-6000-11e7-a7f7-00000aacb35f&acdnat=1499094434_e662ec3381f0db6c7c7f7a0bdf33ee1c. Accessed July 3, 2017.

189. Zhou X, Xiang Y, Garrard WT. The Igk Gene Enhancers, E3' and Ed, Are Essential for Triggering Transcription. *J Immunol*. 2017;185(185):7544-7552. doi:10.4049/jimmunol.1002665

190. Featherstone K, Wood AL, Bowen AJ, Corcoran AE. The mouse immunoglobulin heavy chain V-D intergenic sequence contains insulators that may regulate ordered V(D)J recombination. *J Biol Chem*. 2010;285(13):9327-9338. doi:10.1074/jbc.M109.098251

191. Shih H-Y, Krangel MS. Chromatin architecture, CTCF and V(D)J recombination: managing long-distance relationships at antigen receptor loci. *NIH*. 2014. doi:10.4049/jimmunol.1300218

192. Guo C, Yoon HS, Franklin A, et al. CTCF-binding elements mediate control of V(D)J recombination. *Nature*. 2011;477. doi:10.1038/nature10495

193. Degner SC, Verma-Gaur J, Wong TP, et al. CCCTC-binding factor (CTCF) and cohesin influence the genomic architecture of the Igh locus and antisense transcription in pro-B cells. *Proc Natl Acad Sci*. 2011;108(23):9566-9571. doi:10.1073/pnas.1019391108

194. Ribeiro De Almeida C, Stadhouders R, De Bruijn MJW, et al. The DNA-Binding Protein CTCF Limits Proximal Vκ Recombination and Restricts κ Enhancer Interactions to the Immunoglobulin κ Light Chain Locus. *Immunity*. 2011;35:501-513. doi:10.1016/j.immuni.2011.07.014

195. Vincent-Fabert C, Fiancette R, Pinaud E, et al. Genomic deletion of the whole IgH 3' regulatory region (hs3a, hs1,2, hs3b, and hs4) dramatically affects class switch recombination and Ig secretion to all isotypes. *Blood*. 2010;116(11):1895-1898. doi:10.1182/blood-2010-01-264689

196. Birshtein BK. The role of CTCF binding sites in the 3' immunoglobulin heavy chain regulatory region. *Front Genet*. 2012;3:251. doi:10.3389/fgene.2012.00251

197. Guo C, Yoon HS, Franklin A, et al. CTCF-binding elements mediate control of V(D)J recombination. *Nature*. 2011;477. doi:10.1038/nature10495

198. Zhang Z, Espinoza CR, Yu Z, et al. Transcription factor Pax5 (BSAP) transactivates the RAG-mediated V(H)-to-DJ(H) rearrangement of immunoglobulin genes. *Nat*

Immunol. 2006;7(6):616-624. doi:10.1038/ni1339

199. Bolland DJ, Wood AL, Johnston CM, et al. Antisense intergenic transcription in V(D)J recombination. *Nat Immunol*. 2004;5(6):630-637. doi:10.1038/ni1068

200. Ji Y, Resch W, Corbett E, Yamane A, Casellas R, Schatz DG. The in vivo pattern of binding of RAG1 and RAG2 to antigen receptor loci. *Cell*. 2010;141(3):419-431. doi:10.1016/j.cell.2010.03.010

201. Schatz DG, Ji Y. Recombination centres and the orchestration of V(D)J recombination. *Nat Rev Immunol*. 2011;11(4):251-263. doi:10.1038/nri2941

202. Stubbington MJT, Corcoran AE. Non-coding transcription and large-scale nuclear organisation of immunoglobulin recombination. *Curr Opin Genet Dev*. 2013;23(2):81-88. doi:10.1016/j.gde.2013.01.001

203. West KL, Singha NC, De Ioannes P, et al. A direct interaction between the RAG2 C terminus and the core histones is required for efficient V(D)J recombination. *Immunity*. 2005;23(2):203-212. doi:10.1016/j.immuni.2005.07.004

204. Subrahmanyam R, Du H, Ivanova I, et al. Localized epigenetic changes induced by DH recombination restricts recombinase to DJH junctions. *Nat Immunol*. 2012;13(12):1205-1212. doi:10.1038/ni.2447

205. Su IH, Basavaraj A, Krutchinsky AN, et al. Ezh2 controls B cell development through histone H3 methylation and Igh rearrangement. *Nat Immunol*. 2003;4(2):124-131. doi:10.1038/ni876

206. Espinoza CR, Feeney AJ. The extent of histone acetylation correlates with the differential rearrangement frequency of individual VH genes in pro-B cells. *J Immunol*. 2005;175(10):6668-6675. doi:10.4049/jimmunol.175.10.6668

207. Selimyan R, Gerstein RM, Ivanova I, et al. Localized DNA Demethylation at Recombination Intermediates during Immunoglobulin Heavy Chain Gene Assembly. Nemazee D, ed. *PLoS Biol*. 2013;11(1):e1001475. doi:10.1371/journal.pbio.1001475

208. Benner C, Isoda T, Murre C. New roles for DNA cytosine modification, eRNA, anchors, and superanchors in developing B cell progenitors. *Proc Natl Acad Sci U S A*. 2015;112(41):12776-12781. doi:10.1073/pnas.1512995112

209. Bolland DJ, Koohy H, Wood AL, et al. Two Mutually Exclusive Local Chromatin States Drive Efficient V(D)J Recombination. *Cell Rep*. 2016;15(11):2475-2487. doi:10.1016/j.celrep.2016.05.020

210. Stubbington MJT, Corcoran AE. Non-coding transcription and large-scale nuclear organisation of immunoglobulin recombination. *Curr Opin Genet Dev*. 2013;23(2):81-88. doi:10.1016/j.gde.2013.01.001

211. Franceschi C, Garagnani P, Morsiani C, et al. The Continuum of Aging and Age-Related Diseases: Common Mechanisms but Different Rates. *Front Med*. 2018;5:61. doi:10.3389/fmed.2018.00061

212. López-Otín C, Blasco MA, Partridge L, Serrano M, Kroemer G. The hallmarks of aging. *Cell*. 2013;153(6):1194-1217. http://www.cell.com/article/S0092867413006454/fulltext. Accessed July 10, 2014.

213. Aird KM, Zhang R. Detection of senescence-associated heterochromatin foci (SAHF). *Methods Mol Biol*. 2013;965:185-196. doi:10.1007/978-1-62703-239-1_12

214. Chandra T, Kirschner K, Thuret J-Y, et al. Independence of repressive histone marks and chromatin compaction during senescent heterochromatic layer formation. *Mol Cell*. 2012;47(2):203-214. doi:10.1016/j.molcel.2012.06.010

215. Zhang R, Chen W, Adams PD. Molecular dissection of formation of senescence-associated heterochromatin foci. *Mol Cell Biol*. 2007;27(6):2343-2358. doi:10.1128/MCB.02019-06

216. Singhal RP, Mays-Hoopes LL, Eichhorn GL. DNA methylation in aging of mice. *Mech Ageing Dev*. 1987;41(3):199-210. doi:10.1016/0047-6374(87)90040-6

217. Saksouk N, Simboeck E, Déjardin J. Constitutive heterochromatin formation and transcription in mammals. *Epigenetics and Chromatin*. 2015;8(1):1-17. doi:10.1186/1756-8935-8-3

218. Pinello L, Xu J, Orkin SH, Yuan G-C. Analysis of chromatin-state plasticity identifies cell-type-specific regulators of H3K27me3 patterns. *Proc Natl Acad Sci U S A*. 2014;111(3):E344-E353. doi:10.1073/pnas.1322570111

219. Maleszewska M, Mawer JSP, Tessarz P. Histone Modifications in Ageing and Lifespan Regulation. *Curr Mol Biol Reports*. 2016;2(1):26-35. doi:10.1007/s40610-016-0031-9

220. Siebold AP, Banerjee R, Tie F, Kiss DL, Moskowitz J, Harte PJ. Polycomb Repressive Complex 2 and Trithorax modulate Drosophila longevity and stress resistance. *Proc Natl Acad Sci U S A*. 2010;107(1):169-174. doi:10.1073/pnas.0907739107

221. Maures TJ, Greer EL, Hauswirth AG, Brunet A. The H3K27 demethylase UTX-1 regulates C. elegans lifespan in a germline-independent, insulin-dependent manner. *Aging Cell*. 2011;10(6):980-990. doi:10.1111/j.1474-9726.2011.00738.x

222. Dozmorov MG. Polycomb repressive complex 2 epigenomic signature defines age-associated hypermethylation and gene expression changes. *Epigenetics*. 2015;10(6):484-495. doi:10.1080/15592294.2015.1040619

223. Alvares SM, Mayberry GA, Joyner EY, Lakowski B, Ahmed S. H3K4 demethylase activities repress proliferative and postmitotic aging. *Aging Cell*. 2014;13(2):245-253. doi:10.1111/acel.12166

224. Sun D, Luo M, Jeong M, et al. Epigenomic profiling of young and aged HSCs reveals concerted changes during aging that reinforce self-renewal. *Cell Stem Cell*. 2014;14(5):673-688. doi:10.1016/j.stem.2014.03.002

225. Harman D. Aging: a theory based on free radical and radiation chemistry. *J Gerontol*. 1956;11(3):298-300. doi:10.1093/geronj/11.3.298

226. Simmons JD, Lee Y-L, Mulekar S, et al. Elevated levels of plasma mitochondrial DNA DAMPs are linked to clinical outcome in severely injured human subjects. *Ann Surg*. 2013;258(4):591-598. doi:10.1097/SLA.0b013e3182a4ea46

227. Picca A, Lezza AMS, Leeuwenburgh C, et al. Circulating Mitochondrial DNA at the Crossroads of Mitochondrial Dysfunction and Inflammation During Aging and Muscle Wasting Disorders. *Rejuvenation Res*. 2018;21(4):350-359. doi:10.1089/rej.2017.1989

228. Pinti M, Cevenini E, Nasi M, et al. Circulating mitochondrial DNA increases with age and is a familiar trait: Implications for “inflamm-aging.” *Eur J Immunol*. 2014;44(5):1552-1562. doi:10.1002/eji.201343921

229. Yen TC, Chen YS, King KL, Yeh SH, Wei YH. Liver mitochondrial respiratory functions decline with age. *Biochem Biophys Res Commun*. 1989;165(3):944-1003. doi:10.1016/0006-291x(89)92701-0

230. Bratic A, Larsson NG. The role of mitochondria in aging. *J Clin Invest*. 2013;123(3):951-957. doi:10.1172/JCI64125

231. van den Beld AW, Kaufman J-M, Zillikens MC, Lamberts SWJ, Egan JM, van der Lely AJ. The physiology of endocrine systems with ageing. *lancet Diabetes Endocrinol*. 2018;6(8):647-658. doi:10.1016/S2213-8587(18)30026-3

232. Vestergaard PF, Hansen M, Frystyk J, et al. Serum levels of bioactive IGF1 and physiological markers of ageing in healthy adults. *Eur J Endocrinol*. 2014;170(2):229-236. doi:10.1530/EJE-13-0661

233. Zadik Z, Chalew SA, McCarter RJJ, Meistas M, Kowarski AA. The influence of age on the 24-hour integrated concentration of growth hormone in normal individuals. *J Clin Endocrinol Metab*. 1985;60(3):513-516. doi:10.1210/jcem-60-3-513

234. Cawthon PM, Ensrud KE, Laughlin GA, et al. Sex Hormones and Frailty in Older Men: The Osteoporotic Fractures in Men (MrOS) Study. *J Clin Endocrinol Metab*. 2009;94(10):3806-3815. doi:10.1210/jc.2009-0417

235. Gielen E, O'neill TW, Pye SR, et al. Endocrine determinants of incident sarcopenia in middle-aged and elderly European men. *J Cachexia Sarcopenia Muscle*. 2015;6(3):242-252. doi:10.1002/jcsm.12030

236. Kimura KD, Tissenbaum HA, Liu Y, Ruvkun G. Daf-2, an insulin receptor-like gene that regulates longevity and diapause in Caenorhabditis elegans. *Science (80-)*. 1997;277(5328):942-946. doi:10.1126/science.277.5328.942

237. Tatar M, Kopelman A, Epstein D, Tu MP, Yin CM, Garofalo RS. A mutant Drosophila insulin receptor homolog that extends life-span and impairs neuroendocrine function. *Science*. 2001;292(5514):107-110. doi:10.1126/science.1057987

238. Holzenberger M, Dupont J, Ducos B, et al. IGF-1 receptor regulates lifespan and resistance to oxidative stress in mice. *Nature*. 2003;421(6919):182-187. doi:10.1038/nature01298

239. Bokov AF, Garg N, Ikeno Y, et al. Does reduced IGF-1R signaling in Igf1r+/- mice alter aging? *PLoS One*. 2011;6(11):e26891-e26891. doi:10.1371/journal.pone.0026891

240. Selman C, Lingard S, Choudhury AI, et al. Evidence for lifespan extension and delayed age-related biomarkers in insulin receptor substrate 1 null mice. *FASEB J Off Publ Fed Am Soc Exp Biol*. 2008;22(3):807-818. doi:10.1096/fj.07-9261com

241. Selman C, Partridge L, Withers DJ. Replication of extended lifespan phenotype in mice with deletion of insulin receptor substrate 1. *PLoS One*. 2011;6(1):e16144. doi:10.1371/journal.pone.0016144

242. Junnila RK, List EO, Berryman DE, Murrey JW, Kopchick JJ. The GH/IGF-1 axis in ageing and longevity. *Nat Rev Endocrinol*. 2013;9(6):366-376. doi:10.1038/nrendo.2013.67

243. Conover CA, Bale LK. Loss of pregnancy-associated plasma protein A extends lifespan in mice. *Aging Cell*. 2007;6(5):727-729. doi:10.1111/j.1474-9726.2007.00328.x

244. Conover CA, Bale LK, Mader JR, Mason MA, Keenan KP, Marler RJ. Longevity and age-related pathology of mice deficient in pregnancy-associated plasma protein-A. *J Gerontol A Biol Sci Med Sci*. 2010;65(6):590-599. doi:10.1093/gerona/glq032

245. Mao K, Quipildor GF, Tabrizian T, et al. Late-life targeting of the IGF-1 receptor improves healthspan and lifespan in female mice. *Nat Commun*. 2018;9(1):2394. doi:10.1038/s41467-018-04805-5

246. Colman RJ, Anderson RM, Johnson SC, et al. Caloric restriction delays disease onset and mortality in rhesus monkeys. *Science*. 2009;325(5937):201-204. doi:10.1126/science.1173635

247. McCay CM, Crowell MF, Maynard LA. The Effect of Retarded Growth Upon the Length of Life Span and Upon the Ultimate Body Size: One Figure. *J Nutr*. 1935;10(1):63-79. doi:10.1093/jn/10.1.63

248. Colman RJ, Beasley TM, Kemnitz JW, Johnson SC, Weindruch R, Anderson RM. Caloric restriction reduces age-related and all-cause mortality in rhesus monkeys. *Nat Commun*. 2014;5:3557. doi:10.1038/ncomms4557

249. Goodwin K, Viboud C, Simonsen L. Antibody response to influenza vaccination in the elderly: A quantitative review. *Vaccine*. 2006;24(8):1159-1169. doi:10.1016/j.vaccine.2005.08.105

250. Palmer DB. The effect of age on thymic function. *Front Immunol*. 2013;4(OCT):316. doi:10.3389/fimmu.2013.00316

251. Yager EJ, Ahmed M, Lanzer K, Randall TD, Woodland DL, Blackman MA. Age-associated decline in T cell repertoire diversity leads to holes in the repertoire and impaired immunity to influenza virus. *J Exp Med*. 2008;205(3):711-723. doi:10.1084/jem.20071140

252. Tabibian-Keissar H, Hazanov L, Schiby G, et al. Aging affects B-cell antigen receptor repertoire diversity in primary and secondary lymphoid tissues. *Eur J Immunol*. 2016;46(2):480-492. doi:10.1002/eji.201545586

253. Gibson KL, Wu Y-C, Barnett Y, et al. B-cell diversity decreases in old age and is correlated with poor health status. *Aging Cell*. 2009;8(1):18-25. doi:10.1111/j.1474-9726.2008.00443.x

254. Ma S, Wang C, Mao X, Hao Y. B Cells dysfunction associated with aging and autoimmune disease. *Front Immunol*. 2019;10(FEB):318. doi:10.3389/fimmu.2019.00318

255. Martin V, Bryan Wu Y-C, Kipling D, Dunn-Walters D. Ageing of the B-cell repertoire. *Philos Trans R Soc London Ser B, Biol Sci*. 2015;370(1676). doi:10.1098/rstb.2014.0237

256. Dunn-Walters DK, Stewart AT, Sinclair EL, Serangeli I. Age-Related Changes in B Cells Relevant to Vaccine Responses. *Interdiscip Top Gerontol Geriatr*. 2020;43:56-72. doi:10.1159/000504479

257. Han S, Yang K, Ozen Z, et al. Enhanced differentiation of splenic plasma cells but diminished long-lived high-affinity bone marrow plasma cells in aged mice. *J Immunol*. 2003;170(3):1267-1273. doi:10.4049/jimmunol.170.3.1267

258. Speziali E, Santiago AF, Fernandes RM, Vaz NM, Menezes JS, Faria AMC. Specific immune responses but not basal functions of B and T cells are impaired in aged mice. *Cell Immunol*. 2009;256(1-2):1-5. doi:10.1016/j.cellimm.2009.01.010

259. Frasca D, Diaz A, Romero M, Landin AM, Blomberg BB. Age effects on B cells and humoral immunity in humans. *Ageing Res Rev*. 2011;10(3):330-335. doi:10.1016/j.arr.2010.08.004

260. Ademokun A, Wu YC, Dunn-Walters D. The ageing B cell population: Composition and function. *Biogerontology*. 2010;11(2):125-137. doi:10.1007/s10522-009-9256-9

261. Frasca D, Van der Put E, Riley RL, Blomberg BB. Reduced Ig class switch in aged mice correlates with decreased E47 and activation-induced cytidine deaminase. *J Immunol*. 2004;172(4):2155-2162. doi:10.4049/jimmunol.172.4.2155

262. Hernandez-Segura A, de Jong T V, Melov S, Guryev V, Campisi J, Demaria M. Unmasking Transcriptional Heterogeneity in Senescent Cells. *Curr Biol*. 2017;27(17):2652-2660.e4. doi:10.1016/j.cub.2017.07.033

263. Youm Y-H, Grant RW, McCabe LR, et al. Canonical Nlrp3 inflammasome links systemic low-grade inflammation to functional decline in aging. *Cell Metab*. 2013;18(4):519-532. doi:10.1016/j.cmet.2013.09.010

264. Ratliff M, Alter S, Frasca D, Blomberg BB, Riley RL. In senescence, age-associated b cells secrete tnfα and inhibit survival of b-cell precursors. *Aging Cell*. 2013;12(2):303-311. doi:10.1111/acel.12055

265. Hao Y, O'Neill P, Naradikian MS, Scholz JL, Cancro MP. A B-cell subset uniquely responsive to innate stimuli accumulates in aged mice. *Blood*. 2011;118(5):1294-1304. doi:10.1182/blood-2011-01-330530

266. Ambrosi TH, Scialdone A, Graja A, et al. Adipocyte Accumulation in the Bone Marrow during Obesity and Aging Impairs Stem Cell-Based Hematopoietic and Bone Regeneration. *Cell Stem Cell*. 2017;20(6):771-784.e6. doi:10.1016/j.stem.2017.02.009

267. Kovtonyuk L V, Fritsch K, Feng X, Manz MG, Takizawa H. Inflamm-Aging of Hematopoiesis, Hematopoietic Stem Cells, and the Bone Marrow Microenvironment. *Front Immunol*. 2016;7:502. doi:10.3389/fimmu.2016.00502

268. Sudo K, Ema H, Morita Y, Nakauchi H. Age-associated characteristics of murine hematopoietic stem cells. *J Exp Med*. 2000;192(9):1273-1280.

doi:10.1084/jem.192.9.1273

269. Linton PJ, Dorshkind K. Age-related changes in lymphocyte development and function. *Nat Immunol*. 2004;5(2):133-139. doi:10.1038/ni1033

270. Mori DN, Shen H, Galan A, Goldstein DR. Aged B cells alter immune regulation of allografts in mice. *Eur J Immunol*. 2016:1-9. doi:10.1002/eji.201646353

271. Tuljapurkar SR, McGuire TR, Brusnahan SK, et al. Changes in human bone marrow fat content associated with changes in hematopoietic stem cell numbers and cytokine levels with aging. *J Anat*. 2011;219(5):574-581. doi:10.1111/j.1469-7580.2011.01423.x

272. Chen C-Y, Tseng K-Y, Lai Y-L, Chen Y-S, Lin F-H, Lin S. Overexpression of Insulin-Like Growth Factor 1 Enhanced the Osteogenic Capability of Aging Bone Marrow Mesenchymal Stem Cells. *Theranostics*. 2017;7(6):1598-1611. doi:10.7150/thno.16637

273. Yeh LCC, Wilkerson M, Lee JC, Adamo ML. IGF-1 receptor insufficiency leads to age-dependent attenuation of osteoblast differentiation. *Endocrinology*. 2015;156(8):2872-2879. doi:10.1210/en.2014-1945

274. Zharhary D. Age-related changes in the capability of the bone marrow to generate B cells. *J Immunol*. 1988;141(6):1863-1869.

275. Koohy H, Bolland DJ, Matheson LS, et al. Genome organization and chromatin analysis identify transcriptional downregulation of insulin-like growth factor signaling as a hallmark of aging in developing B cells. *Genome Biol*. 2018;19(1):126. doi:10.1186/s13059-018-1489-y

276. Kruidenier L, Chung CW, Cheng Z, et al. A selective jumonji H3K27 demethylase inhibitor modulates the proinflammatory macrophage response. *Nature*. 2012;488(7411):404-408. doi:10.1038/nature11262

277. Béguelin W, Popovic R, Teater M, et al. EZH2 Is Required for Germinal Center Formation and Somatic EZH2 Mutations Promote Lymphoid Transformation. *Cancer Cell*. 2013;23(5):677-692. doi:10.1016/j.ccr.2013.04.011

278. Lee J, Breton G, Aljoufi A, et al. Clonal analysis of human dendritic cell progenitor using a stromal cell culture. *J Immunol Methods*. 2015;425:21-26.

doi:10.1016/j.jim.2015.06.004

279. Chovanec P, Bolland DJ, Matheson LS, et al. Unbiased quantification of immunoglobulin diversity at the DNA level with VDJ-seq. *Nat Protoc*. 2018;13(6):1232-1252. doi:10.1038/nprot.2018.021

280. Cao J, Packer JS, Ramani V, et al. Comprehensive single-cell transcriptional profiling of a multicellular organism. *Science (80-)*. 2017;357(6352):661-667. doi:10.1126/science.aam8940

281. Kim D, Langmead B, Salzberg SL. HISAT: a fast spliced aligner with low memory requirements. *Nat Methods*. 2015;12(4):357-360. doi:10.1038/nmeth.3317

282. Love MI, Huber W, Anders S. Moderated estimation of fold change and dispersion for RNA-seq data with DESeq2. *Genome Biol*. 2014;15(12):550. doi:10.1186/s13059-014-0550-8

283. Subramanian A, Tamayo P, Mootha VK, et al. Gene set enrichment analysis: a knowledge-based approach for interpreting genome-wide expression profiles. *Proc Natl Acad Sci U S A*. 2005;102(43):15545-15550. doi:10.1073/pnas.0506580102

284. Ye J, Ma N, Madden TL, Ostell JM. IgBLAST: an immunoglobulin variable domain sequence analysis tool. *Nucleic Acids Res*. 2013;41(Web Server issue):W34-40. doi:10.1093/nar/gkt382

285. Yu VWC, Lymperi S, Oki T, et al. Distinctive Mesenchymal-Parenchymal Cell Pairings Govern B Cell Differentiation in the Bone Marrow. *Stem Cell Reports*. 2016;7(2):220-235. doi:10.1016/j.stemcr.2016.06.009

286. Junnila RK, List EO, Berryman DE, Murrey JW, Kopchick JJ. The GH/IGF-1 axis in ageing and longevity. *Nat Rev Endocrinol*. 2013;9(6):366-376. doi:10.1038/nrendo.2013.67

287. Sonntag WE, Lynch C, Thornton P, Khan A, Bennett S, Ingram R. The effects of growth hormone and IGF-1 deficiency on cerebrovascular and brain ageing. *J Anat*. 2000;197(4):575-585. doi:10.1017/S002187829900713X

288. Sandri M, Barberi L, Bijlsma AY, et al. Signalling pathways regulating muscle mass in ageing skeletal muscle. the role of the IGF1-Akt-mTOR-FoxO pathway.

Biogerontology. 2013;14(3):303-323. doi:10.1007/s10522-013-9432-9

289. Rincon M, Muzumdar R, Atzmon G, Barzilai N. The paradox of the insulin/IGF-1 signaling pathway in longevity. *Mech Ageing Dev*. 2004;125(6):397-403. doi:10.1016/j.mad.2004.03.006

290. Chen YR, Li YH, Hsieh TC, et al. Aging-induced Akt activation involves in aging-related pathologies and Aβ-induced toxicity. *Aging Cell*. 2019;18(4). doi:10.1111/acel.12989

291. Manning BD, Toker A. AKT/PKB Signaling: Navigating the Network. *Cell*. 2017;169(3):381-405. doi:10.1016/j.cell.2017.04.001

292. Yoon MS, Choi CS. The role of amino acid-induced mammalian target of rapamycin complex 1(mTORC1) signaling in insulin resistance. *Exp Mol Med*. 2016;48(1):e201-e201. doi:10.1038/emm.2015.93

293. Angelidis I, Simon LM, Fernandez IE, et al. An atlas of the aging lung mapped by single cell transcriptomics and deep tissue proteomics. *Nat Commun*. 2019;10(1):1-17. doi:10.1038/s41467-019-08831-9

294. Kowalczyk MS, Tirosh I, Heckl D, et al. Single-cell RNA-seq reveals changes in cell cycle and differentiation programs upon aging of hematopoietic stem cells. *Genome Res*. 2015;25(12):1860-1872. doi:10.1101/gr.192237.115

295. Martinez-Jimenez CP, Eling N, Chen H-C, et al. Aging increases cell-to-cell transcriptional variability upon immune stimulation. *Science*. 2017;355(6332):1433-1436. doi:10.1126/science.aah4115

296. Kimmel JC, Penland L, Rubinstein ND, Hendrickson DG, Kelley DR, Rosenthal AZ. Murine single-cell RNA-seq reveals cell-identity- And tissue-specific trajectories of aging. *Genome Res*. 2019;29(12):2088-2103. doi:10.1101/gr.253880.119

297. Georgiou G, Ippolito GC, Beausang J, Busse CE, Wardemann H, Quake SR. The promise and challenge of high-throughput sequencing of the antibody repertoire. *Nat Biotechnol*. 2014;32(2):158-168. doi:10.1038/nbt.2782

298. Weksler ME, Szabo P. The effect of age on the B-cell repertoire. *J Clin Immunol*. 2000;20(4):240-249. doi:10.1023/A:1006659401385

299. Barnes MJ, Aksoylar H, Krebs P, et al. Loss of T Cell and B Cell Quiescence Precedes the Onset of Microbial Flora-Dependent Wasting Disease and Intestinal Inflammation in Gimap5-Deficient Mice. *J Immunol*. 2010;184(7):3743-3754. doi:10.4049/jimmunol.0903164

300. Aksoylar HI, Lampe K, Barnes MJ, Plas DR, Hoebe K. Loss of Immunological Tolerance in Gimap5-Deficient Mice Is Associated with Loss of Foxo in CD4 + T Cells . *J Immunol*. 2012;188(1):146-154. doi:10.4049/jimmunol.1101206

301. Galloway A, Saveliev A, Łukasiak S, et al. RNA-binding proteins ZFP36L1 and ZFP36L2 promote cell quiescence. *Science (80-)*. 2016;352(6284):453-459. doi:10.1126/science.aad5978

302. Zhou Y, Zhang Z, Wang N, et al. Suppressor of cytokine signalling-2 limits IGF1R-mediated regulation of epithelial-mesenchymal transition in lung adenocarcinoma article. *Cell Death Dis*. 2018;9(4):1-14. doi:10.1038/s41419-018-0457-5

303. Dey BR, Spence SL, Nissley P, Furlanetto RW. Interaction of human suppressor of cytokine signaling (SOCS)-2 with the insulin-like growth factor-I receptor. *J Biol Chem*. 1998;273(37):24095-24101. doi:10.1074/jbc.273.37.24095

304. Severino V, Alessio N, Farina A, et al. Insulin-like growth factor binding proteins 4 and 7 released by senescent cells promote premature senescence in mesenchymal stem cells. *Cell Death Dis*. 2013;4(11):e911-e911. doi:10.1038/cddis.2013.445

305. Zhou R, Flaswinkel H, Schneider MR, et al. Insulin-like growth factor-binding protein-4 inhibits growth of the thymus in transgenic mice. *J Mol Endocrinol*. 2004;32(2):349-364. doi:10.1677/jme.0.0320349

306. Balasooriya GI, Johnson JA, Basson MA, Rawlins EL. An FGFR1-SPRY2 Signaling Axis Limits Basal Cell Proliferation in the Steady-State Airway Epithelium. *Dev Cell*. 2016;37(1):85-97. doi:10.1016/j.devcel.2016.03.001

307. Rho SB, Song YJ, Lim MC, Lee S-H, Kim B-R, Park S-Y. Programmed cell death 6 (PDCD6) inhibits angiogenesis through PI3K/mTOR/p70S6K pathway by interacting of VEGFR-2. *Cell Signal*. 2012;24(1):131-139.

doi:10.1016/j.cellsig.2011.08.013

308. Yang M, Mailhot G, MacKay CA, Mason-Savas A, Aubin J, Odgren PR. Chemokine and chemokine receptor expression during colony stimulating factor-1-induced osteoclast differentiation in the toothless osteopetrotic rat: A key role for CCL9 (MIP-1γ) in osteoclastogenesis in vivo and in vitro. *Blood*. 2006;107(6):2262-2270. doi:10.1182/blood-2005-08-3365

309. Franceschi C, Garagnani P, Parini P, Giuliani C, Santoro A. Inflammaging: a new immune–metabolic viewpoint for age-related diseases. *Nat Rev Endocrinol*. 2018;14(10):576-590. doi:10.1038/s41574-018-0059-4

310. Franceschi C, Garagnani P, Vitale G, Capri M, Salvioli S. Inflammaging and 'Garb-aging.' *Trends Endocrinol Metab*. 2017;28(3):199-212. doi:10.1016/j.tem.2016.09.005

311. Du W, Amarachintha S, Wilson A, Pang Q. The immune receptor Trem1 cooperates with diminished DNA damage response to induce preleukemic stem cell expansion. *Leukemia*. 2017;31(2):423-433. doi:10.1038/leu.2016.242

312. Klinngam W, Fu R, Janga SR, Edman MC, Hamm-Alvarez SF. Cathepsin s alters the expression of pro-inflammatory cytokines and MMP-9, partially through protease—activated receptor-2, in human corneal epithelial cells. *Int J Mol Sci*. 2018;19(11). doi:10.3390/ijms19113530

313. Johnston CM, Wood AL, Bolland DJ, Corcoran AE. Complete Sequence Assembly and Characterization of the C57BL/6 Mouse Ig Heavy Chain V Region. *J Immunol*. 2006;176(7):4221-4234. doi:10.4049/jimmunol.176.7.4221

314. Chen J, Cheung F, Shi R, et al. PBMC fixation and processing for Chromium single-cell RNA sequencing. *J Transl Med*. 2018;16(1). doi:10.1186/s12967-018-1578-4

315. Lu L, Sun K, Chen X, et al. Genome-wide survey by ChIP-seq reveals YY1 regulation of lincRNAs in skeletal myogenesis. *EMBO J*. 2013;32(19):2575-2588. doi:10.1038/emboj.2013.182

316. Wang JW, Wu JR. Overexpression of a novel gene, Cms1, can rescue the growth arrest of a Saccharomyces cerevisiae mcm10 suppressor. *Cell Res*. 2001;11(4):285-291. doi:10.1038/sj.cr.7290098

317. Labrie JE, Borghesi L, Gerstein RM. Bone marrow microenvironmental changes in aged mice compromise V(D)J recombinase activity and B cell generation. *Semin Immunol*. 2005;17(5):347-355. doi:10.1016/j.smim.2005.05.012

318. Stephan RP, Reilly CR, Witte PL. Impaired Ability of Bone Marrow Stromal Cells to Support B-Lymphopoiesis With Age. 1998.

319. Pence BD, Yarbro JR. Aging impairs mitochondrial respiratory capacity in classical monocytes. *Exp Gerontol*. 2018;108:112-117. doi:10.1016/j.exger.2018.04.008

320. Kurupati RK, Haut LH, Schmader KE, Ertl HCJ. Age-related changes in B cell metabolism. *Aging (Albany NY)*. 2019;11(13):4367-4381. doi:10.18632/aging.102058

321. Urbanczyk S, Stein M, Schuh W, Jäck HM, Mougiakakos D, Mielenz D. Regulation of energy metabolism during early B lymphocyte development. *Int J Mol Sci*. 2018;19(8). doi:10.3390/ijms19082192

322. Kojima H, Kobayashi A, Sakurai D, et al. Differentiation Stage-Specific Requirement in Hypoxia-Inducible Factor-1α–Regulated Glycolytic Pathway during Murine B Cell Development in Bone Marrow. *J Immunol*. 2010;184(1):154-163. doi:10.4049/jimmunol.0800167

323. Goetz CA, Harmon IR, O'Neil JJ, Burchill MA, Farrar MA. STAT5 Activation Underlies IL7 Receptor-Dependent B Cell Development. *J Immunol*. 2004;172(8):4770-4778. doi:10.4049/jimmunol.172.8.4770

324. Abdelrasoul H, Werner M, Setz CS, Okkenhaug K, Jumaa H. PI3K induces B-cell development and regulates B cell identity. *Sci Rep*. 2018;8(1):1-15. doi:10.1038/s41598-018-19460-5

325. Young K, Eudy E, Loberg M, Bell R, Trowbridge J. Decline in Insulin-like Growth Factor-1 (IGF1) from Aged Mesenchymal Stromal Cells Is a Targetable Mechanism to Rescue Hematopoietic Stem Cell Aging. *Blood*. 2019;134(Supplement_1):526-526. doi:10.1182/blood-2019-124534

326. Landreth KS, Narayanan R, Dorshkind K. Insulin-like Growth Factor-I Regulates Pro-B Cell Differentiation. http://www.bloodjournal.org/content/bloodjournal/80/5/1207.full.pdf.

Accessed July 13, 2017.

327. Engels N, Wollscheid B, Wienands J. Association of SLP-65 / BLNK with the B cell antigen receptor through a non-ITAM tyrosine of Ig-α. *Eur J Immunol*. 2001;31(7):2126-2134. doi:10.1002/1521-4141(200107)31:7<2126::AID-IMMU2126>3.0.CO;2-O

328. Fu C, Turck CW, Kurosaki T, Chan AC. BLNK: A central linker protein in B cell activation. *Immunity*. 1998;9(1):93-103. doi:10.1016/S1074-7613(00)80591-9

329. Hers I, Tavaré JM. Mechanism of feedback regulation of insulin receptor substrate-1 phosphorylation in primary adipocytes. *Biochem J*. 2005;388(2):713-720. doi:10.1042/BJ20041531

330. Zhang J, Gao Z, Yin J, Quon MJ, Ye J. S6K directly phosphorylates IRS-1 on Ser-270 to promote insulin resistance in response to TNF-α signaling through IKK2. *J Biol Chem*. 2008;283(51):35375-35382. doi:10.1074/jbc.M806480200

331. Rui L, Aguirre V, Kim JK, et al. Insulin/IGF-1 and TNF-α stimulate phosphorylation of IRS-1 at inhibitory Ser307 via distinct pathways. *J Clin Invest*. 2001;107(2):181-189. doi:10.1172/JCI10934

332. Seok S, Kim YC, Byun S, et al. Fasting-induced JMJD3 histone demethylase epigenetically activates mitochondrial fatty acid ß-oxidation. *J Clin Invest*. 2018;128(7):3144-3159. doi:10.1172/JCI97736

333. de Gonzalo-Calvo D, Neitzert K, Fernández M, et al. Differential inflammatory responses in aging and disease: TNF-α and IL-6 as possible biomarkers. *Free Radic Biol Med*. 2010;49(5):733-737. doi:10.1016/j.freeradbiomed.2010.05.019

334. Davizon-Castillo P, McMahon B, Aguila S, et al. TNF-a–driven inflammation and mitochondrial dysfunction define the platelet hyperreactivity of aging. *Blood*. 2019;134(9):727-740. doi:10.1182/blood.2019000200

335. Saklatvala J. Interleukin 1 (IL1) and tumour necrosis factor (TNF) signal transduction. *Philos Trans R Soc B Biol Sci*. 1996;351(1336):151-157. doi:10.1098/rstb.1996.0011

336. Majewska E, Paleolog E, Baj Z, Kralisz U, Feldmann M, Tchórzewski H. Role of tyrosine kinase enzymes in TNF-α and IL-1 induced expression of ICAM-1 and

VCAM-1 on human umbilical vein endothelial cells. *Scand J Immunol*. 1997;45(4):385-392. doi:10.1046/j.1365-3083.1997.d01-412.x

337. EM P, S Y, AC S, RV M, M F, RN M. Modulation of Angiogenic Vascular Endothelial Growth Factor by Tumor Necrosis Factor Alpha and interleukin-1 in Rheumatoid Arthritis. *Arthritis Rheum*. 1998;41(7). doi:10.1002/1529-0131(199807)41:7<1258::AID-ART17>3.0.CO;2-1

338. Vosshenrich CAJ, Cumano A, Müller W, Di Santo JP, Vieira P. Pre-B cell receptor expression is necessary for thymic stromal lymphopoietin responsiveness in the bone marrow but not in the liver environment. *Proc Natl Acad Sci U S A*. 2004;101(30):11070-11075. doi:10.1073/pnas.0402919101

339. Carpino N, Thierfelder WE, Chang M-S, et al. Absence of an Essential Role for Thymic Stromal Lymphopoietin Receptor in Murine B-Cell Development. *Mol Cell Biol*. 2004;24(6):2584-2592. doi:10.1128/mcb.24.6.2584-2592.2004

340. Peschon JJ, Morrissey PJ, Grabstein KH, et al. Early Lymphocyte Expansion Is Severely Impaired in Interleukin 7 Receptor-deficient Mice. *J Exp Med*. 1994;180(5):1955-1960. doi:10.1084/jem.180.5.1955

341. Corcoran AE, Smart FM, Cowling RJ, Crompton1 T, Owen1 MJ, Venkitaraman2 AR. The interleukin-7 receptor a chain transmits distinct signals for proliferation and differentiation during B lymphopoiesis receptor/phos- phatidylinositol 3-kinase/retrovirus-mediated gene trans- fer/signal transduction. *EMBO J*. 1996;15(8):1924-1932. doi:10.1016/j.archoralbio.2011.07.006

342. Tokoyoda K, Egawa T, Sugiyama T, Choi B Il, Nagasawa T. Cellular niches controlling B lymphocyte behavior within bone marrow during development. *Immunity*. 2004;20(6):707-718. doi:10.1016/j.immuni.2004.05.001

343. Cho SK, Webber TD, Carlyle JR, Nakano T, Lewis SM, Zuniga-Pflucker JC. Functional characterization of B lymphocytes generated in vitro from embryonic stem cells. *Proc Natl Acad Sci U S A*. 1999;96(17):9797-9802. doi:10.1073/pnas.96.17.9797

344. Holl TM, Haynes BF, Kelsoe G. Stromal cell independent B cell development in vitro: Generation and recovery of autoreactive clones. *J Immunol Methods*. 2010;354(1-2):53-67. doi:10.1016/j.jim.2010.01.007

345. Ratliff M, Alter S, Frasca D, Blomberg BB, Riley RL. In senescence, age-associated B cells secrete TNFα and inhibit survival of B-cell precursors. *Aging Cell*. 2013;12(2):303-311. doi:10.1111/acel.12055

346. Vieira P, Cumano A. Differentiation of B lymphocytes from hematopoietic stem cells. *Methods Mol Biol*. 2004;271:67-76. doi:10.1385/1-59259-796-3:067

347. Rolink A, Kudo A, Karasuyama H, Kikuchi Y, Melchers F. Long-term proliferating early pre B cell lines and clones with the potential to develop to surface Ig-positive, mitogen reactive B cells in vitro and in vivo. *EMBO J*. 1991;10(2):327-336. doi:10.1002/j.1460-2075.1991.tb07953.x

348. Nguyen TTT, Baumgarth N. Natural IgM and the development of B cell-mediated autoimmune diseases. *Crit Rev Immunol*. 2016;36(2):163-177. doi:10.1615/CritRevImmunol.2016018175

349. Heinemann B, Nielsen JM, Hudlebusch HR, et al. Inhibition of demethylases by GSK-J1/J4. *Nature*. 2014;514(7520):E1-E2. doi:10.1038/nature13688

350. Béguelin W, Popovic R, Teater M, et al. EZH2 Is Required for Germinal Center Formation and Somatic EZH2 Mutations Promote Lymphoid Transformation. *Cancer Cell*. 2013;23(5):677-692. doi:10.1016/j.ccr.2013.04.011

351. Coleclough C. Chance, necessity and antibody gene dynamics. *Nature*. 1983;303(5912):23-26. doi:10.1038/303023a0

352. Clark MR, Mandal M, Ochiai K, Singh H. Orchestrating B cell lymphopoiesis through interplay of IL-7 receptor and pre-B cell receptor signalling. *Nat Rev Immunol*. 2014;14(2):69-80. doi:10.1038/nri3570

353. Lazorchak AS, Liu D, Facchinetti V, et al. Sin1-mTORC2 suppresses rag and il7r gene expression through Akt2 in B cells. *Mol Cell*. 2010;39(3):433-443. doi:10.1016/j.molcel.2010.07.031

354. Suzuki Y, Yamashita R, Shirota M, et al. Sequence comparison of human and mouse genes reveals a homologous block structure in the promoter regions. *Genome Res*. 2004;14(9):1711-1718. doi:10.1101/gr.2435604

355. Bendall SC, Davis KL, Amir EAD, et al. Single-cell trajectory detection uncovers progression and regulatory coordination in human b cell development. *Cell*.

2014;157(3):714-725. doi:10.1016/j.cell.2014.04.005

356. Bagwell CB, Hill BL, Wood BL, et al. Human B-cell and progenitor stages as determined by probability state modeling of multidimensional cytometry data. *Cytom Part B - Clin Cytom*. 2015;88(4):214-226. doi:10.1002/cyto.b.21243

357. Arnaout R, Lee W, Cahill P, et al. High-Resolution Description of Antibody Heavy-Chain Repertoires in Humans. Reindl M, ed. *PLoS One*. 2011;6(8):e22365. doi:10.1371/journal.pone.0022365

358. Martin VG, Wu YCB, Townsend CL, et al. Transitional B cells in early human B cell development - Time to revisit the paradigm? *Front Immunol*. 2016;7(DEC):546. doi:10.3389/fimmu.2016.00546

359. Lefranc M-PL and G. *The Immunoglobulin FactsBook*. 1st ed.; 2001. https://www.elsevier.com/books/the-immunoglobulin-factsbook/lefranc/978-0-12-441351-1.

360. Rodig SJ, Shahsafaei A, Li B, Dorfman DM. The CD45 isoform B220 identifies select subsets of human B cells and B-cell lymphoproliferative disorders. *Hum Pathol*. 2005;36(1):51-57. doi:10.1016/j.humpath.2004.10.016

361. Kalled SL, Siva N, Stein H, Reinherz EL. The distribution of CD10 (NEP 24.11, CALLA) in humans and mice is similar in non-lymphoid organs but differs within the hematopoietic system: absence on murine T and B lymphoid progenitors. *Eur J Immunol*. 1995;25(3):677-687. doi:10.1002/eji.1830250308

362. Egawa T, Kawabata K, Kawamoto H, et al. The earliest stages of B cell development require a chemokine stromal cell-derived factor/pre-B cell growth-stimulating factor. *Immunity*. 2001;15(2):323-334. doi:10.1016/s1074-7613(01)00185-6

363. Prieyl JA, LeBien TW. Interleukin 7 independent development of human B cells. *Proc Natl Acad Sci*. 1996;93(19):10348-10353. doi:10.1073/pnas.93.19.10348

364. Parrish YK, Baez I, Milford T-A, et al. IL-7 Dependence in Human B Lymphopoiesis Increases during Progression of Ontogeny from Cord Blood to Bone Marrow. *J Immunol*. 2009;182(7):4255-4266. doi:10.4049/jimmunol.0800489

365. Nakamori Y, Liu B, Ohishi K, et al. Human bone marrow stromal cells

simultaneously support B and T/NK lineage development from human haematopoietic progenitors: A principal role for flt3 ligand in lymphopoiesis. *Br J Haematol*. 2012;157(6):674-686. doi:10.1111/j.1365-2141.2012.09109.x

366. Taguchi T, Takenouchi H, Matsui J, et al. Involvement of insulin-like growth factor-I and insulin-like growth factor binding proteins in pro-B-cell development. *Exp Hematol*. 2006;34(4):508-518. doi:10.1016/j.exphem.2006.01.009

367. Nuñez C, Nishimoto N, Gartland GL, et al. B cells are generated throughout life in humans. *J Immunol*. 1996;156(2):866-872. http://www.ncbi.nlm.nih.gov/pubmed/8543844. Accessed May 28, 2020.

368. Rossi MID, Yokota T, Medina KL, et al. B lymphopoiesis is active throughout human life, but there are developmental age-related changes. *Blood*. 2003;101(2):576-584. doi:10.1182/blood-2002-03-0896

369. McKenna RW, Washington LBT, Aquino DB, Picker LJ, Kroft SH. Immunophenotypic analysis of hematogones (B-lymphocyte precursors) in 662 consecutive bone marrow specimens by 4-color flow cytometry. *Blood*. 2001;98(8):2498-2507. doi:10.1182/blood.V98.8.2498

370. Johnson SA, Rozzo SJ, Cambier JC. Aging-dependent exclusion of antigen-inexperienced cells from the peripheral B cell repertoire. *J Immunol*. 2002;168(10):5014-5023. doi:10.4049/jimmunol.168.10.5014

371. Rubtsov A V, Rubtsova K, Fischer A, et al. Toll-like receptor 7 (TLR7)-driven accumulation of a novel CD11c^{+} B-cell population is important for the development of autoimmunity. *Blood*. 2011;118(5):1305-1315. doi:10.1182/blood-2011-01-331462

372. Dunn-Walters DK, Stewart AT, Sinclair EL, Serangeli I. Age-Related Changes in B Cells Relevant to Vaccine Responses. *Interdiscip Top Gerontol Geriatr*. 2020;43:56-72. doi:10.1159/000504479

373. Aberle JH, Stiasny K, Kundi M, Heinz FX. Mechanistic insights into the impairment of memory B cells and antibody production in the elderly. *Age (Omaha)*. 2013;35(2):371-381. doi:10.1007/s11357-011-9371-9

374. Smulski CR, Eibel H. BAFF and BAFF-receptor in B cell selection and survival. *Front*

Immunol. 2018;9(OCT):2285. doi:10.3389/fimmu.2018.02285

375. Winters T, McNicoll F, Jessberger R. Meiotic cohesin STAG3 is required for chromosome axis formation and sister chromatid cohesion. *EMBO J*. 2014;33(11):1256-1270. doi:10.1002/embj.201387330

376. Patwari P, Emilsson V, Schadt EE, et al. The arrestin domain-containing 3 protein regulates body mass and energy expenditure. *Cell Metab*. 2011;14(5):671-683. doi:10.1016/j.cmet.2011.08.011

377. Batista TM, Dagdeviren S, Carroll SH, et al. Arrestin domain-containing 3 (Arrdc3) modulates insulin action and glucose metabolism in liver. *Proc Natl Acad Sci U S A*. 2020;117(12):6733-6740. doi:10.1073/pnas.1922370117

378. Flurkey K, Currer JM H DE. *The Mouse in Biomedical Research*. 2nd ed. (JG F, ed.). American College Laboratory Animal Medicine (Elsevier); 2007.

379. Kraus H, Kaiser S, Aumann K, et al. A Feeder-Free Differentiation System Identifies Autonomously Proliferating B Cell Precursors in Human Bone Marrow. *J Immunol*. 2014;192(3):1044-1054. doi:10.4049/jimmunol.1301815

380. Shaw BE. Human leukocyte antigen matching, compatibility testing and donor selection. In: *Hematopoietic Stem Cell Transplantation in Clinical Practice*. Elsevier Ltd; 2009:239-247. doi:10.1016/B978-0-443-10147-2.50027-8

381. Alegre ML. The initiation of graft-versus-host disease. *Am J Transplant*. 2020;20(1):3. doi:10.1111/ajt.15731

382. Shimabukuro-Vornhagen A, Hallek MJ, Storb RF, Von Bergwelt-Baildon MS. The role of B cells in the pathogenesis of graft-versus-host disease. *Blood*. 2009;114(24):4919-4927. doi:10.1182/blood-2008-10-161638

383. Nakane T, Fukuda T, Kanda J, et al. Age influences post-graft-versus-host disease non-relapse mortality in adults with acute graft-versus-host disease of varying severity following allogeneic hematopoietic cell transplant. *Leuk Lymphoma*. 2015;56(8):2392-2397. doi:10.3109/10428194.2015.1009056

384. Schrack JA, Knuth ND, Simonsick EM, Ferrucci L. “IDEAL” aging is associated with lower resting metabolic rate: The baltimore longitudinal study of aging. *J Am Geriatr Soc*. 2014;62(4):667-672. doi:10.1111/jgs.12740

385. Coll RC, Holley CL, Schroder K. Mitochondrial DNA synthesis fuels NLRP3 inflammasome. *Cell Res*. 2018;28(11):1046-1047. doi:10.1038/s41422-018-0093-8

386. Ma Z, Wang H, Cai Y, et al. Epigenetic drift of H3K27me3 in aging links glycolysis to healthy longevity in Drosophila. *Elife*. 2018;7. doi:10.7554/eLife.35368

387. Southworth LK, Owen AB, Kim SK. Aging mice show a decreasing correlation of gene expression within genetic modules. *PLoS Genet*. 2009;5(12):e1000776. doi:10.1371/journal.pgen.1000776

388. Ren R, Ocampo A, Liu G-H, Izpisua Belmonte JC. Regulation of Stem Cell Aging by Metabolism and Epigenetics. *Cell Metab*. 2017;26(3):460-474. doi:10.1016/j.cmet.2017.07.019

389. Labrie JE, Sah AP, Allman DM, Cancro MP, Gerstein RM. Bone marrow microenvironmental changes underlie reduced RAG-mediated recombination and B cell generation in aged mice. *J Exp Med*. 2004;200(4):411-423. doi:10.1084/jem.20040845

390. Fukushima HS, Takeda H, Nakamura R. Targeted in vivo epigenome editing of H3K27me3. *Epigenetics Chromatin*. 2019;12(1):17. doi:10.1186/s13072-019-0263-z

391. Lima JF, Carvalho J, Pinto-Ribeiro I, et al. Targeting miR-9 in gastric cancer cells using locked nucleic acid oligonucleotides. *BMC Mol Biol*. 2018;19(1):6. doi:10.1186/s12867-018-0107-6

392. Henry CJ, Casás-Selves M, Kim J, et al. Aging-associated inflammation promotes selection for adaptive oncogenic events in B cell progenitors. *J Clin Invest*. 2015;125(12):4666-4680. doi:10.1172/JCI83024

393. Latz E, Duewell P. NLRP3 inflammasome activation in inflammaging. *Semin Immunol*. 2018;40:61-73. doi:10.1016/j.smim.2018.09.001

394. Ali MF, Dasari H, Van Keulen VP, Carmona EM. Canonical Stimulation of the NLRP3 Inflammasome by Fungal Antigens Links Innate and Adaptive B-Lymphocyte Responses by Modulating IL-1β and IgM Production. *Front Immunol*. 2017;8:1504. doi:10.3389/fimmu.2017.01504

395. Mohan S, Nakao Y, Honda Y, et al. Studies on the mechanisms by which insulin-like growth factor (IGF) binding protein-4 (IGFBP-4) and IGFBP-5 modulate IGF actions in bone cells. *J Biol Chem*. 1995;270(35):20424-20431. doi:10.1074/jbc.270.35.20424

396. Neumann D, Lienenklaus S, Rosati O, Martin MU. IL-1beta-induced phosphorylation of PKB/Akt depends on the presence of IRAK-1. *Eur J Immunol*. 2002;32(12):3689-3698. doi:10.1002/1521-4141(200212)32:12<3689::AID-IMMU3689>3.0.CO;2-X

397. Rozengurt E, Soares HP, Sinnet-Smith J. Suppression of feedback loops mediated by PI3K/mTOR induces multiple overactivation of compensatory pathways: an unintended consequence leading to drug resistance. *Mol Cancer Ther*. 2014;13(11):2477-2488. doi:10.1158/1535-7163.MCT-14-0330

398. Medford A, Vaupel JW. Human lifespan records are not remarkable but their durations are. Mappes T, ed. *PLoS One*. 2019;14(3):e0212345. doi:10.1371/journal.pone.0212345

8 APPENDICES

APPENDIX 1 – SCIRNASEQ

8.1 sciRNAseq oligo-dT primer sequences

Part of the "Single-cell combinatorial indexing RNAseq (sciRNAseq)" section of Materials & Methods.

Well #	Sequence (5'-3')	Barcode	Sample ID
A1	ACGACGCTCTTCCGATCTNNNNNNNNTTCTCGCATGTTTTTTTTTTTTTTTTTTTTTTTTTTTTTVN	TTCTCGCATG	Young1
A2	ACGACGCTCTTCCGATCTNNNNNNNNTCCTACCAGTTTTTTTTTTTTTTTTTTTTTTTTTTTTTVN	TCCTACCAGT	Young1
A3	ACGACGCTCTTCCGATCTNNNNNNNNGCGTTGGAGCTTTTTTTTTTTTTTTTTTTTTTTTTTTTVN	GCGTTGGAGC	Young1
A4	ACGACGCTCTTCCGATCTNNNNNNNNGATCTTACGCTTTTTTTTTTTTTTTTTTTTTTTTTTTTVN	GATCTTACGC	Young1
A5	ACGACGCTCTTCCGATCTNNNNNNNNCTGATGGTCATTTTTTTTTTTTTTTTTTTTTTTTTTTTVN	CTGATGGTCA	Young1
A6	ACGACGCTCTTCCGATCTNNNNNNNNCCGAGAATCCTTTTTTTTTTTTTTTTTTTTTTTTTTTTVN	CCGAGAATCC	Young1
A7	ACGACGCTCTTCCGATCTNNNNNNNNGCCGCAACGATTTTTTTTTTTTTTTTTTTTTTTTTTTTVN	GCCGCAACGA	Young1
A8	ACGACGCTCTTCCGATCTNNNNNNNNTGAGTCTGGCTTTTTTTTTTTTTTTTTTTTTTTTTTTTVN	TGAGTCTGGC	Young1
B1	ACGACGCTCTTCCGATCTNNNNNNNNTAGAATTAACTTTTTTTTTTTTTTTTTTTTTTTTTTTTVN	TAGAATTAAC	Young1
B2	ACGACGCTCTTCCGATCTNNNNNNNNGCCATTCTCCTTTTTTTTTTTTTTTTTTTTTTTTTTTTVN	GCCATTCTCC	Young1
B3	ACGACGCTCTTCCGATCTNNNNNNNNTGCCGGCAGATTTTTTTTTTTTTTTTTTTTTTTTTTTTTVN	TGCCGGCAGA	Young1
B4	ACGACGCTCTTCCGATCTNNNNNNNNTTACCGAGGCTTTTTTTTTTTTTTTTTTTTTTTTTTTTVN	TTACCGAGGC	Young1
B5	ACGACGCTCTTCCGATCTNNNNNNNNATCATATTAGTTTTTTTTTTTTTTTTTTTTTTTTTTTTVN	ATCATATTAG	Young1
B6	ACGACGCTCTTCCGATCTNNNNNNNNTGGTCAGCCATTTTTTTTTTTTTTTTTTTTTTTTTTTTVN	TGGTCAGCCA	Young1
B7	ACGACGCTCTTCCGATCTNNNNNNNNACTATGCAATTTTTTTTTTTTTTTTTTTTTTTTTTTTTVN	ACTATGCAAT	Young1
B8	ACGACGCTCTTCCGATCTNNNNNNNNCGACGCGACTTTTTTTTTTTTTTTTTTTTTTTTTTTTTVN	CGACGCGACT	Young1
C1	ACGACGCTCTTCCGATCTNNNNNNNNAGAGAAGGTTTTTTTTTTTTTTTTTTTTTTTTTTTTTVN	AGAGAAGGTT	Young1
C2	ACGACGCTCTTCCGATCTNNNNNNNNCATACTCCGATTTTTTTTTTTTTTTTTTTTTTTTTTTTTVN	CATACTCCGA	Young1
C3	ACGACGCTCTTCCGATCTNNNNNNNNGCTAACTTGCTTTTTTTTTTTTTTTTTTTTTTTTTTTTVN	GCTAACTTGC	Young1
C4	ACGACGCTCTTCCGATCTNNNNNNNNAATCCATCTTTTTTTTTTTTTTTTTTTTTTTTTTTTTVN	AATCCATCTT	Young1
C5	ACGACGCTCTTCCGATCTNNNNNNNNGGCTGAGCTCTTTTTTTTTTTTTTTTTTTTTTTTTTTTVN	GGCTGAGCTC	Young1
C6	ACGACGCTCTTCCGATCTNNNNNNNNCCGATTCCTGTTTTTTTTTTTTTTTTTTTTTTTTTTTTVN	CCGATTCCTG	Young1
C7	ACGACGCTCTTCCGATCTNNNNNNNNACCGCCAACCTTTTTTTTTTTTTTTTTTTTTTTTTTTTVN	ACCGCCAACC	Young1
C8	ACGACGCTCTTCCGATCTNNNNNNNNTGGCCTGAAGTTTTTTTTTTTTTTTTTTTTTTTTTTTTVN	TGGCCTGAAG	Young1
D1	ACGACGCTCTTCCGATCTNNNNNNNNTATATACTAATTTTTTTTTTTTTTTTTTTTTTTTTTTTTVN	TATATACTAA	Young1
D2	ACGACGCTCTTCCGATCTNNNNNNNNACTTGCTAGATTTTTTTTTTTTTTTTTTTTTTTTTTTTTVN	ACTTGCTAGA	Young1
D3	ACGACGCTCTTCCGATCTNNNNNNNNAACCATTGGATTTTTTTTTTTTTTTTTTTTTTTTTTTTTVN	AACCATTGGA	Young1
D4	ACGACGCTCTTCCGATCTNNNNNNNNTCGCGGTTGGTTTTTTTTTTTTTTTTTTTTTTTTTTTTVN	TCGCGGTTGG	Young1
D5	ACGACGCTCTTCCGATCTNNNNNNNNCGTAGTTACCTTTTTTTTTTTTTTTTTTTTTTTTTTTTVN	CGTAGTTACC	Young1
D6	ACGACGCTCTTCCGATCTNNNNNNNNTCCAATCATCTTTTTTTTTTTTTTTTTTTTTTTTTTTTVN	TCCAATCATC	Young1
D7	ACGACGCTCTTCCGATCTNNNNNNNNAATCGATAATTTTTTTTTTTTTTTTTTTTTTTTTTTTTVN	AATCGATAAT	Young1
D8	ACGACGCTCTTCCGATCTNNNNNNNNCCATTATCTATTTTTTTTTTTTTTTTTTTTTTTTTTTTVN	CCATTATCTA	Young1
E1	ACGACGCTCTTCCGATCTNNNNNNNNCGGTCAAGAATTTTTTTTTTTTTTTTTTTTTTTTTTTTVN	CGGTCAAGAA	Young1

E2	ACGACGCTCTTCCGATCTNNNNNNNNCGCTCCTAACTTTTTTTTTTTTTTTTTTTTTTTTTTTTTVN	CGCTCCTAAC	Young1
E3	ACGACGCTCTTCCGATCTNNNNNNNNATCCATGACTTTTTTTTTTTTTTTTTTTTTTTTTTTTTTVN	ATCCATGACT	Young1
E4	ACGACGCTCTTCCGATCTNNNNNNNNAACCTGGTCTTTTTTTTTTTTTTTTTTTTTTTTTTTTTTVN	AACCTGGTCT	Young1
E5	ACGACGCTCTTCCGATCTNNNNNNNNACCGAAGACCTTTTTTTTTTTTTTTTTTTTTTTTTTTTTTVN	ACCGAAGACC	Young1
E6	ACGACGCTCTTCCGATCTNNNNNNNNGGTACCGGCATTTTTTTTTTTTTTTTTTTTTTTTTTTTTTVN	GGTACCGGCA	Young1
E7	ACGACGCTCTTCCGATCTNNNNNNNNAAGCCAGTTATTTTTTTTTTTTTTTTTTTTTTTTTTTTTVN	AAGCCAGTTA	Young1
E8	ACGACGCTCTTCCGATCTNNNNNNNNTCTTGCCGACTTTTTTTTTTTTTTTTTTTTTTTTTTTTTVN	TCTTGCCGAC	Young1
F1	ACGACGCTCTTCCGATCTNNNNNNNNTCAATCGCATTTTTTTTTTTTTTTTTTTTTTTTTTTTTTVN	TCAATCGCAT	Young1
F2	ACGACGCTCTTCCGATCTNNNNNNNNTTCTTAATAATTTTTTTTTTTTTTTTTTTTTTTTTTTTTVN	TTCTTAATAA	Young1
F3	ACGACGCTCTTCCGATCTNNNNNNNNGTCCTAGAGGTTTTTTTTTTTTTTTTTTTTTTTTTTTTTVN	GTCCTAGAGG	Young1
F4	ACGACGCTCTTCCGATCTNNNNNNNNATATTGATACTTTTTTTTTTTTTTTTTTTTTTTTTTTTTVN	ATATTGATAC	Young1
F5	ACGACGCTCTTCCGATCTNNNNNNNNCCGCTGCCAGTTTTTTTTTTTTTTTTTTTTTTTTTTTTTVN	CCGCTGCCAG	Young1
F6	ACGACGCTCTTCCGATCTNNNNNNNNCCTAGTACGTTTTTTTTTTTTTTTTTTTTTTTTTTTTTVN	CCTAGTACGT	Young1
F7	ACGACGCTCTTCCGATCTNNNNNNNNCAATTACCGTTTTTTTTTTTTTTTTTTTTTTTTTTTTTVN	CAATTACCGT	Young1
F8	ACGACGCTCTTCCGATCTNNNNNNNNGGCCGTAGTCTTTTTTTTTTTTTTTTTTTTTTTTTTTTTVN	GGCCGTAGTC	Young1
G1	ACGACGCTCTTCCGATCTNNNNNNNNGCTCAGCCGGTTTTTTTTTTTTTTTTTTTTTTTTTTTTTVN	GCTCAGCCGG	Young1
G2	ACGACGCTCTTCCGATCTNNNNNNNNACGTCCGCAGTTTTTTTTTTTTTTTTTTTTTTTTTTTTTVN	ACGTCCGCAG	Young1
G3	ACGACGCTCTTCCGATCTNNNNNNNNTTGACTGACGTTTTTTTTTTTTTTTTTTTTTTTTTTTTTVN	TTGACTGACG	Young1
G4	ACGACGCTCTTCCGATCTNNNNNNNNTTGCGAGGCATTTTTTTTTTTTTTTTTTTTTTTTTTTTTVN	TTGCGAGGCA	Young1
G5	ACGACGCTCTTCCGATCTNNNNNNNNTTCCAACCGCTTTTTTTTTTTTTTTTTTTTTTTTTTTTTVN	TTCCAACCGC	Young1
G6	ACGACGCTCTTCCGATCTNNNNNNNNTAACCTTCGGTTTTTTTTTTTTTTTTTTTTTTTTTTTTTVN	TAACCTTCGG	Young1
G7	ACGACGCTCTTCCGATCTNNNNNNNNTCAAGCCGATTTTTTTTTTTTTTTTTTTTTTTTTTTTTTVN	TCAAGCCGAT	Young1
G8	ACGACGCTCTTCCGATCTNNNNNNNNCTTGCAACCTTTTTTTTTTTTTTTTTTTTTTTTTTTTTTVN	CTTGCAACCT	Young1
H1	ACGACGCTCTTCCGATCTNNNNNNNNTTGCCTTGGCTTTTTTTTTTTTTTTTTTTTTTTTTTTTTVN	TTGCCTTGGC	Young1
H2	ACGACGCTCTTCCGATCTNNNNNNNNTGCTAATTCTTTTTTTTTTTTTTTTTTTTTTTTTTTTTTVN	TGCTAATTCT	Young1
H3	ACGACGCTCTTCCGATCTNNNNNNNNGTCCTACTTGTTTTTTTTTTTTTTTTTTTTTTTTTTTTTVN	GTCCTACTTG	Young1
H4	ACGACGCTCTTCCGATCTNNNNNNNNGGTAGGTTAGTTTTTTTTTTTTTTTTTTTTTTTTTTTTTVN	GGTAGGTTAG	Young1
H5	ACGACGCTCTTCCGATCTNNNNNNNNGAGCATCATTTTTTTTTTTTTTTTTTTTTTTTTTTTTTTVN	GAGCATCATT	Young1
H6	ACGACGCTCTTCCGATCTNNNNNNNNCCGCTCCGGCTTTTTTTTTTTTTTTTTTTTTTTTTTTTTVN	CCGCTCCGGC	Young1
H7	ACGACGCTCTTCCGATCTNNNNNNNNTTCTTCCGGTTTTTTTTTTTTTTTTTTTTTTTTTTTTTTVN	TTCTTCCGGT	Young1
H8	ACGACGCTCTTCCGATCTNNNNNNNNAGGAGAGAACTTTTTTTTTTTTTTTTTTTTTTTTTTTTTTTVN	AGGAGAGAAC	Young1
A9	ACGACGCTCTTCCGATCTNNNNNNNNTGCGGACCTATTTTTTTTTTTTTTTTTTTTTTTTTTTTTTVN	TGCGGACCTA	Young2
A10	ACGACGCTCTTCCGATCTNNNNNNNNACCTCGTTGATTTTTTTTTTTTTTTTTTTTTTTTTTTTTTVN	ACCTCGTTGA	Young2
A11	ACGACGCTCTTCCGATCTNNNNNNNNACGGAGGCGGTTTTTTTTTTTTTTTTTTTTTTTTTTTTTTTVN	ACGGAGGCGG	Young2
A12	ACGACGCTCTTCCGATCTNNNNNNNNTAGATCTACTTTTTTTTTTTTTTTTTTTTTTTTTTTTTTTVN	TAGATCTACT	Young2
A13	ACGACGCTCTTCCGATCTNNNNNNNNAATTAAGACTTTTTTTTTTTTTTTTTTTTTTTTTTTTTTTVN	AATTAAGACT	Young2
A14	ACGACGCTCTTCCGATCTNNNNNNNNCCATTGCGTTTTTTTTTTTTTTTTTTTTTTTTTTTTTTTVN	CCATTGCGTT	Young2
A15	ACGACGCTCTTCCGATCTNNNNNNNNTTATTCATTCTTTTTTTTTTTTTTTTTTTTTTTTTTTTTVN	TTATTCATTC	Young2
B9	ACGACGCTCTTCCGATCTNNNNNNNNGATACGGAACTTTTTTTTTTTTTTTTTTTTTTTTTTTTTTVN	GATACGGAAC	Young2
B10	ACGACGCTCTTCCGATCTNNNNNNNNTTATCCGGATTTTTTTTTTTTTTTTTTTTTTTTTTTTTTVN	TTATCCGGAT	Young2
B11	ACGACGCTCTTCCGATCTNNNNNNNNTAGAGTAATATTTTTTTTTTTTTTTTTTTTTTTTTTTTTVN	TAGAGTAATA	Young2
B12	ACGACGCTCTTCCGATCTNNNNNNNNGCAGGTCCGTTTTTTTTTTTTTTTTTTTTTTTTTTTTTTVN	GCAGGTCCGT	Young2
B13	ACGACGCTCTTCCGATCTNNNNNNNNTCGGCCTTACTTTTTTTTTTTTTTTTTTTTTTTTTTTTTVN	TCGGCCTTAC	Young2
B14	ACGACGCTCTTCCGATCTNNNNNNNNAGAACGTCTCTTTTTTTTTTTTTTTTTTTTTTTTTTTTTVN	AGAACGTCTC	Young2
B15	ACGACGCTCTTCCGATCTNNNNNNNNCCAGTTCCAATTTTTTTTTTTTTTTTTTTTTTTTTTTTTVN	CCAGTTCCAA	Young2
C9	ACGACGCTCTTCCGATCTNNNNNNNNAACCTCATTCTTTTTTTTTTTTTTTTTTTTTTTTTTTTTVN	AACCTCATTC	Young2
C10	ACGACGCTCTTCCGATCTNNNNNNNNATAAGGAGCATTTTTTTTTTTTTTTTTTTTTTTTTTTTTTVN	ATAAGGAGCA	Young2
C11	ACGACGCTCTTCCGATCTNNNNNNNNCGAACGCCGGTTTTTTTTTTTTTTTTTTTTTTTTTTTTTTVN	CGAACGCCGG	Young2

C12	ACGACGCTCTTCCGATCTNNNNNNNNGGTATGCTTGTTTTTTTTTTTTTTTTTTTTTTTTTTTTTVN	GGTATGCTTG	Young2
C13	ACGACGCTCTTCCGATCTNNNNNNNNAACCTGCGTATTTTTTTTTTTTTTTTTTTTTTTTTTTTTTVN	AACCTGCGTA	Young2
C14	ACGACGCTCTTCCGATCTNNNNNNNNGGCAGACGCCTTTTTTTTTTTTTTTTTTTTTTTTTTTTTTVN	GGCAGACGCC	Young2
C15	ACGACGCTCTTCCGATCTNNNNNNNNTAGCCGTCATTTTTTTTTTTTTTTTTTTTTTTTTTTTTTVN	TAGCCGTCAT	Young2
D9	ACGACGCTCTTCCGATCTNNNNNNNNTCAACGTAAGTTTTTTTTTTTTTTTTTTTTTTTTTTTTTTVN	TCAACGTAAG	Young2
D10	ACGACGCTCTTCCGATCTNNNNNNNNTCTAATAGTATTTTTTTTTTTTTTTTTTTTTTTTTTTTTTVN	TCTAATAGTA	Young2
D11	ACGACGCTCTTCCGATCTNNNNNNNNAACCGCTGGTTTTTTTTTTTTTTTTTTTTTTTTTTTTTTVN	AACCGCTGGT	Young2
D12	ACGACGCTCTTCCGATCTNNNNNNNNGATCGCTTCTTTTTTTTTTTTTTTTTTTTTTTTTTTTTTVN	GATCGCTTCT	Young2
D13	ACGACGCTCTTCCGATCTNNNNNNNNCTAACTAGATTTTTTTTTTTTTTTTTTTTTTTTTTTTTTVN	CTAACTAGAT	Young2
D14	ACGACGCTCTTCCGATCTNNNNNNNNGCTGGAACTTTTTTTTTTTTTTTTTTTTTTTTTTTTTTVN	GCTGGAACTT	Young2
D15	ACGACGCTCTTCCGATCTNNNNNNNNAGGTTAGTTCTTTTTTTTTTTTTTTTTTTTTTTTTTTTTVN	AGGTTAGTTC	Young2
E9	ACGACGCTCTTCCGATCTNNNNNNNNAAGACCGTTGTTTTTTTTTTTTTTTTTTTTTTTTTTTTTVN	AAGACCGTTG	Young2
E10	ACGACGCTCTTCCGATCTNNNNNNNNAGGTTAGCATTTTTTTTTTTTTTTTTTTTTTTTTTTTTTVN	AGGTTAGCAT	Young2
E11	ACGACGCTCTTCCGATCTNNNNNNNNTTCGCCTCCATTTTTTTTTTTTTTTTTTTTTTTTTTTTTVN	TTCGCCTCCA	Young2
E12	ACGACGCTCTTCCGATCTNNNNNNNNAGAGCCAAGGTTTTTTTTTTTTTTTTTTTTTTTTTTTTTTVN	AGAGCCAAGG	Young2
E13	ACGACGCTCTTCCGATCTNNNNNNNNAATACCATCCTTTTTTTTTTTTTTTTTTTTTTTTTTTTTTVN	AATACCATCC	Young2
E14	ACGACGCTCTTCCGATCTNNNNNNNNAGCTCTCCTCTTTTTTTTTTTTTTTTTTTTTTTTTTTTTTVN	AGCTCTCCTC	Young2
E15	ACGACGCTCTTCCGATCTNNNNNNNNCTTGATTGCCTTTTTTTTTTTTTTTTTTTTTTTTTTTTTTVN	CTTGATTGCC	Young2
F9	ACGACGCTCTTCCGATCTNNNNNNNNCGATTACGGCTTTTTTTTTTTTTTTTTTTTTTTTTTTTTTVN	CGATTACGGC	Young2
F10	ACGACGCTCTTCCGATCTNNNNNNNNTAATGAACGATTTTTTTTTTTTTTTTTTTTTTTTTTTTTTVN	TAATGAACGA	Young2
F11	ACGACGCTCTTCCGATCTNNNNNNNNCCGTTCCTTATTTTTTTTTTTTTTTTTTTTTTTTTTTTTVN	CCGTTCCTTA	Young2
F12	ACGACGCTCTTCCGATCTNNNNNNNNGGTACCATATTTTTTTTTTTTTTTTTTTTTTTTTTTTTTTVN	GGTACCATAT	Young2
F13	ACGACGCTCTTCCGATCTNNNNNNNNCCGATTCGCATTTTTTTTTTTTTTTTTTTTTTTTTTTTTTVN	CCGATTCGCA	Young2
F14	ACGACGCTCTTCCGATCTNNNNNNNNATGGCTCTGCTTTTTTTTTTTTTTTTTTTTTTTTTTTTTTVN	ATGGCTCTGC	Young2
F15	ACGACGCTCTTCCGATCTNNNNNNNNGTATAATACGTTTTTTTTTTTTTTTTTTTTTTTTTTTTTTVN	GTATAATACG	Young2
G9	ACGACGCTCTTCCGATCTNNNNNNNNCCATCGCGAATTTTTTTTTTTTTTTTTTTTTTTTTTTTTTVN	CCATCGCGAA	Young2
G10	ACGACGCTCTTCCGATCTNNNNNNNNTAGACTTCTTTTTTTTTTTTTTTTTTTTTTTTTTTTTTVN	TAGACTTCTT	Young2
G11	ACGACGCTCTTCCGATCTNNNNNNNNGTCCTTAAGATTTTTTTTTTTTTTTTTTTTTTTTTTTTTTVN	GTCCTTAAGA	Young2
G12	ACGACGCTCTTCCGATCTNNNNNNNNAGTAACGGTCTTTTTTTTTTTTTTTTTTTTTTTTTTTTTTVN	AGTAACGGTC	Young2
G13	ACGACGCTCTTCCGATCTNNNNNNNNGTTCGTCAGATTTTTTTTTTTTTTTTTTTTTTTTTTTTTTVN	GTTCGTCAGA	Young2
G14	ACGACGCTCTTCCGATCTNNNNNNNNCGCCTAATGCTTTTTTTTTTTTTTTTTTTTTTTTTTTTTTVN	CGCCTAATGC	Young2
G15	ACGACGCTCTTCCGATCTNNNNNNNNACCGGAATTATTTTTTTTTTTTTTTTTTTTTTTTTTTTTTVN	ACCGGAATTA	Young2
H9	ACGACGCTCTTCCGATCTNNNNNNNNTAACTCAATTTTTTTTTTTTTTTTTTTTTTTTTTTTTTTVN	TAACTCAATT	Young2
H10	ACGACGCTCTTCCGATCTNNNNNNNNACTATAGGTTTTTTTTTTTTTTTTTTTTTTTTTTTTTTTVN	ACTATAGGTT	Young2
H11	ACGACGCTCTTCCGATCTNNNNNNNNCAAGATGCCGTTTTTTTTTTTTTTTTTTTTTTTTTTTTTTVN	CAAGATGCCG	Young2
H12	ACGACGCTCTTCCGATCTNNNNNNNNAACGTCTAGTTTTTTTTTTTTTTTTTTTTTTTTTTTTTTVN	AACGTCTAGT	Young2
H13	ACGACGCTCTTCCGATCTNNNNNNNNAGGTATACTCTTTTTTTTTTTTTTTTTTTTTTTTTTTTTTVN	AGGTATACTC	Young2
H14	ACGACGCTCTTCCGATCTNNNNNNNNTTCATAGGACTTTTTTTTTTTTTTTTTTTTTTTTTTTTTTVN	TTCATAGGAC	Young2
H15	ACGACGCTCTTCCGATCTNNNNNNNNGGAGGCCTCCTTTTTTTTTTTTTTTTTTTTTTTTTTTTTTVN	GGAGGCCTCC	Young2
A16	ACGACGCTCTTCCGATCTNNNNNNNNATCTCCGAACTTTTTTTTTTTTTTTTTTTTTTTTTTTTTTVN	ATCTCCGAAC	Young3
A17	ACGACGCTCTTCCGATCTNNNNNNNNTTGACTTCAGTTTTTTTTTTTTTTTTTTTTTTTTTTTTTTVN	TTGACTTCAG	Young3
A18	ACGACGCTCTTCCGATCTNNNNNNNNGGCAGGTATTTTTTTTTTTTTTTTTTTTTTTTTTTTTTTVN	GGCAGGTATT	Young3
A19	ACGACGCTCTTCCGATCTNNNNNNNNAGAGCTATAATTTTTTTTTTTTTTTTTTTTTTTTTTTTTTVN	AGAGCTATAA	Young3
A20	ACGACGCTCTTCCGATCTNNNNNNNNCTAAGAGAAGTTTTTTTTTTTTTTTTTTTTTTTTTTTTTTVN	CTAAGAGAAG	Young3
A21	ACGACGCTCTTCCGATCTNNNNNNNNACTCAATAGGTTTTTTTTTTTTTTTTTTTTTTTTTTTTTTVN	ACTCAATAGG	Young3
A22	ACGACGCTCTTCCGATCTNNNNNNNNCTTGCGCCGCTTTTTTTTTTTTTTTTTTTTTTTTTTTTTTVN	CTTGCGCCGC	Young3
A23	ACGACGCTCTTCCGATCTNNNNNNNNAATCGTAGCGTTTTTTTTTTTTTTTTTTTTTTTTTTTTTTVN	AATCGTAGCG	Young3
A24	ACGACGCTCTTCCGATCTNNNNNNNNGGTACTGCCTTTTTTTTTTTTTTTTTTTTTTTTTTTTTTVN	GGTACTGCCT	Young3

B16	ACGACGCTCTTCCGATCTNNNNNNNNGGCGTTAAGGTTTTTTTTTTTTTTTTTTTTTTTTTTTTTTVN	GGCGTTAAGG	Young3
B17	ACGACGCTCTTCCGATCTNNNNNNNNACTTAACCTTTTTTTTTTTTTTTTTTTTTTTTTTTTTTVN	ACTTAACCTT	Young3
B18	ACGACGCTCTTCCGATCTNNNNNNNNCAACCGCTAATTTTTTTTTTTTTTTTTTTTTTTTTTTTTTVN	CAACCGCTAA	Young3
B19	ACGACGCTCTTCCGATCTNNNNNNNNGACCTTGATATTTTTTTTTTTTTTTTTTTTTTTTTTTTTTVN	GACCTTGATA	Young3
B20	ACGACGCTCTTCCGATCTNNNNNNNNTCTGATACCATTTTTTTTTTTTTTTTTTTTTTTTTTTTTTVN	TCTGATACCA	Young3
B21	ACGACGCTCTTCCGATCTNNNNNNNNGAAGATCGAGTTTTTTTTTTTTTTTTTTTTTTTTTTTTTTVN	GAAGATCGAG	Young3
B22	ACGACGCTCTTCCGATCTNNNNNNNNAGGAGCGGTATTTTTTTTTTTTTTTTTTTTTTTTTTTTTTVN	AGGAGCGGTA	Young3
B23	ACGACGCTCTTCCGATCTNNNNNNNNAAGAAGCTAGTTTTTTTTTTTTTTTTTTTTTTTTTTTTTTVN	AAGAAGCTAG	Young3
B24	ACGACGCTCTTCCGATCTNNNNNNNNTCCGGCCTCGTTTTTTTTTTTTTTTTTTTTTTTTTTTTTTVN	TCCGGCCTCG	Young3
C16	ACGACGCTCTTCCGATCTNNNNNNNNCCTGGAAGAGTTTTTTTTTTTTTTTTTTTTTTTTTTTTTTVN	CCTGGAAGAG	Young3
C17	ACGACGCTCTTCCGATCTNNNNNNNNGGAGGTTCTATTTTTTTTTTTTTTTTTTTTTTTTTTTTTTVN	GGAGGTTCTA	Young3
C18	ACGACGCTCTTCCGATCTNNNNNNNNCTAGTAGTCTTTTTTTTTTTTTTTTTTTTTTTTTTTTTTVN	CTAGTAGTCT	Young3
C19	ACGACGCTCTTCCGATCTNNNNNNNNATCATCAACGTTTTTTTTTTTTTTTTTTTTTTTTTTTTTTVN	ATCATCAACG	Young3
C20	ACGACGCTCTTCCGATCTNNNNNNNNACGCGAGATTTTTTTTTTTTTTTTTTTTTTTTTTTTTTTVN	ACGCGAGATT	Young3
C21	ACGACGCTCTTCCGATCTNNNNNNNNGAAGAGGCATTTTTTTTTTTTTTTTTTTTTTTTTTTTTTTVN	GAAGAGGCAT	Young3
C22	ACGACGCTCTTCCGATCTNNNNNNNNGGTATCCGCCTTTTTTTTTTTTTTTTTTTTTTTTTTTTTTVN	GGTATCCGCC	Young3
C23	ACGACGCTCTTCCGATCTNNNNNNNNAACTAGGCGCTTTTTTTTTTTTTTTTTTTTTTTTTTTTTTVN	AACTAGGCGC	Young3
C24	ACGACGCTCTTCCGATCTNNNNNNNNTCGCTAAGCATTTTTTTTTTTTTTTTTTTTTTTTTTTTTTVN	TCGCTAAGCA	Young3
D16	ACGACGCTCTTCCGATCTNNNNNNNNCATTCGACGGTTTTTTTTTTTTTTTTTTTTTTTTTTTTTTVN	CATTCGACGG	Young3
D17	ACGACGCTCTTCCGATCTNNNNNNNNCATTCAATCATTTTTTTTTTTTTTTTTTTTTTTTTTTTTTVN	CATTCAATCA	Young3
D18	ACGACGCTCTTCCGATCTNNNNNNNNCGGATTAGAATTTTTTTTTTTTTTTTTTTTTTTTTTTTTTVN	CGGATTAGAA	Young3
D19	ACGACGCTCTTCCGATCTNNNNNNNNATCGGCTATCTTTTTTTTTTTTTTTTTTTTTTTTTTTTTTVN	ATCGGCTATC	Young3
D20	ACGACGCTCTTCCGATCTNNNNNNNNCCTTGATCGTTTTTTTTTTTTTTTTTTTTTTTTTTTTTTVN	CCTTGATCGT	Young3
D21	ACGACGCTCTTCCGATCTNNNNNNNNACGAAGTCAATTTTTTTTTTTTTTTTTTTTTTTTTTTTTTVN	ACGAAGTCAA	Young3
D22	ACGACGCTCTTCCGATCTNNNNNNNNTTACCTCGACTTTTTTTTTTTTTTTTTTTTTTTTTTTTTTVN	TTACCTCGAC	Young3
D23	ACGACGCTCTTCCGATCTNNNNNNNNGGAGGATAGCTTTTTTTTTTTTTTTTTTTTTTTTTTTTTTVN	GGAGGATAGC	Young3
D24	ACGACGCTCTTCCGATCTNNNNNNNNGGCTCTCTATTTTTTTTTTTTTTTTTTTTTTTTTTTTTTVN	GGCTCTCTAT	Young3
E16	ACGACGCTCTTCCGATCTNNNNNNNNAGCTTATCCGTTTTTTTTTTTTTTTTTTTTTTTTTTTTTTVN	AGCTTATCCG	Young3
E17	ACGACGCTCTTCCGATCTNNNNNNNNAAGAATCTGATTTTTTTTTTTTTTTTTTTTTTTTTTTTTTVN	AAGAATCTGA	Young3
E18	ACGACGCTCTTCCGATCTNNNNNNNNCATCTCTGCATTTTTTTTTTTTTTTTTTTTTTTTTTTTTTVN	CATCTCTGCA	Young3
E19	ACGACGCTCTTCCGATCTNNNNNNNNACCTGGCCAATTTTTTTTTTTTTTTTTTTTTTTTTTTTTTVN	ACCTGGCCAA	Young3
E20	ACGACGCTCTTCCGATCTNNNNNNNNTAACTGGTTATTTTTTTTTTTTTTTTTTTTTTTTTTTTTTVN	TAACTGGTTA	Young3
E21	ACGACGCTCTTCCGATCTNNNNNNNNTTGCTAACGGTTTTTTTTTTTTTTTTTTTTTTTTTTTTTTVN	TTGCTAACGG	Young3
E22	ACGACGCTCTTCCGATCTNNNNNNNNACTAGAGAGTTTTTTTTTTTTTTTTTTTTTTTTTTTTTTVN	ACTAGAGAGT	Young3
E23	ACGACGCTCTTCCGATCTNNNNNNNNAATGCCGCTTTTTTTTTTTTTTTTTTTTTTTTTTTTTTVN	AATGCCGCTT	Young3
E24	ACGACGCTCTTCCGATCTNNNNNNNNTATAGACGCATTTTTTTTTTTTTTTTTTTTTTTTTTTTTTVN	TATAGACGCA	Young3
F16	ACGACGCTCTTCCGATCTNNNNNNNNATCAGCAAGTTTTTTTTTTTTTTTTTTTTTTTTTTTTTTVN	ATCAGCAAGT	Young3
F17	ACGACGCTCTTCCGATCTNNNNNNNNGGCGAACTCGTTTTTTTTTTTTTTTTTTTTTTTTTTTTTTVN	GGCGAACTCG	Young3
F18	ACGACGCTCTTCCGATCTNNNNNNNNTTAATTGAATTTTTTTTTTTTTTTTTTTTTTTTTTTTTTVN	TTAATTGAAT	Young3
F19	ACGACGCTCTTCCGATCTNNNNNNNNTTAGGACCGGTTTTTTTTTTTTTTTTTTTTTTTTTTTTTTVN	TTAGGACCGG	Young3
F20	ACGACGCTCTTCCGATCTNNNNNNNNAAGTAAGAGCTTTTTTTTTTTTTTTTTTTTTTTTTTTTTTVN	AAGTAAGAGC	Young3
F21	ACGACGCTCTTCCGATCTNNNNNNNNCCTTGGTCCATTTTTTTTTTTTTTTTTTTTTTTTTTTTTTVN	CCTTGGTCCA	Young3
F22	ACGACGCTCTTCCGATCTNNNNNNNNCATCAGAATGTTTTTTTTTTTTTTTTTTTTTTTTTTTTTTVN	CATCAGAATG	Young3
F23	ACGACGCTCTTCCGATCTNNNNNNNNTTATAGCAGATTTTTTTTTTTTTTTTTTTTTTTTTTTTTTVN	TTATAGCAGA	Young3
F24	ACGACGCTCTTCCGATCTNNNNNNNNTTACTTGGAATTTTTTTTTTTTTTTTTTTTTTTTTTTTTTVN	TTACTTGGAA	Young3
G16	ACGACGCTCTTCCGATCTNNNNNNNNTAGGCCATAGTTTTTTTTTTTTTTTTTTTTTTTTTTTTTTVN	TAGGCCATAG	Young3
G17	ACGACGCTCTTCCGATCTNNNNNNNNTAACTCTTAGTTTTTTTTTTTTTTTTTTTTTTTTTTTTTTVN	TAACTCTTAG	Young3
G18	ACGACGCTCTTCCGATCTNNNNNNNNTATGAGTTAATTTTTTTTTTTTTTTTTTTTTTTTTTTTTTVN	TATGAGTTAA	Young3

G19	ACGACGCTCTTCCGATCTNNNNNNNNNTATCATGATCTTTTTTTTTTTTTTTTTTTTTTTTTTTTTVN	TATCATGATC	Young3
G20	ACGACGCTCTTCCGATCTNNNNNNNNGAGCATATGGTTTTTTTTTTTTTTTTTTTTTTTTTTTTTVN	GAGCATATGG	Young3
G21	ACGACGCTCTTCCGATCTNNNNNNNNNTAACGATCCATTTTTTTTTTTTTTTTTTTTTTTTTTTTTVN	TAACGATCCA	Young3
G22	ACGACGCTCTTCCGATCTNNNNNNNNNCGGCGTAACTTTTTTTTTTTTTTTTTTTTTTTTTTTTVN	CGGCGTAACT	Young3
G23	ACGACGCTCTTCCGATCTNNNNNNNNNCGTCGCAGCCTTTTTTTTTTTTTTTTTTTTTTTTTTTTVN	CGTCGCAGCC	Young3
G24	ACGACGCTCTTCCGATCTNNNNNNNNNGTAGCTCCATTTTTTTTTTTTTTTTTTTTTTTTTTTTTVN	GTAGCTCCAT	Young3
H16	ACGACGCTCTTCCGATCTNNNNNNNNNTTCAATATAATTTTTTTTTTTTTTTTTTTTTTTTTTTTVN	TTCAATATAA	Young3
H17	ACGACGCTCTTCCGATCTNNNNNNNNNACGTCATATATTTTTTTTTTTTTTTTTTTTTTTTTTTTVN	ACGTCATATA	Young3
H18	ACGACGCTCTTCCGATCTNNNNNNNNNTTGACCAGGATTTTTTTTTTTTTTTTTTTTTTTTTTTTVN	TTGACCAGGA	Young3
H19	ACGACGCTCTTCCGATCTNNNNNNNNNCGGTTGCGCGTTTTTTTTTTTTTTTTTTTTTTTTTTTTVN	CGGTTGCGCG	Young3
H20	ACGACGCTCTTCCGATCTNNNNNNNNNCAAGGAGGTCTTTTTTTTTTTTTTTTTTTTTTTTTTTTVN	CAAGGAGGTC	Young3
H21	ACGACGCTCTTCCGATCTNNNNNNNNNTTACGATGAATTTTTTTTTTTTTTTTTTTTTTTTTTTTVN	TTACGATGAA	Young3
H22	ACGACGCTCTTCCGATCTNNNNNNNNNTTGCTGGCATTTTTTTTTTTTTTTTTTTTTTTTTTTTVN	TTGCTGGCAT	Young3
H23	ACGACGCTCTTCCGATCTNNNNNNNNNGAGGCATCAATTTTTTTTTTTTTTTTTTTTTTTTTTTTVN	GAGGCATCAA	Young3
H24	ACGACGCTCTTCCGATCTNNNNNNNNNATTCGACCAATTTTTTTTTTTTTTTTTTTTTTTTTTTTVN	ATTCGACCAA	Young3
I1	ACGACGCTCTTCCGATCTNNNNNNNNNCCGCGGCTCATTTTTTTTTTTTTTTTTTTTTTTTTTTTVN	CCGCGGCTCA	Aged1
I2	ACGACGCTCTTCCGATCTNNNNNNNNNGGCTCCTCGTTTTTTTTTTTTTTTTTTTTTTTTTTTTVN	GGCTCCTCGT	Aged1
I3	ACGACGCTCTTCCGATCTNNNNNNNNNGTTACGCAAGTTTTTTTTTTTTTTTTTTTTTTTTTTTTVN	GTTACGCAAG	Aged1
I4	ACGACGCTCTTCCGATCTNNNNNNNNNAGCCGGTACCTTTTTTTTTTTTTTTTTTTTTTTTTTTTVN	AGCCGGTACC	Aged1
I5	ACGACGCTCTTCCGATCTNNNNNNNNNACCTCTATCTTTTTTTTTTTTTTTTTTTTTTTTTTTTVN	ACCTCTATCT	Aged1
I6	ACGACGCTCTTCCGATCTNNNNNNNNNGGACTACTACTTTTTTTTTTTTTTTTTTTTTTTTTTTTVN	GGACTACTAC	Aged1
I7	ACGACGCTCTTCCGATCTNNNNNNNNNGTATCATCGATTTTTTTTTTTTTTTTTTTTTTTTTTTTTVN	GTATCATCGA	Aged1
I8	ACGACGCTCTTCCGATCTNNNNNNNNNCCGCGATTATTTTTTTTTTTTTTTTTTTTTTTTTTTTTVN	CCGCGATTAT	Aged1
J1	ACGACGCTCTTCCGATCTNNNNNNNNNCAGGAGGAGATTTTTTTTTTTTTTTTTTTTTTTTTTTTTTVN	CAGGAGGAGA	Aged1
J2	ACGACGCTCTTCCGATCTNNNNNNNNNGATATCGGCGTTTTTTTTTTTTTTTTTTTTTTTTTTTTTVN	GATATCGGCG	Aged1
J3	ACGACGCTCTTCCGATCTNNNNNNNNNCCAGTCCTCTTTTTTTTTTTTTTTTTTTTTTTTTTTTTVN	CCAGTCCTCT	Aged1
J4	ACGACGCTCTTCCGATCTNNNNNNNNNCATAGTTCGGTTTTTTTTTTTTTTTTTTTTTTTTTTTTTVN	CATAGTTCGG	Aged1
J5	ACGACGCTCTTCCGATCTNNNNNNNNNCGTAATGCAGTTTTTTTTTTTTTTTTTTTTTTTTTTTTTVN	CGTAATGCAG	Aged1
J6	ACGACGCTCTTCCGATCTNNNNNNNNNCCGTTCGGATTTTTTTTTTTTTTTTTTTTTTTTTTTTTVN	CCGTTCGGAT	Aged1
J7	ACGACGCTCTTCCGATCTNNNNNNNNNCCATAAGTCCTTTTTTTTTTTTTTTTTTTTTTTTTTTTTVN	CCATAAGTCC	Aged1
J8	ACGACGCTCTTCCGATCTNNNNNNNNNGGCAATGAGATTTTTTTTTTTTTTTTTTTTTTTTTTTTTTVN	GGCAATGAGA	Aged1
K1	ACGACGCTCTTCCGATCTNNNNNNNNNCGGTCGTTAATTTTTTTTTTTTTTTTTTTTTTTTTTTTTVN	CGGTCGTTAA	Aged1
K2	ACGACGCTCTTCCGATCTNNNNNNNNNATGGCGGATCTTTTTTTTTTTTTTTTTTTTTTTTTTTTTVN	ATGGCGGATC	Aged1
K3	ACGACGCTCTTCCGATCTNNNNNNNNNCTCTGATCAGTTTTTTTTTTTTTTTTTTTTTTTTTTTTTVN	CTCTGATCAG	Aged1
K4	ACGACGCTCTTCCGATCTNNNNNNNNNGGCCAGTCCGTTTTTTTTTTTTTTTTTTTTTTTTTTTTTVN	GGCCAGTCCG	Aged1
K5	ACGACGCTCTTCCGATCTNNNNNNNNNCGGAAGATATTTTTTTTTTTTTTTTTTTTTTTTTTTTTTVN	CGGAAGATAT	Aged1
K6	ACGACGCTCTTCCGATCTNNNNNNNNNTGGCTGATGATTTTTTTTTTTTTTTTTTTTTTTTTTTTTVN	TGGCTGATGA	Aged1
K7	ACGACGCTCTTCCGATCTNNNNNNNNNGAAGGTTGCCTTTTTTTTTTTTTTTTTTTTTTTTTTTTTVN	GAAGGTTGCC	Aged1
K8	ACGACGCTCTTCCGATCTNNNNNNNNNGTTGAAGGATTTTTTTTTTTTTTTTTTTTTTTTTTTTTTVN	GTTGAAGGAT	Aged1
L1	ACGACGCTCTTCCGATCTNNNNNNNNNAGACTCAAGCTTTTTTTTTTTTTTTTTTTTTTTTTTTTTVN	AGACTCAAGC	Aged1
L2	ACGACGCTCTTCCGATCTNNNNNNNNNGCAGGCGACGTTTTTTTTTTTTTTTTTTTTTTTTTTTTTVN	GCAGGCGACG	Aged1
L3	ACGACGCTCTTCCGATCTNNNNNNNNNAATACTCTTCTTTTTTTTTTTTTTTTTTTTTTTTTTTTTVN	AATACTCTTC	Aged1
L4	ACGACGCTCTTCCGATCTNNNNNNNNNCCAACTAACCTTTTTTTTTTTTTTTTTTTTTTTTTTTTTVN	CCAACTAACC	Aged1
L5	ACGACGCTCTTCCGATCTNNNNNNNNNTATCCTCAATTTTTTTTTTTTTTTTTTTTTTTTTTTTTTVN	TATCCTCAAT	Aged1
L6	ACGACGCTCTTCCGATCTNNNNNNNNNGCCGTCGCGTTTTTTTTTTTTTTTTTTTTTTTTTTTTTTVN	GCCGTCGCGT	Aged1
L7	ACGACGCTCTTCCGATCTNNNNNNNNNCCGCTGCTTCTTTTTTTTTTTTTTTTTTTTTTTTTTTTTVN	CCGCTGCTTC	Aged1
L8	ACGACGCTCTTCCGATCTNNNNNNNNNTGACCGAATCTTTTTTTTTTTTTTTTTTTTTTTTTTTTTVN	TGACCGAATC	Aged1
M1	ACGACGCTCTTCCGATCTNNNNNNNNNGCCGTATGCTTTTTTTTTTTTTTTTTTTTTTTTTTTTTVN	GCCGTATGCT	Aged1

M2	ACGACGCTCTTCCGATCTNNNNNNNNCTGAACTGGTTTTTTTTTTTTTTTTTTTTTTTTTTTTTVN	CTGAACTGGT	Aged1
M3	ACGACGCTCTTCCGATCTNNNNNNNNCATAACCAGCTTTTTTTTTTTTTTTTTTTTTTTTTTTTTVN	CATAACCAGC	Aged1
M4	ACGACGCTCTTCCGATCTNNNNNNNNAAGTTGCCATTTTTTTTTTTTTTTTTTTTTTTTTTTTTVN	AAGTTGCCAT	Aged1
M5	ACGACGCTCTTCCGATCTNNNNNNNNAGGCCGCTCGTTTTTTTTTTTTTTTTTTTTTTTTTTTTVN	AGGCCGCTCG	Aged1
M6	ACGACGCTCTTCCGATCTNNNNNNNNAGGTAATAGGTTTTTTTTTTTTTTTTTTTTTTTTTTTTVN	AGGTAATAGG	Aged1
M7	ACGACGCTCTTCCGATCTNNNNNNNNGTACTAGTAATTTTTTTTTTTTTTTTTTTTTTTTTTTTVN	GTACTAGTAA	Aged1
M8	ACGACGCTCTTCCGATCTNNNNNNNNGCGCGGTAGTTTTTTTTTTTTTTTTTTTTTTTTTTTTVN	GCGCGGTAGT	Aged1
N1	ACGACGCTCTTCCGATCTNNNNNNNNTCAGCTCTAATTTTTTTTTTTTTTTTTTTTTTTTTTTTVN	TCAGCTCTAA	Aged1
N2	ACGACGCTCTTCCGATCTNNNNNNNNCGAATAGATGTTTTTTTTTTTTTTTTTTTTTTTTTTTTVN	CGAATAGATG	Aged1
N3	ACGACGCTCTTCCGATCTNNNNNNNNCGGAGATCCGTTTTTTTTTTTTTTTTTTTTTTTTTTTTVN	CGGAGATCCG	Aged1
N4	ACGACGCTCTTCCGATCTNNNNNNNNACCGCAGAATTTTTTTTTTTTTTTTTTTTTTTTTTTTTVN	ACCGCAGAAT	Aged1
N5	ACGACGCTCTTCCGATCTNNNNNNNNTCTCCTATAATTTTTTTTTTTTTTTTTTTTTTTTTTTTVN	TCTCCTATAA	Aged1
N6	ACGACGCTCTTCCGATCTNNNNNNNNCAACCTATATTTTTTTTTTTTTTTTTTTTTTTTTTTTTVN	CAACCTATAT	Aged1
N7	ACGACGCTCTTCCGATCTNNNNNNNNAGTCGAGAAGTTTTTTTTTTTTTTTTTTTTTTTTTTTTVN	AGTCGAGAAG	Aged1
N8	ACGACGCTCTTCCGATCTNNNNNNNNAAGACGGCCATTTTTTTTTTTTTTTTTTTTTTTTTTTTVN	AAGACGGCCA	Aged1
O1	ACGACGCTCTTCCGATCTNNNNNNNNCAGATTCGATTTTTTTTTTTTTTTTTTTTTTTTTTTTTVN	CAGATTCGAT	Aged1
O2	ACGACGCTCTTCCGATCTNNNNNNNNTGCATATAACTTTTTTTTTTTTTTTTTTTTTTTTTTTTVN	TGCATATAAC	Aged1
O3	ACGACGCTCTTCCGATCTNNNNNNNNTAGGCAGATATTTTTTTTTTTTTTTTTTTTTTTTTTTTVN	TAGGCAGATA	Aged1
O4	ACGACGCTCTTCCGATCTNNNNNNNNTATGCCGAGTTTTTTTTTTTTTTTTTTTTTTTTTTTTVN	TATGCCGAGT	Aged1
O5	ACGACGCTCTTCCGATCTNNNNNNNNATAGTCGTAGTTTTTTTTTTTTTTTTTTTTTTTTTTTTVN	ATAGTCGTAG	Aged1
O6	ACGACGCTCTTCCGATCTNNNNNNNNGGATGCAGCATTTTTTTTTTTTTTTTTTTTTTTTTTTTVN	GGATGCAGCA	Aged1
O7	ACGACGCTCTTCCGATCTNNNNNNNNCCGCTATATTTTTTTTTTTTTTTTTTTTTTTTTTTTTVN	CCGCTATATT	Aged1
O8	ACGACGCTCTTCCGATCTNNNNNNNNATCGAGTCGCTTTTTTTTTTTTTTTTTTTTTTTTTTTTVN	ATCGAGTCGC	Aged1
P1	ACGACGCTCTTCCGATCTNNNNNNNNAACTGATCTTTTTTTTTTTTTTTTTTTTTTTTTTTTTVN	AACTGATCTT	Aged1
P2	ACGACGCTCTTCCGATCTNNNNNNNNCCGCGGACCGTTTTTTTTTTTTTTTTTTTTTTTTTTTTVN	CCGCGGACCG	Aged1
P3	ACGACGCTCTTCCGATCTNNNNNNNNAATACGCAGGTTTTTTTTTTTTTTTTTTTTTTTTTTTTVN	AATACGCAGG	Aged1
P4	ACGACGCTCTTCCGATCTNNNNNNNNGGTCGCGTCATTTTTTTTTTTTTTTTTTTTTTTTTTTTVN	GGTCGCGTCA	Aged1
P5	ACGACGCTCTTCCGATCTNNNNNNNNAATTATCAGCTTTTTTTTTTTTTTTTTTTTTTTTTTTTVN	AATTATCAGC	Aged1
P6	ACGACGCTCTTCCGATCTNNNNNNNNCAGCTATCGTTTTTTTTTTTTTTTTTTTTTTTTTTTTVN	CAGCTATCGT	Aged1
P7	ACGACGCTCTTCCGATCTNNNNNNNNATTGCGCTGATTTTTTTTTTTTTTTTTTTTTTTTTTTTVN	ATTGCGCTGA	Aged1
P8	ACGACGCTCTTCCGATCTNNNNNNNNTTGGTAGGCGTTTTTTTTTTTTTTTTTTTTTTTTTTTTVN	TTGGTAGGCG	Aged1
I9	ACGACGCTCTTCCGATCTNNNNNNNNATTCAGGTACTTTTTTTTTTTTTTTTTTTTTTTTTTTTVN	ATTCAGGTAC	Aged2
I10	ACGACGCTCTTCCGATCTNNNNNNNNATGGAATTGGTTTTTTTTTTTTTTTTTTTTTTTTTTTTVN	ATGGAATTGG	Aged2
I11	ACGACGCTCTTCCGATCTNNNNNNNNGACGAAGCGTTTTTTTTTTTTTTTTTTTTTTTTTTTTVN	GACGAAGCGT	Aged2
I12	ACGACGCTCTTCCGATCTNNNNNNNNCTTGCAGTAGTTTTTTTTTTTTTTTTTTTTTTTTTTTTVN	CTTGCAGTAG	Aged2
I13	ACGACGCTCTTCCGATCTNNNNNNNNCTTGGTAATGTTTTTTTTTTTTTTTTTTTTTTTTTTTTVN	CTTGGTAATG	Aged2
I14	ACGACGCTCTTCCGATCTNNNNNNNNCAAGTCGACCTTTTTTTTTTTTTTTTTTTTTTTTTTTTVN	CAAGTCGACC	Aged2
I15	ACGACGCTCTTCCGATCTNNNNNNNNTAACGAATTGTTTTTTTTTTTTTTTTTTTTTTTTTTTTVN	TAACGAATTG	Aged2
I16	ACGACGCTCTTCCGATCTNNNNNNNNTGAGAACCAATTTTTTTTTTTTTTTTTTTTTTTTTTTTVN	TGAGAACCAA	Aged2
J9	ACGACGCTCTTCCGATCTNNNNNNNNCGGTTATGCCTTTTTTTTTTTTTTTTTTTTTTTTTTTTVN	CGGTTATGCC	Aged2
J10	ACGACGCTCTTCCGATCTNNNNNNNNTGGCCGGCCTTTTTTTTTTTTTTTTTTTTTTTTTTTTVN	TGGCCGGCCT	Aged2
J11	ACGACGCTCTTCCGATCTNNNNNNNNAGCTGCAATATTTTTTTTTTTTTTTTTTTTTTTTTTTTVN	AGCTGCAATA	Aged2
J12	ACGACGCTCTTCCGATCTNNNNNNNNTGGCCATGCATTTTTTTTTTTTTTTTTTTTTTTTTTTTVN	TGGCCATGCA	Aged2
J13	ACGACGCTCTTCCGATCTNNNNNNNNTGACGCTCCGTTTTTTTTTTTTTTTTTTTTTTTTTTTTVN	TGACGCTCCG	Aged2
J14	ACGACGCTCTTCCGATCTNNNNNNNNAACTGCTGCCTTTTTTTTTTTTTTTTTTTTTTTTTTTTVN	AACTGCTGCC	Aged2
J15	ACGACGCTCTTCCGATCTNNNNNNNNTGCGCGATGCTTTTTTTTTTTTTTTTTTTTTTTTTTTTVN	TGCGCGATGC	Aged2
J16	ACGACGCTCTTCCGATCTNNNNNNNNATTGAGATTGTTTTTTTTTTTTTTTTTTTTTTTTTTTTVN	ATTGAGATTG	Aged2
K9	ACGACGCTCTTCCGATCTNNNNNNNNCCATTCGTAATTTTTTTTTTTTTTTTTTTTTTTTTTTTVN	CCATTCGTAA	Aged2

K10	ACGACGCTCTTCCGATCTNNNNNNNNNTGCGCCAGAATTTTTTTTTTTTTTTTTTTTTTTTTTTTTVN	TGCGCCAGAA	Aged2
K11	ACGACGCTCTTCCGATCTNNNNNNNNCGAATAATTCTTTTTTTTTTTTTTTTTTTTTTTTTTTTTVN	CGAATAATTC	Aged2
K12	ACGACGCTCTTCCGATCTNNNNNNNNGCGACGCCTTTTTTTTTTTTTTTTTTTTTTTTTTTTTTVN	GCGACGCCTT	Aged2
K13	ACGACGCTCTTCCGATCTNNNNNNNNNATCAACGATTTTTTTTTTTTTTTTTTTTTTTTTTTTTTVN	ATCAACGATT	Aged2
K14	ACGACGCTCTTCCGATCTNNNNNNNNGTTCTGAATTTTTTTTTTTTTTTTTTTTTTTTTTTTTTVN	GTTCTGAATT	Aged2
K15	ACGACGCTCTTCCGATCTNNNNNNNNGCTAACCTCATTTTTTTTTTTTTTTTTTTTTTTTTTTTTVN	GCTAACCTCA	Aged2
K16	ACGACGCTCTTCCGATCTNNNNNNNNCAAGCAACTGTTTTTTTTTTTTTTTTTTTTTTTTTTTTTVN	CAAGCAACTG	Aged2
L9	ACGACGCTCTTCCGATCTNNNNNNNNGTCTCCAGAGTTTTTTTTTTTTTTTTTTTTTTTTTTTTTVN	GTCTCCAGAG	Aged2
L10	ACGACGCTCTTCCGATCTNNNNNNNNAATGCTAGTCTTTTTTTTTTTTTTTTTTTTTTTTTTTTTVN	AATGCTAGTC	Aged2
L11	ACGACGCTCTTCCGATCTNNNNNNNNGACGACCTGCTTTTTTTTTTTTTTTTTTTTTTTTTTTTTVN	GACGACCTGC	Aged2
L12	ACGACGCTCTTCCGATCTNNNNNNNNAGAGCCAGCCTTTTTTTTTTTTTTTTTTTTTTTTTTTTTVN	AGAGCCAGCC	Aged2
L13	ACGACGCTCTTCCGATCTNNNNNNNNCCAGGCCGCATTTTTTTTTTTTTTTTTTTTTTTTTTTTTVN	CCAGGCCGCA	Aged2
L14	ACGACGCTCTTCCGATCTNNNNNNNNCAGGTATGGATTTTTTTTTTTTTTTTTTTTTTTTTTTTTVN	CAGGTATGGA	Aged2
L15	ACGACGCTCTTCCGATCTNNNNNNNNCCGGAGTTGCTTTTTTTTTTTTTTTTTTTTTTTTTTTTTVN	CCGGAGTTGC	Aged2
L16	ACGACGCTCTTCCGATCTNNNNNNNNTTAATTATTGTTTTTTTTTTTTTTTTTTTTTTTTTTTTTVN	TTAATTATTG	Aged2
M9	ACGACGCTCTTCCGATCTNNNNNNNNCTGGATTAGTTTTTTTTTTTTTTTTTTTTTTTTTTTTTVN	CTGGATTAGT	Aged2
M10	ACGACGCTCTTCCGATCTNNNNNNNNTTGGATCCTTTTTTTTTTTTTTTTTTTTTTTTTTTTTVN	TTGGATCCTT	Aged2
M11	ACGACGCTCTTCCGATCTNNNNNNNNTTGGAATCTCTTTTTTTTTTTTTTTTTTTTTTTTTTTTVN	TTGGAATCTC	Aged2
M12	ACGACGCTCTTCCGATCTNNNNNNNNACCTGGACGCTTTTTTTTTTTTTTTTTTTTTTTTTTTTTVN	ACCTGGACGC	Aged2
M13	ACGACGCTCTTCCGATCTNNNNNNNNCCTGACGTTCTTTTTTTTTTTTTTTTTTTTTTTTTTTTVN	CCTGACGTTC	Aged2
M14	ACGACGCTCTTCCGATCTNNNNNNNNGCGTTCAGCTTTTTTTTTTTTTTTTTTTTTTTTTTTTTVN	GCGTTCAGCT	Aged2
M15	ACGACGCTCTTCCGATCTNNNNNNNNTTAGCAATAATTTTTTTTTTTTTTTTTTTTTTTTTTTTTVN	TTAGCAATAA	Aged2
M16	ACGACGCTCTTCCGATCTNNNNNNNNTTGATGCTATTTTTTTTTTTTTTTTTTTTTTTTTTTTTVN	TTGATGCTAT	Aged2
N9	ACGACGCTCTTCCGATCTNNNNNNNNGCCAACGCCATTTTTTTTTTTTTTTTTTTTTTTTTTTTTVN	GCCAACGCCA	Aged2
N10	ACGACGCTCTTCCGATCTNNNNNNNNTCTACCATTATTTTTTTTTTTTTTTTTTTTTTTTTTTTTVN	TCTACCATTA	Aged2
N11	ACGACGCTCTTCCGATCTNNNNNNNNCTTGCGGTCTTTTTTTTTTTTTTTTTTTTTTTTTTTTTVN	CTTGCGGTCT	Aged2
N12	ACGACGCTCTTCCGATCTNNNNNNNNTTACGTATACTTTTTTTTTTTTTTTTTTTTTTTTTTTTTVN	TTACGTATAC	Aged2
N13	ACGACGCTCTTCCGATCTNNNNNNNNCGATTGGTTATTTTTTTTTTTTTTTTTTTTTTTTTTTTTVN	CGATTGGTTA	Aged2
N14	ACGACGCTCTTCCGATCTNNNNNNNNACTTAACTAGTTTTTTTTTTTTTTTTTTTTTTTTTTTTTVN	ACTTAACTAG	Aged2
N15	ACGACGCTCTTCCGATCTNNNNNNNNGCAGACCGGTTTTTTTTTTTTTTTTTTTTTTTTTTTTTVN	GCAGACCGGT	Aged2
N16	ACGACGCTCTTCCGATCTNNNNNNNNTGAGTCCAGATTTTTTTTTTTTTTTTTTTTTTTTTTTTTVN	TGAGTCCAGA	Aged2
O9	ACGACGCTCTTCCGATCTNNNNNNNNGCGACGCAGATTTTTTTTTTTTTTTTTTTTTTTTTTTTTVN	GCGACGCAGA	Aged2
O10	ACGACGCTCTTCCGATCTNNNNNNNNAATGGTCGACTTTTTTTTTTTTTTTTTTTTTTTTTTTTTVN	AATGGTCGAC	Aged2
O11	ACGACGCTCTTCCGATCTNNNNNNNNTGGAACTAGATTTTTTTTTTTTTTTTTTTTTTTTTTTTTVN	TGGAACTAGA	Aged2
O12	ACGACGCTCTTCCGATCTNNNNNNNNGTCCAACTCATTTTTTTTTTTTTTTTTTTTTTTTTTTTTVN	GTCCAACTCA	Aged2
O13	ACGACGCTCTTCCGATCTNNNNNNNNGTTATGGATCTTTTTTTTTTTTTTTTTTTTTTTTTTTTTVN	GTTATGGATC	Aged2
O14	ACGACGCTCTTCCGATCTNNNNNNNNTTATAAGAACTTTTTTTTTTTTTTTTTTTTTTTTTTTTTVN	TTATAAGAAC	Aged2
O15	ACGACGCTCTTCCGATCTNNNNNNNNCAAGCTTCATTTTTTTTTTTTTTTTTTTTTTTTTTTTTVN	CAAGCTTCAT	Aged2
O16	ACGACGCTCTTCCGATCTNNNNNNNNCTGATTAAGATTTTTTTTTTTTTTTTTTTTTTTTTTTTTVN	CTGATTAAGA	Aged2
P9	ACGACGCTCTTCCGATCTNNNNNNNNAGCTAAGGTATTTTTTTTTTTTTTTTTTTTTTTTTTTTTVN	AGCTAAGGTA	Aged2
P10	ACGACGCTCTTCCGATCTNNNNNNNNTCGTAGAGAATTTTTTTTTTTTTTTTTTTTTTTTTTTTTVN	TCGTAGAGAA	Aged2
P11	ACGACGCTCTTCCGATCTNNNNNNNNTGATGGCCTTTTTTTTTTTTTTTTTTTTTTTTTTTTTTVN	TGATGGCCTT	Aged2
P12	ACGACGCTCTTCCGATCTNNNNNNNNTGGAAGTACCTTTTTTTTTTTTTTTTTTTTTTTTTTTTTVN	TGGAAGTACC	Aged2
P13	ACGACGCTCTTCCGATCTNNNNNNNNCTCCAAGGATTTTTTTTTTTTTTTTTTTTTTTTTTTTTTVN	CTCCAAGGAT	Aged2
P14	ACGACGCTCTTCCGATCTNNNNNNNNAGATATATCGTTTTTTTTTTTTTTTTTTTTTTTTTTTTTVN	AGATATATCG	Aged2
P15	ACGACGCTCTTCCGATCTNNNNNNNNCATGCTGGTTTTTTTTTTTTTTTTTTTTTTTTTTTTTTVN	CATGCTGGTT	Aged2
P16	ACGACGCTCTTCCGATCTNNNNNNNNTCCTCGAGTCTTTTTTTTTTTTTTTTTTTTTTTTTTTTTVN	TCCTCGAGTC	Aged2
I17	ACGACGCTCTTCCGATCTNNNNNNNNTTATTCTGAGTTTTTTTTTTTTTTTTTTTTTTTTTTTTTVN	TTATTCTGAG	Aged3

I18	ACGACGCTCTTCCGATCTNNNNNNNNTTATTATGGTTTTTTTTTTTTTTTTTTTTTTTTTTTTTVN	TTATTATGGT	Aged3
I19	ACGACGCTCTTCCGATCTNNNNNNNNATATGAGCCATTTTTTTTTTTTTTTTTTTTTTTTTTTTTVN	ATATGAGCCA	Aged3
I20	ACGACGCTCTTCCGATCTNNNNNNNNCAACCAGTACTTTTTTTTTTTTTTTTTTTTTTTTTTTTVN	CAACCAGTAC	Aged3
I21	ACGACGCTCTTCCGATCTNNNNNNNNCATCCGACTATTTTTTTTTTTTTTTTTTTTTTTTTTTTVN	CATCCGACTA	Aged3
I22	ACGACGCTCTTCCGATCTNNNNNNNNATCATGGCTGTTTTTTTTTTTTTTTTTTTTTTTTTTTTVN	ATCATGGCTG	Aged3
I23	ACGACGCTCTTCCGATCTNNNNNNNNCCGCAAGTTCTTTTTTTTTTTTTTTTTTTTTTTTTTTTVN	CCGCAAGTTC	Aged3
I24	ACGACGCTCTTCCGATCTNNNNNNNNCTTCTCATTGTTTTTTTTTTTTTTTTTTTTTTTTTTTTVN	CTTCTCATTG	Aged3
J17	ACGACGCTCTTCCGATCTNNNNNNNNTTGATATATTTTTTTTTTTTTTTTTTTTTTTTTTTTTVN	TTGATATATT	Aged3
J18	ACGACGCTCTTCCGATCTNNNNNNNNCGGTAGGAATTTTTTTTTTTTTTTTTTTTTTTTTTTTTVN	CGGTAGGAAT	Aged3
J19	ACGACGCTCTTCCGATCTNNNNNNNNACCAGCGCAGTTTTTTTTTTTTTTTTTTTTTTTTTTTTVN	ACCAGCGCAG	Aged3
J20	ACGACGCTCTTCCGATCTNNNNNNNNCGAATGAGCTTTTTTTTTTTTTTTTTTTTTTTTTTTTTVN	CGAATGAGCT	Aged3
J21	ACGACGCTCTTCCGATCTNNNNNNNNAGTTCGAGTATTTTTTTTTTTTTTTTTTTTTTTTTTTTVN	AGTTCGAGTA	Aged3
J22	ACGACGCTCTTCCGATCTNNNNNNNNTTGGACGCTGTTTTTTTTTTTTTTTTTTTTTTTTTTTTVN	TTGGACGCTG	Aged3
J23	ACGACGCTCTTCCGATCTNNNNNNNNATAGACTAGGTTTTTTTTTTTTTTTTTTTTTTTTTTTTVN	ATAGACTAGG	Aged3
J24	ACGACGCTCTTCCGATCTNNNNNNNNTATAGTAAGCTTTTTTTTTTTTTTTTTTTTTTTTTTTTVN	TATAGTAAGC	Aged3
K17	ACGACGCTCTTCCGATCTNNNNNNNNGGAGCGGCCGTTTTTTTTTTTTTTTTTTTTTTTTTTTTTVN	GGAGCGGCCG	Aged3
K18	ACGACGCTCTTCCGATCTNNNNNNNNCGCGTACGACTTTTTTTTTTTTTTTTTTTTTTTTTTTTTVN	CGCGTACGAC	Aged3
K19	ACGACGCTCTTCCGATCTNNNNNNNNCGATGGCGCCTTTTTTTTTTTTTTTTTTTTTTTTTTTTTVN	CGATGGCGCC	Aged3
K20	ACGACGCTCTTCCGATCTNNNNNNNNTGGTATTCATTTTTTTTTTTTTTTTTTTTTTTTTTTTTVN	TGGTATTCAT	Aged3
K21	ACGACGCTCTTCCGATCTNNNNNNNNGATAAGGCAATTTTTTTTTTTTTTTTTTTTTTTTTTTTTVN	GATAAGGCAA	Aged3
K22	ACGACGCTCTTCCGATCTNNNNNNNNGCCGGTCGAGTTTTTTTTTTTTTTTTTTTTTTTTTTTTTVN	GCCGGTCGAG	Aged3
K23	ACGACGCTCTTCCGATCTNNNNNNNNTGCGCCATCTTTTTTTTTTTTTTTTTTTTTTTTTTTTTVN	TGCGCCATCT	Aged3
K24	ACGACGCTCTTCCGATCTNNNNNNNNAAGTCTTCCGTTTTTTTTTTTTTTTTTTTTTTTTTTTTTVN	AAGTCTTCCG	Aged3
L17	ACGACGCTCTTCCGATCTNNNNNNNNAATCAGCTGCTTTTTTTTTTTTTTTTTTTTTTTTTTTTTVN	AATCAGCTGC	Aged3
L18	ACGACGCTCTTCCGATCTNNNNNNNNCCGTTGACTTTTTTTTTTTTTTTTTTTTTTTTTTTTTTVN	CCGTTGACTT	Aged3
L19	ACGACGCTCTTCCGATCTNNNNNNNNGCCAGGATCATTTTTTTTTTTTTTTTTTTTTTTTTTTTTVN	GCCAGGATCA	Aged3
L20	ACGACGCTCTTCCGATCTNNNNNNNNCTTCGGCGCATTTTTTTTTTTTTTTTTTTTTTTTTTTTTVN	CTTCGGCGCA	Aged3
L21	ACGACGCTCTTCCGATCTNNNNNNNNCAAGGCATTCTTTTTTTTTTTTTTTTTTTTTTTTTTTTTVN	CAAGGCATTC	Aged3
L22	ACGACGCTCTTCCGATCTNNNNNNNNAAGAATGGAATTTTTTTTTTTTTTTTTTTTTTTTTTTTTVN	AAGAATGGAA	Aged3
L23	ACGACGCTCTTCCGATCTNNNNNNNNCGGATGAAGGTTTTTTTTTTTTTTTTTTTTTTTTTTTTTVN	CGGATGAAGG	Aged3
L24	ACGACGCTCTTCCGATCTNNNNNNNNTATCGTCGGCTTTTTTTTTTTTTTTTTTTTTTTTTTTTTVN	TATCGTCGGC	Aged3
M17	ACGACGCTCTTCCGATCTNNNNNNNNCTCTGCGGCATTTTTTTTTTTTTTTTTTTTTTTTTTTTTVN	CTCTGCGGCA	Aged3
M18	ACGACGCTCTTCCGATCTNNNNNNNNAATAATACCATTTTTTTTTTTTTTTTTTTTTTTTTTTTTTVN	AATAATACCA	Aged3
M19	ACGACGCTCTTCCGATCTNNNNNNNNACGCCGTTCATTTTTTTTTTTTTTTTTTTTTTTTTTTTTVN	ACGCCGTTCA	Aged3
M20	ACGACGCTCTTCCGATCTNNNNNNNNTTCGCTTACGTTTTTTTTTTTTTTTTTTTTTTTTTTTTTVN	TTCGCTTACG	Aged3
M21	ACGACGCTCTTCCGATCTNNNNNNNNTACGGCTACGTTTTTTTTTTTTTTTTTTTTTTTTTTTTTVN	TACGGCTACG	Aged3
M22	ACGACGCTCTTCCGATCTNNNNNNNNTTCTTATCGATTTTTTTTTTTTTTTTTTTTTTTTTTTTTVN	TTCTTATCGA	Aged3
M23	ACGACGCTCTTCCGATCTNNNNNNNNTTCCATGGCATTTTTTTTTTTTTTTTTTTTTTTTTTTTTVN	TTCCATGGCA	Aged3
M24	ACGACGCTCTTCCGATCTNNNNNNNNAAGTAGTCAGTTTTTTTTTTTTTTTTTTTTTTTTTTTTTVN	AAGTAGTCAG	Aged3
N17	ACGACGCTCTTCCGATCTNNNNNNNNTGGAGAATTCTTTTTTTTTTTTTTTTTTTTTTTTTTTTTVN	TGGAGAATTC	Aged3
N18	ACGACGCTCTTCCGATCTNNNNNNNNACCAGCCTTATTTTTTTTTTTTTTTTTTTTTTTTTTTTTVN	ACCAGCCTTA	Aged3
N19	ACGACGCTCTTCCGATCTNNNNNNNNGGCGAGCTTATTTTTTTTTTTTTTTTTTTTTTTTTTTTTVN	GGCGAGCTTA	Aged3
N20	ACGACGCTCTTCCGATCTNNNNNNNNTCGAGGAGTATTTTTTTTTTTTTTTTTTTTTTTTTTTTTVN	TCGAGGAGTA	Aged3
N21	ACGACGCTCTTCCGATCTNNNNNNNNCCTTACTCCTTTTTTTTTTTTTTTTTTTTTTTTTTTTTVN	CCTTACTCCT	Aged3
N22	ACGACGCTCTTCCGATCTNNNNNNNNTCAGACGAACTTTTTTTTTTTTTTTTTTTTTTTTTTTTTVN	TCAGACGAAC	Aged3
N23	ACGACGCTCTTCCGATCTNNNNNNNNCCGTCCAGTATTTTTTTTTTTTTTTTTTTTTTTTTTTTTVN	CCGTCCAGTA	Aged3
N24	ACGACGCTCTTCCGATCTNNNNNNNNGTTCCGCTAATTTTTTTTTTTTTTTTTTTTTTTTTTTTTVN	GTTCCGCTAA	Aged3
O17	ACGACGCTCTTCCGATCTNNNNNNNNTACTTACTTATTTTTTTTTTTTTTTTTTTTTTTTTTTTTVN	TACTTACTTA	Aged3

O18	ACGACGCTCTTCCGATCTNNNNNNNNGGATCTGCAGTTTTTTTTTTTTTTTTTTTTTTTTTTTTVN	GGATCTGCAG	Aged3
O19	ACGACGCTCTTCCGATCTNNNNNNNNATGCAATATGTTTTTTTTTTTTTTTTTTTTTTTTTTTTVN	ATGCAATATG	Aged3
O20	ACGACGCTCTTCCGATCTNNNNNNNNTTCCTAGACCTTTTTTTTTTTTTTTTTTTTTTTTTTTVN	TTCCTAGACC	Aged3
O21	ACGACGCTCTTCCGATCTNNNNNNNNACTGCCGATATTTTTTTTTTTTTTTTTTTTTTTTTTTTVN	ACTGCCGATA	Aged3
O22	ACGACGCTCTTCCGATCTNNNNNNNNTCCAGAAGGTTTTTTTTTTTTTTTTTTTTTTTTTTTTVN	TCCAGAAGGT	Aged3
O23	ACGACGCTCTTCCGATCTNNNNNNNNTTCAAGACCATTTTTTTTTTTTTTTTTTTTTTTTTTTTVN	TTCAAGACCA	Aged3
O24	ACGACGCTCTTCCGATCTNNNNNNNNTATTACTCATTTTTTTTTTTTTTTTTTTTTTTTTTTTVN	TATTACTCAT	Aged3
P17	ACGACGCTCTTCCGATCTNNNNNNNNGCAAGGAATATTTTTTTTTTTTTTTTTTTTTTTTTTTTVN	GCAAGGAATA	Aged3
P18	ACGACGCTCTTCCGATCTNNNNNNNNGGCATAGCTTTTTTTTTTTTTTTTTTTTTTTTTTTTVN	GGCATAGCTT	Aged3
P19	ACGACGCTCTTCCGATCTNNNNNNNNCTACGGTAGCTTTTTTTTTTTTTTTTTTTTTTTTTTTVN	CTACGGTAGC	Aged3
P20	ACGACGCTCTTCCGATCTNNNNNNNNAGTAAGCATATTTTTTTTTTTTTTTTTTTTTTTTTTTTVN	AGTAAGCATA	Aged3
P21	ACGACGCTCTTCCGATCTNNNNNNNNCGCCTCGAACTTTTTTTTTTTTTTTTTTTTTTTTTTTVN	CGCCTCGAAC	Aged3
P22	ACGACGCTCTTCCGATCTNNNNNNNNTTAGGATCTATTTTTTTTTTTTTTTTTTTTTTTTTTTTVN	TTAGGATCTA	Aged3
P23	ACGACGCTCTTCCGATCTNNNNNNNNACTACTGAAGTTTTTTTTTTTTTTTTTTTTTTTTTTTTVN	ACTACTGAAG	Aged3
P24	ACGACGCTCTTCCGATCTNNNNNNNNAATCTGGAGTTTTTTTTTTTTTTTTTTTTTTTTTTTTVN	AATCTGGAGT	Aged3

Figure 8-1: sciRNAseq oligo-dT primer sequences. N= 8-base UMI; sampleID= mouse (young n=3, aged n=3).

8.2 GO Terms "Cell Cycle G1/S Phase Transition" and "Cell Cycle G2/M Phase Transition"

For use in "sciRNAseq analysis" using SeuratR package and the *Cell-Cycle Scoring and Regression* Vignette.

Cell cycle G1/S phase transition

Acvr1, Acvr1b, Adam17, Adamts1, Aif1, Akt1, Ankrd17, Anp32b, Anxa1, Apex1, Appl1, Appl2, Atp2b4, Bach1, Bcl2, Bid, Brd4, Brd7, Btn2a2, Cables1, Cacnb4, Cacul1, Camk2a, Camk2b, Camk2d, Camk2g, Casp2, Ccl12, Ccna2, Ccnd1, Ccnd2, Ccnd3, Ccne1, Ccne2, Cdc25a, Cdc45, Cdc73, Cdk2, Cdk2ap2, Cdk4, Cdkn1a, Cdkn1b, Cdkn2a, Cdkn2b, Cdkn2c, Cdkn2d, Cirbp, Cradd, Crebbp, Crlf3, Crnn, Ctdsp1, Ctdsp2, Ctdspl, Cul4a, Cul4b, Cyp1a1, Dact1, Dbf4, Dcun1d3, Ddx3x, Dgkz, E2f1, E2f3, E2f4, E2f5, E2f6, E2f7, Ecd, Egfr, Eif4e, Eif4ebp1, Eif4g1, Esrrb, Ezh2, Fam83d, Fam107a, Fbxo7, Fbxo31, Fgf10, Fhl1, Gas1, Gigyf2, Gjc2, Gli1, Gpnmb, Gpr132, Hacd1, Haspin, Hinfp, Hyal1, Id2, Id4, Inhba, Ino80, Iqgap3, Itgb1, Jade1, Kank2, Kcna5, Kif14, Klf4, Klf11, Kmt2e, Larp7, Lats1, Lats2, Lsm10, Lsm11, Map3k11, Mdm2, Men1, Mepce, Mir26a-1, Mir26a-2, Mir26b, Mnat1, Mtbp,

Myb, Nacc2, Nasp, Nfatc1, Npat, Paf1, Pagr1a, Pagr1b, Pdpn, Phb2, Phf8, Pias1, Pidd1, Pim2, Pkd1, Pkd2, Plcb1, Plk2, Plk3, Plk5, Plrg1, Pml, Pole, Ppp2r3d, Ppp3ca, Prkdc, Prmt2, Psme1, Psme2, Psme3, Pten, Ptpn6, Ptprv, Rb1, Rbbp8, Rbl1, Rbl2, Rbm38, Rcc1, Rdx, Rfwd3, Rgcc, Rhou, Ripk1, Rpa2, Rpl17, Rpl26, Rps6, Rps6kb1, Rps27l, Rptor, Senp2, Septin7, Skp2, Slfn1, Sox4, Spdya, Stxbp4, Susd2, Taf10, Tcf3, Tcf19, Tcim, Tert, Tfdp1, Tjp3, Tm4sf5, Trim39, Trim71, Trp53, Trp63, Ube2e2, Usp26, Usp29, Usp37, Zc3h12d, Zfp655, Zpr1

Cell cycle G2/M phase transition

Abcb1a, Abraxas1, Akap8, Akap8l, App, Arpp19, Atad5, Atf5, Atm, Babam1, Babam2, Bach1, Birc5, Blm, Brca1, Brcc3, Brd4, Brsk1, Brsk2, Calm1, Calm2, Calm3, Camk2d, Ccna2, Ccnb1, Ccnb3, Ccnd1, Ccng1, Ccny, Cdc6, Cdc7, Cdc14b, Cdc25a, Cdc25b, Cdc25c, Cdk1, Cdk2, Cdk4, Cdk5rap3, Cdk14, Cdkn1a, Cdkn2a, Cdkn2b, Cenpf, Chek1, Chek2, Chmp4c, Cit, Clspn, Ctc1, D7Ertd443e, Donson, Dtl, Dyrk3, Esrrb, Fbxl3, Fbxl7, Fbxl8, Fbxl12, Fbxl15, Fbxl18, Fbxl21, Fbxl22, Fbxo5, Fhl1, Foxm1, Foxo4, Fzr1, Gpr132, Hacd1, Hspa2, Hus1, Hus1b, Ier3, Kat14, Kcnh5, Kdm8, Kif14, Lats1, Lmnb1, Macroh2a1, Mastl, Mbd4, Mecp2, Miip, Mre11a, Mrnip, Mta3, Nae1, Nbn, Nek10, Nop53, Npm1, Orc1, Pagr1a, Paxip1, Pbx1, Pinx1, Pkia, Plcb1, Plk1, Ppm1d, Prkcq, Rab11a, Rad17, Rad21, Rad51b, Rad51c, Rcc2, Rint1, Rnaseh2b, Sin3a, Skp2, Smarcd3, Stox1, Syf2, Taf2, Taok1, Taok2, Taok3, Ticrr, Topbp1, Tpd52l1, Trim39, Uimc1, Ush1c, Usp47, Vps4a, Vps4b, Wnt10b, Zfp830, Zfyve19

APPENDIX 2 – SUPPLEMENTARY APPENDIX

Supplementary to the contents of this thesis, I provide a separate appendix document containing complete gene list datasets for the bulk RNAseq, VDJseq, and single-cell sciRNAseq analyses performed. Below is a summary of the gene lists provided in this supplementary appendix, which will be provided alongside this main thesis document.

8.3 Bulk RNAseq DESeq2 differentially-expressed gene lists

Bulk RNAseq:	
ProB All (916DE)	DESeq2 Differentially-expressed genes (p<0.05) between Young (n=4) and Aged (n=12) ProB
ProB Mild (115DE)	DESeq2 Differentially-expressed genes (p<0.05) between Young (n=4) and Mild (n=4) ProB
ProB Moderate (143DE)	DESeq2 Differentially-expressed genes (p<0.05) between Young (n=4) and Moderate (n=4) ProB
ProB Severe (761DE)	DESeq2 Differentially-expressed genes (p<0.05) between Young (n=4) and Severe (n=4) ProB
PreB All (1164DE)	DESeq2 Differentially-expressed genes (p<0.05) between Young (n=4) and Aged (n=12) PreB
PreB Mild (148DE)	DESeq2 Differentially-expressed genes (p<0.05) between Young (n=4) and Mild (n=4) PreB
PreB Moderate (2561DE)	DESeq2 Differentially-expressed genes (p<0.05) between Young (n=4) and Moderate (n=4) PreB
PreB Severe (3596DE)	DESeq2 Differentially-expressed genes (p<0.05) between Young (n=4) and Severe (n=4) PreB
Human CD19+ (665DE)	DESeq2 Differentially-expressed genes (p<0.05) between Young (n=3) and Aged (n=3) Human CD19+

8.4 DNA VDJseq V_H gene usage lists

DNA VDJseq:	
ProB	Vh-gene usage (% Repertoire) between Young (n=4) and Aged (n=12) ProB
PreB	Vh-gene usage (% Repertoire) between Young (n=4) and Mild/Moderate/Severe (n=3x4) PreB

8.5 sciRNAseq – Cluster ID gene lists

sciRNAseq - Cluster ID:	
c0 (Transitioning PreB)	Seurat Differentially expressed genes between clusters that are conserved across both Young and Aged groups: c0
c1 (Cycling Early PreB)	Seurat Differentially expressed genes between clusters that are conserved across both Young and Aged groups: c1
c2 (Resting Late PreB)	Seurat Differentially expressed genes between clusters that are conserved across both Young and Aged groups: c2
c3 (Immature B)	Seurat Differentially expressed genes between clusters that are conserved across both Young and Aged groups: c3
c4 (Pro B)	Seurat Differentially expressed genes between clusters that are conserved across both Young and Aged groups: c4
c5 (Mature B)	Seurat Differentially expressed genes between clusters that are conserved across both Young and Aged groups: c5
c6 (Other B)	Seurat Differentially expressed genes between clusters that are conserved across both Young and Aged groups: c6
c7 (PreProB)	Seurat Differentially expressed genes between clusters that are conserved across both Young and Aged groups: c7
c8 (CLP)	Seurat Differentially expressed genes between clusters that are conserved across both Young and Aged groups: c8

8.6 sciRNAseq – Young versus aged gene lists

sciRNAseq - Young versus Aged:	
CLP	Seurat Differentially-expressed genes (p<0.05) between Young and Aged (n=3) CLP
PreProB	Seurat Differentially-expressed genes (p<0.05) between Young and Aged (n=3) PreProB
ProB	Seurat Differentially-expressed genes (p<0.05) between Young and Aged (n=3) ProB
Cycling Early PreB	Seurat Differentially-expressed genes (p<0.05) between Young and Aged (n=3) Cycling Early PreB
Transitioning PreB	Seurat Differentially-expressed genes (p<0.05) between Young and Aged (n=3) Transitioning PreB
Resting Late PreB	Seurat Differentially-expressed genes (p<0.05) between Young and Aged (n=3) Resting Late PreB
Immature B	Seurat Differentially-expressed genes (i<0.05) between Young and Aged (n=3) Immature B
Mature B	Seurat Differentially-expressed genes (m<0.05) between Young and Aged (n=3) Mature B